보안 과제( ), 일반 과제(✓) / 공개(✓), 비공개( ) ISBN 979-11-88683-20-8

국토교통기술촉진 연구사업 제3차 연도 최종보고서

R&D / 18CTAP-C144787-01

재난 대응 및 복구 지원을 위한 급속 손상도평가 및 의사결정시스템 개발 최종보고서

2021. 01 . 13.

주관연구기관 / 서울대학교
공동연구기관 / Georgia Institute of Technology

국 토 교 통 부
국토교통과학기술진흥원

제 출 문

국토교통과학기술진흥원 귀하

‘재난 대응 및 복구 지원을 위한 급속 손상도평가 및 의사결정시스템 개발’(연구개발 기간 : 2018.04.10 ~ 2020.12.31) 과제의 최종보고서 7부를 제출합니다.

2021 . 01 . 13 .

주관연구기관명 : 서울대학교 산학협력단 (대표자) 김용진 (인)

공동연구기관명 : Georgia Tech Research Corporation (대표자) (인)

주관연구기관책임자: 강준석
공동연구기관책임자: Yong Kwon Cho

국토교통부소관 연구개발사업 운영규정 제29조에 따라 최종보고서 열람에 동의합니다.

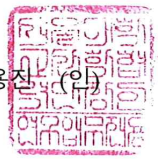
제 출 문

국토교통과학기술진흥원 귀하

'재난 대응 및 복구 지원을 위한 급속 손상도평가 및 의사결정시스템 개발'(연구개발 기간 : 2018.04.10 ~ 2020.12.31) 과제의 최종보고서 7부를 제출합니다.

2021 . 01 . 13 .

주관연구기관명 : 서울대학교 산학협력단 (대표자) 김용진 (인)



공동연구기관명 : Georgia Tech Research Corporation (대표자) (인)

주관연구기관책임자: 강준석
공동연구기관책임자: Yong Kwon Cho

국토교통부소관 연구개발사업 운영규정 제29조에 따라 최종보고서 열람에 동의합니다.

Cover Letter

To President of Korea Agency for Infrastructure Technology Advancement,

We, hereby, submit seven copies of the final report of the research project, 'Rapid damage assessment and situation mapping system to support disaster response and recovery (research period: 04/10/2018 - 12/31/2020)'

2021 . 01 . 12 .

Primary organization: Seoul National University

(representative) Yongjin Kim (signature)

Cooperative organization: Georgia Tech Research Corporation

(representative) Jatri Amin (signature)

PI : Junsuk Kang
Co-PI: Yong Kwon Cho

We agree to open the final report pursuant to Article 29 of the Regulations for the Operation of Research and Development Projects under the jurisdiction of the Ministry of Land, Infrastructure and Transport.

보고서 요약서

<table>
<tr><td>과제 고유 번호</td><td>18CTAP-C144787-01</td><td>해당 단계 연구 기간</td><td>2020.01.01. ~2020.12.31.</td><td>단계구분</td><td>(해당단계)3/ (총단계)3</td></tr>
<tr><td rowspan="2">연구사업명</td><td>중사업명</td><td colspan="4">국토교통기술개발연구사업</td></tr>
<tr><td>세부사업명</td><td colspan="4"></td></tr>
<tr><td rowspan="2">연구과제명</td><td>대과제명</td><td colspan="4"></td></tr>
<tr><td>세부과제명</td><td colspan="4">재난 대응 및 복구 지원을 위한 급속 손상도평가 및 의사결정시스템 개발</td></tr>
<tr><td rowspan="2">연구책임자</td><td rowspan="2">강준석</td><td>해당단계 참여연구원 수</td><td>총: 10 명
내부: 10 명
외부: 0 명</td><td>해당단계 연구비</td><td>정부:174,000천원
민간: 천원
정부외: 천원
상대국: 28,000천원
계:202,000천원</td></tr>
<tr><td>총 연구기간 참여연구원 수</td><td>총: 13명
내부: 13명
외부: 명</td><td>총 연구비</td><td>정부:550,000천원
민간: 천원
정부외: 천원
상대국: 84,000천원
계:634,000천원</td></tr>
<tr><td>연구기관명 및 소속 부서명</td><td colspan="3"></td><td colspan="2">참여기업명</td></tr>
<tr><td>국제공동연구</td><td colspan="3">상대국명: USA</td><td colspan="2">상대국 연구기관명:
Georgia Institute of Technology</td></tr>
<tr><td>위탁연구</td><td colspan="3">연구기관명:</td><td colspan="2">연구책임자:</td></tr>
</table>

※ 국내・외의 기술개발 현황은 연구개발계획서에 기재한 내용으로 갈음

연구개발성과의 보안등급 및 사유	일반

9대 성과 등록・기탁번호

구분	논문	특허	보고서 원문	연구시설・장비	기술요약 정보	소프트웨어	화합물	생명자원		신품종	
								생명정보	생물자원	정보	실물
등록・기탁 번호	13	1	1			1					

국가과학기술종합정보시스템에 등록한 연구시설・장비 현황

구입기관	연구시설・장비명	규격 (모델명)	수량	구입연월일	구입가격 (천원)	구입처 (전화)	비고 (설치장소)	NTIS 등록번호

요약

○ 무인비행체를 이용하여 건물의 변형도를 8-12분 내에 감지하여 사전에 구축된 손상도 DB와의 연계를 통해, 건물 주요 부재에 대한 상황 및 위험도 정보를 제공하는 급속 손상도평가 기술 및 의사결정을 지원하는 의사결정시스템 개발
○ 연구 및 개발 기술에 대한 학계의 검증: SCI(E) 논문 13편
○ 개발기술의 지식재산권 획득: 특허 출원 1건, 저작권 1건
○ 개발기술의 모형실험 및 현장실측과의 비교를 통한 성능 검증
○ 의사결정 시스템 시나리오 초안 제시

보고서 면수

176

〈 요약문 〉

연구의 목적 및 내용	- 본 연구는 지진 등과 같은 재난 상황 시 건물외관 변형을 급속 감지하고 건물 전체 주요부재에 대한 상황 및 위험도 정보를 제공함으로서 재난대응 및 복구 의사결정을 지원할 수 있는「**재난대응 및 복구 지원을 위한 급속 손상도평가 및 의사결정시스템**」을 개발하는 것이 최종 목표임. **[지진하중에 종속된 고층건물 외관변형도와 내외부손상도의 매핑 시스템 개발]** ▪ 지진에 의한 고층 아파트의 거동특성 파악 및 3차원 해석모델 개발 ▪ 지진하중 및 내부 폭파에 의한 고층아파트의 파괴거동 해석모델 개발 및 모형실험 ▪ 건물의 외관변형도를 고려한 구조물의 전체 및 주요 부재에 대한 위험도를 타나내는 매핑모델 개발 **[재난대응 및 복구를 위한 무인비행체 기반 재난지역 3차원 매핑 및 이미지 분석기법 개발]** ▪ 드론 및 무인로봇을 활용한 재난지역 3차원 모델링 및 오브젝트 검출기법 개발 ▪ 3D 모델 기반 구조체 변위 및 파손 측정기법 ▪ 한/미 공동 Test-Bed 구축 및 시스템 검증
연구개발성과	[1] 건물외관변형도와 건물내외부 손상도의 상관관계를 보이는 매핑 시스템 개발 [2] 재난대응 및 복구를 위한 무인비행체 기반 재난지역 3차원 매핑 및 이미지 분석기법 개발 [3] 제난 대응 및 복구 지원을 위한 급속 손상도평가 및 의사결정시스템을 개발
연구개발성과의 활용계획 (기대효과)	○ 활용계획 ◦ 기술적 활용방안 - 현장 대응 중심의 기술을 이용한 지진 발생 현장에서의 신속한 대처 - 선진기술의 공유와 이해를 통한 선진국의 기술이전 기피 현상 극복 - 무인 원격화 기술을 사이버물리시스템으로 확장 ◦ 사회적 활용방안 - 신속한 복구시스템을 통한 지진에 대한 전사회적 트라우마 예방가능 - 현장 대응 기술 도입으로 인한 안전사고 위험성 감소 - 예상 불가능한 지진 발생 상황에서의 성공적 대처로 국가적 이미지 향상 ◦ 경제적 활용방안 - 개발기술을 바탕으로 후진국 시장 진출을 통한 Global Frontier 역할 수행 - 인공지능형 현장 복구 기술로 피해규모 최소화 가능 - 시나리오 기반 신속한 현장 대응으로 최단시간 인명구조 및 추가피해 감소 ○ 기대효과 ◦ 복합적 재난 대응 시장 구축을 위한 시발점 - 성공적인 무인 구조 및 복구 시나리오의 적용으로 원천기술에 대한 국내 및 해외 시장 창출 기회 선점 ◦ 국제적 수준의 재난대응 선진국 - 지진 피해의 대응 뿐 아니라 미래의 지진 피해 상황에 대한 시나리오 예측을 가능하게 함으로써 타국에 본 시나리오를 적용하여 국가적 이미지 향상 ◦ 신뢰도 높은 재난 대응 시스템 - 재난 발생 시 신속한 현장 대응 및 효율적 현장 복구로 국민들의 국가 재난대응에 대한 신뢰도 향상 ◦ 경제적 가이드라인 제공 - 인공지능형 현장 대응 기술 개발로 기계와 인력을 효율적으로 분배 및 활용하여 경제적 시너지 기대

핵심어 (5개 이내)	재난	지진	공동주택	손상도평가	의사결정시스템

〈 목 차 〉

1. 연구개발과제의 개요 ····· 1

2. 연구수행내용 및 성과 ····· 12

(1) 1차 연도 ····· 12

(가) 주관연구기관(서울대학교 산학협력단) ····· 12

(나) 협동연구기관(Georgia Institute of Technology) ····· 34

(2) 2차 연도 ····· 41

(가) 주관연구기관(서울대학교 산학협력단) ····· 41

(나) 협동연구기관(Georgia Institute of Technology) ····· 91

(3) 3차 연도 ····· 95

(가) 주관연구기관(서울대학교 산학협력단) ····· 95

(나) 협동연구기관(Georgia Institute of Technology) ····· 117

3. 목표 달성도 및 관련 분야 기여도 ····· 124

4. 연구개발성과의 활용 계획 ····· 130

붙임. 참고 문헌 ····· 133

부록. 의사결정시스템 시나리오 예시 ····· 142

1. 연구개발과제의 개요

가. 연구개발 목적

(1). 연구개발 최종목표

(가) 최종목표

최종목표	본 연구의 목표는 **지진 등과 같은 재난 상황 시 건물외관 변형을 급속 감지**하고 **건물 전체 주요부재에 대한 상황 및 위험도 정보를 제공**함으로서 **재난대응 및 복구 의사결정을 지원**할 수 있는 **「재난대응 및 복구 지원을 위한 급속 손상도평가 및 의사결정시스템」을 개발**하는 것임.

세부 연구목표	**1 세부**	건물외관변형도와 건물내외부 손상도의 상관관계를 보이는 매핑시스템 개발
	2 세부	재난대응 및 복구를 위한 무인비행체 기반 재난지역 3차원 매핑 및 이미지 분석기법 개발

기술개발 범위	**개발범위**	**대상건물**	공동주택	
		대상업무	구조해석, 손상감지, 무인비행체(드론)	
		기술성숙도	TRL 5단계 : 시작품 제작 및 Mock-up test	
	개발목표 수준	**평가항목**	**유형**	**비고(평가방법)**
		[구조해석] 건물외관변형도에 따른 건물내외부 손상도 매핑시스템	시스템	▪ 2차년도의 소형모형 실증실험과 3차년도의 Full-scale 실증실험을 통해 해석모델 및 제안된 매핑시스템의 검증
		[손상 감지] 재난지역 3D 매핑 및 이미지 분석기법	공법·기법	▪ 2차년도의 소형모형 실증실험과 3차년도의 Full-scale 실증실험을 통해 재난지역 3D 매핑 및 이미지 분석기법 검증

핵심 성과물	**구조해석**	건물외관변형도와 건물내외부 손상도의 상관관계를 보이는 매핑시스템
	손상감지	무인비행체 기반 재난지역 3차원 매핑 및 이미지 분석기법

(나) 최종목표의 성격 및 설정근거

■ 세부별 최종목표 설정근거

구 분	최종목표	기술 성격	목표 설정 근거
[1세부연구] 건물외관변형도와 건물내외부 손상도의 상관관계를 보이는 매핑시스템 개발	▪ 다양한 구조물의 지진하중 하에서의 거동데이터를 사전에 축적하여 외형변형도와 구조물의 손상 및 위험도와의 상관관계를 데이터베이스로 만들어 **지진발생 시 외형의 변형도 측정만으로 빠른시간 안에 구조물의 훼손정도를 파악**하여 응급상황 시 신속한 대응 및 복구에 기여 ▪	시스템	▪ 건물내외부의 피해 및 이에 따른 위험도는 측정에 상당한 시간이 소요됨에 따라 외형변형도와 구조물 손상 및 위험도 데이터베이스를 토대로 재난현장 긴급 대응 및 복구에 기여
[2세부연구] 재난대응 및 복구를 위한 무인비행체 기반 재난지역 3차원 매핑 및 이미지 분석기법 개발	▪ 재난 발생 후 구조적 성능평가를 위해 포인트 클라우드 모델에서 각 구조체를 요소단위로 자동으로 검출하여 모델링한 후 재난 발생 후 빌딩의 구조적 성능평가를 위해 빌딩 단위 요소들의 변위 및 손상도를 정량화	공법·기법	▪ 긴급 투입이 가능한 무인비행체를 활용하여 구조물 변위 및 손상도를 효율적으로 감지하여 재난현장 의사결정을 위한 정보 취득 필요

(2) 연차별 연구목표 및 내용

(가) 연구목표 및 내용

연차	연구목표		주요연구내용
1차년도	1세부	■ 지진에 의한 고층 아파트의 거동특성 파악 및 3차원 해석모델 개발	- 해석모델 개발을 위한 고층아파트 재원 및 지진하중에대한 주요변수 파악 - Response-Spectrum Analysis를 통한 Peak Response 파악 - 비선형 동적해석 (Nonlinear Dynamic Analysis)을 통해 구조물의 비선형 거동특성 파악 및 3차원 해석모델 개발 - 해석모델을 이용한 수치해석을 통해 매핑 모델에 사용될 주요변수 파악
	2세부	■ 드론을 활용한 재난지역 3차원 모델링 및 오브젝트 검출기법 개발	- 무인항공기 기반 재난지역 이미지 데이터 취득 - 무인항공기 이미지를 활용한 재난지역 3차원 모델링 - 머신러닝 기반 오브젝트 및 지면상태 자동검출 및 분류기법 개발
2차년도	1세부	■ 지진하중 및 내부 폭파에 의한 고층아파트의 파괴거동 해석모델 개발 및 모형실험	- 소규모 모형실험을 위한 주요변수 파악 및 실험준비 - 소규모 모형실험 수행 - 해석모델 검증 및 보완 - 지진하중에 이은 내부폭파에 종속된 고층 아파트의 유한요소해석 모델개발
	2세부	■ 3D 모델 기반 구조체 변위 및 파손 측정기법	- 재난 및 이벤트 전/후 3D 모델 매칭 - 구조체 변형 및 손상 정량화 - 무인항공체 이미지 및 적외선 카메라 데이터 퓨전 방식 개발 - 측정 데이터 연동
3차년도	1세부	■ 건물의 외관변형도를 고려한 구조물의 전체 및 주요 부재에 대한 위험도를 나타내는 매핑시스템 개발	- 실증실험을 위한 대상구조물 선정 및 구조물 변위 및 손상도 측정방법 연구 - 구조물의 Full-scale 실증실험 - 3가지 실험결과(구조물 직접계측, LiDAR 계측, 드론계측)와 유한요소해석결과의 비교분석을 통한 개발된 모델검증 - 실증실험 및 해석모델 수치해석결과를 활용한 건물변형도-내부손상도 매핑 모델 개발
	2세부	■ 한/미 공동 Test-Bed 구축 및 시스템 검증	- Test-Bed 구축 - 시스템 검증 - 시스템 연동

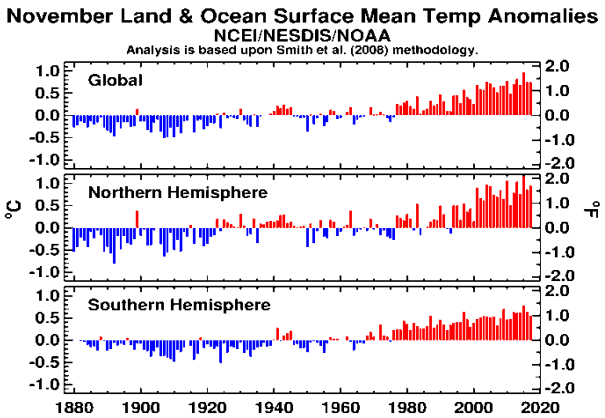
나. 연구개발의 필요성

(1) 연구개발과제의 설명

(가) 연구개발과제 추진배경

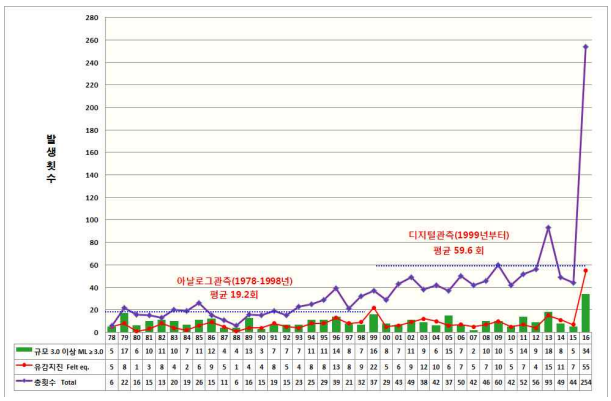
■ 자연 재해로 사회·경제적 피해액 증가

- 국제재해경감전략기구 (UNIDRS)에서 발표된 연도별 보고서에 따르면, 2015년은 기록 이래 가장 따뜻한 해였으며, 지구온난화로 인한 다양한 형태의 기상재해가 발생되고 있음.
- 전 세계적으로 발생한 각종 자연재해로 약 1억명(총 사망자수의 72%가 아시아에서 발생)이 재해 영향을 받았으며 경제적인 손실은 미국의 경우 250억 달러로 가장 많은 손실이 발생함.
- 국내의 자연재난 발생 현황으로 볼 때, 이상 고온으로 인한 폭염, 태풍 등이 인명과 재산에 피해를 주는 주요 자연재난으로 볼 수 있으나, 최근 지진에 의한 재해 피해가 급격하게 증가하고 있음.



참조 : 관계부처합동(2016), 2016년 이상기후 보고서

그림 1-1 전지구 평균기온 편차 시계열



참조 : 기상청보도자료(2017), 2016년 국내외 지진발생 현환

그림 1-2 연도별 지진발생추이

■ 국내 지진 재난에 의한 건축물 붕괴 위험에 노출

- 국내 규모 2.0 이상 지진 발생빈도가 예년(1999년부터 2015년까지) 평균 (47.5회)보다 2016년 252회로 5배 이상 높음.
- 우리나라 건축물의 내진설계화가 지진이 빈번하게 발생하는 국가에 비하여 현저히 늦어져, 지진 발생에 대한 안전성을 확인할 수 없음. 즉, 내진설계가 적용되지 않은 건축물을 주변에 쉽게 찾아볼 수 있어 지진에 의한 건축물 붕괴 위험에 노출되어 있음.

표 1-1 최근 10년간 우리나라 지진발생 현황

(단위 : 건)

	2007	2008	2009	2010	2011	2012	2013	2014	2015	2016	계
계	42	46	60	42	47	56	93	49	44	252	731
서울/경기		5	6	1	6	5	19	3	6	3	54
충청/강원	13	2	6	10	7	6	40	7	6	10	107
전라/제주	3	13	17	12	9	14	8	13	12	17	118
경상도	18	14	16	9	15	24	19	16	17	199	347
기타지역	8	12	15	10	10	7	7	10	3	23	105

참조 : 행정안전부(2016), 2016 재해연보

■ 재난/재해 발생 시 피해 현장 분석 및 대응 기술 부족

- 대형재난이 발생하면 재난현장에는 많은 인력과 장비가 동원되나, 체계적이며 통합적인 지휘체계가 수립되지 못하여 재난대응을 효율적으로 수행하는데 많은 어려움이 존재함. 재난 발생의 초기 대응에 있어 우선적인 활동을 지시하고 인명과 재산피해를 최소화하여 재난의 확산 방지하고 순조롭게 복구활동을 수행하는 것이 매우 중요함.
- 그러나 2016년 우리나라의 재난·재해·안전 분야 국가전략기술 수준은 최고기술국인 미국을 기준으로 기술수준 73.5%, 기술격차 5.4년으로 10대 국가전략기술 평균 기술수준 78.6%, 기술격차 4.2년 대비 낮은 편임. (미래창조과학부, 2016)
- 현재까지는 국내에서는 발생 빈도가 상대적으로 빈번한 태풍 및 호수와 같은 단일 재난요소 분석 시뮬레이션, 화재 및 피난 시뮬레이션 관련 연구가 주를 이루어 새롭게 제기되고 있는 지진에 의한 재난이나 복합 재해에 대응할 수 있는 역량강화에 집중할 필요가 있음.

표 1-2 주요 5개국의 국가전략기술 수준 (2016년)

(단위 : 기술수준(%), 기술격차(년))

분야	한국		미국		유럽(EU)		일본		중국	
	기술수준	기술격차	기술수준	기술격차	기술수준	기술격차	기술수준	기술격차	기술수준	기술격차
국가 전략 기술	78.6	4.2	100	0	94.4	1.1	92.7	1.5	71.1	5.2
재난 · 재해 · 안전	73.5	5.4	100	0	91.2	2.1	92.9	1.8	65.7	7.0

참조 : 미래창조과학부(2016), 2016기술 수준 평가

■ 재난/재해 발생 시 초기 대응 기반 구축 필요

- 재난 및 안전기술관련 연구개발 활동을 통합 조정하여 국가의 재난저감 및 목적에 맞게 협력·연계추진에 대한 필요성을 제기하고 있으나, 재난/재해 발생 시 빠르고 안전하게 대처할 수 있는 재난 대응 기술 기반을 마련할 필요가 있음.
- 그러나 재난에 의한 구조물의 붕괴 및 파괴형상에 대한 시뮬레이션만으로는 재난 발생 현장에 적절한 의사결정을 지원할 수 없으며, 재난 상황에 맞게 빠르고 효율적인 대응 방안을 제시할 수 있는 기술이 필요함.
- 이를 위하여, 재난/재해 발생으로 인한 구조물의 피해 시나리오를 마련하고 실제 구조물 피해 상황을 재현함으로써, 무인 항공기 등을 활용한 재난 현장 실시간 모니터링을 통해 빠르고 정확한 의사결정을 지원하는 기반 기술이 요구됨.
- 미국 조지아(Georgia) 주, 뉴욕시(New York City)에는 재난 후 붕괴된 건축물을 재현한 Multi-Purpose Collapsed Structures가 재현되어 있으므로, 국내의 시뮬레이션 기술과 더불어, 선진국의 국제적인 실험환경 및 기술 협업을 통하여, 재난/재해 발생 시 초기 대응 기반 연구가 필요함.

(나) 연구개발기술의 정의

「자연재해 대응 선진 기술 확보」,「실시간 현장 분석」,「재해 발생 초기 신속한 대응」목표 달성을 위한 **재난대응 및 복구 지원을 위한 급속 손상도평가 및 의사결정시스템**

본 연구과제에서 개발되는 “재난 대응 및 복구 지원을 위한 급속 손상도평가 및 의사결정시스템”은 무인비행체를 지진 등과 같은 재난 상황 시 피해 시설물에 긴급 투입한 후, 건물외관 변형을 3D 매핑 및 이미지 프로세싱을 통해 급속 감지하여 건물 전체 주요부재에 대한 상황 및 위험도 정보를 제공함으로서 재난대응 및 복구 의사결정을 지원하는 IT 융복합기술로 정의

○ **「건물외관변형도에 따른 건물내외부 손상도 매핑시스템 개발 연구」**이라 함은 다양한 구조물의 지진하중 하에서의 거동데이터를 사전에 축적하여 외형변형도와 구조물의 손상 및 위험도와의 상관관계를 데이터베이스로 만들어 지진발생 시 외형의 변형도 측정만으로 빠른시간 안에 구조물의 훼손정도를 파악하는 연구임.

○ **「재난대응 및 복구를 위한 무인비행체 기반 재난지역 3차원 매핑 및 이미지 분석기법 개발 연구」**이라 함은 머신러닝 기술을 활용하여 3차원 포인트 클라우드 모델에서 빌딩 요소(기둥, 벽체, 바닥판 등)를 자동으로 검출 및 분류하고, 특징점 기반 3차원 모델 매칭 기술을 활용하여 구조물의 변위 및 손상도를 정량화하는 연구임.

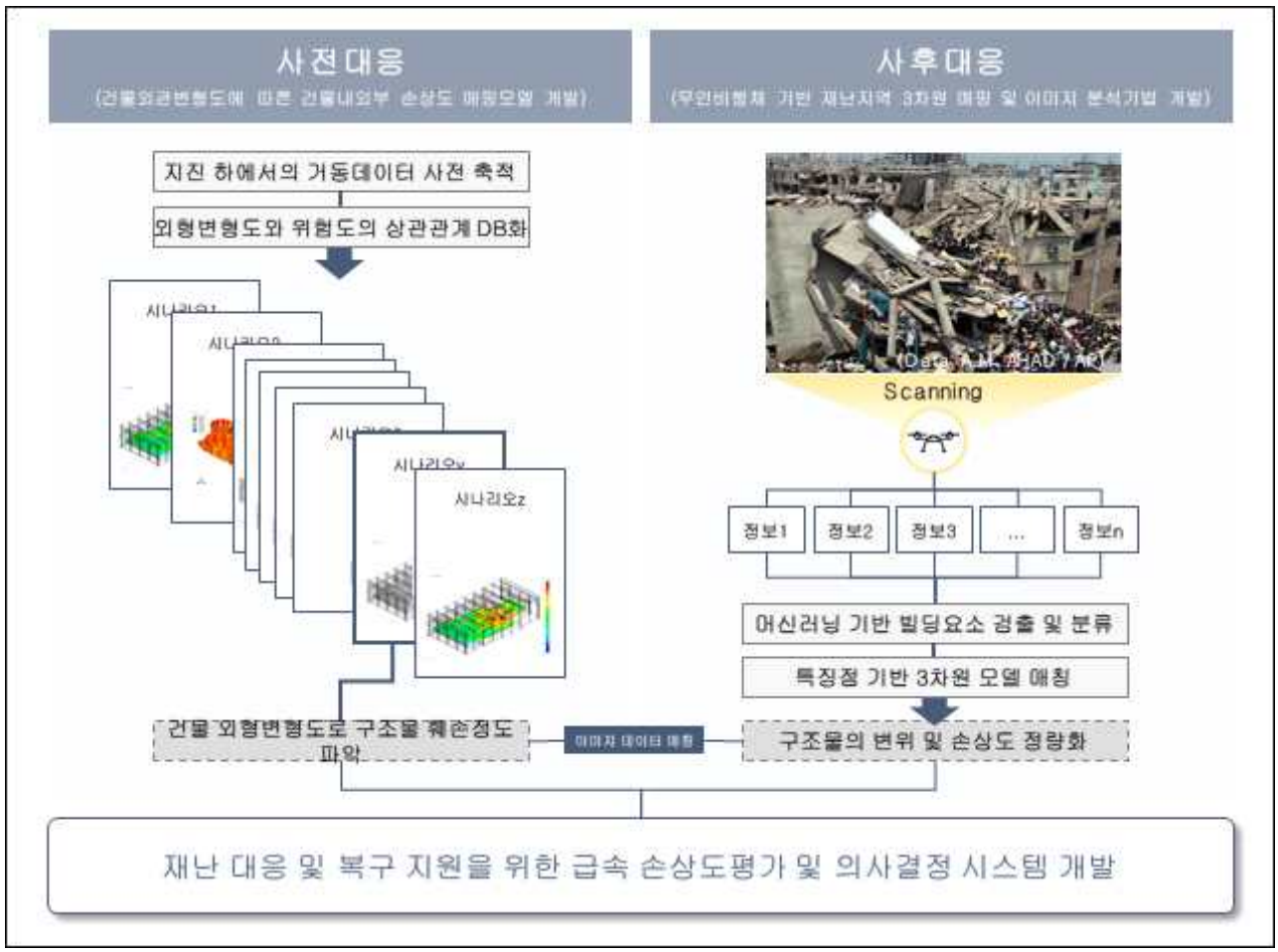


그림 1-3 연구개념도

(2) 연구개발의 중요성

(가) 기술적 측면

■ 광범위하고 복잡한 재난 현장 분석 기술 부족

- 최근 들어 국내를 포함한 전 세계적으로 지진과 이상 기후에 의한 태풍, 폭설, 홍수, 산사태 등 연쇄적으로 발생하여 과거에 비해 광범위한 피해를 야기하고 있음.

- 재난 및 재해로 인한 시설물 붕괴 사고 발생 시 재난 현장은 비정화된 환경이며, 2차 피해가 발생하기 쉬운 복잡하고 위험한 환경임.

- 도시개발 사업 때의 구조물의 다양화, 노후화, 인구집중, 시스템의 복잡성 등으로 과거와 비교해 서 재난, 대형사고 예측이 어렵고, 다양한 시나리오의 개발과 파악된 현장과 시나리오를 매칭 하는 기술이 필요.

■ 재난/재해 발생 시 초기 대응을 위한 현장 지원 시스템 미비

- 재난 현장에 인력 및 기존 중장비 투입이 어려우므로, 신속한 투입이 가능한 소형 로봇 및 무인 항공기 등의 소형 장비 활용하여 재난 상황을 정확히 파악할 필요가 있음.

- 재난/재해 상황 시 인명 및 기타 피해를 최소화하기 위하여 발생 초기 즉각적으로 투입하여 골든타임(재난 발생 후 2~72시간) 내에 초동 대응이 가능한 의사결정이 필요.

- 재난/재해 복구 및 건설 기술 등의 로봇분야 기술개발과 연계하고 현장 상황을 정확하게 인식하여 재난 대응 및 복구를 지원할 수 있는 재난현장 분석 기술이 필요함.

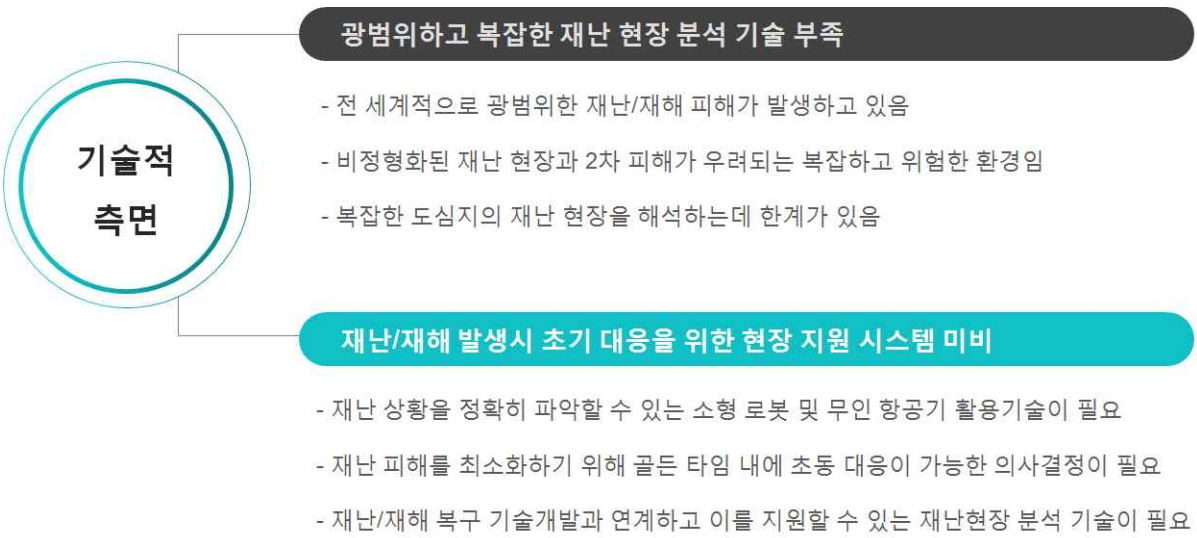


그림 1-4 기술적 측면의 중요성

(나) 경제·산업적 측면

■ 재난/재해에 대한 신속한 초기 대응으로 재난 피해 확산 방지 필요

- 지진을 포함한 기후변화에 따른 자연력으로 인한 구조물 손상과 붕괴는 막대한 인명 및 재산 피해를 초래하여 국가적 재난을 야기할 수 있음.

- 또한, 재해 발생 시 초기 대응 미흡으로 2차적인 피해로 이어질 수 있으며, 도시화와 산업화로 인하여 피해가 기하급수적으로 증가할 것으로 판단됨.

- 재난 및 사고 상황 발생 시 시나리오 개발 및 재난 현장 지원 시스템 구축을 바탕으로 빠른 초기대응과 신속한 복구 작업을 수행함으로써 관련된 직접적인 피해비용, 복구비용, 간접적인 피해비용 등 인명과 재산피해를 최소화 할 수 있음.

■ 재난/재해 발생에 따른 신속한 초기 대응 기술 확보

- 전 세계적으로 증가하는 재난/재해 발생에 따른 신속하고 초기 대응 기술이 필요하며, 복잡하고 위험한 재난 현장에 정확한 정보 분석 기술이 필요함.

- 예측할 수 없는 비정상하중의 작용에 따른 구조물의 붕괴 시 이미지 스캐닝과 시나리오와의 매칭기술을 통하여 빠른 의사 결정을 지원하여 초기 대응의 신속성으로 인력 및 시간 단축이 필요함.

- 본 과제 관련 기술인 드론, 로봇, 스캐닝, 데이터 매칭 기술 등의 발전을 통한 최근 부상하고 있는 4차 산업혁명 트렌드로서 새로운 성장산업 전환이 가능함

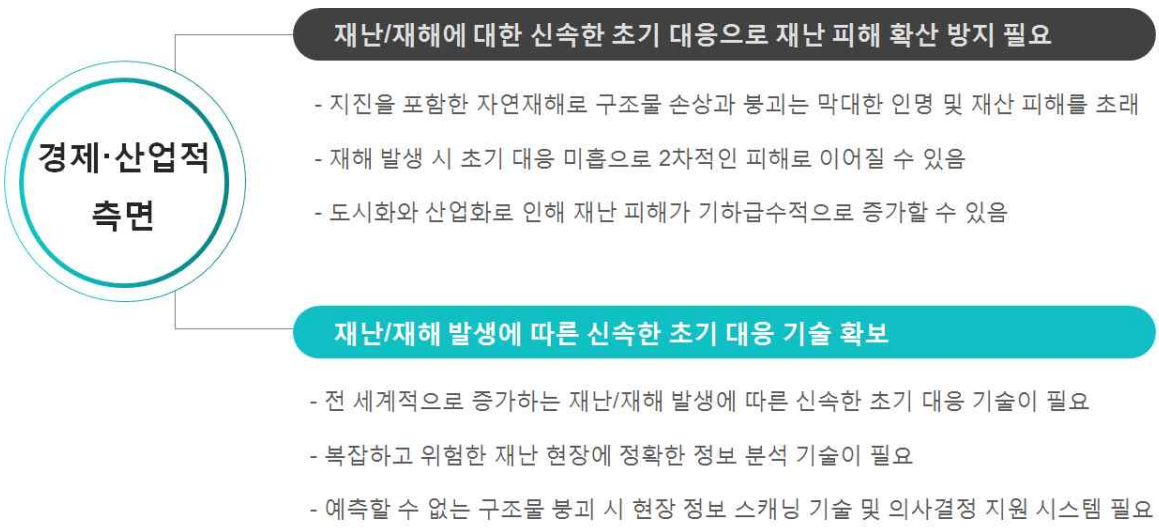


그림 1-5 경제·산업적 측면의 중요성

(다) 사회·문화적 측면

■ 재난/재해 피해 발생 시 신속한 대응 및 사회적 안전성 확보 필요

- 지진 및 전 세계적으로 발생하고 있는 환경변화에 적극 대응이라는 측면에서 재난 발생 시 신속한 대응 및 안전성 확보에 대한 사회적 요구가 급격하게 증가하고 있음.

- 재난/재해 상황 발생 시 즉각적인 투입과 신속한 복구 작업을 국가가 주도하여 수행함으로써 사회적인 신뢰도를 회복하고 추가적인 피해를 예방함.

- 중대 재난에 대한 전개 시나리오와 적절한 대응 방안은 사회적 안전성을 확보하고 추가적인 피해에 대한 불안감 해소, 사회적 갈등을 예방함.

■ 재난/재해 발생 시 신속한 대응에 대한 사회적 요구 증가

- 재난/재해로 인한 붕괴 사고 피해 발생 건수 및 인명피해가 점점 증가하고 있는 상황에서, 건물의 구조적 안정성 및 붕괴 위험에 관한 관심도가 높아지고 있으므로 재난 사고에 대한 시나리오 구축 및 대비를 통하여 사회적 불안감 및 문제 해결.

- 최근 우리나라에 빈번한 지진발생으로 인하여 건축물 붕괴 사고 및 인명 피해가 발생함에 따라, 신속하고 체계적인 대응 방안 마련에 대한 사회적 요구가 증가하고 있으므로 사회문화적 측면에서 해당 연구의 필요성이 매우 크다고 사료됨.

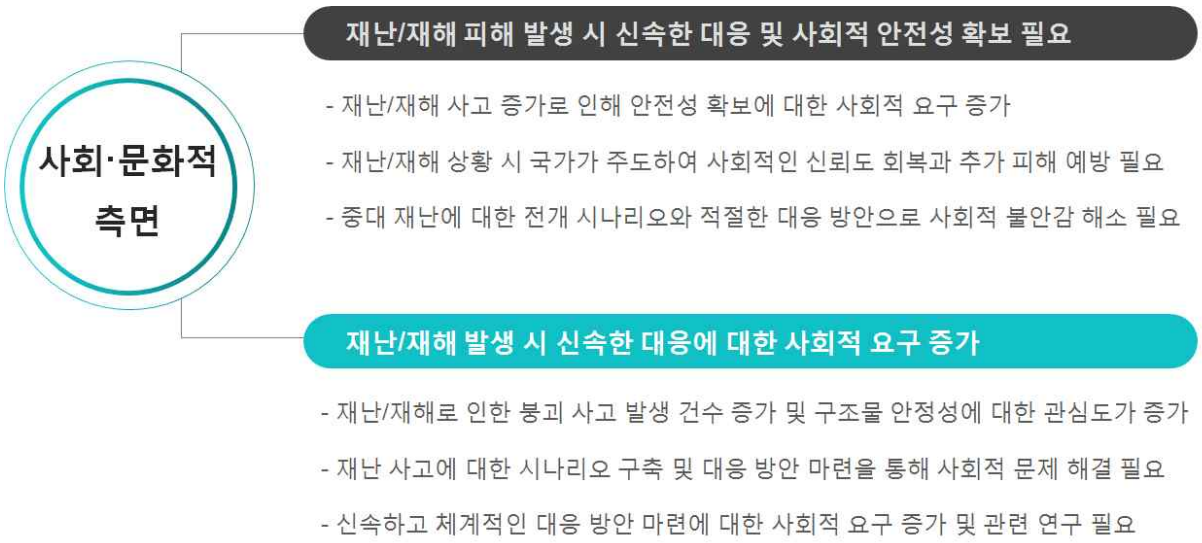


그림 1-6 사회·문화적 측면의 중요성

(라) 정부지원의 필요성

■ 국내 재난/재해 상황에 따라 건물 붕괴 시 초기 대응 조치 개발 시급

- 과거 성수대교, 상품 백화점 붕괴 사고 이후 시설물 붕괴에 관한 관심이 높아 졌지만 건물의 붕괴 예방, 성능 평가 등에 관한 관심이 높아 졌을 뿐 붕괴 이후 상황에 대한 관심도는 상대적으로 저조함.

- 그에 따라 붕괴현장에 대한 초기 대응, 복구 정책 등의 제도적 장치가 부족하며 학술적으로도 연구가 부족한 실정이며 정부차원의 인명 구조, 재해 복구 등의 대응 조치를 위한 기술 개발이 필요함.

- 재난 상황의 특성상 활용 빈도가 상대적으로 높지 않은 기술이지만 높은 수준의 기술력과 투자비를 요구함. 따라서 이익을 추구하는 기업의 특성상 재난/재해 상황에 대한 기술투자를 기대하기 어려운 상황으로 정부차원의 기술개발 투자가 요구됨.

■ 국가재난관리전략의 강화

- 최근 경주/포항 지진 발생, 제천/밀양 화재, 타워크레인 붕괴사고 등 대형 재난이 연속해서 발생하면서 재난 안전에 대한 세간의 관심이 높아지고 있으며, 과거 상대적으로 재난의 빈도가 낮은 국내 환경의 특성을 고려하여 기존 재난관리시스템을 개선 보강하는 등 국가재난관리 패러다임의 대전환이 필요함.

- 본 연구사업은 초기 대응 조치를 가능하게 하고 인명 구조 및 복구 정책 등의 가이드라인을 제시하는 동시에 국제 협력을 통하여 국내의 과학기술 발전을 도모하기에 매우 부합한 연구임.

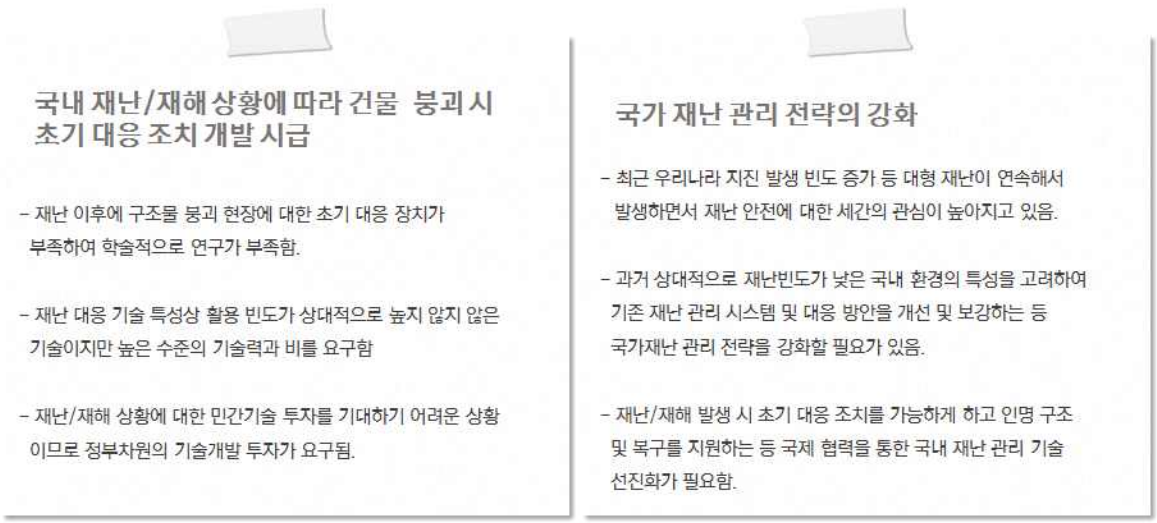


그림 1-7 정부지원의 필요성

(3) 국제협력 필요성

■ 재난/재해 사고에 대한 선진국 역량 활용

- 세계적으로 재난/재해와 관련하여 미국, 유럽, 일본과 같은 선진국에서 국가 차원에서 자연재해에 대비하는 전략을 마련하고, 대응 시스템을 체계화하여 피해를 최소화하는 노력을 기울이고 있는 실정이며, 우리나라도 더 이상 재난 안전지대가 아니기 때문에 재난/재해에 대한 국제적인 협력과 연구가 필요함.

■ 선진 국가의 기술 협력 필요성

- 재난사고 시나리오 국외 운용 사례를 검토하고 재난사고 시나리오 작성 및 고도화를 위하여 재난/재해 사례 연구 및 기술이 구축된 선진 국가와 공동연구가 필요함.

- 또한, 재난 현장을 실시간으로 파악하여 초동 대응을 마련하기 위해서 재난/재해 현장 상황을 모니터링하고 분석할 수 있는 이미지 스캐닝 기술이 확보된 선진 국가와 협력이 필요함.

■ 선진 연구 인프라 활용

- 건물 붕괴 발생 시 가장 중요한 일은 인명이 매몰되어 있는 위치를 찾고 구조하는 일임. 그러나 건물 붕괴 상황은 여러 변수가 작용하여 그 현황을 예측하기 어렵고 붕괴의 잔해물 내에 위치한 인명을 구조하는 방법은 쉽지 않음.

- 따라서 붕괴 초기에 인명 피해를 줄이기 위한 빠른 구조를 위하여 다양한 환경을 반영한 연구가 필요함. 이러한 여러 환경에 대한 T/B 실험이 가능한 선진 국가의 연구 인프라를 적극 활용함으로써, 본 연구개발기술에 대한 실질적인 검증이 가능함.

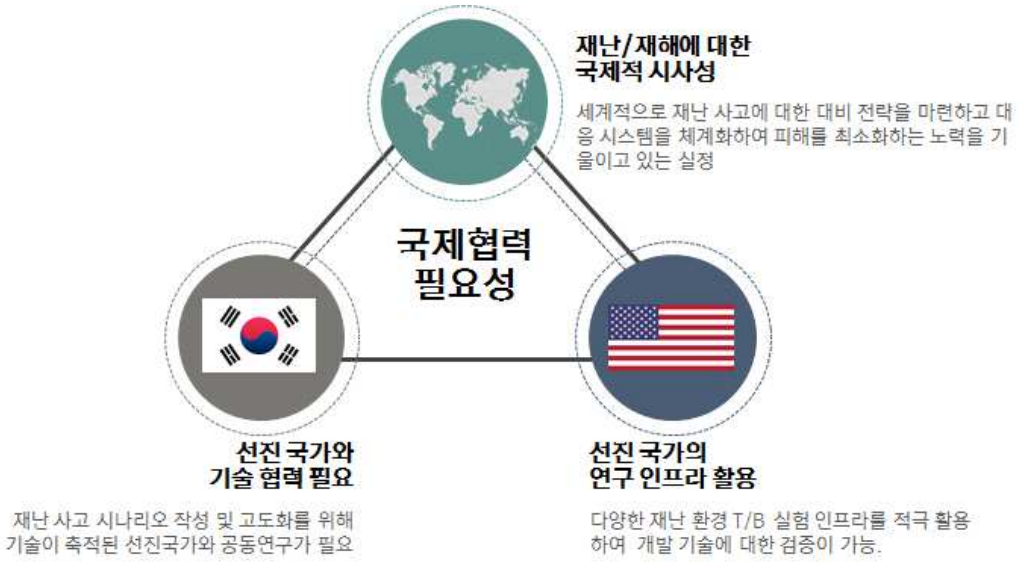


그림 1-8 국제협력의 필요성

2. 연구수행내용 및 성과

가. 연차별 연구개발 목표 및 내용

(1) 1차 연도

(가) 주관연구기관(서울대학교 산학협력단)

① 개발 목표 : 지진에 의한 고층 아파트의 거동특성 파악 및 3차원 해석모델 개발

② 개발 내용 및 범위

①	해석모델 개발을 위한 고층아파트 재원 및 지진하중에대한 주요변수 파악

- 대상 구조물 및 지반: 포항 및 경주지역의 고층아파트, 형상 및 층수
  - 대상 구조물: 연면적 약 22000 m^2, 20층 내외의 철골조 및 철근 콘크리트 공동주택
- 지진규모: 국내 MMI (Modified Mercalli intensity) 진도 4 ~ 8
- 구조물의 재료적 특성 (철골, RC) 및 내진설계 유무로 고려

②	Response-Spectrum Analysis를 통한 Peak Response 파악

- Modal analysis를 통해 해석모델의 Natural frequency와 Mode shape을 파악
- Modal analysis로부터 얻은 1st frequency를 이용하여 Response-spectrum analysis를 통해 Peak response 파악

③	비선형 동적해석 (Nonlinear Dynamic Analysis)을 통해 구조물의 비선형 거동특성 파악 및 3차원 해석모델 개발

- SAP2000을 이용한 고층아파트의 비선형동적해석 수행
- 아파트 전체 및 주요부재에대한 손상도 측정 및 건물외관변형도와의 상관관계 파악 (매핑의 기초자료 수집)

④	해석모델을 이용한 수치해석을 통해 매핑 모델에 사용될 주요변수 파악

- 아파트의 높이 (H) 및 폭 (W), drift angle, 구조물의 회전, 구조물 상단의 전단변형 등과 내부손상도와의 상관관계 파악
- 구조물의 재료적 특성, 지반특성, 내진성능정도를 고려한 구조물 전체 및 주요부재에 대한 위험도 등급 제안.

⑤	소규모 모형실험을 위한 주요변수 파악 및 실험준비

- 1차년도 개발된 해석모델 및 결과에 기반한 축소모형제작 및 실증실험위한 주요변수 파악
- 소규모 모형실험을 통한 변위 및 손상도 측정 준비
- LiDAR를 이용한 외관변형도의 측정 및 내진실험후 실측변형도와 비교 및 보정을 위한 사전준비

⑥	소규모 모형실험 수행

- 3차년도 실물실증실험전에 해석모델을 기반으로 소규모 모형구조물의 실증실험
- 해석모델 및 결과에 기반한 소형모델의 지진하에서의 변위 및 손상도 측정
- LiDAR를 이용하여 동시에 외관변형도를 측정하여 실측결과와 비교

✓ 대상지 선정
✓ 해석모델 개발

✓ 비선형 동적해석
✓ Modal Analysis

✓ 해석모델 검증
✓ 매핑 주요변수 파악

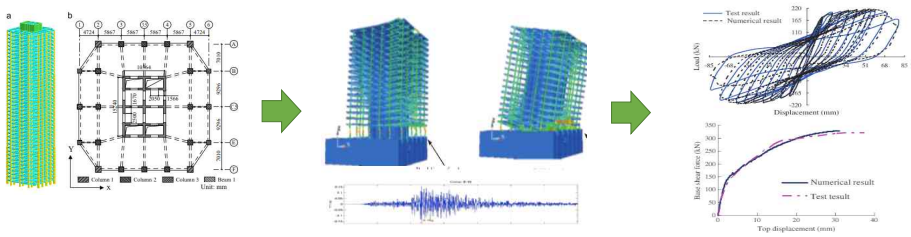


그림 2-1 1차년도 주요연구내용

■ 3차원 해석모델 구축 및 이를 통한 주요변수 파악

20층 높이의 철근 콘크리트 공동주택의 비선형 동적해석을 통하여 구조물의 비선형 거동특성을 파악하고, 해석모델을 통해 높이, 폭, 층밀림, 변형도와 내부손상도의 관계를 파악하고, 재료특성이나 내진성능 등을 고려한 위험도 등급을 제안함.

1. 개요

Earthquake has been one of the major factors in designing structures especially high-rise buildings. Nowadays, along with the advancement of modern technology, modeling buildings under earthquake loadings is a lot easier compared to the previous generations where time-consuming manual computations were needed. Now, utilizing these opportunity, the Seoul National University together with Georgia Institute of Techonology, have come up with a proposal in which you can easily pin point critical areas of the building when it’s struck by an earthquake. As an initial step to this project, this research main objective is to investigate the response of a 20-story high-rise residential building located in the City of Cassino to seismic loading using modal response spectrum analysis. The structure will be modeled in an engineering software developed by Computers and Structures, Inc. (CSI) called SAP 2000.

2. 방법론

There are numerous ways on analyzing structures under seismic loading. Starting with linear method, which can be used to calculate the effects of seismic actions in the case of both dissipative and non-dissipative structures to non-linear methodology. In addition, these two methodologies are further divided into different categories. Linear analysis method can be done through modal response spectrum analysis and equivalent lateral force analysis while non-linear methods can be done through non-linear response history analysis and non-linear static analysis or more commonly known as pushover analysis. This study will used a linear analysis method specifically the modal response spectrum analysis. This method is based on the structural dynamics theory and can be derived from the basic principles. In addition, it also considers the influence of several modes on the seismic behavior of the structure unlike the equivalent lateral force analysis.

3. 3차원 해석모델

3.1. 구조 형상 및 모델링

그림 2-2, 그림 2-3 shows the details plan of the 20-storey residential building with floor area of 1,050 m2 and height of 63.1m. In addition, the distance of the one column to the other is 5 min both x and y direction while the floor height differs at some floors. The floor height for the 1st and 2nd floor is 3.5m while from 3rd to 19th floor is 3.1m and the 20th floor is 3.4m. Beam, column and reinforcement bar sizes per floor will be discussion the proceeding sections. On the other hand, 그림 2-4 shows the three-dimensional (3D) view of the model in SAP2000 with a fixed support boundary condition at the bottom. A diaphragm constraint was use at each floor to mimic the behavior of the concrete slab.

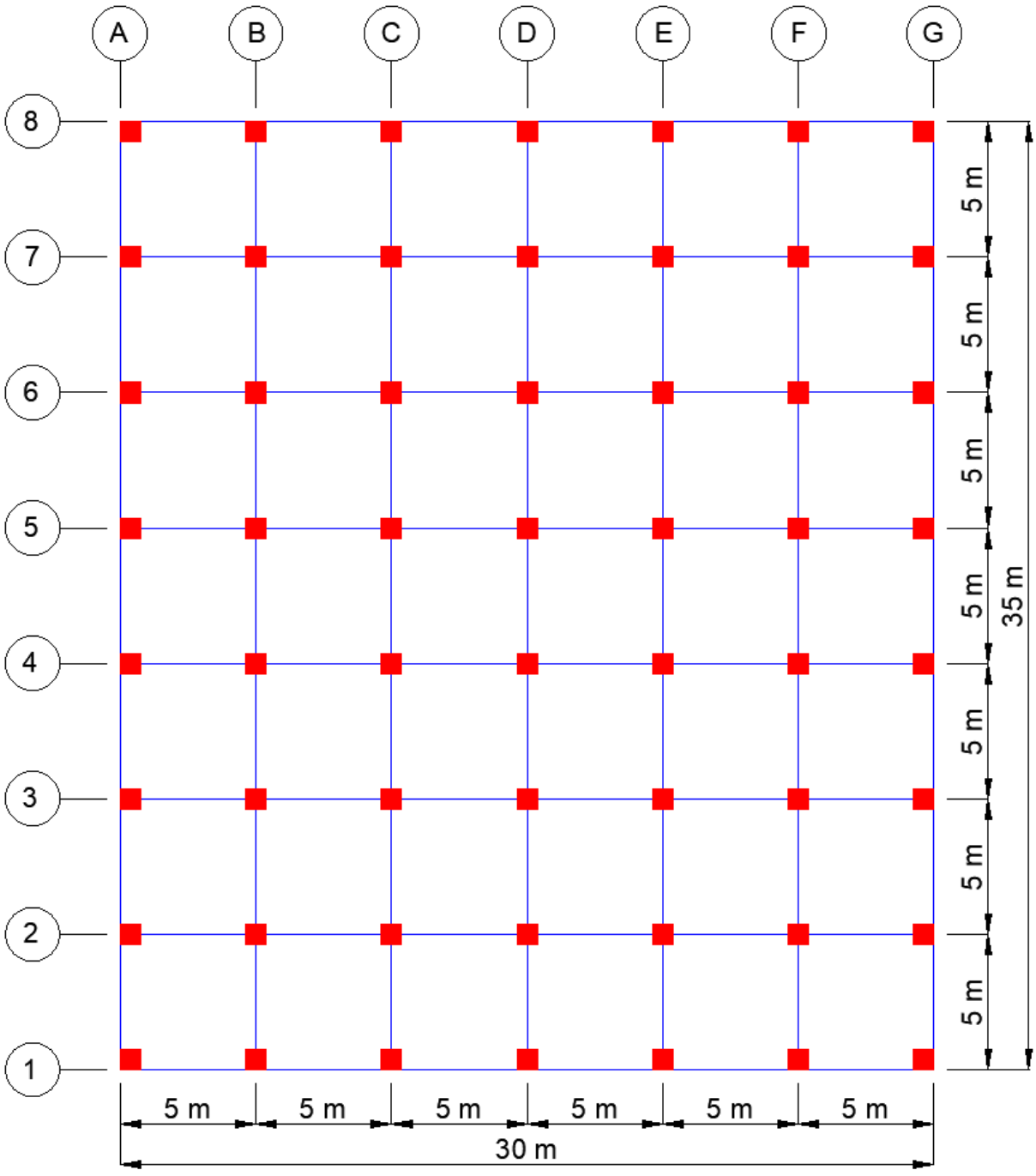
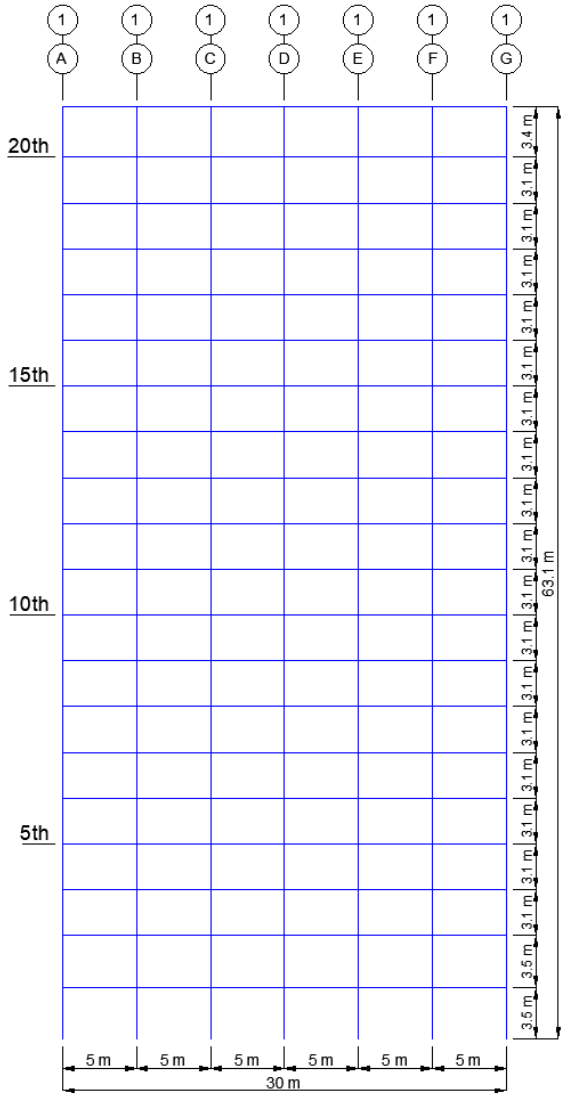
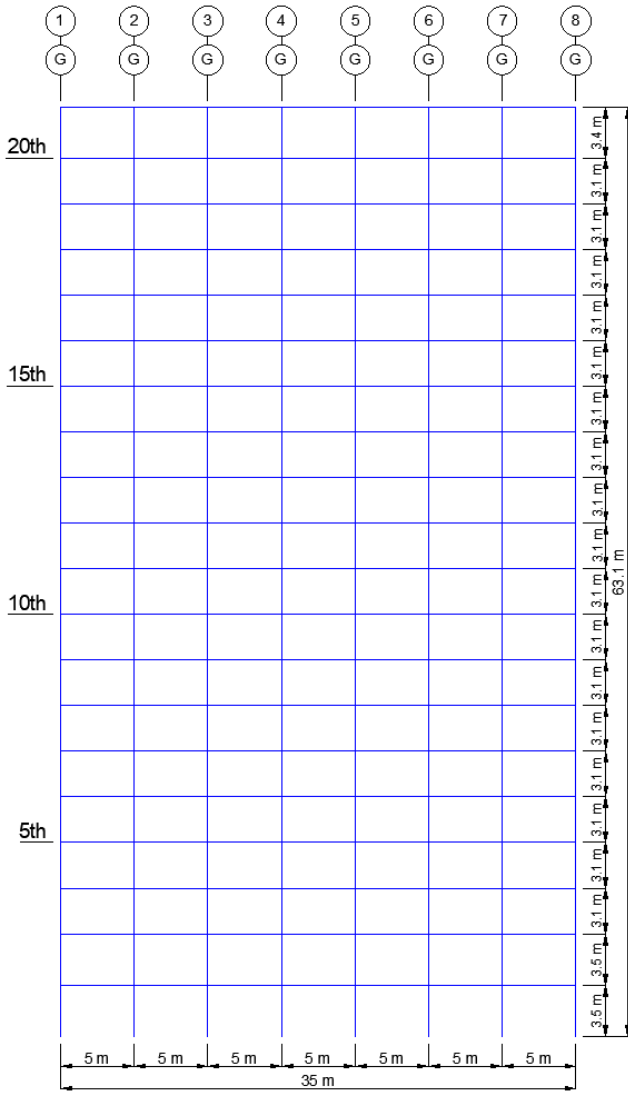


그림 2-2 Typical Floor Plan View



(a) Front View (X-Z axis)



(b) Side View (Y-Z axis)

그림 2-3 Elevation View

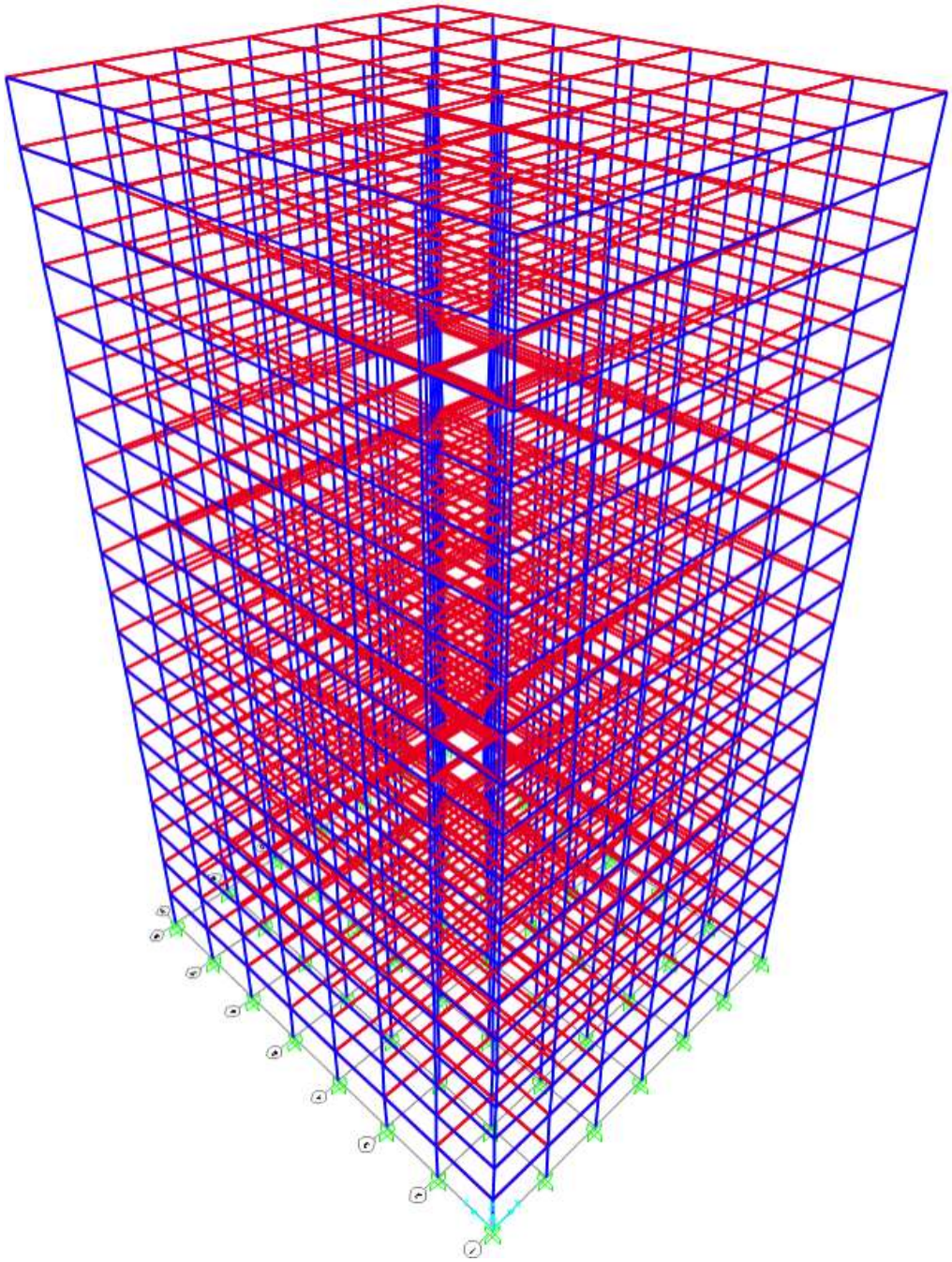


그림 2-4 Three-dimensional view of SAP 2000 model

3.2. 하중

표 3-1 shows the loads that the structure will carry at each floor. It includes it self-weight that will be automatically calculate by SAP 2000, and other loads like slab load, live load, snow and super imposed load in the form of partition walls.

표 2-1 Structural Loads

Floor	Self-weight (kN/m^2)	Slab load (kN/m^2)	Super imposed load (kN/m^2)	Live load (kN/m^2)
$2^{nd}$to 20^{th}	Automatic computation	6.1	6 (partition walls)	2
Roof	Automatic computation	5.4	-	1.3 (snow)

Note: Assume two-way slab

3.3. 재료의 물성치

표 2-2 shows the materials used in modeling the structure and its properties. The concrete and steel follows European design standards (Eurocode) with grade of C25/30 for concrete with 25 MPa compressive strength, and S355 for steel with 355 MPa as its yield strength as listed in 표 2-2. Other properties like modulus of elasticity, Poisson's ratio and shear modulus are also shown in 표 2-2. Beam and column sizes for each floor are summarized in 표 3-3. It also includes the reinforcement bar number and its corresponding diameter size in inches (Note: rebar number is different from number of rebar). In addition, there eight (8) reinforcement bars around each beam and column with concrete cover of 40 mm on each side.

표 3-2 Material Properties

Concrete		Steel	
Design Standard	EN 1992-1-1	Design Standard	EN 1993-1-1
Grade	C25/30	Grade	S355
Compressive strength, $f'c$	25 MPa	Yield strength, F_y	355 MPa
Density, ρ	2400 kg/m^3	Ultimate strength, F_u	510 MPa
Elastic modulus, E	31 MPa	Elastic modulus, E	210 MPa
Poisson's ratio, υ	0.2	Poisson's ratio, υ	0.3
Shear modulus, G	12.92 MPa	Shear modulus, G	80.769 MPa

표 3-3 Beam, Column, and Reinforcement Bar Sizes

Floor	Beam Size	Rebar Number	Column Size	Rebar Number
1st to 7th	400x600 mm	#7 (7/8")	750x750 mm	#11 (11/8")
8th to 14th	400x600 mm	#7 (7/8")	600x600 mm	#9 (9/8")
15th to 20th	400x600 mm	#7 (7/8")	450x450 mm	#7 (7/8")

3.4. 지진 정보

The 20-storey residential building is located at the city of Cassino (+41°48'40" N and +14°36'10" E) with a C type of soil and T1 topography. Other details are listed in 표 3-4. 그림 2-5 shows the response spectra curve or the function of the earthquake applied to the structure having the following characteristics listed in 표 3-4 as per Italian code NTC2008.

표 2-4 Building and Location Details

Place	City of Cassino
Soil Type	C
Topography	T1
Latitude	+41° 48' 40"
Longitude	+14° 36' 10"
Building Type	Residential
Class	III
Limit State Analysis	SLD
Damping Ratio	0.05
Spectrum Type	Elastic Horizontal

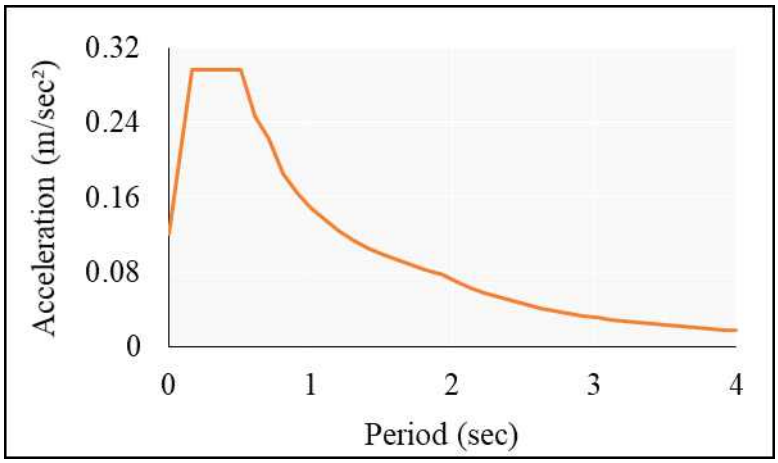


그림 2-5 Response Spectra Curve as per NTC2008 in SAP 2000

The ESL (estimated service life) or simply reference life is defined as the service life that a building or parts of a building would be expected to have in a set of specific in-use conditions, calculated by adjusting the reference in-use conditions in terms of materials, design, environment, use and maintenance. Reference life, VR,can be computed using the following equation:

$$V_R = V_N x O_F \quad (1)$$

Where Nis the nominal life of a structure following the classification listed in 표 3-5, and OF is the corresponding occupancy factor for different building classes categorize in 표 3-6.

표 2-5 Classification for Building's Nominal Life

Structure	Nominal Life (V_N)
Temporary, provisional, etc.	10
Normal buildings, bridges, infrastructures, dams, etc.	50
Special structures, strategic bridges, infrastructures, dams, etc.	100

표 2-6 Building Class Occupancy Factor

Class	Occupancy Factor
I: Agricultural facilities, etc.	0.7
II: Normal buildings	1.0
III: Buildings with large crowds, etc.	1.5
IV: Public facilities (e.g. hospitals), strategic buildings, etc.	2.0

표 2-7 shows the different return period of earthquake for various limit design states for different reference life.

표 3-7 Return Period for Different Limit States and Reference Life

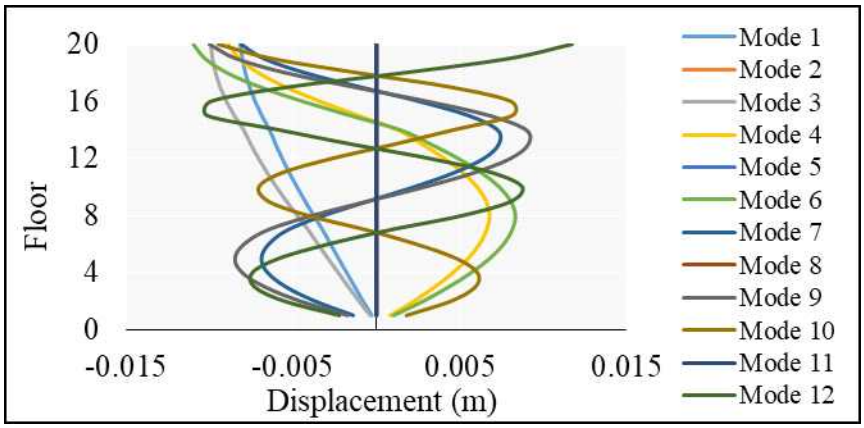
Limit States		Exceedance Probability in the Reference Life	Reference Life (V_R) Return Period			
Serviceability	SLO	81%	21	30	45	60
	SLD	63%	35	50	75	100
Ultimate	SLV	10%	332	475	712	949
	SLC	5%	682	975	1462	1950

Note: SLO = Operationality; SLD = Damage; SLV = Life safety; SLC = Collapse

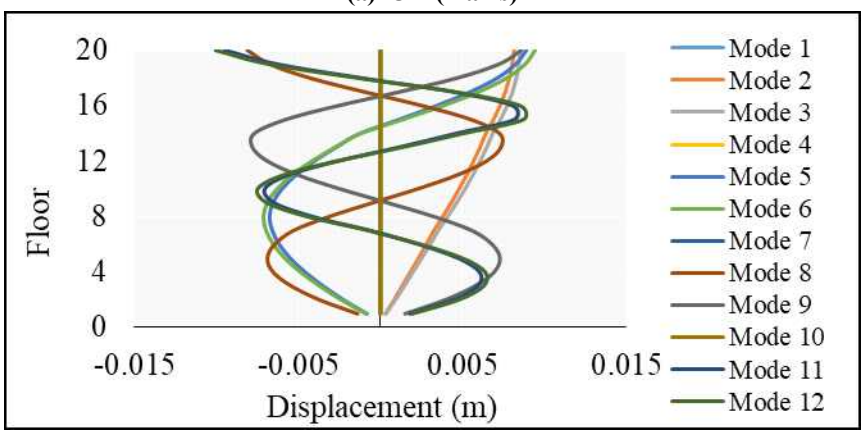
4. 해석 결과

4.1. 변위

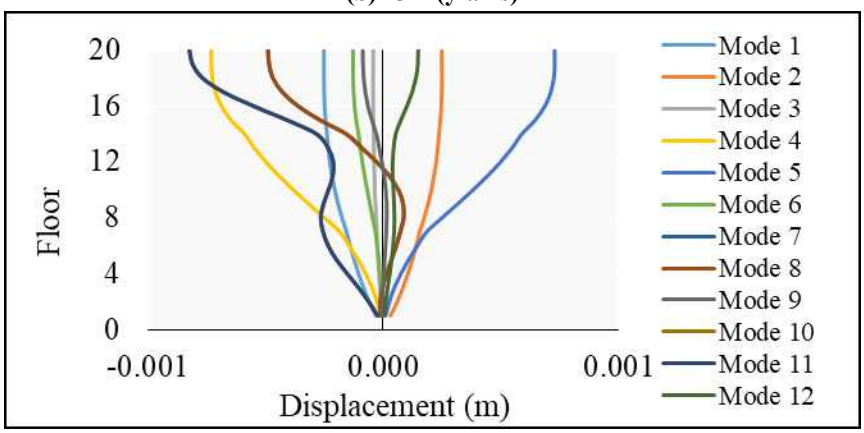
그림 2-6 shows the displacement of the structure at various direction as it experience dynamic loading using modal analysis procedure. Based from the results, the maximum displacement of the structure is 11.73, 10.06, and 0.82 mm at x, y, and z-direction, respectively. In addition, the maximum displacement of the structure at x and y-direction can be found in Mode 12 while for the z-direction is at Mode 11. Furthermore, 표 2-8 shows the different deformed shaped of the structure at different modes for various directions.



(a) U1 (x-axis)



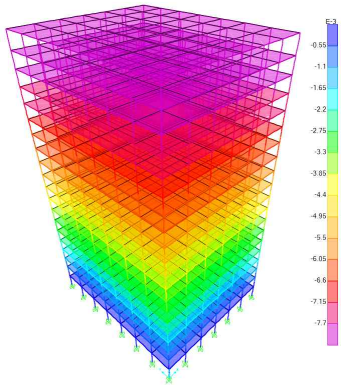
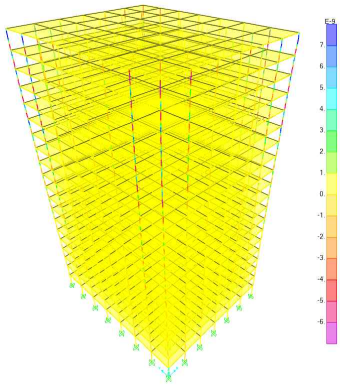
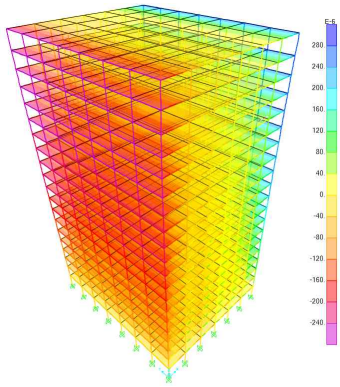
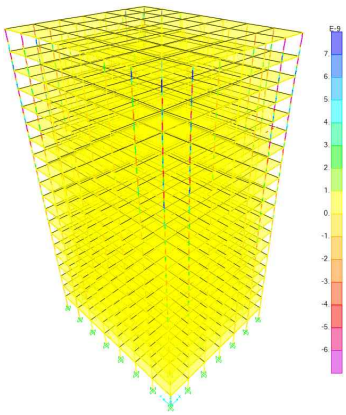
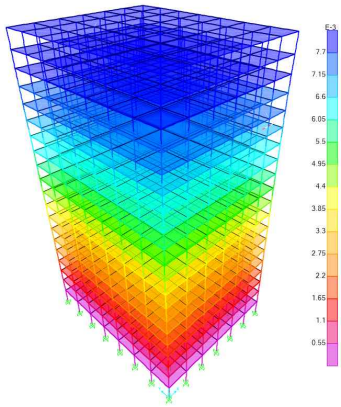
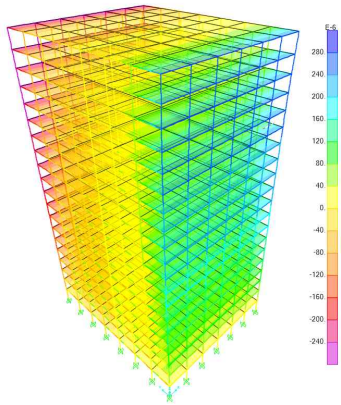
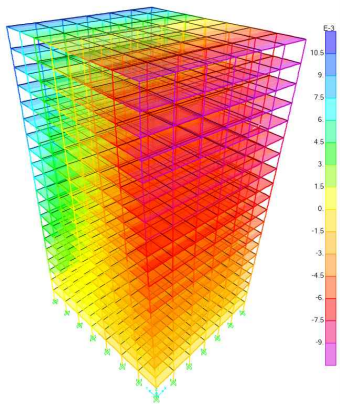
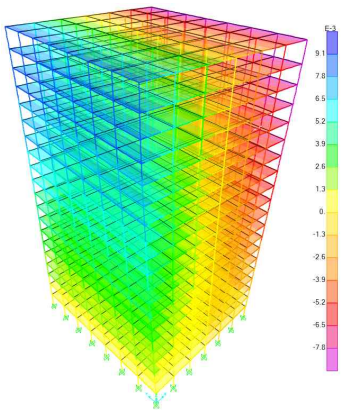
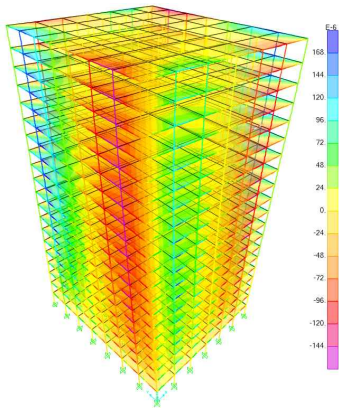
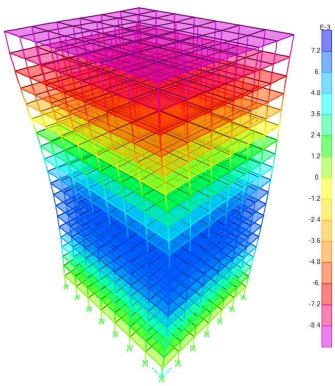
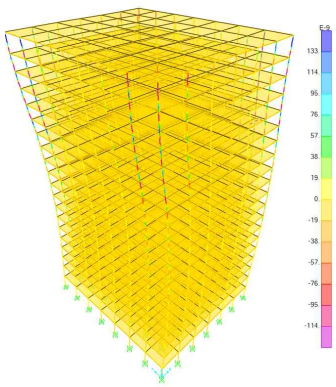
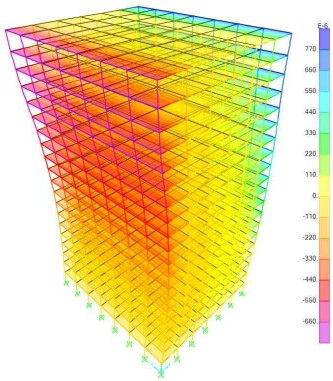
(b) U2 (y-axis)

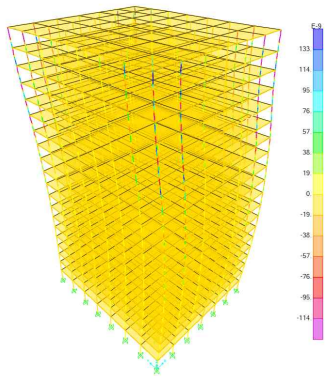
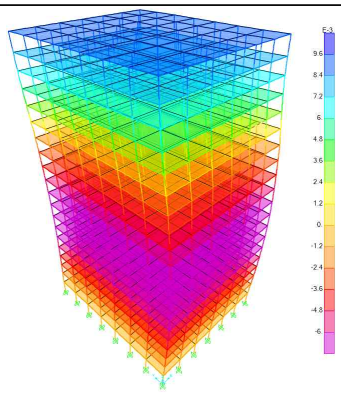
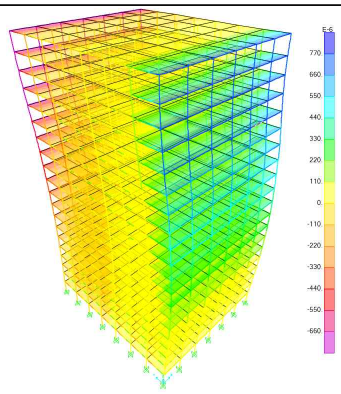
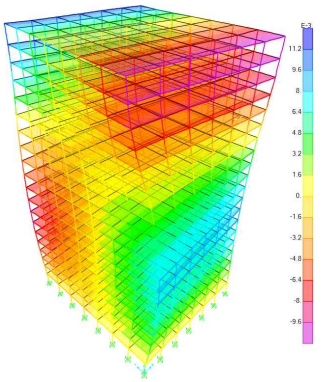
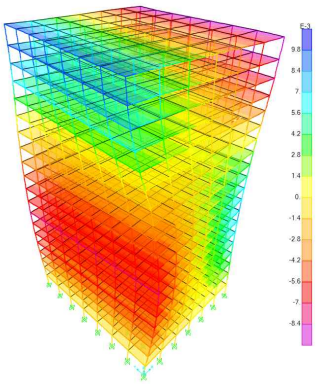
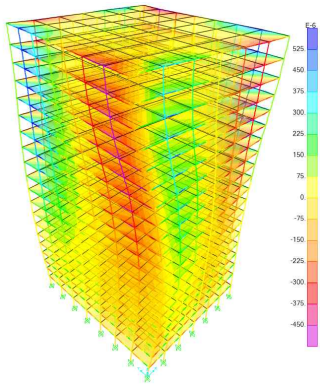
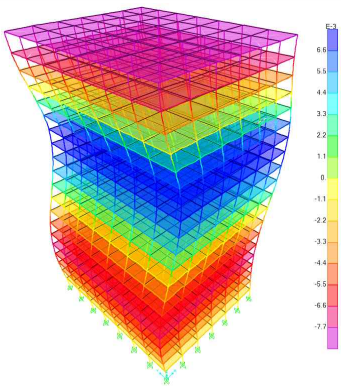
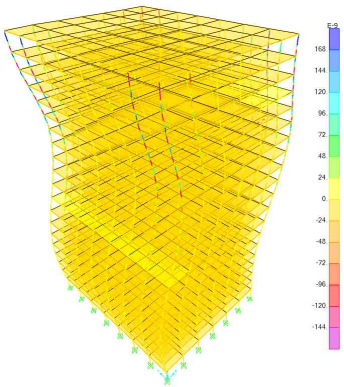
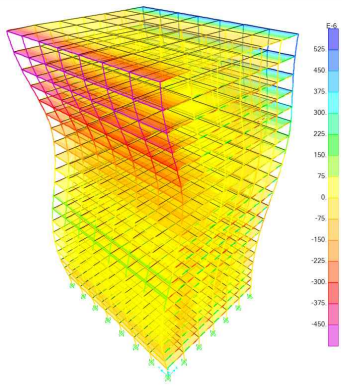
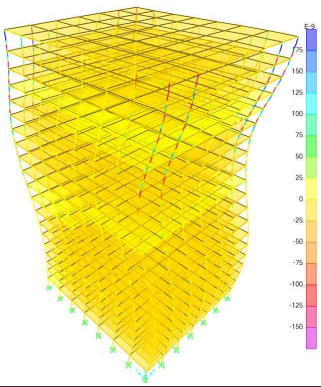
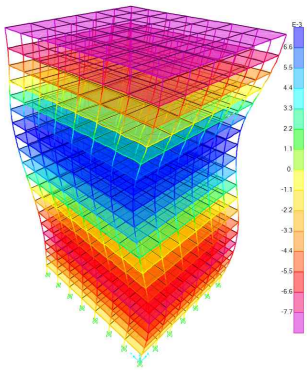
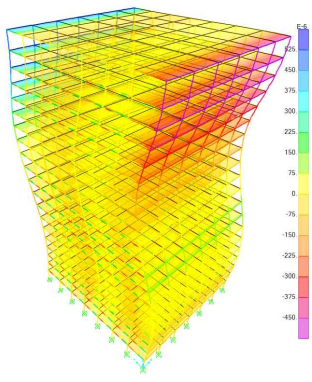
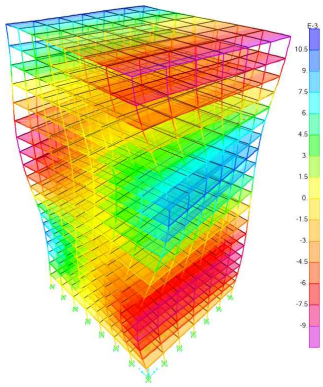
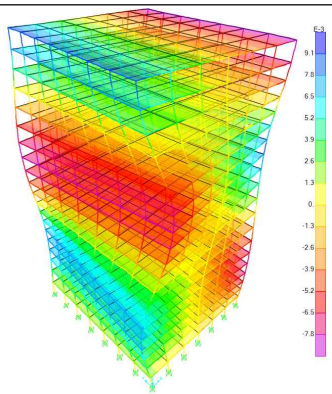
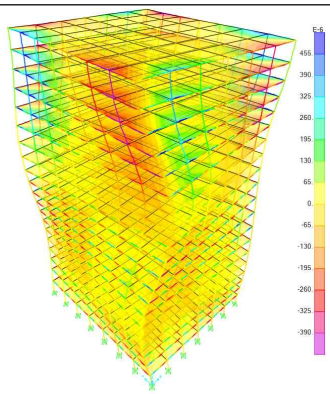


(c) U3 (z-axis)

그림 2-6 Story Displacement at Different Direction (Modal Analysis)

표 2-8 Structure's Deformed Shape (Modal Analysis)

Mode No.	Ux	Uy	Uz
1			
2			
3			
4			

5			
6			
7			
8			
9			

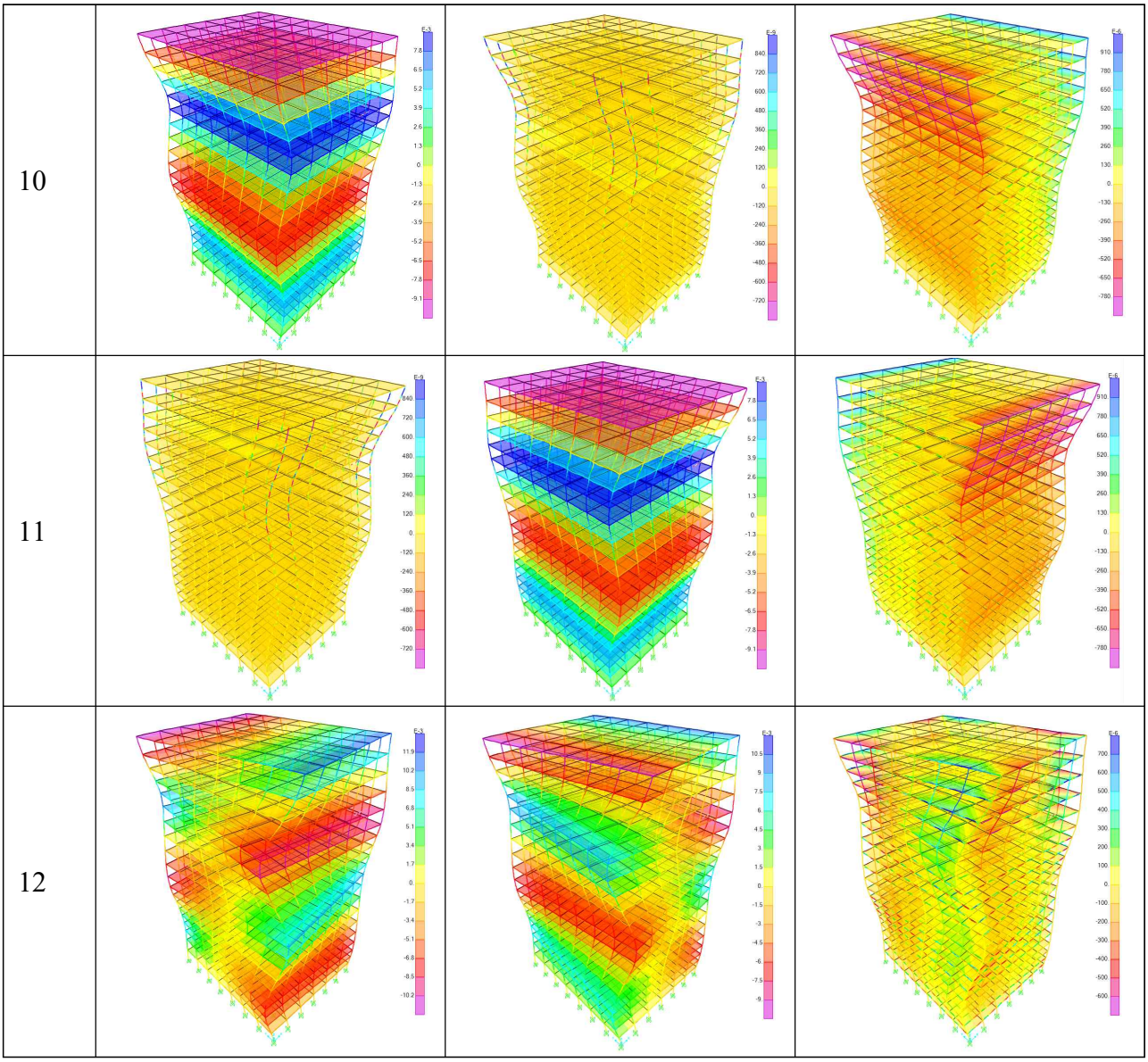
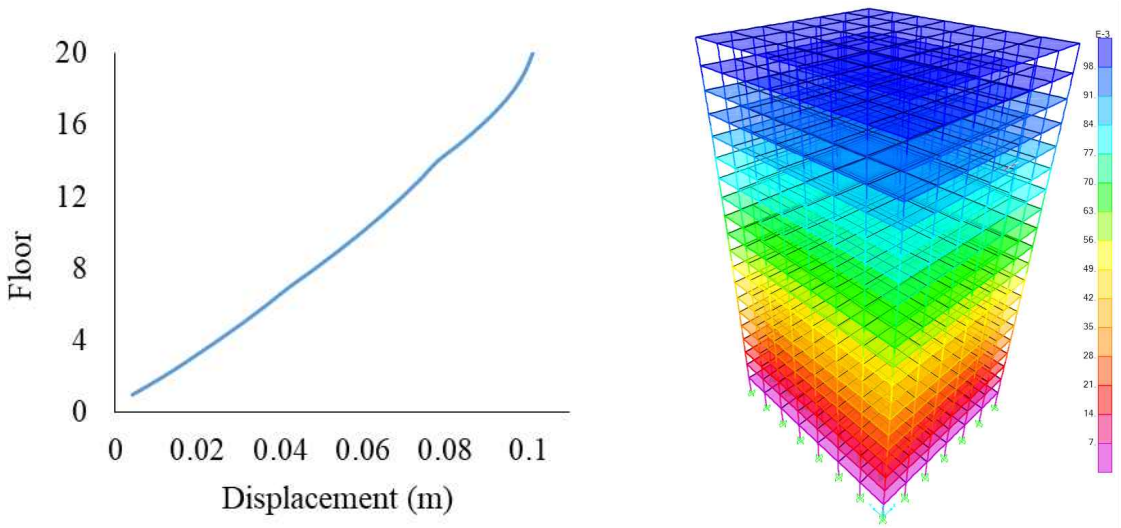


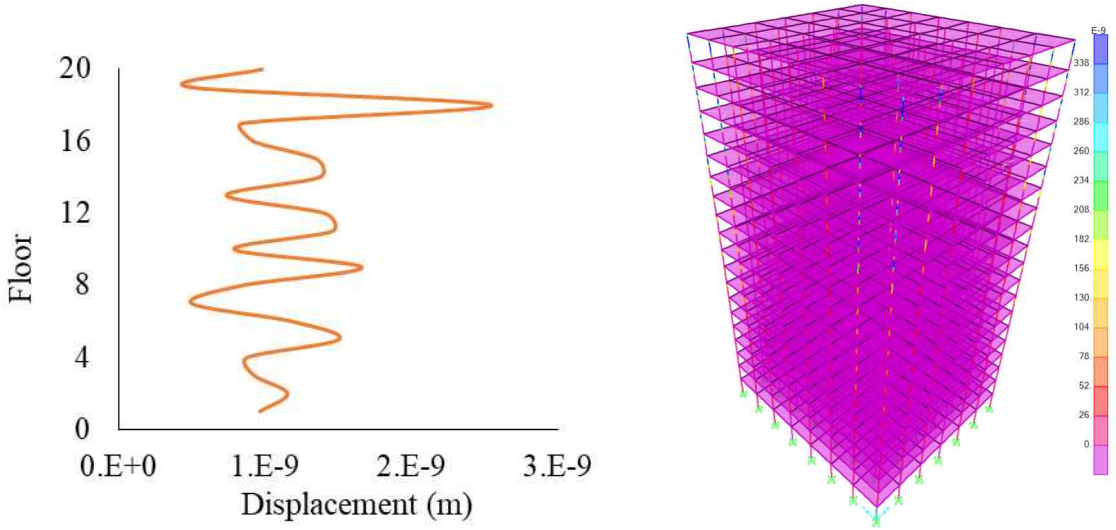
그림 2-7 shows the displacement and actual deformation of the structure at various direction as it experience dynamic loading using response spectrum analysis. Based from the results, the maximum displacement of the structure is 0.101, 9E-10, and 0.003 m at x, y, and z-direction, respectively. In addition, it can be observed that when considering U1 upper floors are more critical then lower floors while upon considering U2 and U3 the most critical part where the column near the perimeter of the upper floors.

4.2. 응력

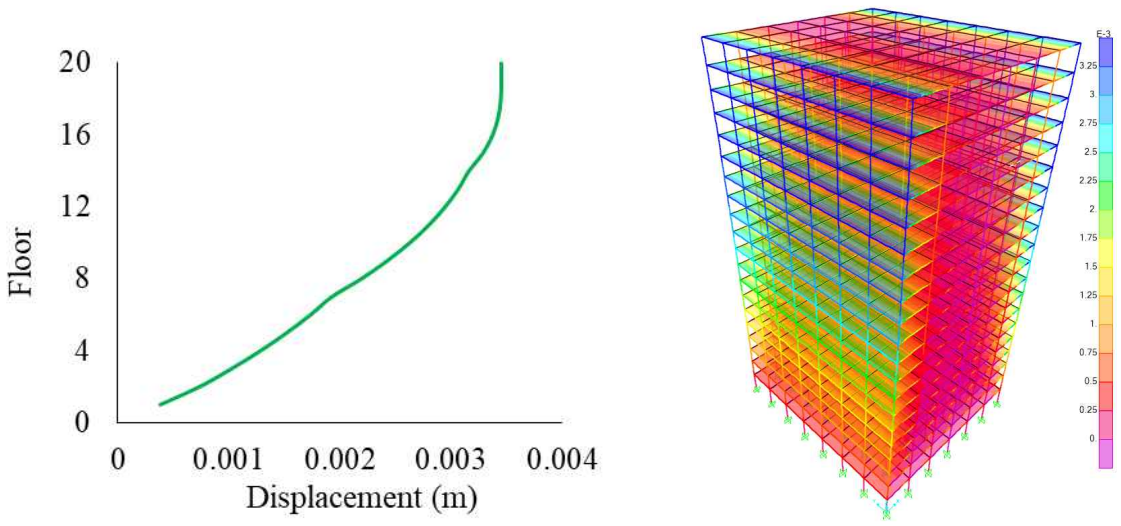
표 2-10 to 3-12 shows the axial force, moment and stress experienced by the structure as it is subjected to dynamic loading using modal analysis for all the 12 modes. Based from the results, the critical sections of the building varies for different modes of different components. Blue shaded shapes mean positive values while red shaded shapes mean negative values. The 표 2-10 to 3-12 also shows force at the x-z direction as well as the moment and stress at the x-z and y-z direction.



a. U1 (x-axis)



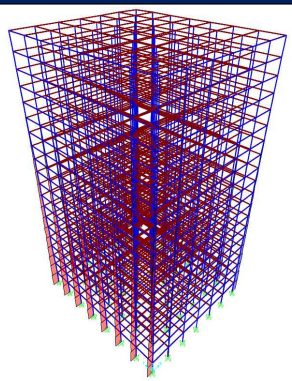
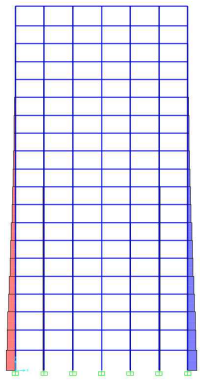
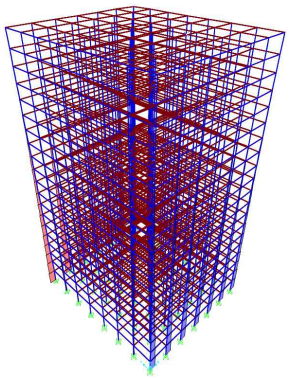
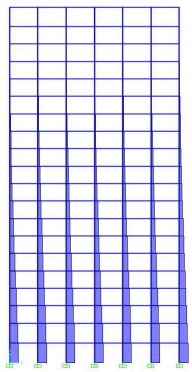
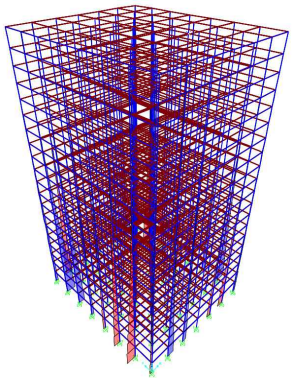
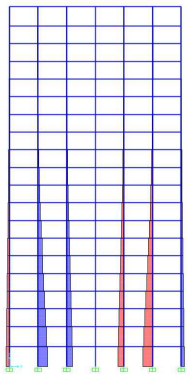
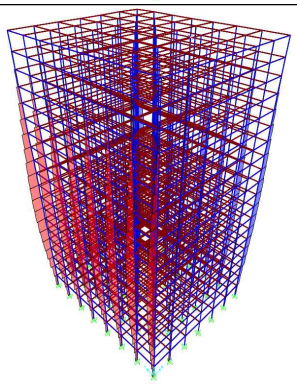
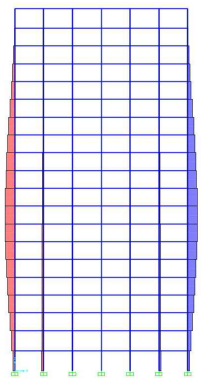
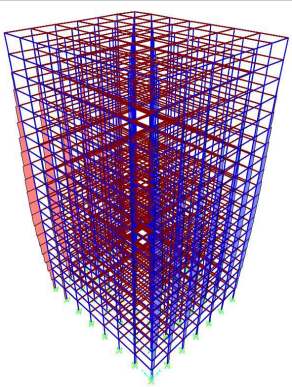
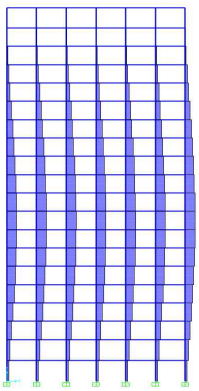
b. U2 (y-axis)

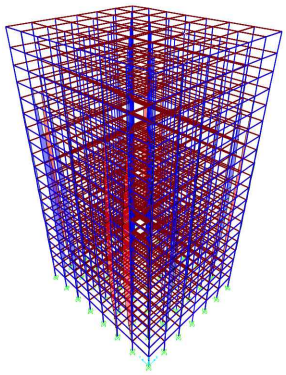
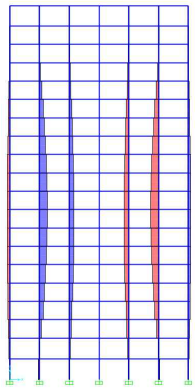
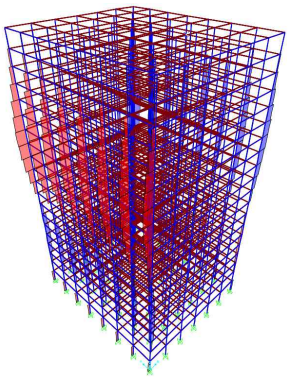
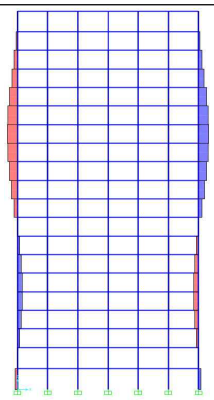
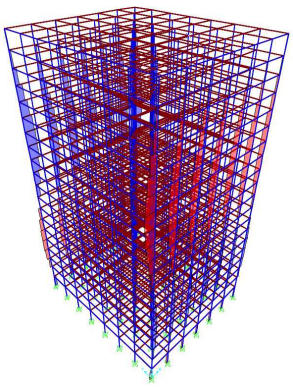
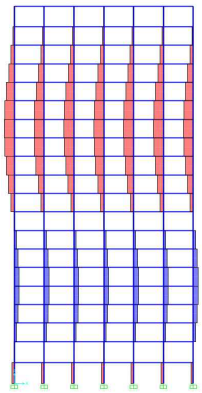
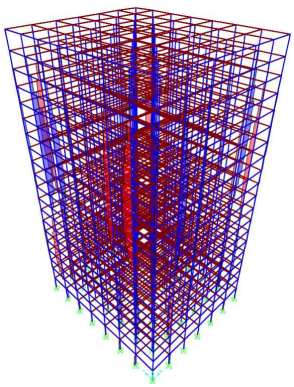
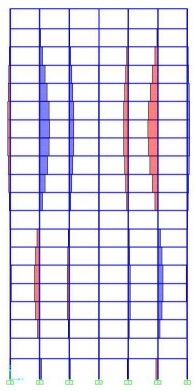
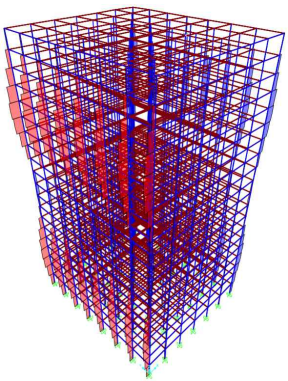
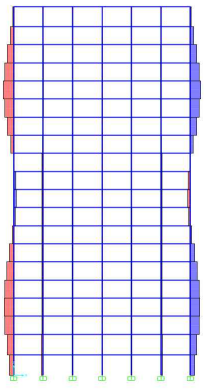


c. U3 (z-axis)

그림 2-7 Structure's Deformed Shape (Response Spectrum Analysis)

표 **2-10** Structure's Axial Force (Modal Analysis)

Mode No.	3D	X-Z Direction
1		
2		
3		
4		
5		

6		
7		
8		
9		
10		

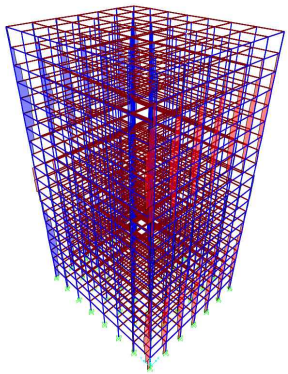
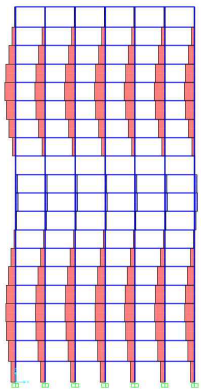
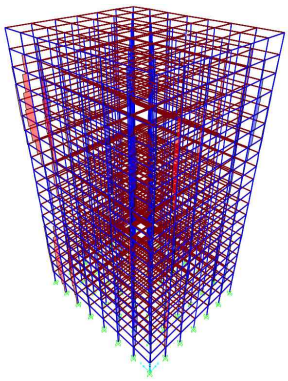
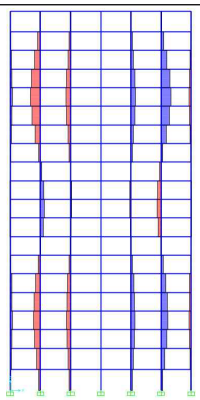
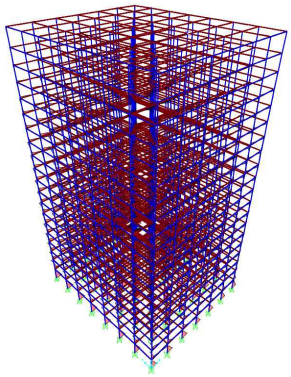
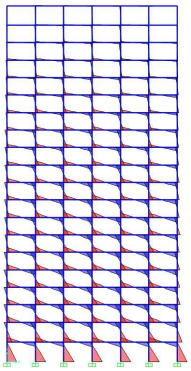
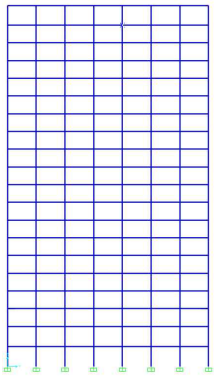
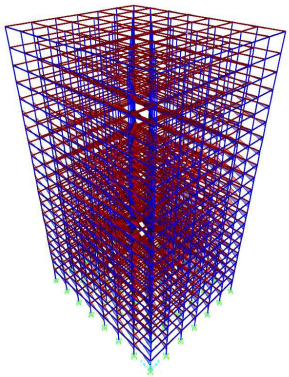
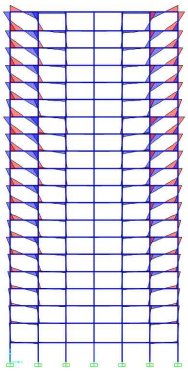
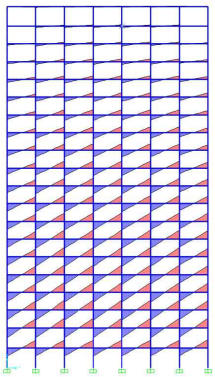
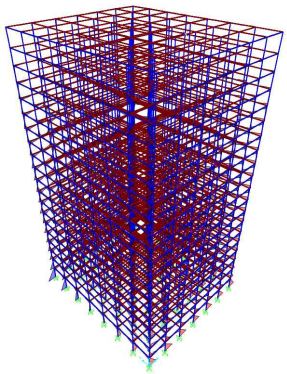
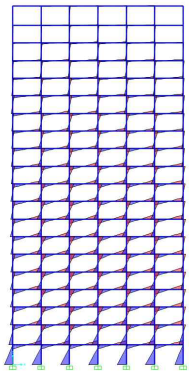
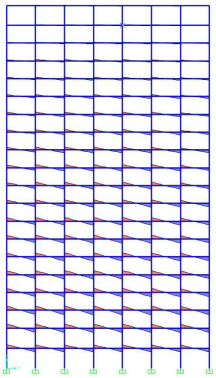
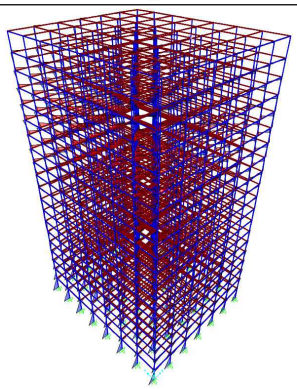
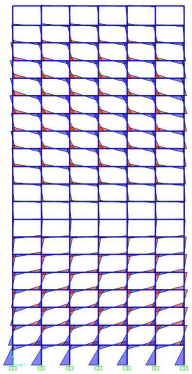
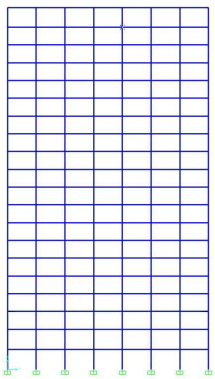
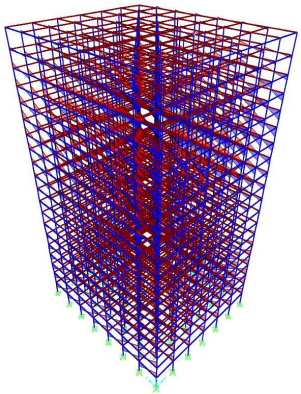
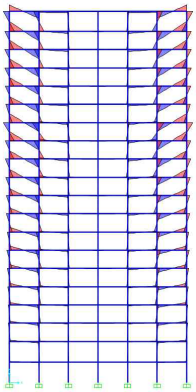
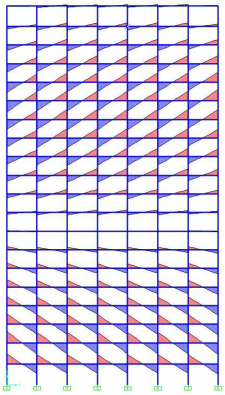
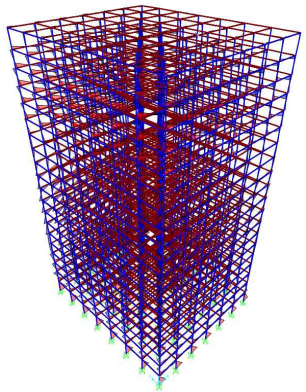
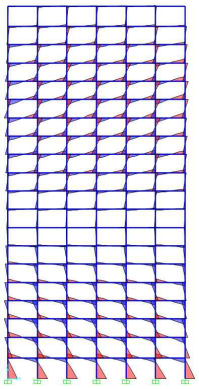
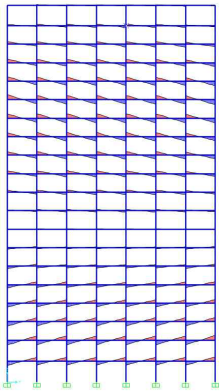
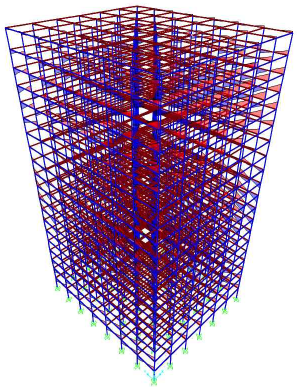
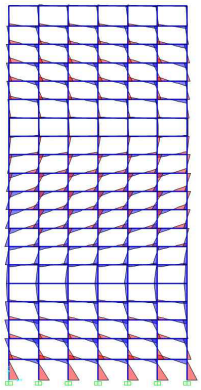
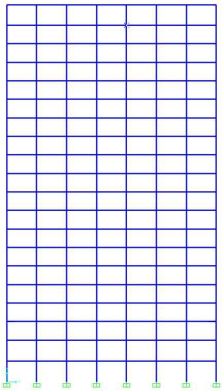
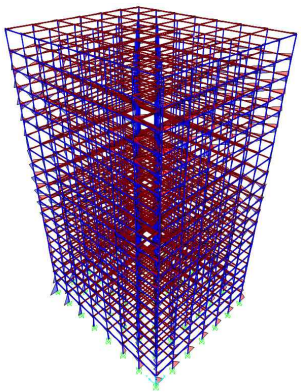
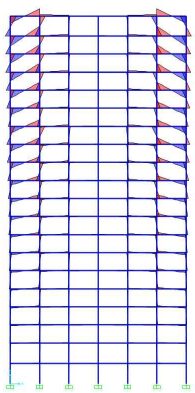
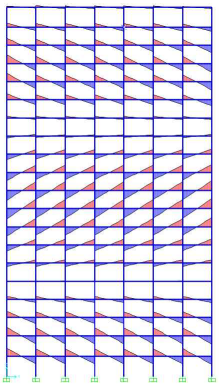
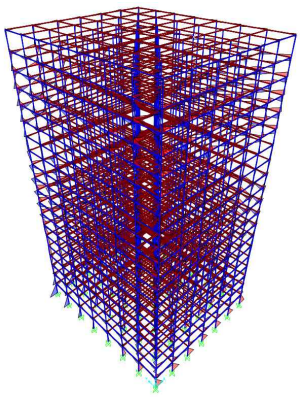
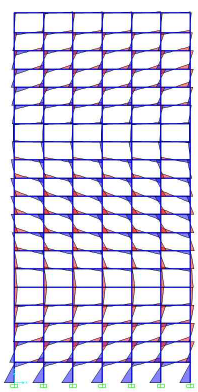
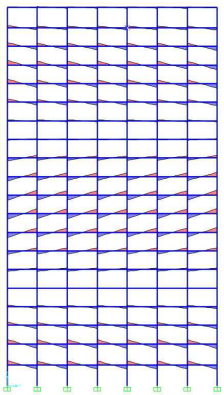
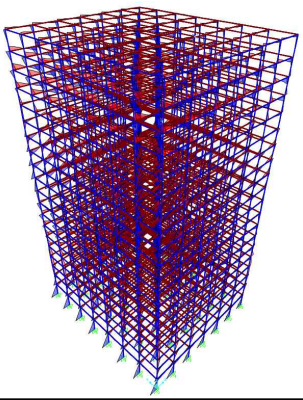
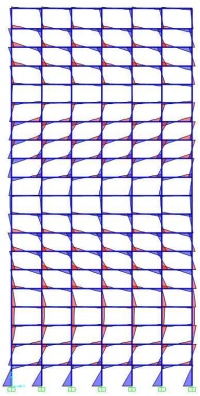
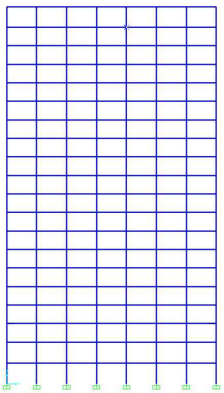
11		
12		

표 **2-11** Structure's Moment 3-3 (Modal Analysis)

Mode No.	3D	X-Z Direction	Y-Z Direction
1			
2			
3			
4			
5			

6			
7			
8			
9			
10			

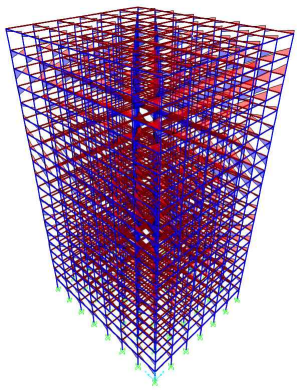
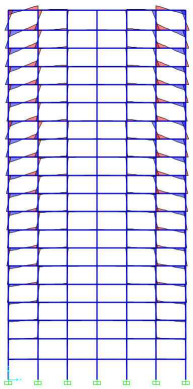
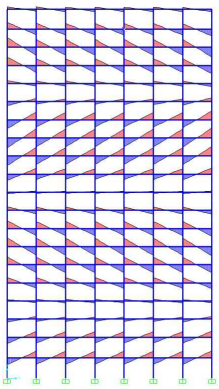
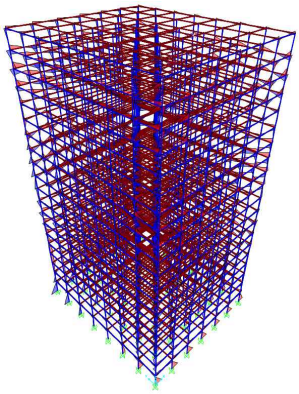
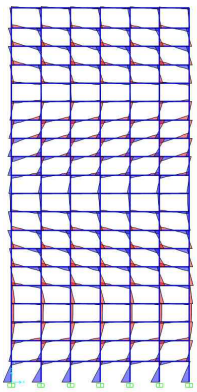
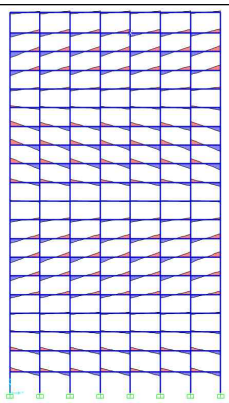
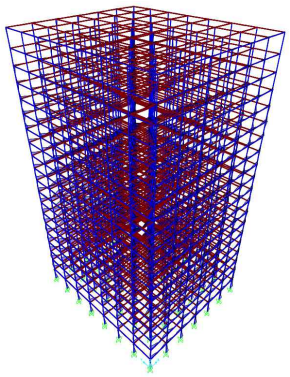
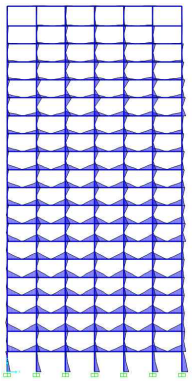
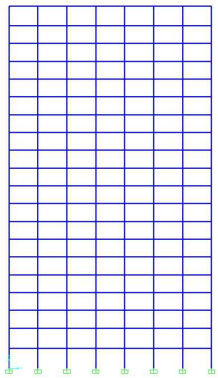
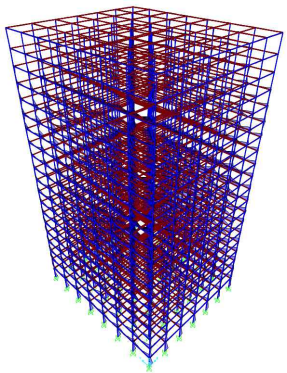
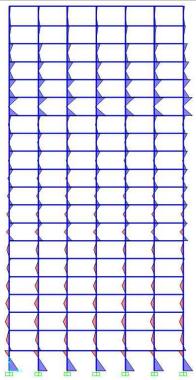
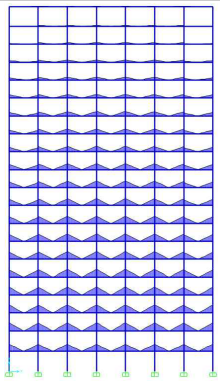
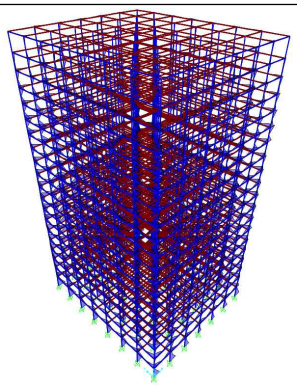
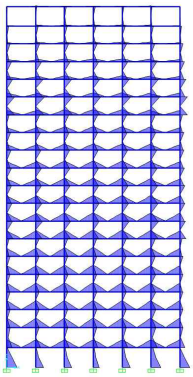
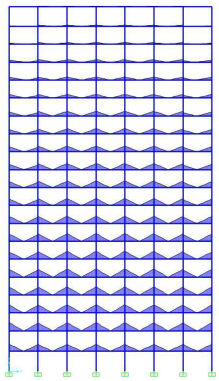
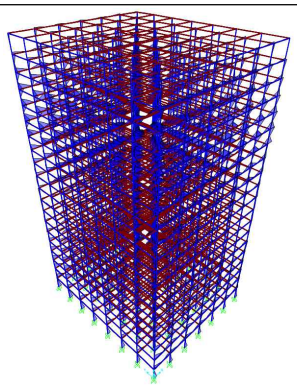
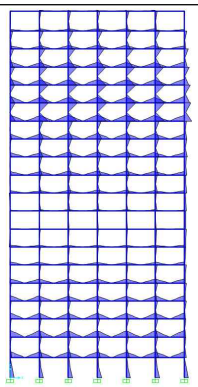
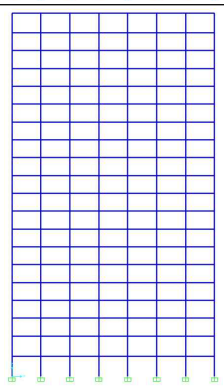
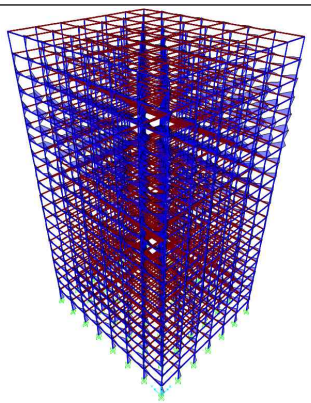
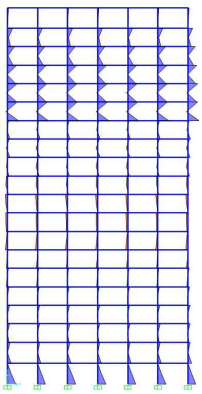
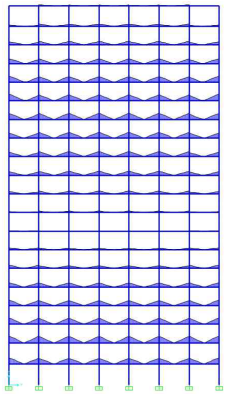
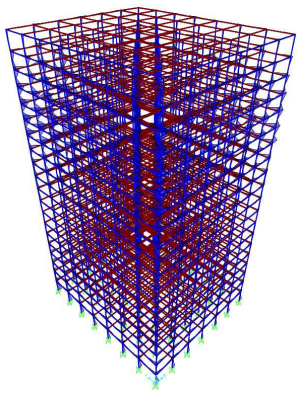
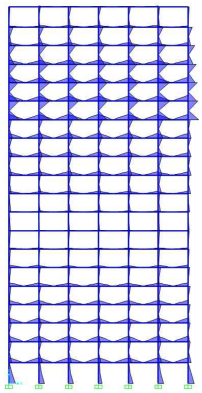
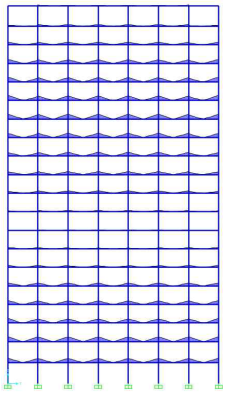
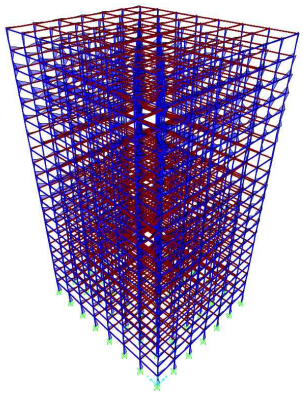
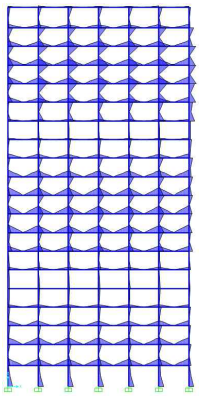
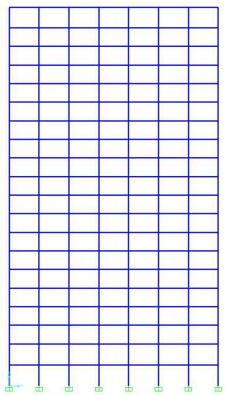
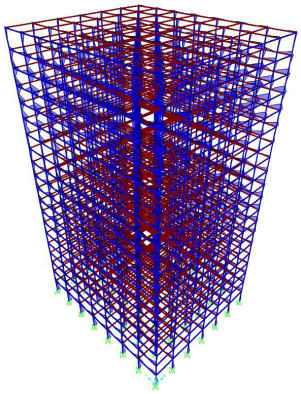
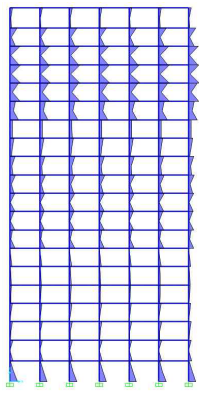
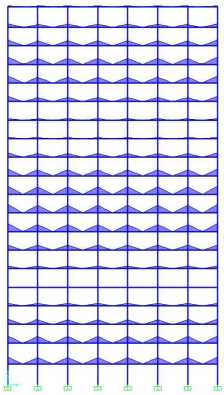
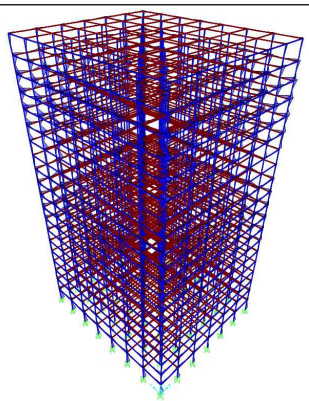
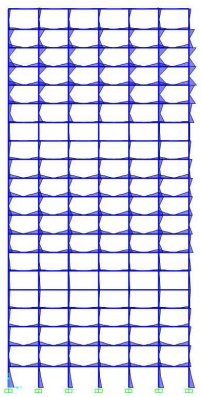
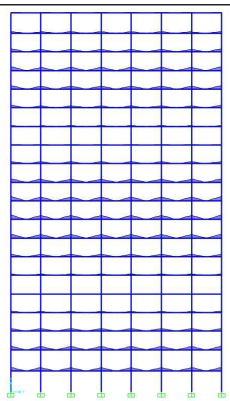
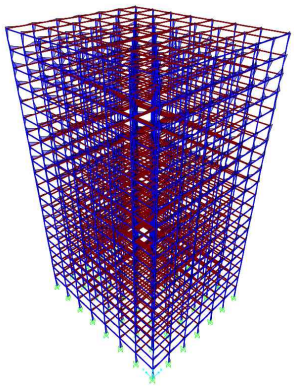
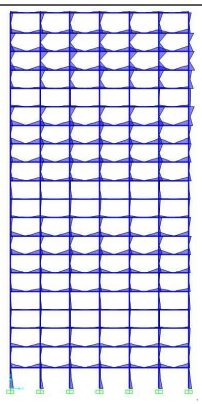
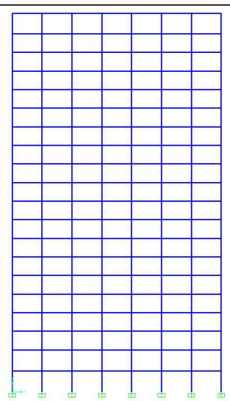
11			
12			

표 **2-12** Structure's S11 Stress (Modal Analysis)

Mode No.	3D	X-Z Direction	Y-Z Direction
1			
2			
3			
4			
5			

6			
7			
8			
9			
10			

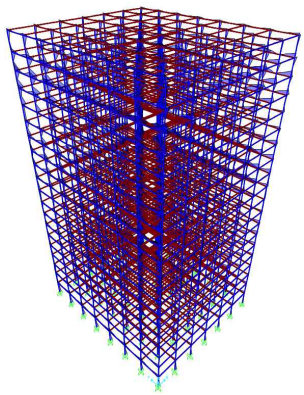
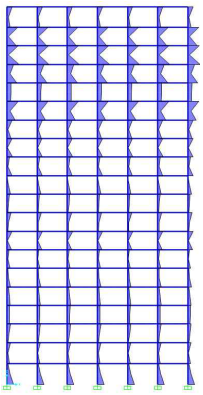
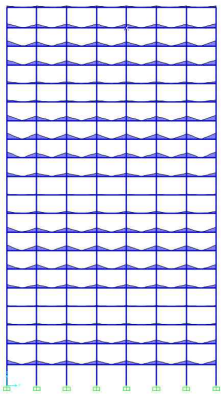
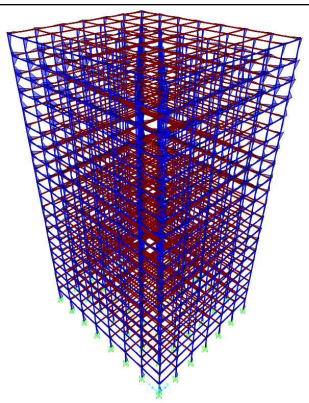
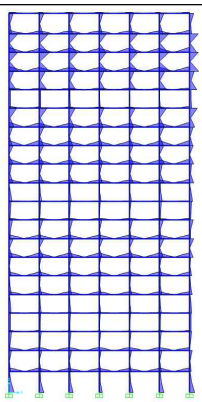
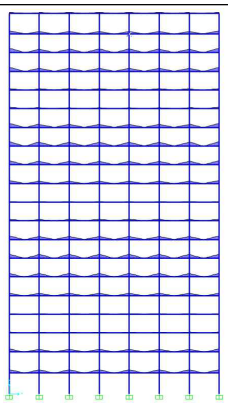
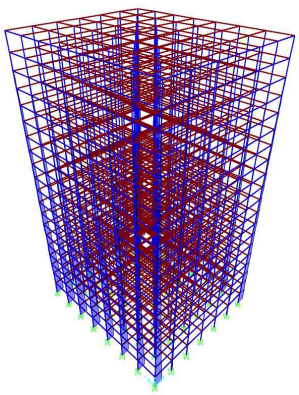
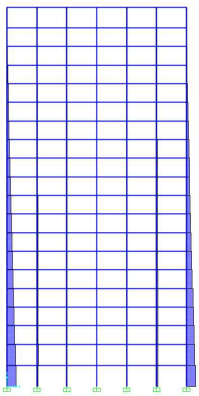
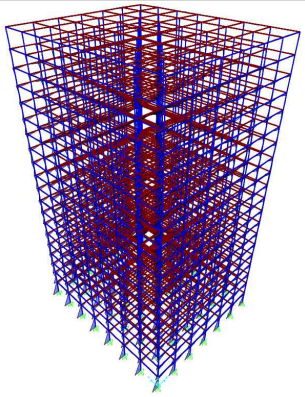
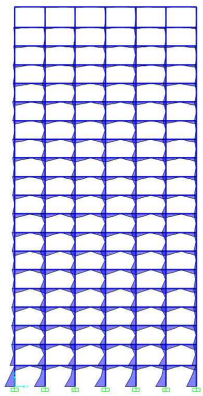
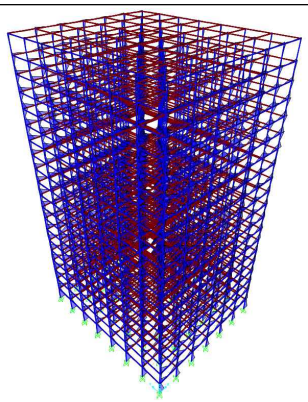
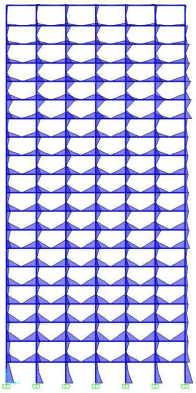
11			
12			

표 2-13 shows the axial force, moment and stress experienced by the structure as it is subjected to dynamic loading using response spectrum analysis. Based from the results, the all the critical sections can be found at the lower floors, especially at the ground floor or first floor. The maximum axial force is 1899.39 kN located at the side of the building as shown in 표 2-13. In addition, the maximum moment is 877.55 kN-m located at the inner columns near the perimeter of the building while the maximum stress (S11) is 19876.3 kN/m2 located at the beam in the third floor as illustrated in 표 2-13.

표 2-13 Structure's Forces/Stress (Response Spectrum Analysis)

	3D	X-Z Direction
Axial Force		

Moment 3-3		
Stress S11		

5. 결론

The main objective of this research was to investigate the seismic performance of a 20-story high-rise residential building located in the City of Cassino using a modal response spectrum analysis. The structure was analyzed and modeled through the used of a finite element program, SAP 2000. Based on the results, the following conclusions have been made:

- For seismic analysis using modal analysis of the 20-storey high-rise residential building, it would be difficult to precisely pin point the exact critical areas for displacement, axial force, moment, and stress as it is different for various mode cases. Thus, other factors and methodologies are advice to conduct.
- For seismic analysis using response spectrum analysis of the 20-storey high-rise residential building, the critical sections considering the maximum displacement can be observed at the upper floors while the critical sections upon considering the maximum axial force, moment and stress can be observed at the lower floors.

6. 실증실험 및 추가적인 변수 파악을 위하여 추가로 고려해야 할 점들

The following are the recommendations for future studies with respect to seismic analysis of high-rise buildings:

- Conduct a similar case study using other linear analysis such as equivalent lateral force analysis and time history analysis.
- Create a similar study using non-linear analysis such as pushover analysis and time history analysis.
- Perform or model the same structure in other structural software such as ETABS and ABAQUS and also used existing design codes to verify the results of the study.
- Make a similar structure using steel frames and composites structures.

(나) 협동연구기관(Georgia Institute of Technology)

① 개발 목표 :

무인항공기를 활용한 재난지역 3차원 모델링 및 오브젝트 검출기법 개발

② 개발 내용 및 범위(그림을 이용하여 시스템 구성도, 구조 등을 구체적으로 표현)

①	무인항공기 기반 재난지역 이미지 데이터 취득

- 모의 재난지역 스캐닝 시험 장소 확보
- 재난지역 스캐닝을 위한 임무 수행계획도 작성
- 객체 단위 혹은 타운 단위 스캐닝 데이터 수집

②	무인항공기 이미지를 활용한 재난지역 3차원 모델링

- Structure from Motion (SfM) 알고리즘 기반 Photogrammetric Analysis
- 고밀도 3D-RGB 포인트 클라우드 모델 생성

③	머신러닝 기반 오브젝트 자동검출 및 분류기법 개발

- 포인트 클라우드 다운샘플링 및 노이즈 제거 기법 구현
- 평면 요소 분할 및 개별 오브젝트 분리 기법 개발
- 손상 및 비손상 오브젝트 분류를 위한 트레이닝 모델 정형화
- 머신러닝 기술을 활용한 지면 상태 및 잔해 검출

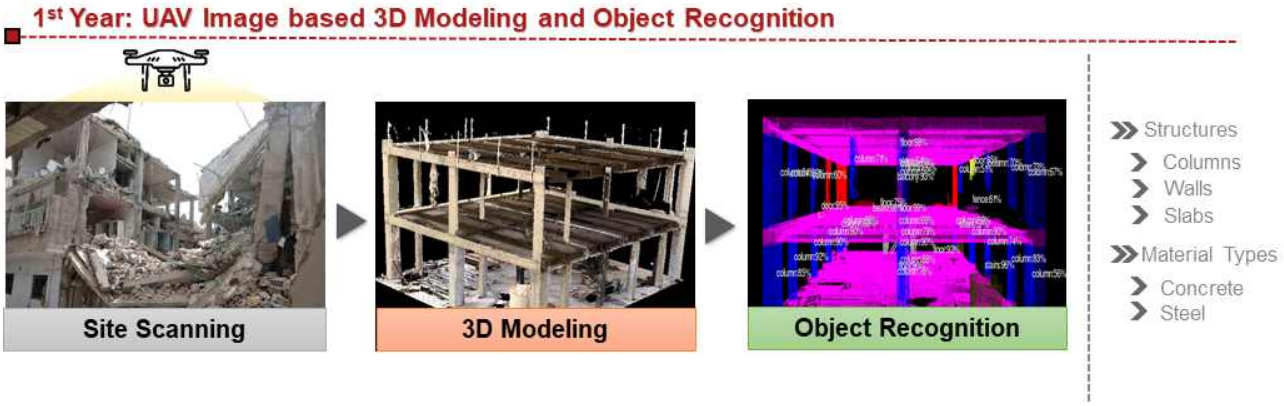


그림 2-8 1차년도 주요연구내용

③ 연구성과물

○ 모의 재난지역 데이터 취득 및 3차원 모델링

■ 드론 및 지상레이저를 활용한 모의 재난지역 데이터 취득

▪ National Center for Medical Readiness (NCMR) in Ohio

- 데이터 취득: 지상 레이저 스캐너
- 비고
  - · 재난 대비 및 대응 훈련을 위한 모의 재난 현장
  - · 다양한 사고 및 충돌 현장 모사
  - · 약 202,343m2
  - · 약 25m 높이의 콘크리트 구조물 및 운송 장비 잔해
  - · 취득 시간: 10시간



그림 2-9 NCMR in Ohio

▪ Structures Lab in Georgia Tech

- 데이터 취득: 지상 레이저 스캐너, 드론
- 비고
  - · 모의 지진실험을 위한 콘크리트 구조물
  - · 주변에 많은 건설 자재 및 구조시험체들이 존재
  - · 약 300 m2
  - · 11m 높이의 콘크리트 구조물
  - · 취득 시간: 30분



그림 2-10 Structures lab in Georgia Tech

■ 모의 재난현장 3차원 모델링

▪ NCMR in Ohio

- RGB point cloud from laser scan
- 총 스캐닝 수: 52 개소



그림 2-11 Point cloud model for NCMR

▪ Structures lab in Georgia Tech

- RGB point cloud from SfM and laser scan
- 총 이미지 수: 48 개
- 총 스캐닝 수: 5 개소



그림 2-12 3D point cloud for the structures lab, 드론 (좌), 지상 레이져 스캐닝 로봇 (우)

○ 드론 및 지상 레이져 스캐닝 데이터 융합 기술 개발 및 검증

■ 2D 이미지 매칭포인트를 활용한 3차원 포인트 클라우드 자동정합 방식 개발

▪ Frame work

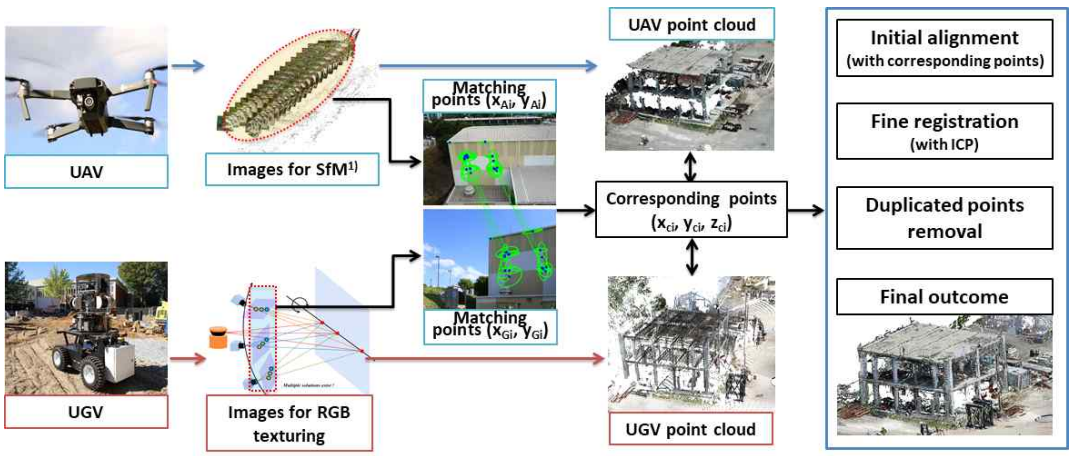


그림 2-13 드론 및 지상 레이져 스캔 데이터 융합 순서도

▪ 현장 실험을 통한 정합 정확도 및 시간 검증

		Proposed registration method	Manual registration
Number of points		36	36
Scale adjustment		9.042	9.032
Translation	T_x	-22.730	-22.264
	T_y	-15.685	-16.774
	T_z	18.099	18.246
Rotation	Θ_x (°)	-89.444	-89.496
	Θ_y (°)	4.538	6.852
	Θ_z (°)	-66.990	-66.239
Mean (m)		0.275	0.199
RMSE (m)		0.216	0.168
Overal time (min)		12	36

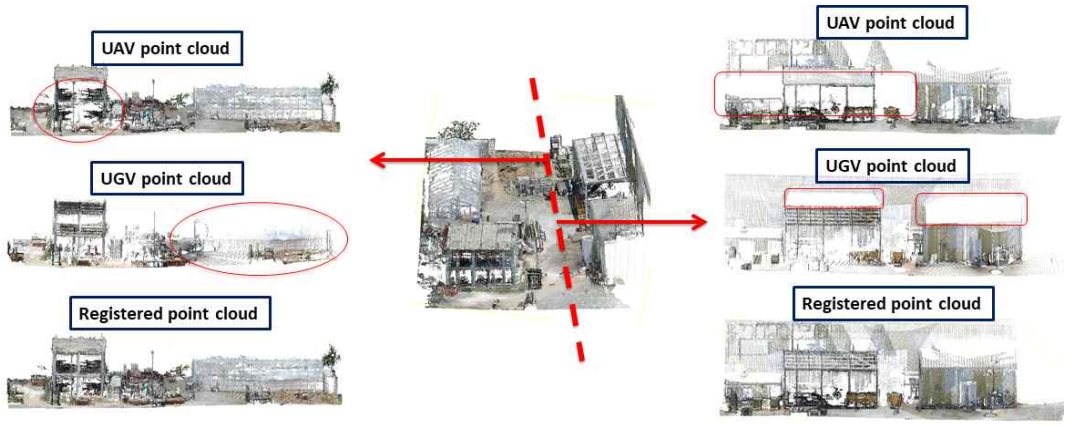


그림 2-14 지상레이져 스캐닝 및 드론 데이터 정합을 통한 고밀도 포인트 클라우드 생성

■ 기대효과

▪ 완전히 자동화된 데이터 취득 및 융합 기술을 통해 재난현장에서 사람의 개입을 최소화

▪ 수동 정합과 비교하여 충분한 정확도를 확보

▪ 데이터 처리 시간을 혁신적으로 줄임으로 인해 더욱 빠른 재난대응 가능

○ 머신러닝 기반 기형 빌딩 오브젝트 자동검출 및 분류기법 개발

■ 머신러닝을 활용한 빌딩 오브젝트 검출 기법

▪ 시스템 구조

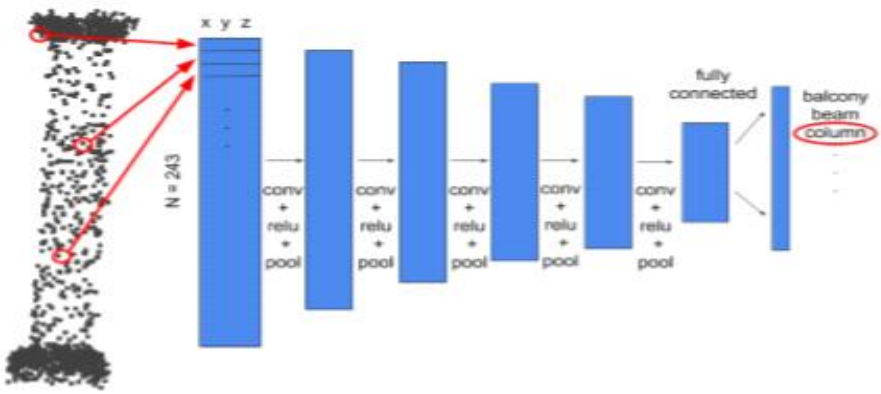


그림 2-15 Architecture design

▪ 시스템 구성

- CAD model 데이터 베이스 구축 (BIMNet10)
- 포인트 클라우드 모델 매칭
- 3D descriptor 기반 빌딩오브젝트 분류

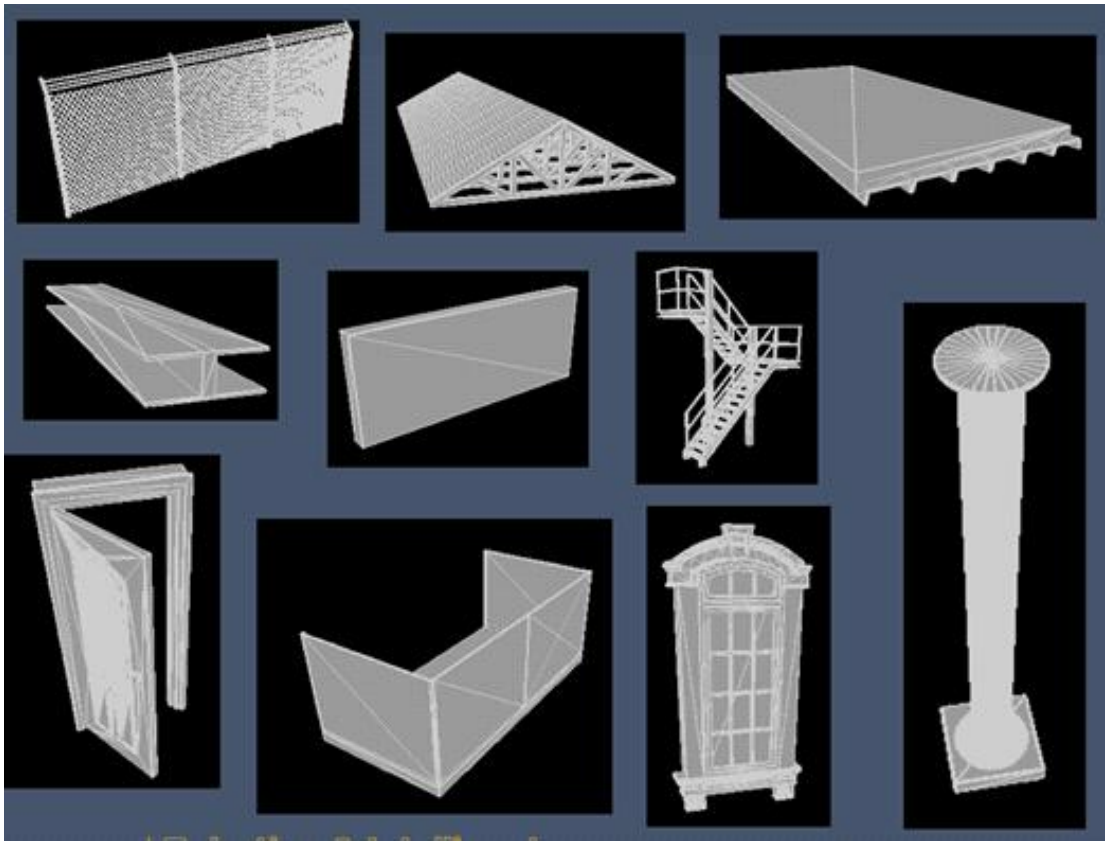


그림 2-16 BIMNet 10 데이터베이스

■ 변형된 빌딩오브젝트 자동검출 및 분류 알고리즘 검증

▪ 검증 방법

- 기존 다른 알고리즘과 비교 검증
- 포인트 클라우드를 특정 형식으로 변형 후 분류 알고리즘 검증
- Rigid trasformation, Outlier noise, Bending, and Truncation

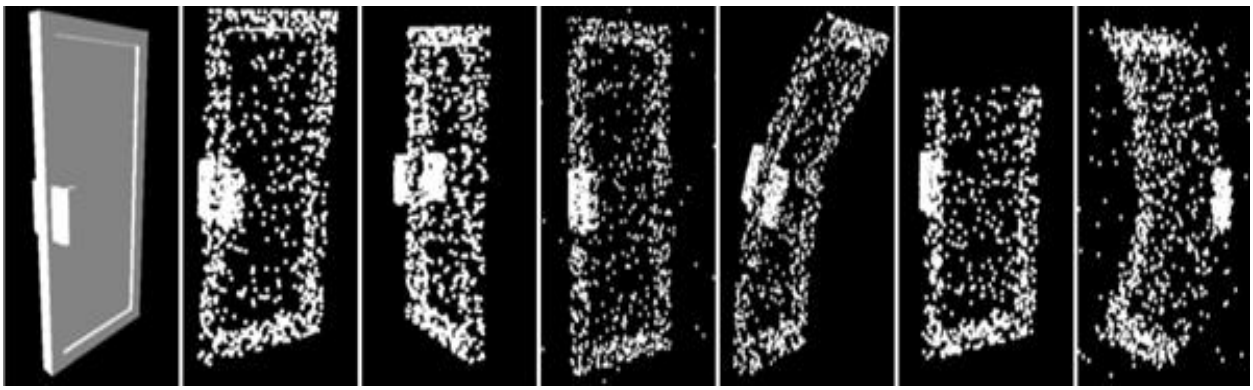


그림 2-17 임의 변형된 포인트 클라우드 모델

▪ 검증 시험 결과

- 각각 다른 데이터셋을 통한 오브젝트 분류 알고리즘 비교 검증
- 최종 소요 시간 및 메모리 할당량 비교를 통한 효율성 검증

표 2-14 빌딩 오브젝트 분류 알고리즘 비교 검증 결과

Dataset / Algorithm	ModelNet40	ModelNet40 + deform	BIMNet10	BIMNet10 + deform
3D-NIM	0.87	0.19	0.70	0.29
3D-NIN (multi-view)	0.89	0.20	**0.77**	0.24
VRN	0.89	0.21	0.64	0.32
VRN (multi-view)	**0.91**	0.20	0.71	0.30
PointNet	0.86	0.08	0.62	0.10
Ours	0.81	0.34	0.69	0.40
Ours (with resample)	0.84	**0.39**	0.68	**0.43**

표 2-15 알고리즘 효율성 검증

	Memory consumption (MB)	Training time (ms)	Inference time (ms)
3D-NIM	36	3.4	1.1
VRN	51	495	90
PointNet	9.4	8.1	1.8
Ours	**3.2**	**0.49**	**0.17**

- 오브젝트 변형 타입에 따른 검출 정확도 검증

표 2-16 변형 타입별 오브젝트 분류 정확도

Dataset	Classification accuracy
ModelNet10	0.86
ModelNet10 + rotation	0.85
ModelNet10 + noise	0.74
ModelNet10 + bending	0.79
ModelNet10 + truncation	0.73
ModelNet10 + rotation + noise + bending + truncation	0.54

- 최종 결과



그림 2-18 < Original point cloud >



그림 2-19 < Building object recognition >

(2) 2차 연도

(가) 주관연구기관(서울대학교 산학협력단)

① 개발 목표 :

지진하중 및 내부폭파에 의한 고층아파트의 파괴거동 해석모델 개발 및 모형실험

② 개발 내용 및 범위(그림을 이용하여 시스템 구성도, 구조 등을 구체적으로 표현)

①	해석모델 검증 및 보완

- 1차년도 해석결과, 소규모실증실험 결과, LiDAR의 계측결과의 상호비교 및 상관관계 분석을 통해 단일 건물의 지진위험도를 전체구조물 및 주요부재에대해 정량화 (위험도 또는 손상도를 5등급으로 분류)

②	지진하중에 이은 내부폭파에 종속된 고층 아파트의 유한요소해석 모델개발

- 내부폭파로 인한 주요부재의 손상도의 변화를 유한요소해석을 통해 정량적으로 해석
- 폭파발생시 부재손상도의 증가를 고려하기위한 폭파변수 (BF, Blast Factor) 제안
- BF값을 지진하중하에서의 위험도에 곱하여 위험도를 보정하는 방법을 제안

③	실증실험을 위한 대상구조물 선정 및 구조물 변위 및 손상도 측정방법 연구

- 1, 2차년도 연구결과를 기반으로 실제구조물(미국 가디언센터내)의 실증실험 준비
- 미국 가디언센터내 철근 콘크리트 또는 철골구조물의 실제스케일 건물 활용
- 실험의 완성도를 높이기 위해 실제구조물의 3차원 지진해석의 수행으로 예비 데이터 구축



Shake-table/earthquake simulation at UCSD (wikipedia)

LiDAR Scanning (Mike Symans 2009)

Post-earthquake fire (Xu 2018)

그림 2-20 2차년도 주요연구내용

■ 해석모델 보완 및 검증

1차년도 해석 결과와 소규모 모형실험 결과, 계측결과를 비교하여 건물의 지진위험도를 건물전체와 부재별로 확인하고 정량화

1. 서론

Constructional steel and composites materials have been widely used for structural applications and construction (Pedro et al. 2009, Mohammadzadeh and Noh 2017, Choi et al. 2018, Kim and Lee 2013, Choi et al. 2018, Choi et al. 2019, Mohammadzadeh et al. 2020). The steel frames were employed frequently to construct the high-rise buildings to which major attention should be paid to resist against applied external loads (Reyes-Salazar et al. 2016, Lee et al. 2014, Hoffman and Fahnestock 2011). Earthquake is the most significant natural disaster making the steel frames vulnerable to failure. There has been a large number of records in the literature reporting the extensive structural damages and destruction due to high demand earthquakes. It has been documented that when buildings located in a region subject to seismic loads, some buildings collapse while some resist and remain undamaged which showed that they utilized a system providing them with better seismic performance to stay resistant (Hou et al. 2109, Hsu et al. 2011, Linzell and Nadakuditi 2011, Choi et al. 2019).

It has been always a real need of constructing a structure resistant against seismic loads generated from earthquakes to increase safety and decrease the maintenance costs. Therefore, many attentions have been attracted to investigate the effects of various important parameters such as architectural design, structural materials, and soil conditions on the seismic resistance of a building (Chung et al. 2015, Ozmen and Unay 2007, Oikonomou and Bougiatioti 2011, Altunışı and Kalkan 2016, Virella and Godoy 2009, Ajamy et al. 2018). In recent decades, construction of the seismic-resistant steel frame buildings retrofitted with the proper lateral load-resisting systems providing ductile and elastic behavior under moderate earthquakes, despite being costly and uneconomic, was great of interest (Sheehan et al. 2015, Özuygur 2016, Lian et al. 2015, Takin et al. 2016).

One of the major concerns that should be paid attention is the vertical irregularities of a building which is appealed in a structure in the form of varying column height in any floor resulting in stiffness irregularity (Mario and Barbara 2008). Structures with irregular horizontal and vertical layouts are more vulnerable to collapse than regular structures. Besides, many public, commercial and institutional buildings have been designed with various irregularities in structural layout because of architectural and aesthetic requirements. The design of buildings with stiffness irregularities requires specific design considerations in comparison with that of regular buildings because of the various seismic demands.

The structural elements can resist a specific amount of plastic hinge rotation beyond which it may experience failure (Mohammadzadeh et al. 2018, Choi et al. 2018, Mohammadzadeh et al. 2019,). To evaluate the structural behavior of a building subject to seismic loads, the linear static, nonlinear static (pushover), linear dynamic and nonlinear dynamic analyses can be

employed (Dya and Oretaa 2015, Mohammadzadeh et al. 2012, Mohammadzadeh and Noh 2014, Li et al. 2017). It has been documented that the most accurate predictions of dynamic responses of irregular structures subject to severe dynamic loads can be obtained by the nonlinear dynamic analysis through which the plastic hinge development evaluated at the ends of the structural elements (Mohammadzadeh and Noh 2019, Benavent-Climent et al. 2014, Davani et al. 2016,).

Georgoussis et al. (2015) presented a method to investigate the seismic behavior of the multi-storey setback building subject to strong ground motions at the preliminary stage of practical design. The accuracy of the method was evaluated by considering asymmetric tall buildings with a mass or stiffness irregularity. Dynamic responses of elastic multi-storey building systems were obtained by analyzing simple (equivalent) single-storey systems. The behavior of the building was also investigated in the post elastic phase considering the stiffness-dependent strength of the various bents and discontinuities.

Vasilopoulos et al (2008) presented a seismic design approach for irregular space steel frames with respect to Eurocodes 8 and 3. The approach used an advanced static and dynamic finite element method considering geometrical and material nonlinearities as well as member and frame imperfections. The pushover analysis was performed by distributing multimodal load along with the height of the building combining the first few modes. The nonlinear dynamic analysis was carried out, in the time domain, using accelerograms obtained from real earthquakes such that to be compatible with the elastic design spectrum of Eurocode 8. Cancellara and Angelis (2019) investigated the dynamic behavior of base-isolated multi-storey structures having high irregularity in the plan. In this regard, two types of dynamic analyses were adopted: a dynamic analysis with a response spectrum and a nonlinear dynamic analysis. The results were presented in the form of deformation, inter-storey drift at different levels, and stresses with the focus on bending moment, and shear in the columns and beams and axial force.in columns.

Although numerous studies have been reported in the literature improving the understanding of the behavior of regular structures subject to seismic loads, the need for assessment of the structural behavior of the irregular structures subject to the earthquake still exists. Therefore, this study was motivated to investigate the seismic performance of the steel frame building of twelve stories with irregularities in both plan and elevation. It helps to figure out to what extend each irregularity can cause damage or failure. To design the building and determine the type and dimensions of the columns and beams, the commercially available structural design package SAP2000 was adopted. The design resulted in the box profiles for the columns with various dimensions along with the building height while a uniform IPE profile was considered for the beams of all floors. The nonlinear time-history analysis was performed employing the FEM package ABAQUS through and dynamic implicit method. The validity of the method of this study was evaluated by making a comparison between the results of the current method and literature (Wijaya et al., 2019). Accordingly, a three-bay steel moment-resisting frame of eight-storey height was analyzed and results were compared with those of literature. Thereafter, a real set of recorded ground acceleration obtained from the Vrancea Earthquake, Romania was considered to be applied to the steel frames of different types in X- and Z-directions at the base under displacement control conditions. Two main types of irregularities were considered;

irregularity in plan and elevation. Each type included two cases; 1) plan: discontinuity in the plan, and torsional irregularity, and 2) elevation: discontinuity along with building height, and set-back. The results were presented in the form of the spectrogram of building deformation, and storey drift. Besides, the fragility curves were derived to evaluate the failure of the steel frames with regard to different peak ground acceleration (PGA).

2. 해석모델

2.1. 해석모델의 개요

This study investigated the seismic performance of the moment-resisting steel frame of twelve stories with and without irregularities. Two main categories of irregularity were considered; 1) plan and 2) elevation. To investigate the irregularity influences on the structural resistance of the buildings, the regular building was analyzed as a control model. This helps to find out the variation of seismic behavior of the irregular building with the regular building. It is worthy to note that the same area and height were considered for regular and irregular buildings. Based on the definitions of building category given in (HAZUS 1999), the high-rise buildings possess more than eight stories, higher than 36.5 m in height, thus, the model of this study laid in the high-rise building category.

2.2. 건물 모델 개요

2.2.1. 통상의 건물

The overall design of the regular building is such that all the stories, from the ground floor to the top, possess an equal height of 3.2 m for each. To illustrate the height of the building and variation between consecutive floors a typical regular building is provided in 그림 2-21.

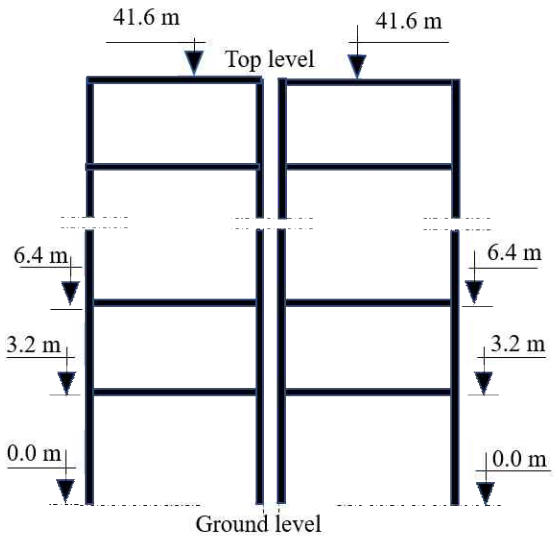
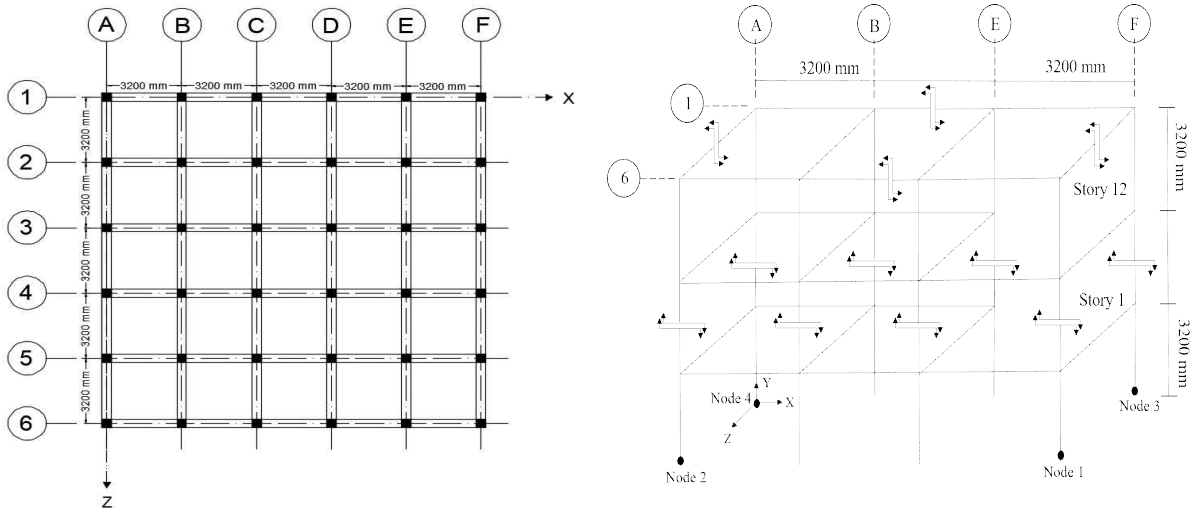


그림 2-21 Illustration of a typical building elevation considered in this study

The plan of the regular building, considered in this study as a control prototype, is given in 그림 2-22 (a) while the 3D schematic of the building is given in 그림 2-22(b). The general plan of the building is a square with six-axis and five spans of 3.2 m in X- and Z-directions.

2.2.2. 비정형성

In earthquake codes, buildings have been mostly classified into two main categories; regular and irregular buildings. Irregularities in buildings and structures are mostly because of



(a) Architectural plan **(b) 3D schematic**

그림 2-22 Illustration of the typical regular building

architectural demands and purposes. Two types of irregularities have been recognized for buildings: One is the irregularity in the plan such as torsional irregularity, floor slab discontinuities, projection in the plan, and nonparallel axes of structural elements. Another is the irregularity in elevation so-called vertical irregularity comprising inter-storey strength (weak storey), inter-storey stiffness (soft storey), and discontinuity of vertical structural elements. These irregularities can cause partial or general failure of the structure, especially, in case of moderate and severe earthquakes. For example, 그림 2-23 shows the severe damages of a building due to the torsional irregularity.



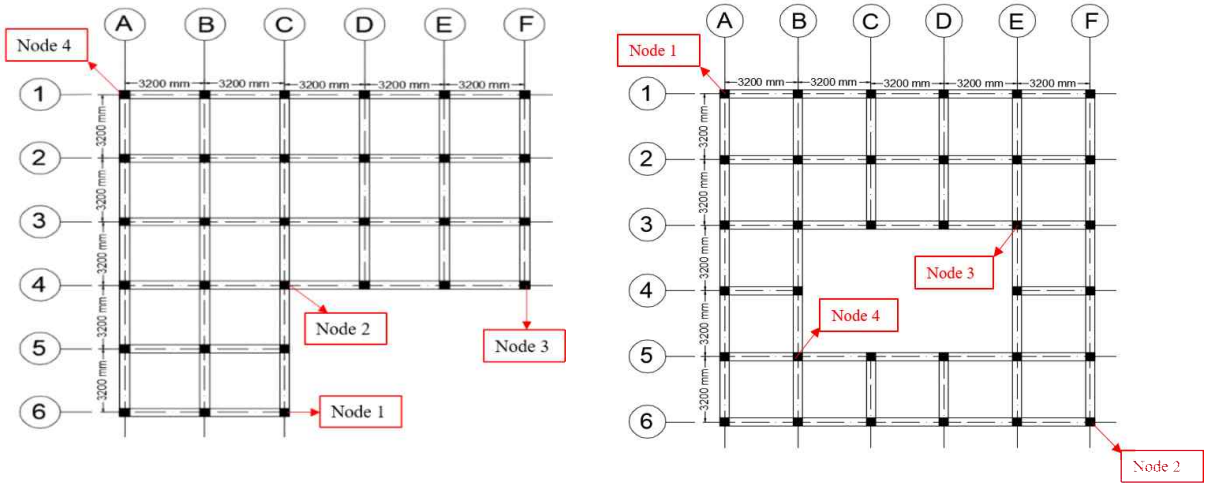
(a) General view **(b) Zoomed-in view**

그림 2-23 Severe damage and partial failure of the building due to torsional irregularity (Ozmen, C., Unay, A.I. 2007)

(a) 도면

Among different types of irregularity in the plan, this study intended to investigate torsional irregularity and the discontinuity in the slab, which have been commonly considered in design and construction. 그림 2-24 illustrates the cases of plan-irregularities of this study.

Torsional irregularity originated from the distance between centers of gravity and rigidity. This eccentricity results in the torsional moments around the center of rigidity causing the shear forces in the columns. The slabs of the floors have the role of transferring the lateral loads, which commonly caused by a seism, to the columns and shear walls. Although, the floor slabs have been supposed to possess an infinite in-plane rigidity, however, the existence of an opening in the slabs may lead to a drastic change in slab rigidity. This can change the distribution of lateral loads and affect the overall seismic behavior of the structure by imposing the extra shear stresses to the columns due to the lateral displacement.

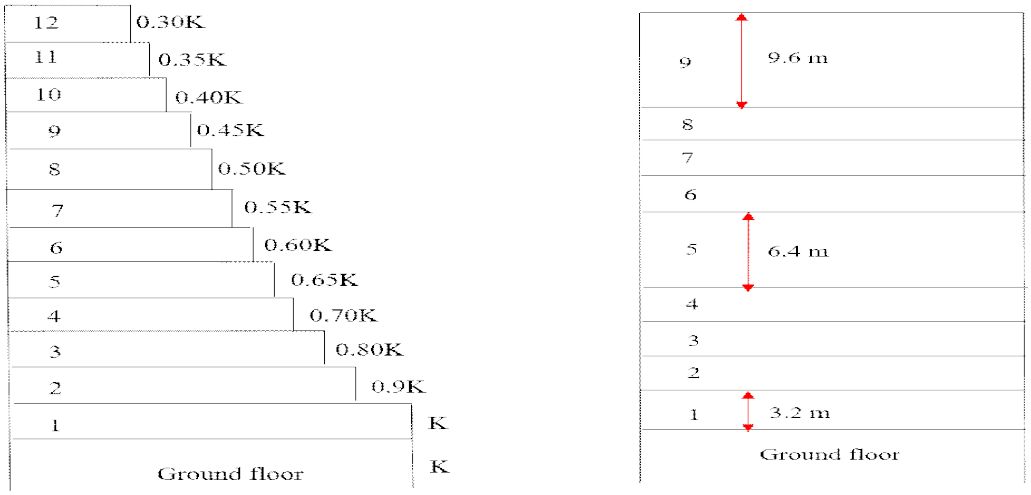


(a) Torsional **(b) Discontinuity**

그림 2-24 Illustrations of irregularities in plan considered in this study

(b) 높이

In this study, two types of vertical irregularities were considered; soft storey and vertical discontinuity. The soft floor or inter-storey stiffness irregularity initiated from the differentiation of lateral displacement of consecutive floors has been commonly seen on the ground floors. In several cases, the soft storey might be observed; one case is when the columns with the same cross-section utilize a longer height than other floors, thus, the lower lateral rigidity increases the displacements. Another one is the case that non-continuous shear walls induce critical shear stresses in the columns. Besides, having partition walls in higher elevations while they are eliminated on the ground floor may result in the development and increase of the shear forces in the columns. For the analysis, a range of variation of stiffness irregularity from K=0.3, at the top, to K=0.9, at lower levels, was considered as illustrated in 그림 2-25(a). Another scenario is the discontinuity in elevation which can result in the instability and increase in the displacement of the storey and drift at the floors with discontinuity. In this regard, two floors of heights 9.60 m at the top and 6.4 m in the middle of the building were considered as illustrated in 그림 2-25(b).



(a) Stiffness irregularity **(b) Elevation discontinuity**

그림 2-25 Illustration of two cases of irregularity in elevation considered in this study

It is worthy to mention that the focus of the current study was the investigation of seismic performance of the irregular buildings of two types of irregularity in plan and elevation to provide a strong background and foundation for future studies that will consider a range of irregularities in building heights, plan and configurations.

3. 유한요소해석

The time-history analysis was performed using the commercially available FE package ABAQUS to investigate the seismic behavior of the high-rise building with and without irregularity.

3.1. 해석모델 상세

In this study, the twelve-stories building was investigated through FEM analysis. To create the model of the structural elements of buildings in ABAQUS, the wire elements were adopted. This helps to reduce the analysis costs and achieve accurate results in a shorter time than the case of modeling with 3D solid elements.

3.1.1. 형상

The first step of FEM analysis is the construction of the model based on the geometry of the problem given in 그림 2-22. In this regard, a reference point was defined to be the origin of the building. It helps to have a precise tool for drawing the structural elements at different stories. Having this reference point, a set of points was created at the level of each storey for the positioning of beams and columns. Then, they have been connected by employing the wire elements and a net of beam and column formed. 그림 2-26 shows the 3D view of the regular building modeled with wire elements.

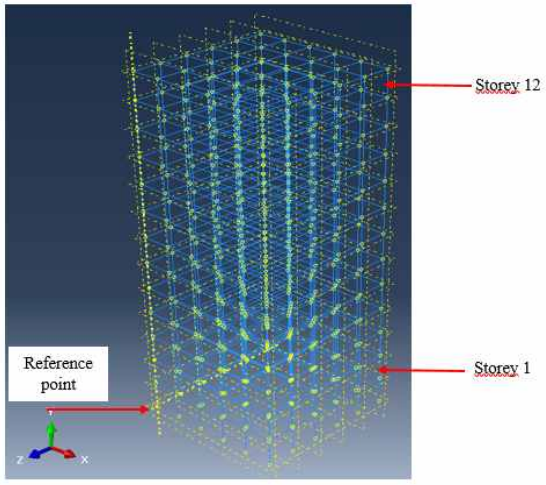


그림 2-26 3D view of the building created by a set of points connected with wire elements

3.1.2. 재료의 물성치 및 강철 프로파일

This study considered the construction steel with the yield strength of 420 MPa, elastic modulus of E=210 GPa, and Poisson's ratio of for the profiles of beam and columns of the building. To perform the nonlinear analysis as a complementary step for the linear analysis, the nonlinearity of steel was defined based on the stress-strain relation illustrated in 그림 2-27.

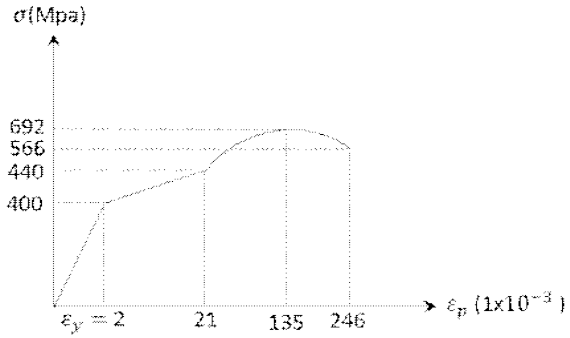


그림 2-27 Nonlinear material properties of the constructional steel

To design the building and to find the dimensions of the steel frame the commercially available design package SAP2000 was employed. From the design process, various BOX profiles were obtained for different stories: one to three: 0.50×0.50×0.05m, four to seven: 0.45×0.45×0.05m, and eight to twelve: 0.40×0.40×0.05m. For the beam of all stories, the steel profile IPE 500 was achieved having the dimensions of W=200 mm, H=500 mm, = 10.2 mm, =16 mm as depicted in 그림 2-28.

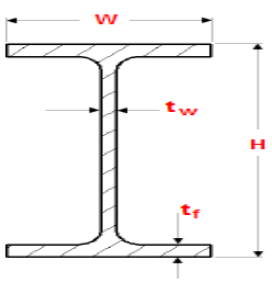


그림 2-28 Illustration of the beam profile IPE 500

Thereafter, the section profiles were specified to the corresponding beam and columns of each storey. 그림 2-29 shows the 3D model of the building after specifying the steel profiles to the structural members.

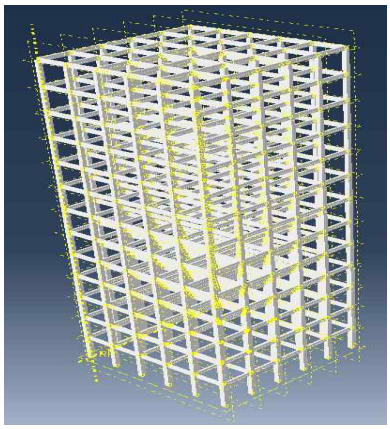


그림 2-29 A 3D model of building with specified steel profiles to the beam and columns

3.2. 하중 및 경계조건

(a) 하중

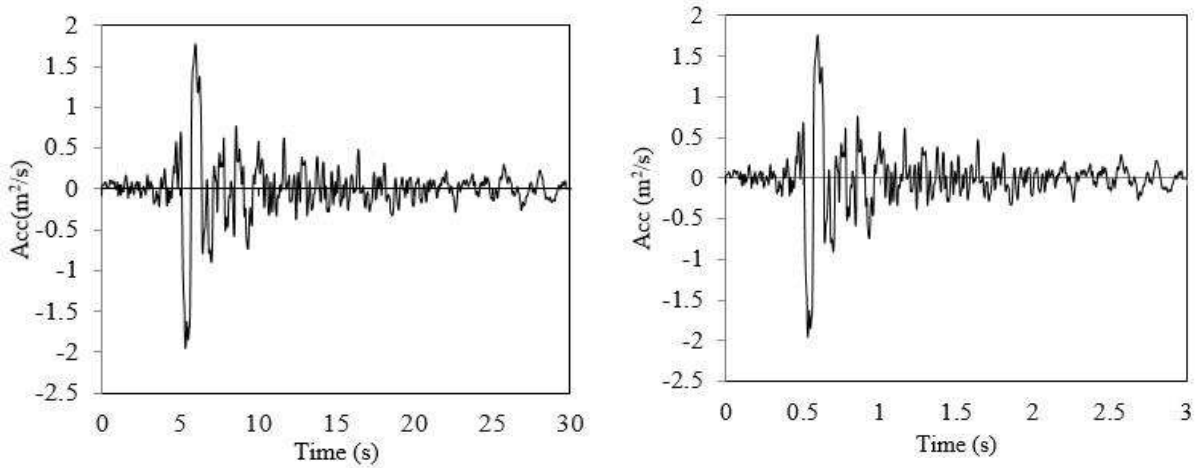
Various types of loads comprising dead and live loads were considered; the superimposed dead load counting for floor coating and interior walls as well as a live load for all residential areas, a line load due to cladding weight of exterior walls on the exterior beams, dead and live loads at the roof elevation. 표 2-17 shows the various portions of the applied load.

표 2-17 Loading pattern comprising dead and live loads of floors and roof

Loading position	Floor (kN/m^2)	Roof (kN/m^2)	Building exterior wall (kN/m)	Roof exterior wall (kN/m)
Dead load	11.38	9.26	7.68	1.99
Live load	3.14	2.35	–	0.98

It is appropriate to note that loads given in 표 2-17 were applied to the building in negative Y-direction. In addition to the above-mentioned loads, a real set of recorded ground accelerations obtained from Vrancea Earthquake, Romania, considered as the seismic load applied to the building for the time history analysis as illustrated in 그림 2-30(a). For the aim of deduction of the analysis costs, the time axis was squeezed by a factor of 10 as shown in 그림 2-30(b).

The seismic load was applied to the base of steel frame under displacement-control conditions with an amplitude defined regarding the load time-history and applied in X- and Z-directions.



Real recorded ground acceleration **Squeezed time axis**

그림 2-30 Real recorded ground acceleration of Vrancea earthquake

(b) 경계조건

To apply boundary conditions (B.C.), the movement in Y-direction and rotation about X- and Z-directions of the columns at the base floor was constrained. Displacements in X- and Z-directions were released to let the seismic load act in these directions under displacement control conditions.

Analysis procedure

The finite element method (FEM) was adopted for the seismic analyses of regular and irregular buildings. FEM is a numerical tool approximating the solutions of governing equations of a target problem. For this aim, the implicit non-linear dynamic procedure was employed through ABAQUS. The implicit method was adopted as it does not need the time-step as very small as that of the explicit method, thus, a less expensive analysis could be achieved. To decrease the analysis costs, the 3D wire elements were taken into account, then, the column and beam sections were created and specified to them. Using 3D solid elements drastically increases the size of the model and results in a very expensive analysis. Besides, tracking the stress through the elements and obtaining the displacement getting tough resulting in a decrease in the analysis accuracy.

In the first step, the validity of the analysis method was examined by making a comparison between the results of the current study and literature. Upon validating the model, different cases of regular and irregular buildings were investigated. In this regard, the regular building was investigated by applying the seismic load together with the dead and live loads corresponding to each storey. Then, two types of irregularities in plan and elevation were dealt with. Each type of irregularity consisted of two cases; torsional irregularity and discontinuity in the plan were considered for the plan while set-back and discontinuity in elevation were taken into account for vertical irregularity. By having the results comprising the deformed shape of steel frames, storey drift, and fragility curves, the effects of irregularity on the seismic performance of the building were studied.

4. 해석 결과

To find the most appropriate element for FEM analysis, the convergence study was performed and the normalized displacements of the basement and top floor were plotted with respect to the number of elements. Afterward, the validity of the FE model was evaluated. The results obtained from seismic analyses of the regular and irregular buildings were reported in the form of deformation spectrograms, storey drift along with the building height, and fragility curves.

4.1. 수렴 연구

To obtain the most appropriate element type and size, the convergence rate of various types of elements was investigated by comparing the maximum displacements of the building at base and top floor with respect to mesh size for the number of elements of sixteen. Having this an optimum design and the least expensive analysis can be achieved. For this aim, the regular building was analyzed for which four types of beam elements were considered; 1) B31, a 2-node linear beam in space, 2) B31H, A 2-node linear beam in space, hybrid formulation, 3) B32, A 3-node quadratic beam in space, and 4) B32H, a 3-node quadratic beam in space, hybrid formulation. 그림 2-31 represents the convergence of the displacements of the top floor and basement with respect to element and mesh size.

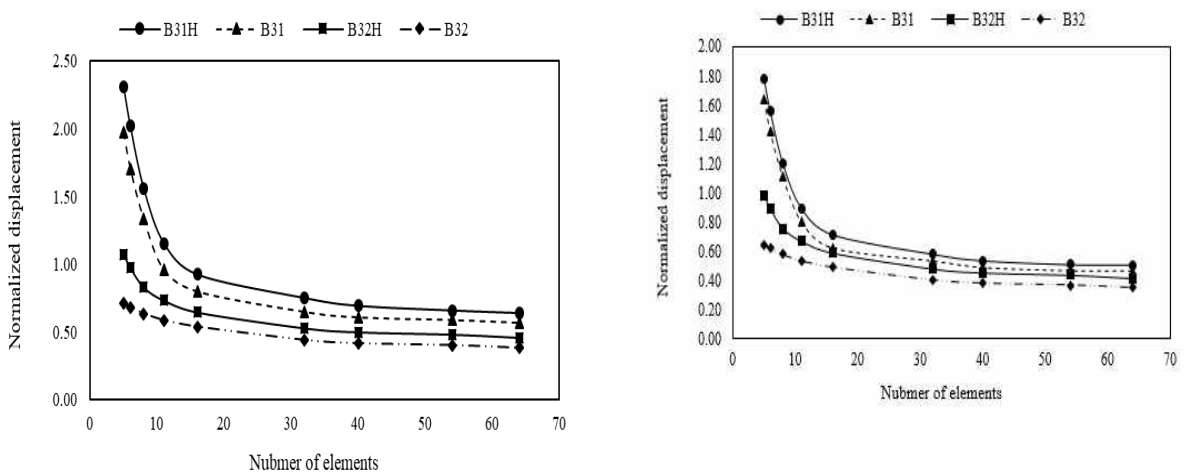


그림 2-31 Convergence study presenting the variation of normalized displacement with respect to the number of elements considering different element types; B31, B31H, B32, B32H.

As can be seen from the convergence study, the accuracy of the results of linear elements was highly dependent on the number of elements. A vast variation can be seen in the graphs for linear elements. The same pattern was observed for the top floor and basement. From the graphs presenting the variation of displacement corresponding to quadratic elements, it can be inferred that the convergence was quickly achieved with a low number of elements. Furthermore, it was concluded that the element type of B32 could result in a better and faster convergence, thus, this study considered the B32 element for further analysis.

4.2. 유한요소해석 타당성 평가

To evaluate the model validity, the comparison was made between the results of the current method and literature. In this regard, an example problem which is given in (Wijaya et al., 2019) was considered; a three-bay steel moment-resisting frame of eight-storey height. The building was designed such that it could resist against the seismic load with respect to Eurocode 8 considering earthquakes having a magnitude up to 5.5. For the analysis, S275 steel was considered. Floors were subjected to the gravity load of 21 kN/m while a load of 13 kN/m was exerted to the building roof. The profile IPE 550 was used for beams of all floors while two different steel profiles were utilized for columns; the profile HD 100x187 from the basement to 4th storey and profile HD 320x74 from 5th to 7th storey. Notably, the beam-column connection is rigid. The bracing was modeled in terms of elastic truss elements remained in the elastic range during upon applying seismic loads. The geometrical nonlinearity was taken into account for the analysis. The illustration of the building geometry is provided in 그림 2-32.

The median and logarithmic standard deviation of first mode spectral accelerations for different return periods of 100, 500, and 1000 years are provided in 표 2-18 for both literature and the present study.

In another attempt for validating the method of this study, the variation of building capacity was plotted with respect to drift at the top floor for both methods of this study and literature as can be seen in 그림 2-33.

표 2-18 Median and logarithmic standard deviation of first mode spectral acceleration

Parameter	Study	Return period		
		100	500	1000
Period (s)	Literature (Wijaya et al., 2019)	1.46	1.46	1.46
	Current	1.44	1.44	1.44
	Variation (%)	1.39	1.39	1.39
Median (g)	Literature (Wijaya et al., 2019)	0.162	0.416	0.653
	Current	0.156	0.403	0.627
	Variation (%)	3.84	3.23	4.15
Standard deviation	Literature (Wijaya et al., 2019)	0.045	0.183	0.265
	Current	0.043	0.175	0.253
	Variation (%)	4.65	4.37	4.74

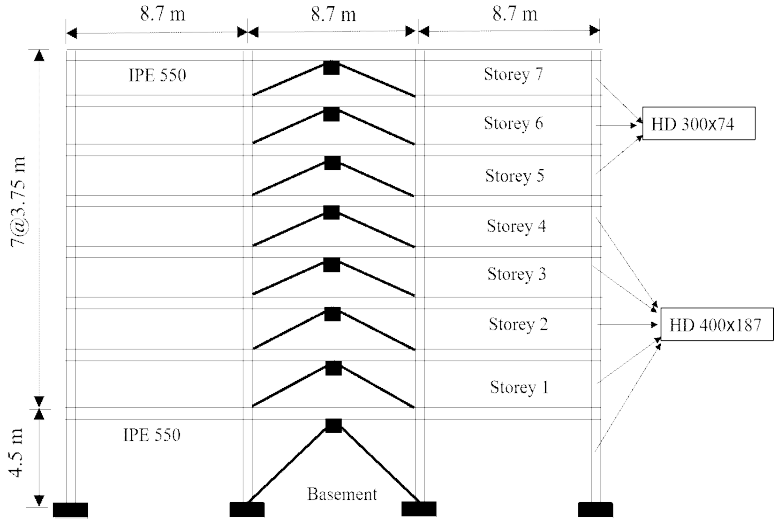


그림 2-32 Illustration of the building of eight stories for method validity

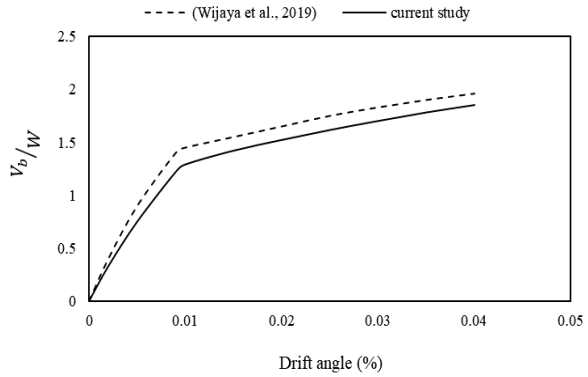


그림 2-33 Capacity curve of the building obtained from the current study and literature at the top floor

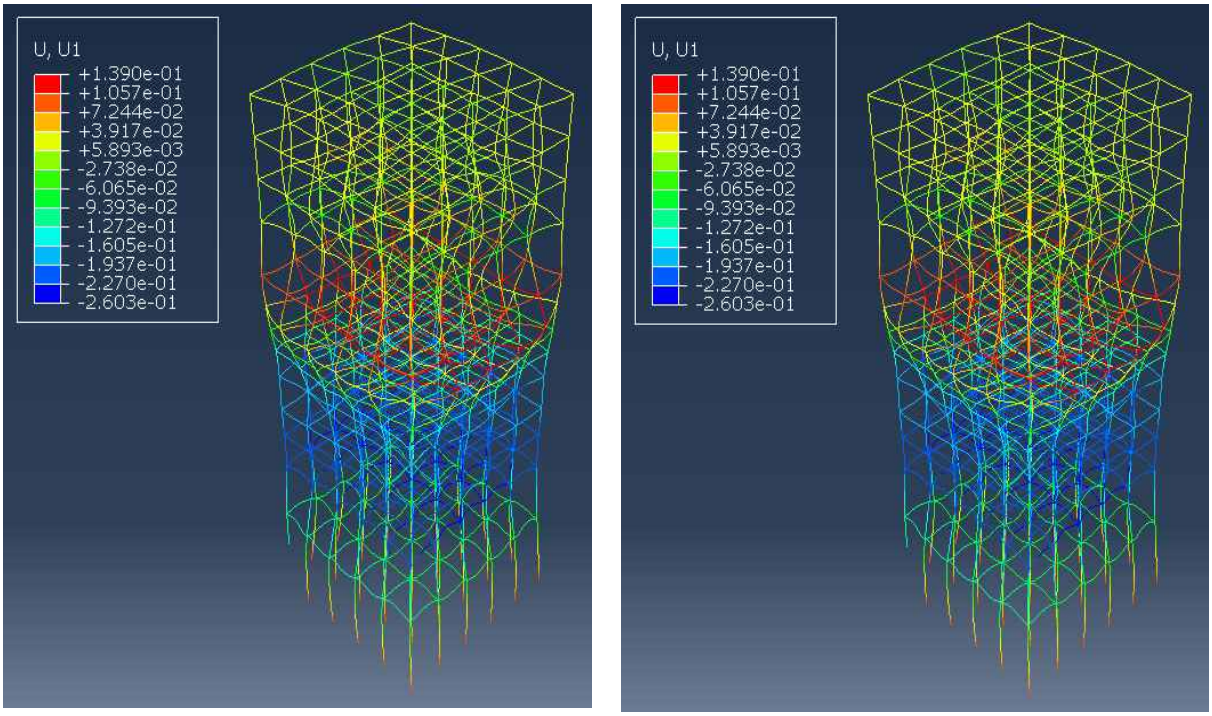
As can be seen from the graphs given in 그림 2-33, a small discrepancy between the building seismic capacity obtained from this study and literature proved the validity of the method of this study, thus, further studies can be reliably done with high accuracy.

4.3. 정형 건물

그림 2-34(a) shows the illustration of the damaged regular building obtained from nonlinear dynamic analysis at a time step of t=0.57s corresponding to negative peak acceleration (maximum compressive load) while the deformation corresponding to positive peak acceleration (maximum tensile load) is shown in 그림 2-34(b) at t= 0.61s. As the plan of the regular building is symmetric, the deformed shape of the building in X-direction is solely enough to be presented. The support reactions of the building, at the four corners, comprising moments and lateral displacements in the plane of the building are provided in 표 2-19.

표 2-19 Support reactions of the regular building at the positive peak

Node	M1	M2	M3	U1	U2	U3
1	-171.1 E+03	0.0	3.1E+06	119.3	0	119.3
4	-3.1E+06	0.0	229.5 E+03	119.3	0	119.3



(a) Negative peak acceleration (t=0.57s) **(b) Positive peak acceleration (t= 0.61s)**

그림 2-34 Deformation of the regular building at negative and positive peak (X-direction)

4.4. 비정형 건물

The seismic analyses of buildings with different types of irregularities were carried out to find out the effects of irregularities on the dynamic behavior and seismic resistance of buildings. Two types of irregularities were imposed on the frame; plan and elevation. In this regard, two cases of irregularities were considered for the plan, namely, torsional irregularity and plan discontinuity while for the vertical irregularities two cases of set back and elevation irregularity were adopted.

4.4.1. 도면

Dynamic characteristics of buildings with irregularity in the plan were investigated considering two cases of irregularities; torsional and discontinuity.

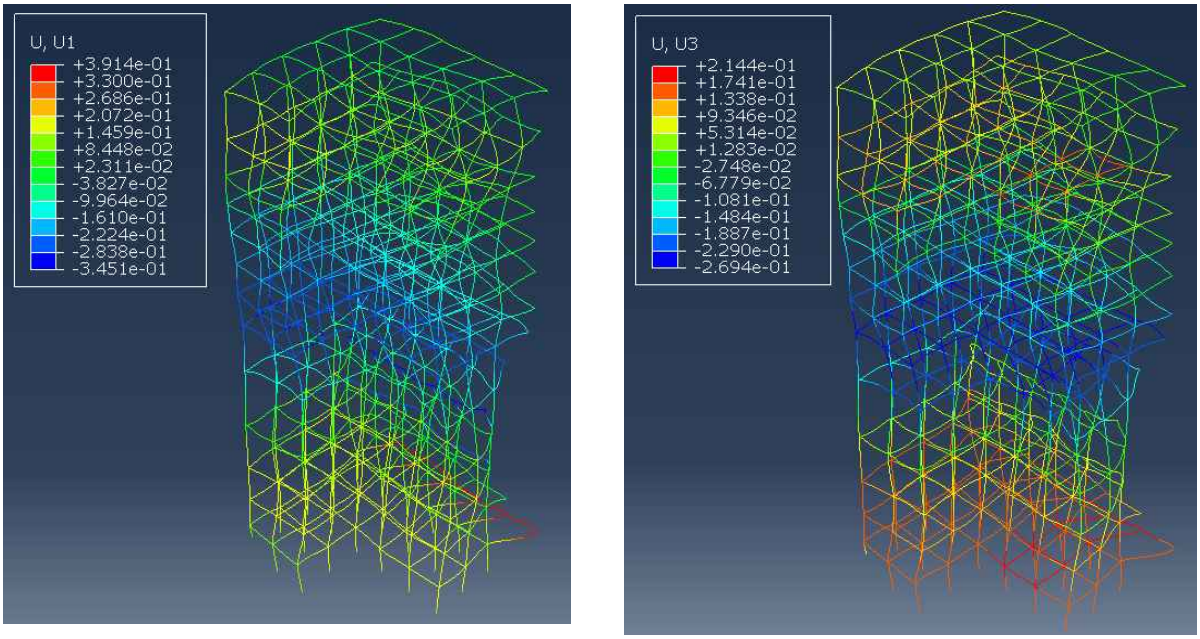
(a) 비틀림 비정형성

The deformed shape of the building with torsional irregularity in X- and Z-directions, just after the positive peak, are shown in 그림 2-35.

To investigate the effects of irregularity in the plan, the support reactions together with the variation of the displacement with respect to those of the regular building were provided in 표 2-19 for nodes 1 and 4 shown in 그림 2-34.

표 2-20 Support reactions of the plan-irregular building at the positive peak

Node	M1(N.m)	M2(N.m)	M3(N.m)	U1(mm)	U2(mm)	U3(mm)
1	-9.8E06	0.0	-2.9E06	142.0	0.0	142.0
Variation (%)	-	-	-	19.03	0	19.03
4	-207.2E3	0.0	3.3E6	142.0	0.0	142.0
Variation (%)	-	-	-	19.03	0	19.03

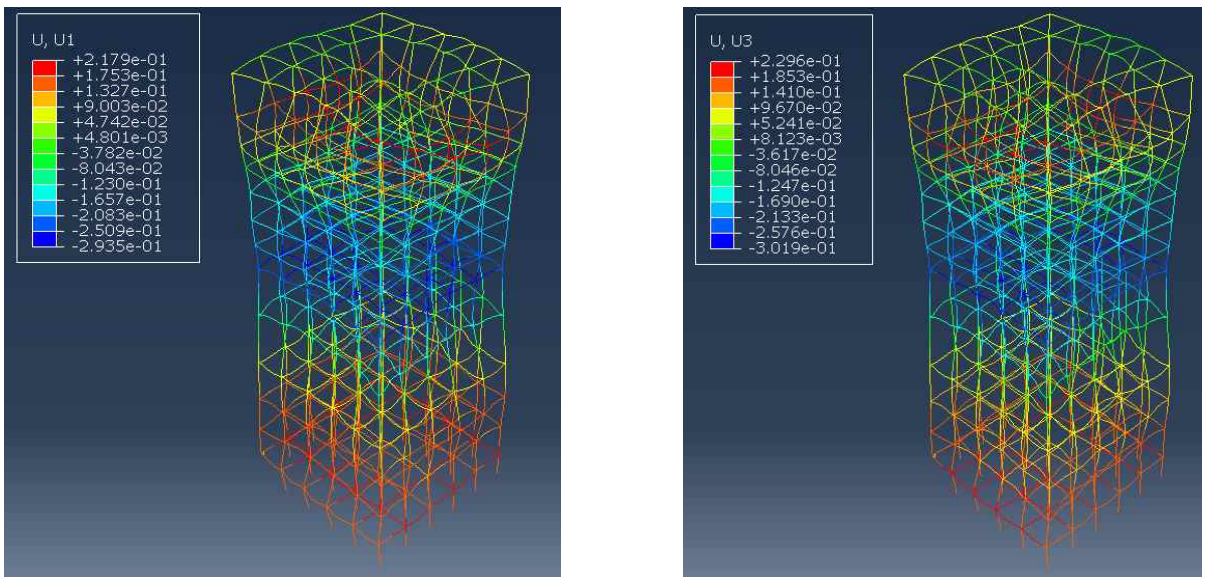


X-direction **Z-direction**

그림 2-35 Deformed shape of the seismic loaded building with torsional irregularity just after the positive peak (t=0.61s)

(b) 불연속성

The effect of discontinuity in the plan of a building on the seismic performance was investigated and the deformed shape of the steel frame was obtained just after peak accelerations as illustrated in 그림 2-36. Having this deformed shape helps to figure out the overall seismic behavior of the high-rise building and find the most critical parts of the building which are highly prone to failure.



X-direction **Z-direction**

그림 2-36 Deformed shape of the seismic loaded building with discontinuity in the plan just after the peak

From the graphs given in 그림 2-36 it can be inferred that the maximum positive displacements occurred in the basement and lower stories while the maximum negative displacements occurred in the middle stories. This holds for displacements in both X- and Z-directions in the plane of the building plan. Moreover, larger displacements were observed in Z-direction, so, the possibility of frame failure is higher than in other directions.

표 2- 21 Support reactions of the plan-irregular building at positive peak

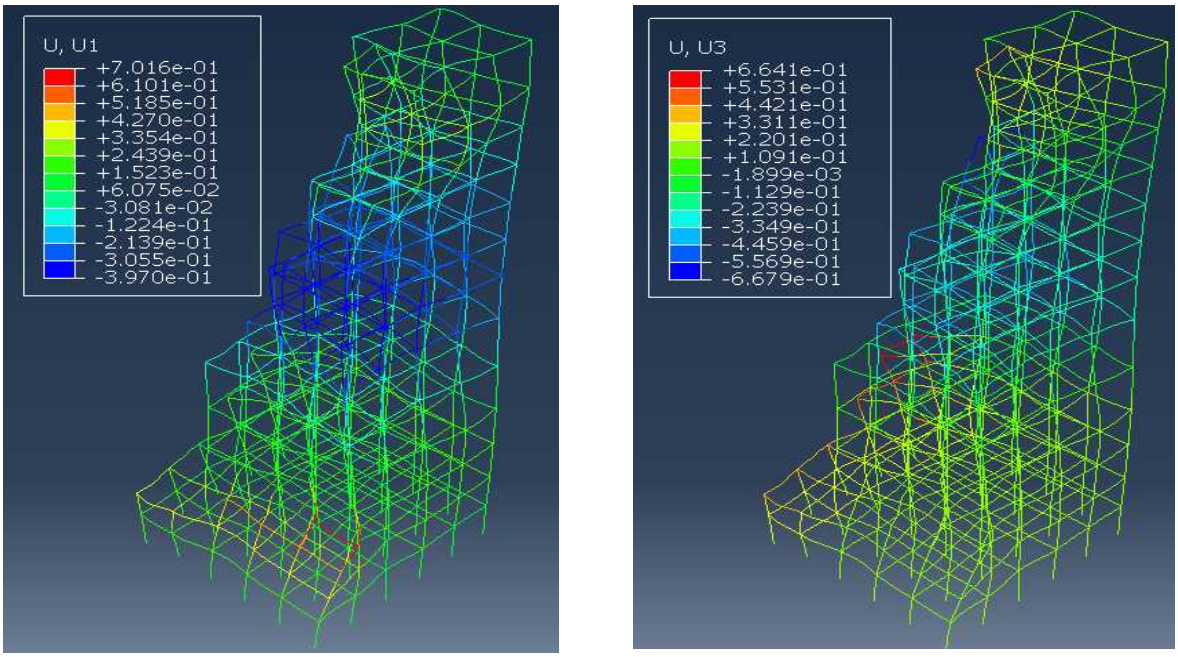
Node	M1(N.m)	M2(N.m)	M3(N.m)	U1(mm)	U2(mm)	U3(mm)
1	-9.8E06	0.0	-2.9E06	151.26	0.0	151.26
Variation (%)	-	-	-	26.79	0	26.79
4	-207.2E3	0.0	3.3E6	151.26	0.0	151.26
Variation (%)	-	-	-	26.79	0	26.79

4.4.2. 높이

Having analyzed the irregularity in elevation using ABAQUS, the seismic responses of the building were achieved. The deformations of the irregular buildings were obtained just after applying the peak ground acceleration.

4.4.3. 셋백 (Set back)

The deformed shape of the steel frame was reported in the form of spectrograms in X- and Z-directions as illustrated in 그림 2-37(a) and (b), respectively.



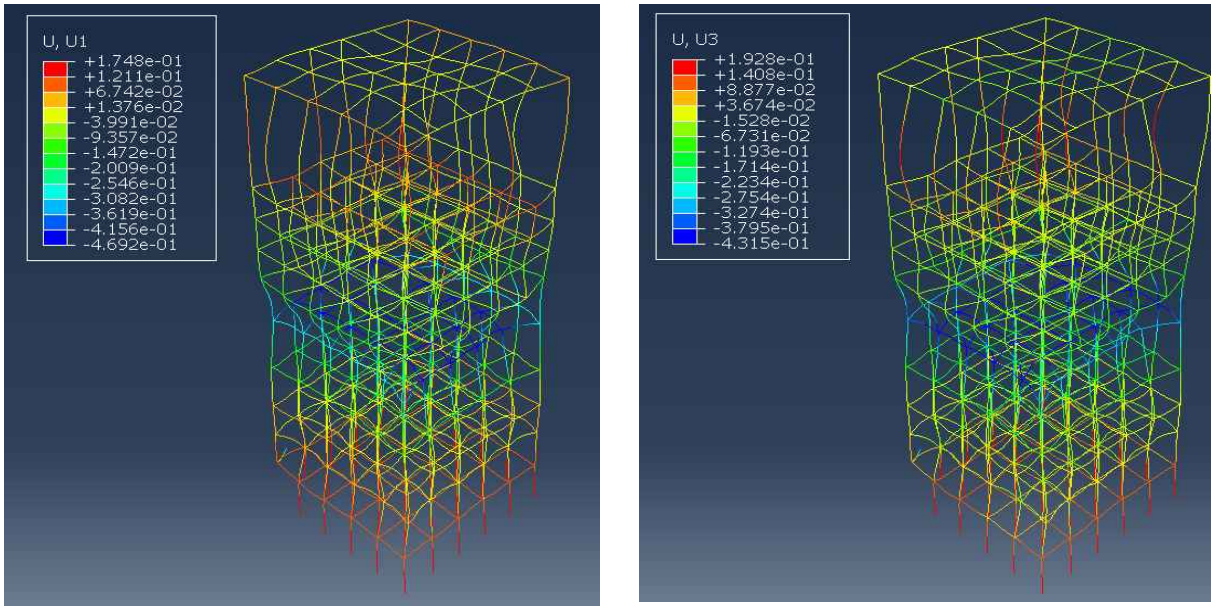
X-direction **Z-direction**

그림 2-37 Deformed shapes of the seismic loaded building with set back just after the peak

As can be seen from the spectrograms given in 그림 2-37, positive displacements in X-direction are higher while the bigger negative displacements were observed in Z-direction. The negative displacements formed in the middle of the building while the positive displacements were seen at the top and bottom of the frame. The frame in Z-direction is more prone to failure since more deformation occurred in this direction.

4.4.4. 수직 불연속성

그림 2-38(a) and (b) show the deformed shapes of the frame with discontinuity in elevation presented in the form of the spectrogram in X-and Z-directions. As can be seen in 그림 2-38, the middle of the building sustained the highest deformation that appeared in the form of constriction.



X-direction **Z-direction**

그림 2-38 Deformed shapes of the seismic loaded building with elevation discontinuity

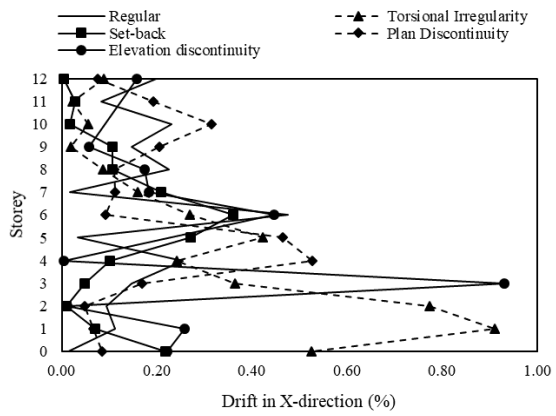
5. 결론

To investigate the effects of irregularity in the plan, the results obtained from the seismic analysis of the regular building were normalized with those of the regular building. The seismic behaviors of the building with and without irregularity were reported in the form of comparative graphs presenting storey drift. The seismic resistance of the steel frame was evaluated by producing the fragility curves for both regular and irregular buildings.

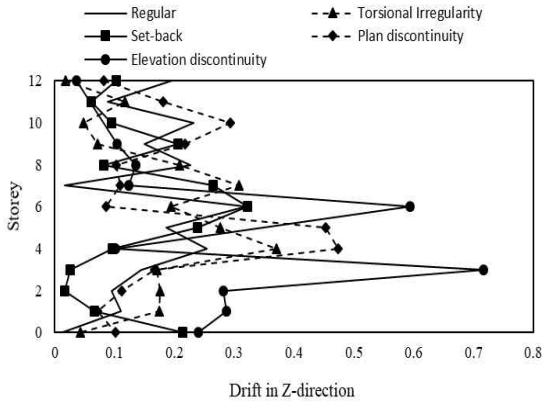
5.1. 층변위 비교

To figure out the effects of irregularity on the seismic performance of the building, the storey drift corresponding to regular and irregular buildings were plotted in comparative graphs. The storey drifts of regular and irregular buildings are provided in comparative graphs given in 그림 2-39(a), (b), and (c) for drifts in X- and Z-direction, respectively.

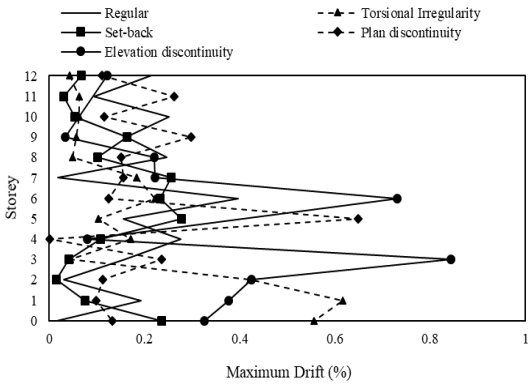
As can be seen from the graphs given in 그림 2-39(a), the torsional irregularity and discontinuity in elevation resulted in the highest drift, especially, in lower levels in the x-direction. Besides, it can be figured out that the irregularity in elevation, stiffness irregularity, did not have significant effects on the building drifts. Having looked at 그림 2-39(b), it can be found that the plan irregularity affects the storey drift, in Z-direction, at mid-height of the building the most. Furthermore, the irregularity in elevation had more effects on storey drift in Z-direction than in X-direction.



(a) X-direction



(b) Z-direction



(c) Maximum

그림 2-39 Variation of storey drift in X-and Y-directions as well as the maximum drift with respect to building height

5.2. 취약도 곡선

To evaluate the probability of the failure of the buildings with and without irregularity, the fragility curves were derived. Fragility curves represent the probability of structural damage due to exceeding a certain limit state such as ground motion intensity measure (IM), peak ground acceleration (PGA), spectral acceleration at the fundamental building period, or any other intensity measures (Dasgupta 2017). Typically, the ground motion is defined as the peak ground acceleration (PGA) or spectral acceleration (Sa) at frequencies consistent with the ground motion (Bojorquez, and Iervolino 2011, Kircil, and Polat 2006). prescribed level of damage to a structure for a wide range of ground motion intensities. Fragility curves are extremely important for estimation of the overall risk to the civil structures from potential earthquakes and for predicting the economic impact of future earthquakes. The probability of being in or exceeding the damage state considering the damage parameter “shear failure” can be evaluated with respect to the formation of plastic hinge using the 식 (2)-(3) for before and after the formation of the plastic hinge, respectively.

$$PF = P[\varepsilon_{sv}(V_s + V_0) > \varepsilon_{Rv}(V_{R0} + V_N)] \quad (2)$$

$$F = P\left[\varepsilon_{sv}(V_s + V_0) > \varepsilon_{Rv}(V_{R0}(1 - 0.05\mu_\theta^{pl}) + V_N)\right] \quad (3)$$

where V_s is the COV of shear demand before plastic hinge, V_{R0}, COV of shear demand before plastic hinge, ε_{sv}, demand uncertainty factor for shear failure, uncertainty factor for

shear capacity, COV of the contribution of axial load to shear resistance (Column), COV of shear force due to gravity load (Beam), , uncertainty factor for the chord rotation ductility.

To produce the fragility curves, a total number of 25 artificial ground motion records were adopted. This helps to provide a thorough estimation of seismic demand accounting for the random nature of the earthquake. In this regard, the artificial ground accelerations were generated using a computer code developed in Matlab based on the method (Parajuli and Shrestha 2018). For all artificial earthquakes a total duration of 30 s was considered together with the moment magnitude of 7.7 Mw, and Epicentral distance of 133 km. To provide a better understanding, an example artificially produced ground acceleration is illustrated in 그림 2-40. The fragility curves illustrating the failure probability for beam and columns of irregular buildings were derived considering the peak ground acceleration (PGA) of 0.3g after the formation of the plastic hinge as provided in 그림 2-41.

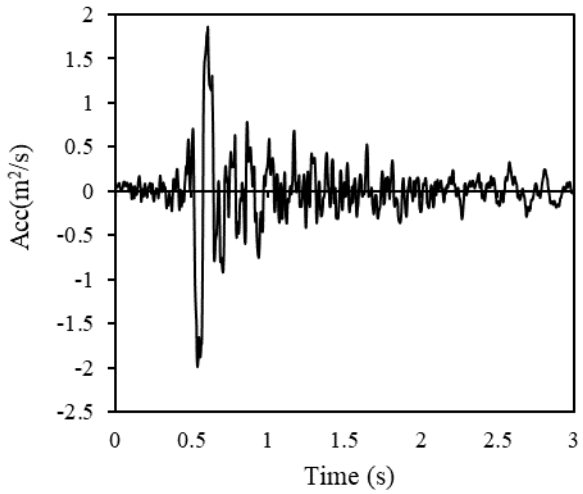
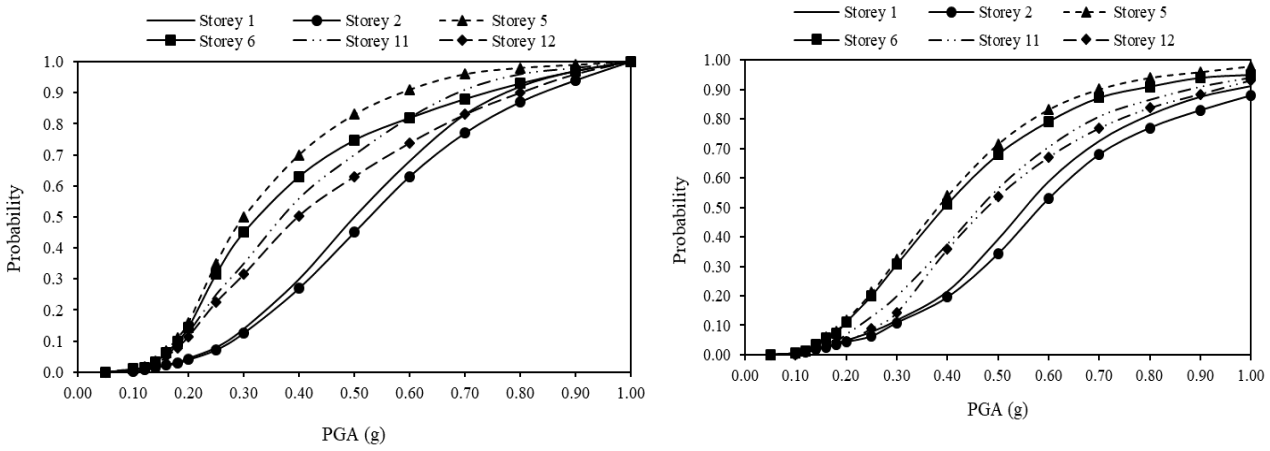
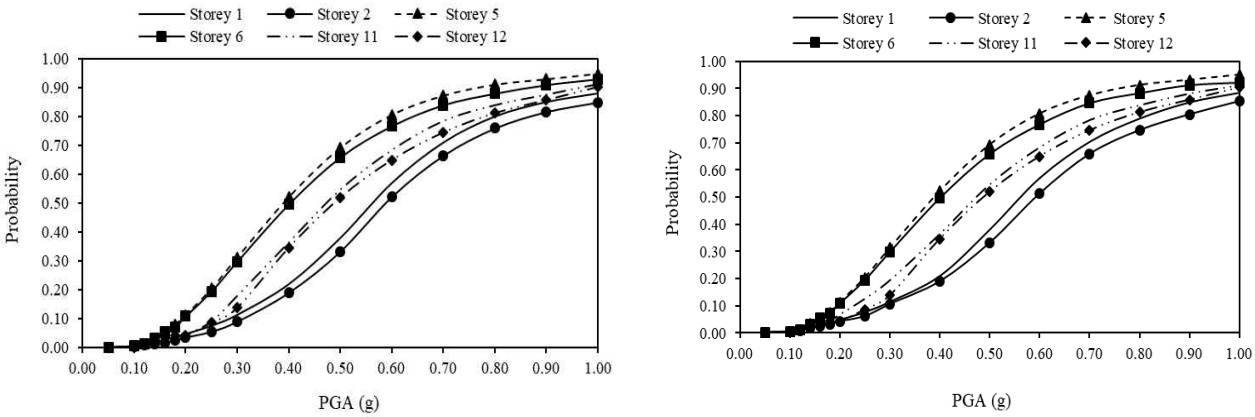


그림 2-40 An example of the artificial ground acceleration

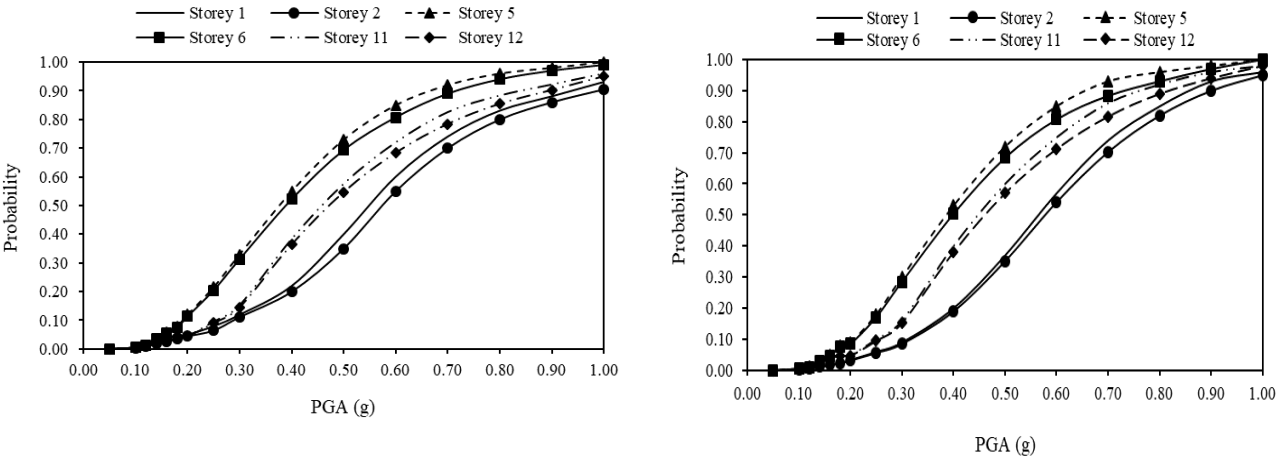
From the fragility curves given in 그림 2-41, it can be found that building with torsional irregularity had the highest probability of failure. It also concluded that the beams are more prone to failure than columns, so, in the design, they should be paid more considerations. Besides, the probability of failure of stories five and six of approximately all cases is higher than 50% for PGA= 0.4g. The lowest probability of failure was obtained for the first storey. After PGA=0.2 a sudden increase can be observed in the probability of failure. The concavities of the slope of fragility curves are similar for all stories showing that all the structural members follow a general pattern up to failure when a seismic load applies.



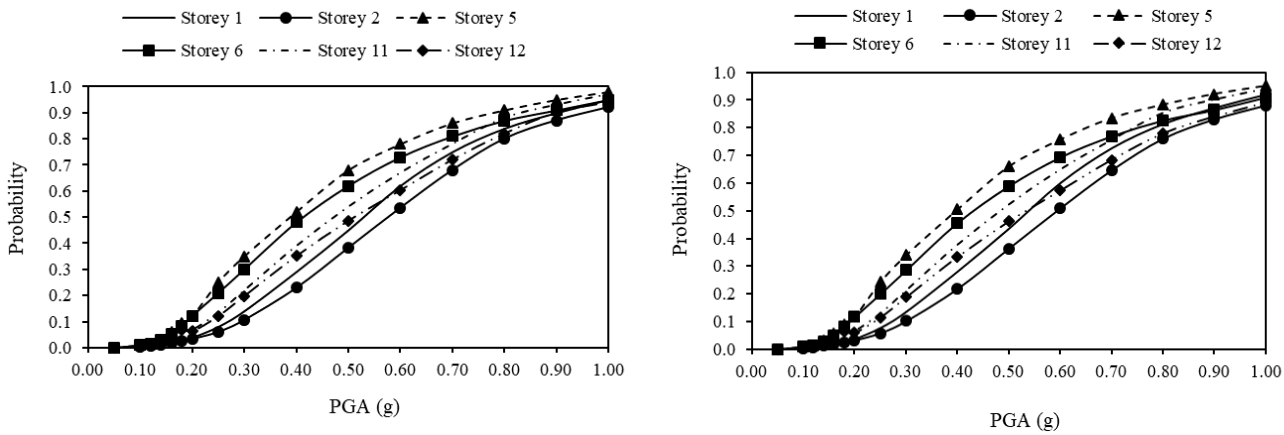
(a) Torsional irregularity



(b) Plan discontinuity



(c) Set-back



(a) Elevation discontinuity

Beam **Column**

그림 2-41 Fragility curves of the irregular building with vertical irregularity (Set-back)

6. 맺음말

The current study investigated the seismic performance of the twelve-storey steel frame buildings of 41.6 m height considering regular building and two main types of irregularity; in plan and elevation. The irregularity in the plan included two cases; torsional irregularity and discontinuity in the plan. For the irregularity in elevation two cases were taken into account; set-back and discontinuity in elevation. At the first step, the regular building was designed using SAP2000 and resulted in different profiles for the column; one to three:

0.50×0.50×0.05m, four to seven: 0.45×0.45×0.05m, and eight to twelve: 0.40×0.40×0.05m. Furthermore, the profile IPE 500 was considered for beams of all stories. After designing the regular building, the FEM software ABAQUS was used for the time-history analysis of the buildings with and without irregularities. First, the validity of the method of this study was evaluated through an example problem given in the literature. Making the comparison between the results of this study and literature, a good agreement was achieved, thus, the method was validated. A real set of ground accelerations of the Vrancea earthquake in Romania was adopted for the nonlinear incremental dynamic analysis of the cases of building adopted in this study. First, the regular building was modeled and analyzed, then, the irregular buildings were investigated. For the regular building, the results were extracted for two negative and positive peaks of seismic. Deformed shapes and corresponding displacements were provided for X-direction due to the symmetric plan of the building laid down in the X-Z plane. The results of irregular buildings were provided for just after the positive peak and were reported in both X- and Z- directions. Thereafter, the support reactions including displacements and moments were reported to provide a good insight into the effects of the irregularity on seismic resistance of the building. The seismic behavior of the buildings of different types and the effects of irregularities were investigated in terms of storey drift. To evaluate the status of the building from the viewpoint of failure, the fragility curves were derived and reported. Having investigated the results, the following outcomes were achieved:

The maximum drift increased with a steep slope as the irregularity degree of the storey increased.

For the residual drift, it could observe that with the increase in the storey irregularity the rate of increase in the residual drift increased compared to the stories with regular storey stiffness.

- From the comparison between regular and irregular buildings, it was found that the regular building significantly showed a better seismic performance than irregular buildings, and lower deformation was observed.
- From the comparison between two different types of irregularities, it was observed that the frame with irregularity in the plan had worse seismic performance than the building with irregularity in elevation.
- The torsional irregularity and discontinuity in elevation resulted in the highest drift, especially, at lower levels in the x-direction.
- In consonance with storey drift, the fragility curves showed that the torsional irregularity had the highest probability of failure.

- The higher probability of failure for stories five and six was obtained, therefore, they should be paid more considerations in the design procedure.

The results of this study would be beneficial for the designer engineers as it provides a valuable insight into the effects of different types of irregularity on the seismic performance and structural resistance of the high-rise buildings. It also provides useful information for the researchers and students to get the idea for further research works. As a further study, the interactive effects of irregularity, foundation, frame materials, building height, and plan on building seismic performance can be investigated.

■ 내부폭파를 고려한 유한요소해석 모델개발

내부폭파로 인한 주요부재의 손상도의 변화를 유한요소해석을 통해 정량적으로 해석하기 위하여 내부폭파에 대한 주요 변수 및 요소들을 구하고, 그 변수 및 요소들의 내부폭파 상황에서의 상관관계를 구하여 내부폭파의 유한요소 모델을 제안

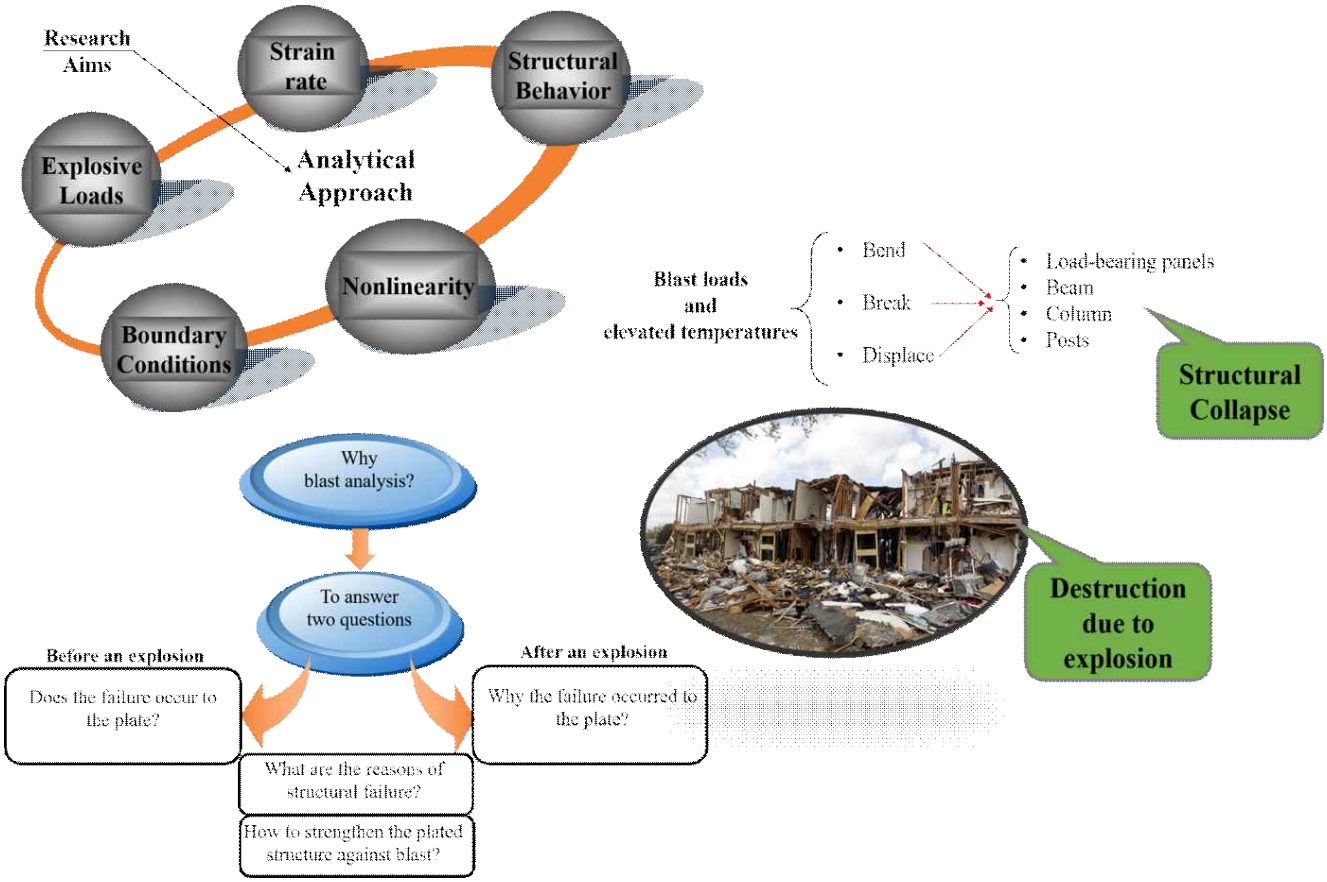


그림 2-42 폭파모델 개발 개념도

1. 서론

Destruction of plated structural elements and structures as a whole subject to explosive loads has raised much attention and significant importance in a wide area of engineering disciplines such as civil, mechanical, aerospace, machine, and vehicle manufacturing (Li, et al., 2020; Xu, et al., 2020). Besides, the dynamic behavior of the plated-structures is of great importance in the design of blast-resistant structures (Syed, et al., 2018; Koneshwaran, Thambiratnam, Gallage, 2015). During an explosion, a large amount of energy is released while producing the blast wave coming in the form of pressure waves and hot gasses (Momeni, et al, 2015; Vapper, Lasn, 2020; Kim, et al, 2011). Hot gasses would expand and occupy the space transmitting spherically through the unbounded surrounding medium (Li, Chen, Hao, 2019; Liu, et al., 2019; Shim, et al, 2013). Along with the produced gasses, the air around the point of burst expands and results in the molecules pile-up well-known as the blast wave and a shock front (Liew, 2008). Blast-induced forces cause substantial damage to the structural elements and result in a total or a partial failure without any proportionality between the initial and the ultimate devastation (Mohammadzadeh, Noh, 2015; Moghimi, Driver, 2015; Formi, Chiaia, Cadoni, 2017).

Having looked into the civil engineering-related literature, numerous studies can be found dealing with dynamic analysis of structures subject to wind, earthquakes, hydrodynamics, and bending (Mohamadzadeh, Noh, 2012; Choi, et al, 2018), however, a few studies can be found dealing with structures exposed to the explosion. Some of them performed experimental works (Clubley, 2014; Rolfe, et al, 2017; Wang, Zhao, 2020) but they were limited due to high costs, and some carried out analytical and numerical analysis (Markose, Rao, 2017; Gharababaei, Darvizeh, A., Darvizeh, H., 2010; Al-Thairy, 2018) but very less due to the inherent complexity of the blast phenomenon and structural responses. There has always been the possibility for a structure comprising civil residential buildings and or industrial containment buildings to be subject to blast waves. No matter a structure is made of concrete or steel, the application of the steel plates, amain structural element of reinforcing element is inevitable, thus, the dynamic behavior of the blast loaded plates has been investigated by several studies (Sabuwala, Linzell, Kraithammer, 2005; Byfield, 2006). The disclosure of the nonlinear behavior of the structures made of ductile materials subject to blast loads is a paramount concern in the fields of industrial, military, and civil engineering (Moriello, et al, 2020). It has been documented that there are three common plate responses to an explosive load; 1) large inelastic deformation, 2) inelastic deformation with tensile-made material rupture, and 3) transverse shear-made rupture with small deformation (Teeling-Smith, Nurick, 1991; Nurick, Shave, 1996). Several studies have reported experimental works investigating the plate responses considering a variety of shapes, namely, square (Li, et al., 2017), rectangular (Zhang, Ye, Qin, 2019), and circular (Schiffer, Tagarielli, 2015) as well as the assessment of the effects of different boundary conditions (Peng, Yang, 2008; Amabili, et al., 2020; Bonorchis, Nurick, 2007) and stiffener configurations (Zhao, et al., 2020).

Kim (2015) conducted a set of numerical, analytical, and experimental works to examine the efficiency and function of a blast-resistant earth-covered magazine manufactured by the use of corrugated steel plates. It was observed that no fracture occurred to the bolted joints of the corrugated steel plates. Besides, the steel surrounding the bolts did not experience destruction. A drawback that can be pointed out was that the experiment was expensive from viewpoints of cost and time. It was a huge obstacle for the investigation of various effective parameters on blast responses of the plate.

Lee (2016) presented a series of elastoplastic design charts for protective structures exposed to explosive forces. The accuracy of the study was evaluated by employing the existing design charts with a finite element method through LS-DYNA. Their study was limited to an SDOF design considering only the location near to the point of explosion i.e. the scaled distance which is a very important parameter in blast-design and analysis was not investigated.

Mohammadzadeh (2016, 2017) presented a comprehensive study including a nonlinear dynamic approach for investigation of the blast loaded sandwich plates with functionally graded material (FGM) face sheets resting on the elastic foundation as well as a simplified analytical method of a steel plate subject to blast load. They employed Hamilton’s principle, higher-order shear deformation theory to obtain a set of differential equations of motion while the Navier’s solution was adopted to solve the equations of motion. To examine the validity of the method,

displacement time-history obtained from the analytical method were compared with FEM using ABAQUS and literature. Their work for steel plate did not consider the nonlinearity and strain rate which affect the blast responses of the plate. Besides, their work for the composite plate was very complicated making it difficult to use, especially, for the intermediate engineers and researchers. Yuan (2013) assessed the deformation and failure of the fully clamped rectangular plates subject to a zero-period impulsive load through a numerical approach. In this regard, the nonlinear analysis of the rectangular plate was carried out to find out the central deflection of the plate for the various aspect ratios. Mirzababaei (2016) provided a theoretical investigation of the inelastic behavior of the fully clamped thin quadrangular plates subject to impulsive forces with two different distributions. The aim was to provide a method of calculating deflections of the quadrangular plate exposed to uniformly distributed and localized loadings. A drawback of this work is that it was limited to one type of boundary conditions and thin-plates only. In real structures, there are various types of plates from viewpoints of boundary conditions and thickness, especially, for protective structures and ship hull which utilize thick plates.

From the literature explained, it can be found that conducting the experimental research works dealing with blast loads needs a high amount of financial resources which limits the work substantially while they encounter serious hazards. Therefore, analytical and numerical approaches could be a potential alternative for the experiments. However, the given analytical approaches face two main drawbacks; one is that they are limited to some of the effective parameters. For example, only one boundary condition was considered, and or the scaled distance was not paid attention. Second is that they could be hardly employed for the analysis of the plated structures due to their complexity, especially, for beginner to intermediate users. Therefore, a need for a simple-to-use approach considering various blast-related effective parameters for prediction of the dynamic responses of plated structures exposed to explosion comes up. Ringing up a simplified analytical approach will be helpful for not only researchers but also engineers and structural designers, to validate their numerical methods of application or their designs, whereas complicated methods using the higher-order shear deformation theory for which definition and calculation of a series of parameters and coefficients are only possible for those having a piece of rich knowledge in this regard. The lake of such a simple method motivated this study to present a novel simplified nonlinear analytical approach for investigation of the isotropic plates subject to explosive loads considering different boundary conditions, material nonlinearity, and strain rate which is of high importance in blast design and analysis. Besides, the stand-off distance (scaled distance), and charge weight were included in the description of the blast load as well as the plate geometry. In this method, analytical formulas were provided for predicting maximum plate deflection and bending moment. For this aim, Navier's solution was adopted to derive analytical formulas. The distribution of the load was assumed as independent of the location on the plate surface. Besides, the material nonlinearity and strain rate were included in the method to provide an accurate nonlinear method. Afterward, the largest deflection and the utmost bending moments around the x and y-axes were obtained for the center point of the plate. The method validation was executed by

making a comparison between the results obtained from the presented method and the finite element method through ABAQUS. Later on, to have a well-comprehension of the efficiency and applicability of the method, a set of parametric studies was carried out to examine the effects of the plate thickness, aspect ratio, and weight of the charge on the dynamic behavior of the plated structures by the use of the presented method. This simple method can be employed for design purposes, especially, at the early stages requiring a swift approximation of the structural behavior and easy-to-use for engineers and researchers of beginner to intermediate levels. The novelty of this work lies in the fact that although this is a simple approach, it included all the most important parameters affecting the dynamic responses of the blast loaded plates; material nonlinearity, time-dependent deformation (strain rate0, geometrical specifications of the plate and boundary conditions.

2. 플레이트 변위의 정의

2.1. 모델링 개요

2.1.1. 플레이트 형상 및 하중 패턴

A schematic of a rectangular plate with a longitudinal dimension of '*a*' along with X-direction, lateral direction of '*c*' along with Y-direction, and a transverse dimension of '*h*' along with Z-direction is illustrated in 그림 2-43.

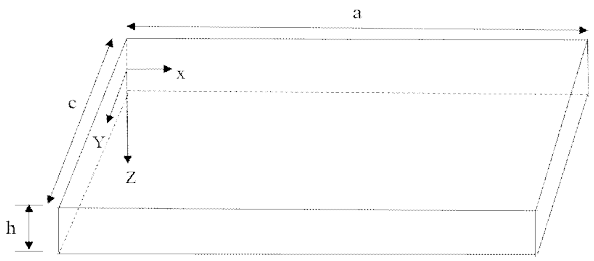
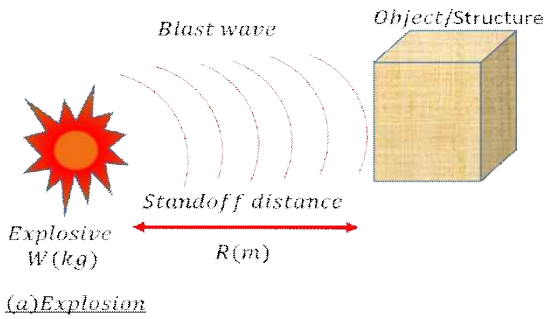


그림 2-43 Schematic of plate

The propagation of a typical blast wave in its surrounding air can be represented in the form of a pressure-time graph as illustrated in 그림 2-44.



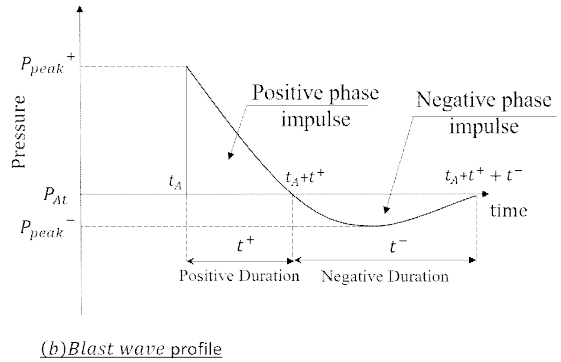


그림 2-44 Schematic of (a) typical explosion and (b) blast wave propagation into surroundings

In 그림 2-44, P_0 represents the ambient atmospheric pressure, P_{s0^+} peak positive pressure (MPa), P_{S0^-} peak negative pressure, t_A the wave arrival time (ms), t_{0^+} positive phase duration (ms), t_{0^-} negative phase duration (ms), b dimensionless wave decay coefficient. Propagation of the blast wave pressure over the surface of the plate can be stated as a function of time, positive phase pressure, and ambient pressure by modifying the Friedlander equation and Bajic's peak pressure equation as shown in 식 (4) (Byfield, 2006):

$$P_{\in}(t) = P_A + \left[0.1\left(1.02\frac{1}{Z} + 4.36\frac{1}{Z^2} + 14\frac{1}{Z^3}\right)\right]\left(1 - \frac{t}{t^+}\right)e^{\left(\frac{-b(t-t_A)}{t^+}\right)}, \quad (4)$$

where $P_{in}(t)$ is the time-dependent blast pressure (MPa), the atmosphere pressure, Z the scaled distance defined as $Z = R/W^{1/3}$ for which W represents charge weight (kg), and R shows the standoff distance (m), the distance from charge to object. This equation expresses the blast load considering the positive impulse only as it is more substantial than the negative phase in terms of structural collapse prevention. The consideration of the negative phase can be examined with respect to the scaled distance, Z. For the scaled distances, Z, if the value is less than 50, the influence of the negative phase can be neglected (Goel, et al., 2012). Consideration of the stand-off distance when R= 1.0 m resulted in the values of Z much smaller than 50, so the positive phase was only considered.

The main aim of the current study was to present a simple analytical equation to find the maximum plate displacement that occurred due to the explosive loads. The damping effect was not included as it has been documented that the damping does not significantly affect the ultimate displacement of the plates subject to blast loads (Mohammadzadeh, Noh, 2015).

2.1.2. 주요 변수 고려

In this method, the most important parameters affecting the blast responses of isotropic plates were considered, namely, thickness, aspect ratio, and boundary condition of the plate as well as the charge weight. Another important parameter included in the method is the scaled distance which represents the distance between the explosive charge and the target object. Besides, the material nonlinearity and strain rate were included in the method as they prevent the overestimation of the plate displacement, thus, an economic design can be achieved.

(a) 플레이트 종횡비:

This parameter was considered to normalize and generalize the plate dimensions which helps to conduct parametric analysis. In practice, plates with different dimensions are used depending on the application and type of load. It has been documented that the plate dimensions have a significant effect on the shell and plate frequency, static and dynamic responses (Kang, Davison 2013; Eslami-Maid, Rahbar-Ranji, 2015), thus, it was taken into account in the method of this study to predict the displacement of the plates subject to blast load.

(b) 플레이트 두께

It has been documented that the plate resistance, static, and dynamic response are significantly dependent on the plate thickness, such that the plate buckling and displacement is a cubic function of plate thickness (Lee, Shepherd, Evernden, 2020). Therefore, this parameter was included in the method to provide a precise prediction of the plate responses subject to the blast load.

(c) 경계조건

Boundary conditions (B.Cs.) have a significant effect on the plate frequency and responses under both static and dynamic loads, especially, from the viewpoint of edge supports (Mijušković, et al., 2020). Two frequently used edge supports in practical applications are simply supported and clamped. Thus, this study included these two B.Cs., into the method to enable the users to have a precise prediction of the plate responses concerning the desired B.C .

(d) 폭약량과 거리

The explosion process is very complicated in terms of charge weight which brings great trouble to a mathematical solution (Li, et al., 2020). The amount of charge directly affects the material and geometrical nonlinearities as well as the displacement of the target plate. As the charge weight increases the amounts of nonlinearity and deflection increase. The importance of this parameter motivated this study to include it into the method to precisely predict the plate displacement. The scaled distance is adopted for the determination of the pressure-time profile of a blast wave. It can be expressed in the form of $Z = R/W^{1/3}$ in which R is the distance of the explosive from the point of interest and W is the charge weight.

(e) 재료비선형성, 경화 및 변형률:

The blast loads cause nonlinearities in the construction material of the target plate and result in a decrease in the stiffness of the materials such that in some cases a material failure is observed (Peng, Yang, Hu, 2020). Besides, the plate displacement and strain changes with time

which can be defined in the form of strain rate, thus, the inclusion of the strain rate is vital for a method used for predicting the dynamic responses of the blast loaded plates.

2.1.3. 지배방정식

The governing differential equation of the plate accounting for the applied blast load can be given in the form represented in 식 (5) (Ventsel, Krauthammer, 2001):

$$\frac{\partial^4 w}{\partial x^4} + 2\frac{\partial^4 w}{\partial x^2 \partial y^2} + \frac{\partial^4 w}{\partial y^4} + \frac{12\rho h(1-\nu^2)}{Eh^3}\frac{\partial^2 w}{\partial t^2} = \frac{12P(t)(1-\nu^2)}{Eh^3}, \tag{5}$$

where w' is displacement along with thickness, 't' is time, 'ρ' is the mass density per unit volume, 'h' is the plate thickness, '$P(t)$' is the blast load, E is the modulus of elasticity, and υ is Poisson's ratio.

2.1.4. 재료 비선형성 고려

For considering the material nonlinearity into the equation of plate displacement, the Ramberg-Osgood model was employed (Ozakgul, 2015). It describes the nonlinear relationship between stress and strain in the materials near the yield point which accounts for the strain-hardening behavior. The total strain composed of elastic and plastic strains can be defined as represented in 식 (6a):

$$\varepsilon = \frac{\sigma}{E} + K\left(\frac{\sigma}{E}\right)^n \tag{6a}$$

where ε is the strain, σ stress, E Young's modulus, K, and n are material constants defining the hardening behavior of the material. The first part of 식 (7a), $\frac{\sigma}{E}$, is the elastic part while the second part, $K\left(\frac{\sigma}{E}\right)^n$, indicates the plastic part. By defining the yield strength of the material, σ_0, K can be represented as $K = \alpha\left(\frac{E}{\sigma_0}\right)^{n-1}$ and 식 (6a) can be rearranged as shown in 식 (6b):

$$\varepsilon = \frac{\sigma}{E} + \alpha\frac{\sigma}{E}\left(\frac{\sigma}{\sigma_0}\right)^{n-1} \tag{6b}$$

where and n dominate the hardening behavior of the material.

2.1.5. 경화 현상 고려

In the Ramberg-Osgood model, the hardening behavior of the material is defined by and n. Since there is a power-law relationship between stress and plastic strain, the plastic strain remains even in case of very low-stress levels. Values for α can be found by fitting to

experimental data or it can be fixed to have the yield offset equal to the permissible value of strain of 0.2%, which means =0.002. The parameter n takes usually the amount of 5 or greater. The usual representation of non-linear behavior can be implied as 식 (7a) represents:

$$\varepsilon = \frac{\sigma}{E} + 0.002(\frac{\sigma}{\sigma_{ys}})^n, \tag{7a}$$

where is yield strength. The tangent modulus is defined by inverting 식 (7b):

$$(E_t)_\Gamma = \left(\frac{E\sigma_{ys}}{\sigma_{ys}+0.002nE\left(\frac{\sigma}{\sigma_{ys}}\right)^{n-1}} \right)_\Gamma \tag{7b}$$

where is the specific direction, x, y, or z.

2.1.6. 변형율 고려

In the case of severe dynamic loading such as seismic loads, the inclusion of strain rate gains importance and helps to achieve more precise results. It is appropriate to note that most of the metallic materials and composites show an increase in the yield stress with increasing strain rate. Strain rate effects can be included by adjusting the material dynamic yield stress as given in 식 (8a):

$$\dot{\varepsilon} = D(R-1)^{\varphi}, \tag{8a}$$

where R is the ratio of the dynamic yield stress to the static yield stress and D and are experimentally defined material coefficients. The material failure occurs instantaneously when the local stress reaches critical stress (the dynamic failure strength of materials); the dynamic failure strength is assumed to be dependent to the local strain rate, and the relation between the dynamic failure strength and the strain rate was taken as an intrinsic property of materials, which can be derived experimentally. 식 (8b), which is known as Cowper-Symonds relation, can be obtained by rearranging 식 (8a).

$$\sigma_y = \sigma_0\left[1 + \left|\frac{\dot{\varepsilon}}{D}\right|^{\frac{1}{\varphi}}\right], \tag{8b}$$

By substituting 식 (8b) into 식 (7b), the tangent modulus including strain rate can be defined as shown in 식 (9):

$$(E_t)_\Gamma = \frac{E\sigma_0\left[1+\left|\frac{\dot{\varepsilon}}{D}\right|^{\frac{1}{\varphi}}\right]}{\sigma_0\left[1+\left|\frac{\dot{\varepsilon}}{D}\right|^{\frac{1}{\varphi}}\right]+0.002nE\left(\frac{\sigma}{\sigma_0\left[1+\left|\frac{\dot{\varepsilon}}{D}\right|^{\frac{1}{\varphi}}\right]}\right)^{\varphi-1}}, \tag{9}$$

In this study for consideration of the strain rate the hardening behavior parameters were adopted as D = 40 s and = 5.

2.2. 경계조건

In this study, to include the edge effects, two cases of boundary conditions (B.Cs) were considered; case 1: simply supported plate and case 2: clamped plate. Case 1 assumes the out of plane deflection (w) at plate edges, the moment about X-axis (at x=0&a, moment about Y-axis () at y=0&c, while the amounts of ,, and w at t=0 is equal to zero.

It has been documented that the clamped plate mode shapes are always highly sinusoidal near the nodal lines, which are occurred in regions far enough removed from the boundaries to be virtually unaffected (Shooshtari, Khadem, 2006; Civalek, Ersoy, 2008). It has been proven that a simply supported edge must be nearly satisfied at every point along such a nodal line. Therefore, every nodal line can be considered equivalent to a simply supported boundary. Mode shapes can be generated by having straight nodal lines being parallel to the plate boundaries. Therefore, vibration modes corresponding to the clamped boundary conditions can be defined by employing the same numbering system, as simple sinusoidal series, as that of a simply supported solution, except in regions very close to the clamped boundary. Accordingly, a clamped plate can be simulated as a part of a simply supported plate mostly in the middle part as illustrated in 그림 2-45.

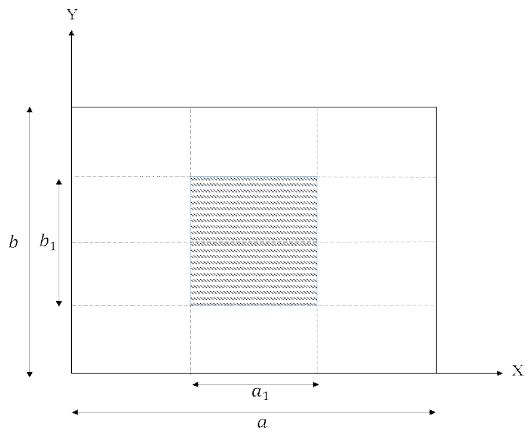


그림 2-45 Illustration of simulation of a clamped plate as a part of a simply supported plate

For considering the effects of edge boundary conditions such as a clamped plate, in this study, it was supposed that the plate is a part of a simply supported plate. Based on this assumption and the abovementioned explanations the boundary conditions can be represented as noted hereunder:

$$w=0, \quad \frac{\partial^2 w}{\partial x^2}=0 \qquad \text{for x=0 and x=}a,$$

$$w=0, \quad \frac{\partial^2 w}{\partial y^2}=0 \qquad \text{for y=0 and y=}c,$$

$$w=0, \quad \frac{\partial w}{\partial t}=0 \qquad \text{at } t=0.$$

2.3. 변위의 해 도출

2.3.1. 급수형태로 하중 및 변위 정의

The applied load, can be represented in the form of series as shown in 식 (10) (Mohammadzadeh, Noh, 2019)

:

$$P(x,y,t) = \sum_{m=1}^{\infty}\sum_{n=1}^{\infty} f_{mn}(t)W_{mn}(x,y). \tag{10}$$

where is the time-dependent part of the applied load, and is the displacement-dependent component of the equation. For the inclusion of the dynamics into the approach of this study, the plate deflection could be defined in terms of the time and the plate geometry. The time and the position deflection of the plate w are represented by the function as shown in 식 (16):

$$w(x,y,t) = \sum_{m=1}^{\infty}\sum_{n=1}^{\infty} F_{mn}(t)W_{mn}(x,y), \tag{11}$$

where the function is the time-dependent part of the deflection while m and n are the mode shape numbers representing the number of half-waves of vibration along with the x and the y directions, respectively. 식 (11) composed of two functions; one is , the time-dependent part expressing the change in the blast wave intensity and plate displacement with respect to time, and the second is stating the displacement over the area of the plate. In this study, the updatable plate frequency was defined for the inclusion of the material nonlinearity. It inherently includes the flexural rigidity and tangential modulus of elasticity as given in 식 (12a) and (12b) for simply supported and clamped boundary conditions, respectively:

$$\omega_{u(mn)}^2 = \frac{\pi^4 (E_t)_{\Gamma} h^2}{12\rho(1-\nu^2)}\left[\left(\frac{m}{a}\right)^2 + \left(\frac{n}{b}\right)^2\right]^2, \tag{12a}$$

$$\omega_{u(mn)}^2 = \frac{\pi^4 (E_t)_{\Gamma} h^2}{12\rho(1-\nu^2)}\left[\left(\frac{m_1}{a_1}\right)^2 + \left(\frac{n_1}{b_1}\right)^2\right]^2, \tag{12b}$$

Where m and n are the numbers of half sine-waves corresponding to the mode shapes of the plate, and are the half sine-waves of mode shapes between the nodal lines closest to the clamped boundary conditions. Parameters a, b, and are dimensions defined in 그림 2-3. Having these all, can be expressed as given in 식 (13):

$$F_{mn}(t) = A_{mn}\cos\omega_{u(mn)}t + B_{mn}\sin\omega_{u(mn)}t + F_{mn}^{(p)}(t), \tag{13}$$

where is considered to be a particular solution of 식 (5), while and are constants which will be obtained later.

2.3.2. 특수해

The function shown in 식 13 must satisfy 식 (14):

$$\ddot{F}_{mn}(t) + \omega_{u(mn)}^2 F_{mn}(t) = \frac{1}{\rho h} f_{mn}(t), \tag{14}$$

where is the second time derivative of , the updated frequency, and is an arbitrary expression. By setting and , the particular solution of 식 (10) was achieved as given in 식 (15):

$$F_{mn}^{(p)}(t) = \frac{exp\left(\frac{-b(t-t_A)}{t^+}\right)}{\rho h\left(\left(\frac{b}{t^+}\right)^2 + \omega_{u(mn)}^2\right)}. \tag{15}$$

2.4. A_{mn}와 B_{mn}의 정의

For solving the governing differential equation of the motion, the Navier method was employed. It was assumed that the solution of the equation of motion, and the plate displacement, are functions of time and displacement. Based on the Navier method, the displacement dependent section was defined in the form of a trigonometric series; y (Zhang Ye, Qin, 2019, Schiffer, Tagarielli, 2015) . It accounts for the fundamental mode and satisfies the boundary conditions. Considering and uniform distribution of the blast load on the plate resulting in and having applied the boundary conditions w=0 and at t=0, indicating that the plate is at rest at an initial moment, and can be obtained as given in 식 (16a) and (16b), respectively:

$$B_{mn} = \frac{b}{t^+ \omega_{u(mn)}} \cdot \frac{exp\left(\frac{bt_A}{t^+}\right)}{\rho h\left(\left(\frac{b}{t^+}\right)^2 + \omega_{u(mn)}^2\right)}, \tag{16a}$$

$$A_{mn} = -\frac{exp\left(\frac{bt_A}{t^+}\right)}{\rho h\left(\left(\frac{b}{t^+}\right)^2 + \omega_{u(mn)}^2\right)}. \tag{16b}$$

2.5. 변위와 휨 모멘트

The equation of the plate deflection was obtained by substituting the equations obtained for and into 식 (11) as given in 식 (17):

$$w = \frac{exp\left(\frac{bt_A}{t^+}\right)}{\rho h\left(\frac{b}{t^+}\right)^2} \sum_{m=1}^{\infty} \sum_{n=1}^{\infty} \frac{1}{\left(1 + \left(\frac{t^+ \omega_{u(mn)}}{b}\right)^2\right)} \left[-1 + \frac{b}{t^+ \omega_{u(mn)}} + exp\left(\frac{-bt}{t^+}\right)\right] G_{mn} \sin \alpha_m x \sin \beta_n y. \tag{17}$$

It is notable vanishes when mode shape numbers take even numbers while having the case of odd numbers , thus, 식 (17) can be rearranged as 식 (18) represents:

$$w = \frac{16P(t)exp\left(\frac{bt_A}{t^+}\right)}{\rho h\pi^2\left(\frac{b}{t^+}\right)^2}\sum_{m=1,3,\cdots}^{\infty}\sum_{n=1,3,\cdots}^{\infty}\frac{1}{mn\left(1+\left(\frac{t^+\omega_{u(mn)}}{b}\right)^2\right)}\left[\frac{b}{t^+\omega_{u(mn)}}+exp\left(\frac{-bt}{t^+}\right)-1\right]\sin\alpha_m x\sin\beta_n y. \quad (18)$$

In this study the updatable flexural rigidity was introduced which itself includes the updated tangential modulus of elasticity of the plate materials representing the material nonlinearity as shown in 식 (19).

$$D_u = \frac{(E_t)_\Gamma h^3}{12(1-\nu^2)} \quad (19)$$

Having and by setting the time-dependent part of 식 (18) to , the maximum bending moments were obtained as given in 식 (17a) and (17b):

$$M_x = \frac{16D_u P(t)exp\left(\frac{bt_A}{t^+}\right)}{\rho h\pi^2\left(\frac{b}{t^+}\right)^2}\sum_{m=1,3,\cdots}^{\infty}\sum_{n=1,3,\cdots}^{\infty}F(t)\left(\frac{m^2\pi^2}{a^2}+\nu\frac{n^2\pi^2}{c^2}\right)\sin\frac{m\pi}{a}x\sin\frac{n\pi}{c}y, \quad (19a)$$

$$M_y = \frac{16D_u P(t)exp\left(\frac{bt_A}{t^+}\right)}{\rho h\pi^2\left(\frac{b}{t^+}\right)^2}\sum_{m=1,3,\cdots}^{\infty}\sum_{n=1,3,\cdots}^{\infty}F(t)\left(\nu\frac{m^2\pi^2}{a^2}+\frac{n^2\pi^2}{c^2}\right)\sin\frac{m\pi}{a}x\sin\frac{n\pi}{c}y. \quad (19b)$$

2.6. 플레이트 중심에서의 변위 평가

It has been documented that the maximum deflection and the bending moments could be occurred, mostly, at the plate center, and Having considered the fundamental mode, m=1, and n=1, as well as the time at which the maximum deflection occurs , the maximum plate deflection can be found by 식 (17):

$$w_{max} = \frac{16P_{s0+}exp\left(\frac{bt_A}{t^+}\right)}{\rho h\pi^2\left(\left(\frac{b}{t^+}\right)^2+\omega_{u(11)}^2\right)}.\left(1-\frac{t_{max}}{t^+}\right).exp\left(\frac{-b(t_{max}-t_A)}{t^+}\right)\left[-1+\frac{b}{t^+\omega_{u(11)}}+exp\left(\frac{-bt_{max}}{t^+}\right)\right] \quad (20)$$

3. ABAQUS를 이용한 유한요소해석

It has been documented that the finite element method (FEM) was extensively used for the analysis of the wide range of structures and systems incorporated with the static and dynamic problems (Khan, Al-Osta, Lbrahim, 2017; Rajendran, Narasimhan, 2006). Some researches employed commercially available FEM packages such as ABAQUS for dynamic analysis of structures (Li, et al., 2017; Gulkhan, Korucu, 2011). Several studies can be found dealing with examining the finite element method efficiency and accuracy for analysis of a variety of structures subjected to the various loading patterns such as compression, blast, and impact loads (Nam, et al., 2008; Imbalzano, et al., 2018).

To examine the credibility of the analytical method, the numerical dynamic analysis of the isotropic steel plate subject to blast loads comprising the time-dependent deformations was performed. For this aim, the commercially available finite element package ABAQUS and adopting the guidelines given in (Farzin, Dibajian, 2012; Tavakoli, Kiakojouri, 2014; Rashid, James, 2009).

3.1. 해석 유효성

The validity of the method was examined by making a comparison between the analytically- and numerically-based time-history and maximum deflection considering different plate thickness, aspect ratio, and charge weight for simply supported plates. 그림 2-46 provides a typical illustration of a simply supported plate subject to a blast wave pressure.

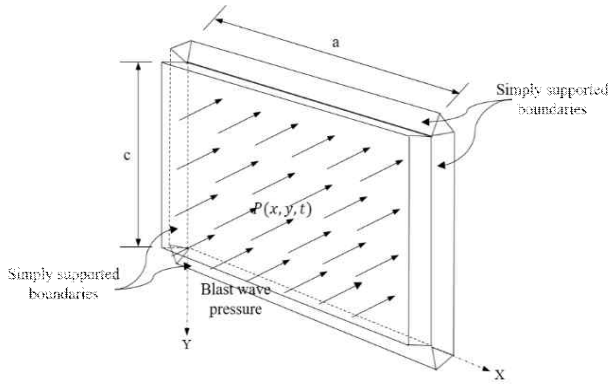


그림 2-46 Typical illustration of the simply supported blast loaded plate

In another attempt the maximum displacement was obtained for a variety of charge weight and two different boundary conditions; simply supported and clamped plates. The explosive load was applied to the plane of the plate in the form of a pressure time-history. Since the magnitude of the pressure wave varies with time time-dependent blast load was expressed in ABAQUS in the form of tabular amplitude considering the positive phase of the blast wave, only. 그림 2-47 depicts the time-history profile of a typical pressure wave due to a charge of 50 kg.

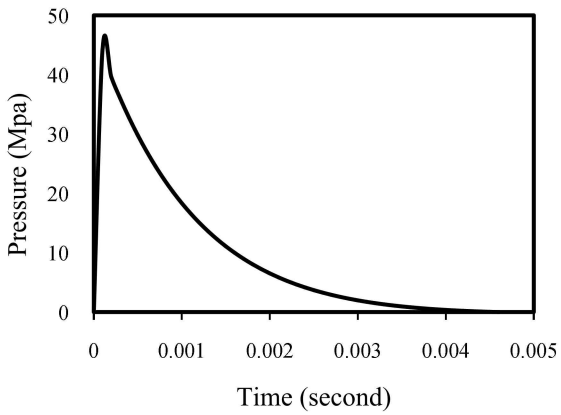


그림 2-47 Positive phase of blast wave pressure due to 50 kg of the explosive charge

To carry out the numerical analyses, the dynamic explicit approach was adopted since for the short-duration phenomenon such as an explosion, it precisely predicts the stress variation as a highly important parameter. For this type of analysis, a very short time-step must is required to achieve convergence and accurate results.

3.2. 수렴 연구

In this study, solid elements were adopted for the modeling of plates in ABAQUS including first-order (linear), and second-order (quadratic) interpolation elements expressed in one, two, or three dimensions. Triangle and quadrilateral elements were categorized as two-dimensional elements while tetrahedral, triangular prisms, and hexahedra known as bricks were presented in three dimensions. It has been proved that the second-order elements are powerful for the modeling of geometric features and can lead to more accurate results as they effectively catch the stress concentrations. For the element stiffness, the full-integration and the reduced-integration elements are available in the library of ABAQUS. The reduced integration saves running time, which is especially true in three dimensions. For example, the element type C3D20 has 27 integration points, while the C3D20R has only 8. Therefore, the element assembly for the C3D20 is roughly 3.5 times more costly than for the C3D20R. The reduced integration is also referred to as the uniform strain or the centroid strain elements with hourglass control. The second-order reduced-integration elements in the ABAQUS generally yield more accurate results than the corresponding fully integrated elements.

In addition to the abovementioned explanations, a convergence study was carried out to find out the most efficient element and optimized size. For this aim, a steel plate of AR=2 and 10 mm thickness having the natural period of was subjected to a blast load due to a burst of 1.0 kg with a loading duration of . The central plate displacement was obtained for different mesh types and variations of the number of elements. Three types of elements were considered; C3D20, and C3D20R, as well as a three-dimensional 8-node, doubly curved thick shell element with reduced integration (S8R). The central displacement of the plate was normalized concerning plate thickness and plotted versus the number of elements as shown in 그림 2-6.

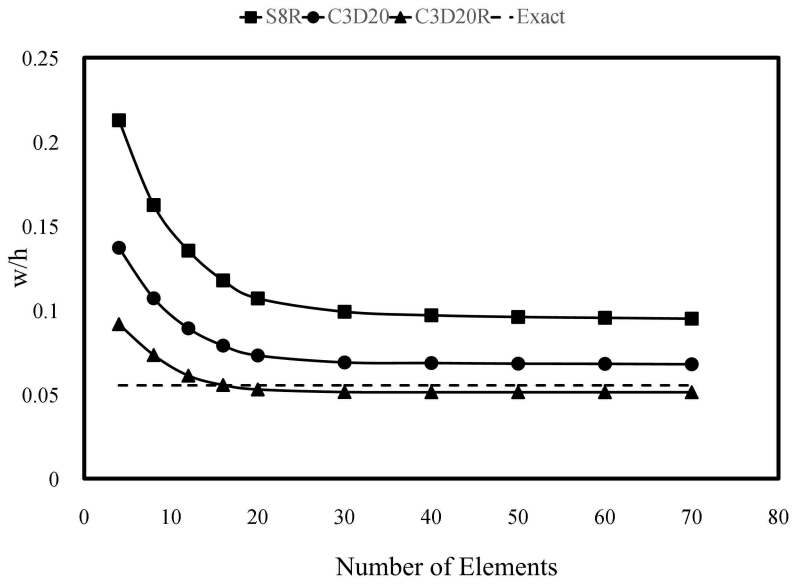


그림 2-48 Convergence study representing the variation of the normalized plate displacement obtained from the numerical model for the number of elements for different element types; S8R, C3D20, C3D20R

From the convergence study illustrated in 그림 2-48 it can be observed that after the number of 30 elements, the results are converged Considering all the explanations above as well as the results of the convergence study given in 그림 2-48, the 20-node quadratic (brick) elements with the reduced integration formulation(C3D20R) were adopted for the numerical modeling and investigation of the target plates of this study.

4. 결과 평가

For the aim of accreditation of the presented method and to generalize the outcomes and achievements, the numerical approach through ABAQUS was adopted. Accordingly, In the first step, the validity of the method was examined by comparing the analytical and numerical results in terms of displacement time-history, and maximum displacement considering various plate thickness, aspect ration, and boundary conditions. Thereafter, the effect of variation of the charge weight, the plate thickness, aspect ratio, and boundary conditions on the blast resistance of the steel plate was investigated through the parametric study.

4.1. 모델 검증

4.1.1. 시간이력 비교

The validation of the proposed method was examined in terms of the loading duration ( ) and the natural period of the plate () since they highly affect the nature of the dynamic responses of a system. If the duration of the applied load is smaller than half of the natural period of the plates, , the maximum response of the plate develops in the free vibration phase. The opposite occurs if , and the maximum response of the plate develops in the forced vibration phase (Chopra, 2001).

In this part, the validity of the presented analytical method was examined by making a comparison between the displacement time-histories of the blast loaded plates obtained from analytical and numerical approaches. For this aim, two main batches of loading duration smaller and greater than the plate natural frequency were considered while for each batch three cases of plate aspect ratio were considered, namely, AR=1, 2, 4 as they are adopted for the parametric studies. This study adopted the construction steel having the material characteristics represented in 그림 2-49 to be assigned to the plate. The modulus of elasticity of steel is E=200 GPa and Poisson’s ratio is

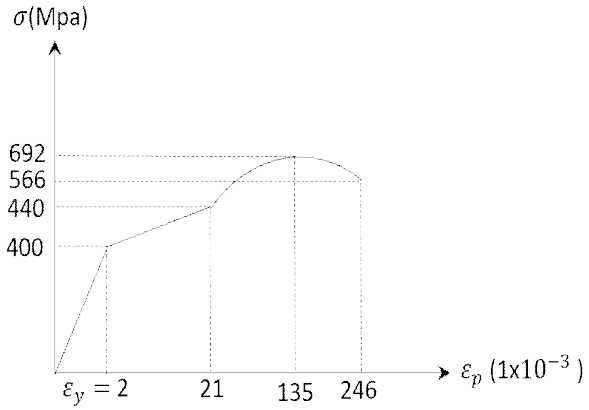


그림 2-49 Nonlinear stress-strain behavior of the steel

(a) $t_d < \frac{T_n}{2}$

For the loading duration smaller than the half of the natural period of the plate three cases were considered; 1) a plate of AR=1, and a thickness of 30 mm having the natural period of =6.92 ms, 2) a plate of AR=2 and a thickness of 15 mm with the natural period of =5.54 ms and 3) a plate of AR=4 and a thickness of 1 mm with the natural period of =4.14 ms. For these three cases, a blast load due to a burst of 150 g explosive charge was considered for which the duration of the applied load was t_d =1.11 ms. Since for both cases the duration of loading is smaller than the half of the natural periods of these plates, ms, and ms, and ms, the maximum displacements of the plates were developed in the free vibration phase. The time step of the analysis was =0.2 ms. 그림 2-50 depicts the displacement time-histories of the plates of the abovementioned three cases which were obtained from both analytical and the numerical approaches at the plate center where x=a/2 and y=c/2.

In the graphs presented in 그림 2-50, the solid line shows the dynamic responses of the blast loaded plates calculated by employing the presented analytical approach, and the results of the numerical approach through ABAQUS were depicted by dashed lines. It has been observed that the examined plates oscillated about their equilibrium condition in the free vibration phase when the loading (blast load positive phase) finished, and no peak developed during the forced vibration phase which agrees with results reported by Chopra (2001), and Tavakoli (2014).

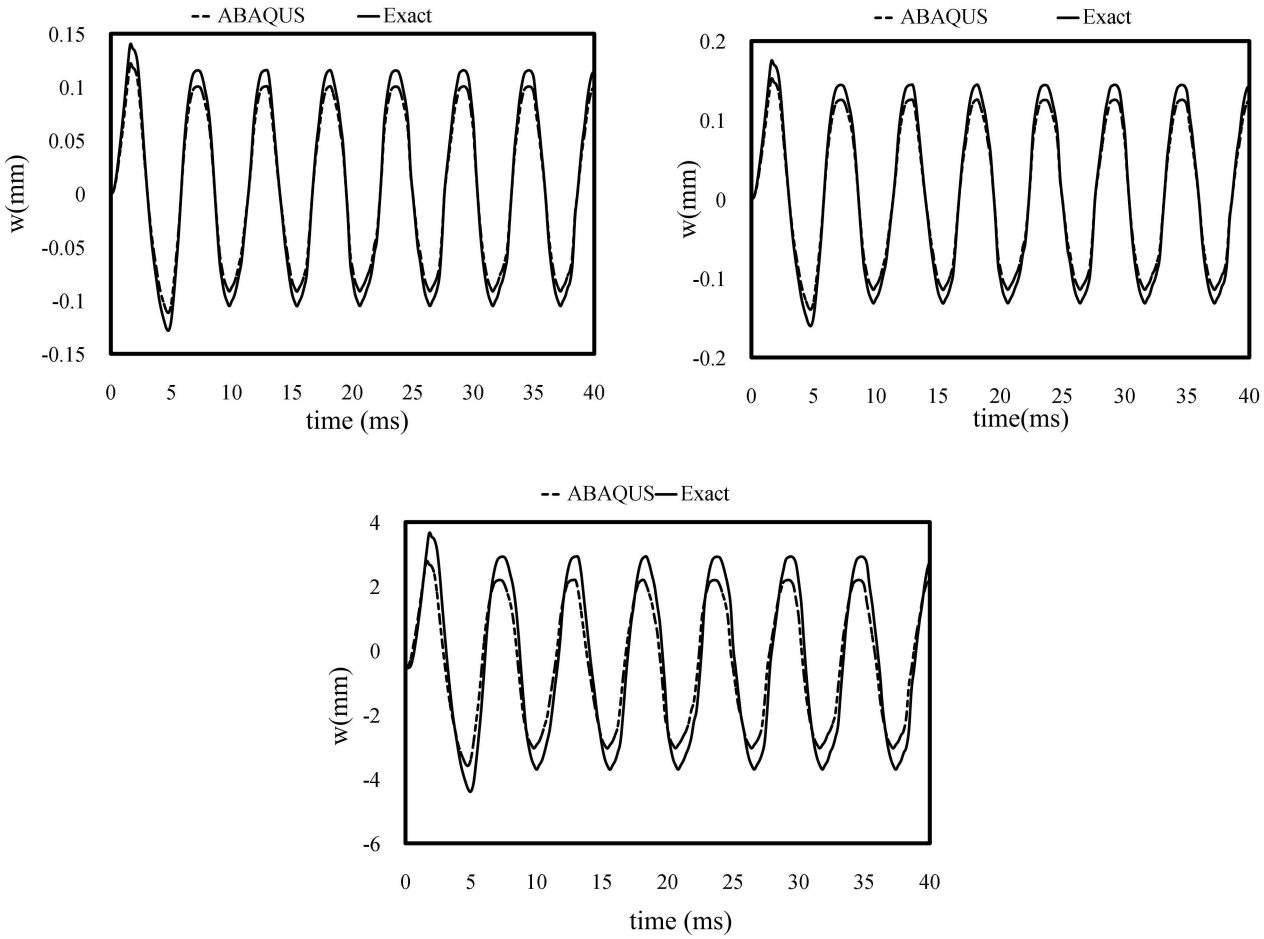


그림 2-50 The time histories of the plates of different aspect ratios and thickness considering and 150g explosive charge: (a) AR=1 and h=30 mm, (b) AR=2 and h=15 mm, (c) AR=4 and h=1 mm

(b) $t_d \rangle \frac{T_n}{2}$

For the batch of loading duration greater than half of the natural period of the plate, three aspect ratios of AR=1, 2, and 4 were also adopted considering the example plates which have been already investigated for except for the AR=4 for which a plate of 10 mm thickness having the natural period of was considered. In this regard, a blast load due to a burst of 20 kg having the loading duration of was applied which satisfies the condition of . The dynamic analyses of the blast loaded plated were carried out considering the time step of =0.18 ms, and the corresponding time histories were plotted from the results evaluated at x=a/2 and y=c/2 as presented in 그림 2-51.

In the graphs presented in 그림 2-51, the solid line depicts the displacement time-history extracted from the analytical method of this study, while the graph shown with the dashed line reflects the time history generated from ABAQUS. For all the graphs it was observed that the maximum plate deflection developed in the forced vibration phase within the loading duration, and agree with results provided by Chopra (2001), and Tavakoli (2014).

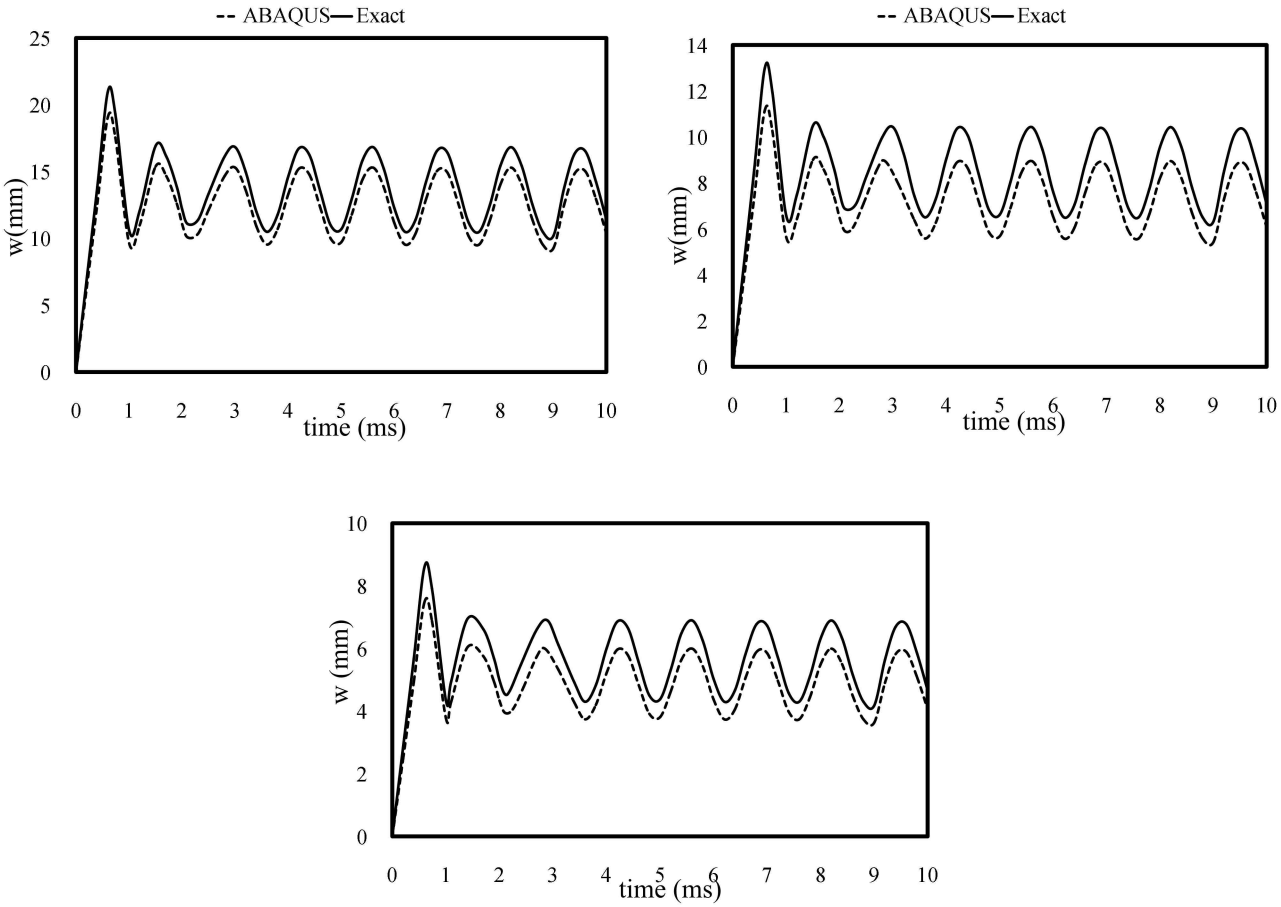


그림 2-51 The time histories of the plates of different aspect ratios and thickness considering and 20 kg explosive charge: (a) AR=1 and h=30 mm, (b) AR=2 and h=15 mm, (c) AR=4 and h=10 mm

4.1.2. 최대 플레이트 휨

In another attempt for evaluation of the validity of the current analytical approach the maximum displacements of the plate obtained analytically were compared with those of numerical method through ABAQUS. In this regard, two cases of boundary conditions were considered; simply supported and clamped plates. Three aspect ratios of AR=1, 2, and 4 were adopted for the plate of a 50 mm thickness subject to a blast load due to the burst of an explosive charge of 200 kg. For all these cases the condition of is met. The dynamic analysis was performed considering a time step of =0.2 ms and the results were provided in 표 2-22.

The small variation between the results of two methods which are shown with variation (%), certified the validity of the current approach, thus, the presented formulas can be reliably used for the practical applications and prediction of the dynamic responses of the blast loaded plates.

표 2- 22 Maximum displacement of the plates having the thickness of 50 mm considering simply supported and clamped boundary conditions subject to a charge of 200 kg for AR=1, 2, 4

BC	AR	Method	W (mm)	Variation (%)
Simply supported	1	Anal.	118.15	4.69
		Num.	112.61	
	2	Anal.	76.89	4.47
		Num.	73.45	
	4	Anal.	20.30	4.24
		Num.	19.44	
Clamped	1	Anal.	13.74	4.13
		Num.	13.17	
	2	Anal.	8.94	4.03
		Num.	8.58	
	4	Anal.	2.37	3.97
		Num.	2.27	

4.1.3. 폭약량, 플레이트 두께와 경계조건의 상호작용

The comparison between the predicted plate deflections obtained from the analytical and numerical analysis was made by utilizing the guidelines and the concepts given in (Jonesm 2012); Laecher, 2007; Ngo, et al., 2007). In this regard, am aspect ratio of AR=2 was considered for the plates of 50 mm and 100 mm thickness having specified two boundary conditions; simply supported (SS) and clamped (Cl). The plate deflections were obtained for a variety of charge weights as provided in 표 2-23, and 3-24, respectively.

표 2-23 Deflections of the plate with a 50 mm thickness considering two B.Cs.; SS and Cl (AR=2)

Charge (kg)	B.C.	w/h Analytical	w/h Numerical	Numerical/Analytical	Variation (%)
2	SS	1.65E-02	1.51E-02	0.9151	8.4848
	Cl	1.70E-03	1.56E-03	0.9198	8.0107
20	SS	1.56E-01	1.45E-01	0.9251	7.4856
	Cl	1.60E-02	1.50E-02	0.9347	6.5269
50	SS	3.79E-01	3.52E-01	0.9303	6.9749
	Cl	3.84E-02	3.61E-02	0.9398	6.0208
75	SS	5.76E-01	5.38E-01	0.9352	6.4802
	Cl	6.16E-02	5.79E-02	0.9402	5.9774
100	SS	7.74E-01	7.26E-01	0.9386	6.1401
	Cl	7.91E-02	7.48E-02	0.9454	5.4635
150	SS	1.20E+00	1.13E+00	0.9403	5.9674
	Cl	1.25E-01	1.19E-01	0.9503	4.9724
200	SS	1.54E+00	1.45E+00	0.9438	5.6249
	Cl	1.59E-01	1.52E-01	0.9546	4.5367

표 2-24 Deflections of the plate with a 100 mm thickness considering two B.Cs.; SS and Cl (AR=2)

Charge (kg)	B.C.	w/h Analytical	w/h Numerical	Numerical/Analytical	Variation (%)
2	SS	1.10E-03	1.20E-03	1.0909	8.3333
	Cl	1.14E-04	1.24E-04	1.0841	7.7616
20	SS	1.06E-02	1.15E-02	1.0849	7.8261
	Cl	1.10E-03	1.18E-03	1.0771	7.1582
50	SS	2.52E-02	2.71E-02	1.0754	7.0111
	Cl	2.58E-03	2.77E-03	1.0699	6.5342
75	SS	3.96E-02	4.25E-02	1.0732	6.8235
	Cl	4.05E-03	4.32E-03	1.0678	6.3472
100	SS	5.23E-02	5.61E-02	1.0727	6.7736
	Cl	5.31E-03	5.68E-03	1.0694	6.4897
150	SS	8.12E-02	8.59E-02	1.0579	5.4715
	Cl	8.22E-03	8.68E-03	1.0557	5.2801
200	SS	1.07E-01	1.12E-01	1.0468	4.4683
	Cl	1.08E-02	1.12E-02	1.0447	4.2759

In 표 2-23, and 3-24 the slight variations of the plate displacements, due to a given blast load, predicted by analytical and numerical approaches prove the validity of the method of this study. Besides, it was observed that the numerical method resulted in an underestimation of the displacement of the plate of 50 mm thickness, while it overestimated the blast-induced displacement for h=100 mm. Besides, it was seen that the clamped boundary condition significantly increased the plate blast resistance compared with the simply supported plate.

4.2. 수치해석

This study performed a parametric study to analyze the blast-resistance and displacement of the isotropic steel plates concerning effective parameters; plate thickness, plate aspect ratio, explosive charge weight, and boundary conditions. This provides a better understanding of the plate behavior subject to a given blast load and helps to assess the accuracy, integrity, and generalization of the method. To generalize the analysis and results, the plate displacement was normalized in terms of the plate thickness and shown with w/h.

4.2.1. 종횡비

It has been documented that the plate aspect ratio has a significant effect on the blast loaded plate displacement. In this regard, this study investigated the variation of the deflections of plates of 50 mm and 100 mm thickness for a variety of charge weights considering three aspect ratios; AR=1, 2, and 4 as depicted in 그림 2-52 and 3-53. In the following graphs, the dashed lines show the perfectly linear paths used to distinguish the variation of the results from the linear behavior and the solid lines with markers indicate the plate displacement obtained from the nonlinear method of this study.

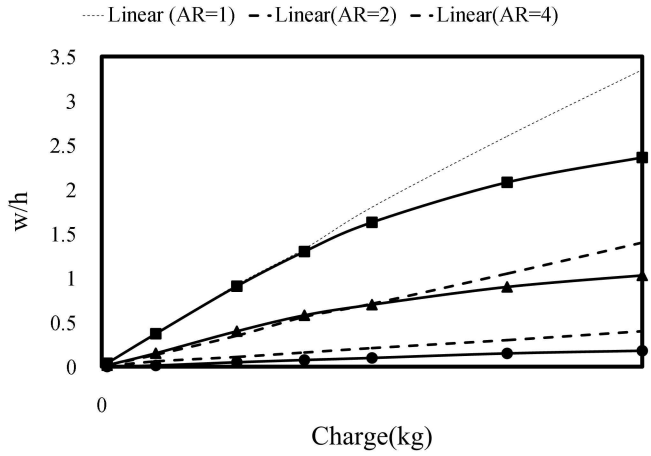


그림 2-52 Variation of plate displacement concerning the variation of charge weight in terms of aspect ratio (h=50mm)

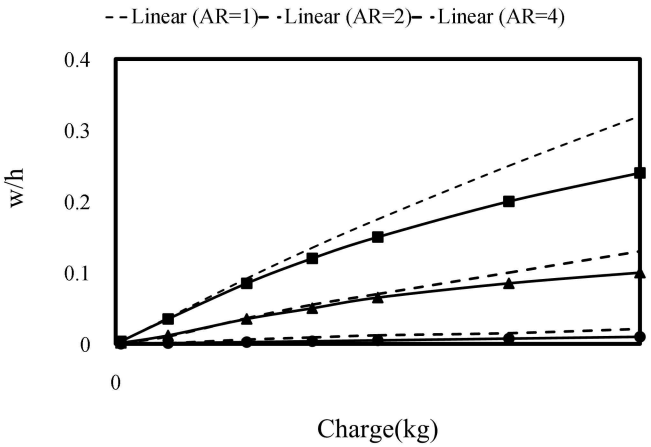


그림 2-53 Variation of plate displacement concerning the variation of charge weight in terms of aspect ratio (h=100mm)

From the graphs given in 그림 2-53, and 3-54 it is observed that the aspect ratio of AR=1 resulted in the highest plate displacement due to exposure to a blast load. In another word, the blast loaded plate displacement is a function of the plate geometry such that the highest displacement was achieved for the square plate while the lowest one was observed for the plate with strip shape. It was also seen that the plate displacement showed a nonlinear increase when the charge weight added up.

4.2.2. 두께와 폭약량

In this study, a variety of the plate thicknesses from h= 50 mm to h=100 mm was adopted for the plates subjected to blast loads due to a burst of a range of charge weight of from 2 kg to 200 kg. 그림 2-54 and 3-55 depict the interactive effects of plate thickness and charge weights on the plate displacement considering two aspect ratios of AR=1, and AR= 4, respectively.

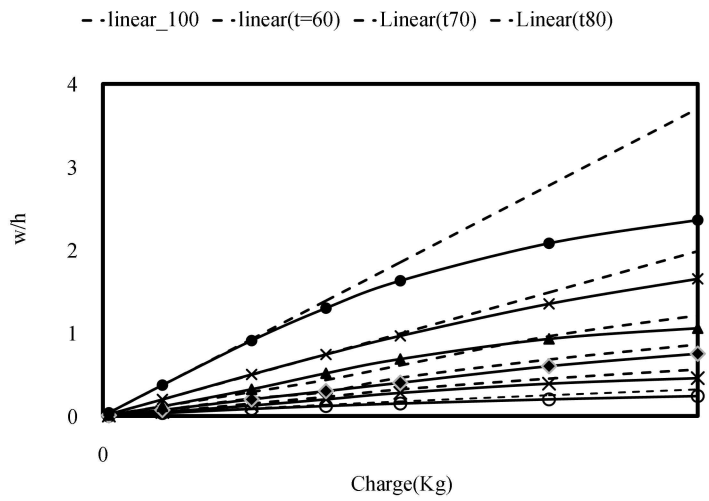


그림 2-54 Variation of plate displacement concerning the variation of charge weight in terms of plate thickness (AR=1)

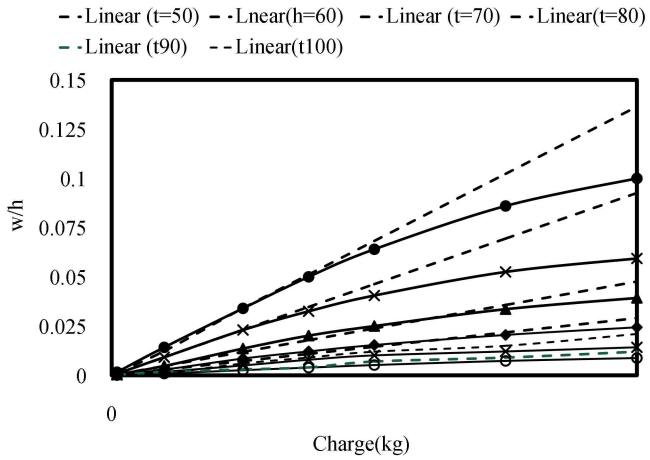


그림 2-55 Variation of plate displacement concerning the variation of charge weight in terms of plate thickness (AR=4)

From 그림 2-54 and 3-55, it is observed that having the charge weight increased, the plate displacement nonlinearly increased. For the high amounts of charge weight, the slope of the graph decreased showing the fact that an increase in the amounts of charge, for example from 180 kg to 200 kg, induced a small increase in plate displacement. A reason for this can be a decrease in material stiffness up to the material failure due to the inclusion of the material nonlinearity. This can be beneficial for design purposes to estimate what would be plate behavior in terms of deflection and failure. However, for low amounts of charge weights, a small addition can result in a big increase in plate deflection. In another attempt, the variation of the plate deflection was plotted versus the variation of plate thickness considering charge weights of W=50, 100, and 200 kg. The results were plotted together with their corresponding results obtained from the linear approach (Mohammadzadeh, Noh, 2019) shown with dashed lines as given in 그림 2-56 and 3-57 for the aspect ratios of 1 and 4, respectively.

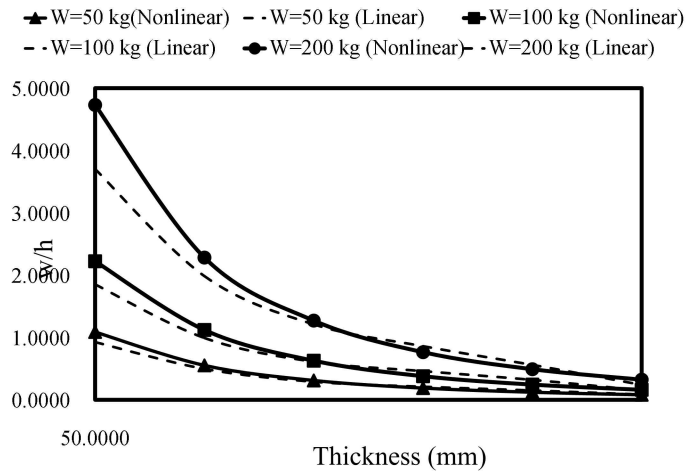


그림 2-56 Variation of plate displacement concerning the variation of the thickness (AR=1, W=50, 100, 200)

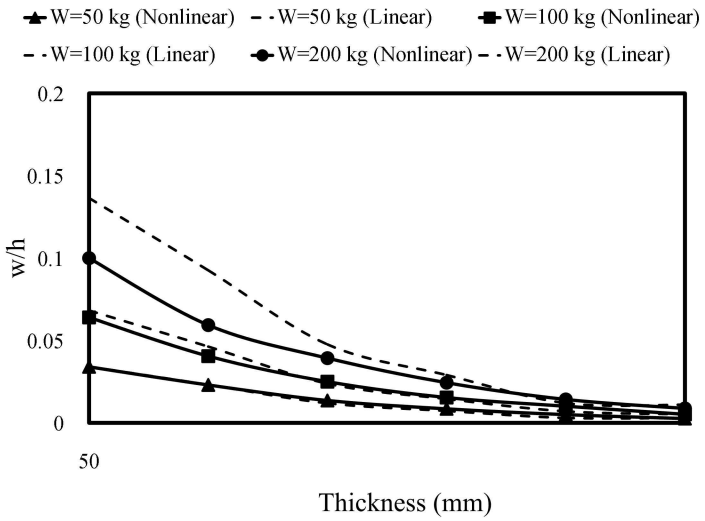


그림 2-57 Variation of plate displacement concerning the variation of the thickness (AR=4, W=50, 100, 200)

In 그림 2-56 and 3-57, solid lines with markers show the variation of plate displacement concerning the plate thickness obtained from the nonlinear method of this study while the dashed line shows the variation of the plate displacement obtained from the linear method presented in (Mohammadzadeh, Noh, 2019). Having looked at the graphs, a nonlinear variation of plate displacement can be observed with respect to the variation of the thickness generated from the fact that the plate displacement is a cubic function of the plate thickness. Consideration of the material nonlinearity resulted in the update in tangential modulus of elasticity of the plate in each step which appeared in the form of a nonlinear increase in the plate deflection. However, the results showed that the inclusion of the material nonlinearity in the method resulted in a small variation of the plate deflection in terms of the plate thickness comparing with the results of the linear method given in (Mohammadzadeh, Noh, 2019), especially, for thick plates having a thickness of over 70 mm.

4.2.3. 경계조건의 영향 평가

To investigate the effects of boundary conditions on the dynamic responses of the blast loaded plates, a comparison was made between time-histories corresponding to two conditions, namely, simply supported and clamped boundary conditions. For this aim, two cases of plate thickness and explosive charge were considered: Case I including a plate of 15 mm thickness subject to a blast load of 200 g charge, and Case II comprising a plate of 50 mm thickness to which an explosive load resulted from 5 kg charge. For both cases, AR=2 was considered. 그림 2-58 and 3-59 illustrate the time histories of case I and case II, respectively.

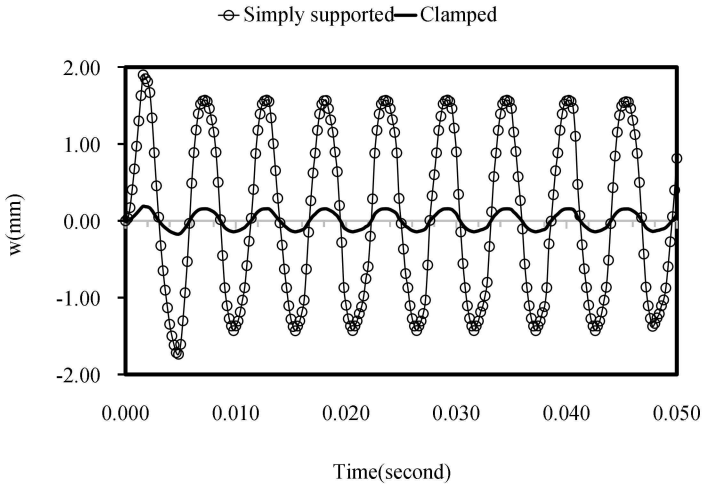


그림 2-58 Comparative time-history of the plate of 15 mm thickness subject to 200 g charge with simply supported and clamped boundary conditions

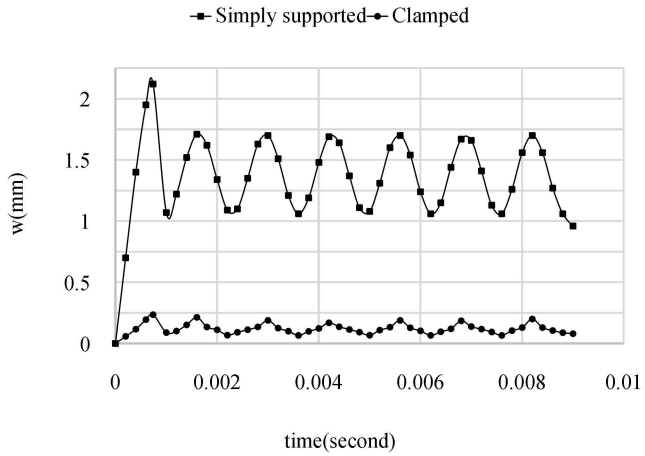


그림 2-59 Comparative time-history of the plate of 50 mm thickness subject to 5 kg charge with simply supported and clamped boundary conditions

It can be observed from comparative graphs given in 그림 2-58 and 3-59 the method could accurately predict the dynamic responses of the clamped plates for different conditions. Also, the results exhibited that the clamped plate showed deflections much smaller than the simply supported plate.

5. 결과

A simplified nonlinear analytical approach was presented to predict the dynamic responses of the isotropic plates subject to blast loads considering two frequently used boundary conditions; simply supported and clamped plates. For this aim, Navier's solution was employed and the nonlinearity of the method was constructed by the inclusion of the material nonlinearity and the strain rate. The geometrical nonlinearity was not included in the method due to its complexity that the first order, and or higher-order shear deformation theories may impose on the method. The method was validated by making a comparison between the results obtained from the presented method and those of ABAQUS concerning the criteria given in the literature; plate natural frequency () and loading duration (). Accordingly, two types of analyses were carried out; , and . The characteristic behaviors of each case were produced successfully with a good agreement between the proposed scheme, numerical analysis, and the literature. In another attempt, the maximum displacement of the plate of 50 mm thickness was calculated considering various aspect ratios of AR=1, 2, and 4, and for simply supported and clamped plates. Parametric studies were carried to investigate the effects of plate aspect ratio, and thickness as well as the charge weight, and different boundary conditions on the blast responses of the isotropic steel plate. From the parametric studies the following outcomes were achieved:

1. Convergence study for the numerical analysis revealed that the 20-node quadratic elements with the reduced integration formulation (C3D20R) resulted in the more precise prediction of plate displacement in comparison with those obtained from the exact solution.
2. From the analysis done for the validation of the presented analytical method, the small variation between calculated displacement using the presented method and numerical analysis through ABAQUS proved the reliability and validity of the presented simple nonlinear analytical method for blast loaded plates. It was also observed that for the condition the maximum displacement of the plate developed in the free vibration phase, while for the maximum plate deflection developed in the forced vibration phase within the loading duration.
3. From the results, it was revealed that as the charge weight increased the normalized displacement of the plate (w/h) nonlinearly increased for a given aspect ratio and the plate thickness. The trend of the nonlinearity of the plate responses in terms of the thickness was relatively severe as the stiffness of the plates is a cubic function of the thickness.
4. It was seen that as the aspect ratio of the plate increased from AR=1 to AR=4, for a specific charge weight and thickness, the plate deflection drastically decreased.
5. From the comparative analysis performed on the plates of 50 mm and 100 mm thickness, it was observed that the numerical method underestimated the plate deflection for the 50 mm-thickness while it resulted in the overestimation of the plane-normal displacement of the plate of 100 mm thickness.

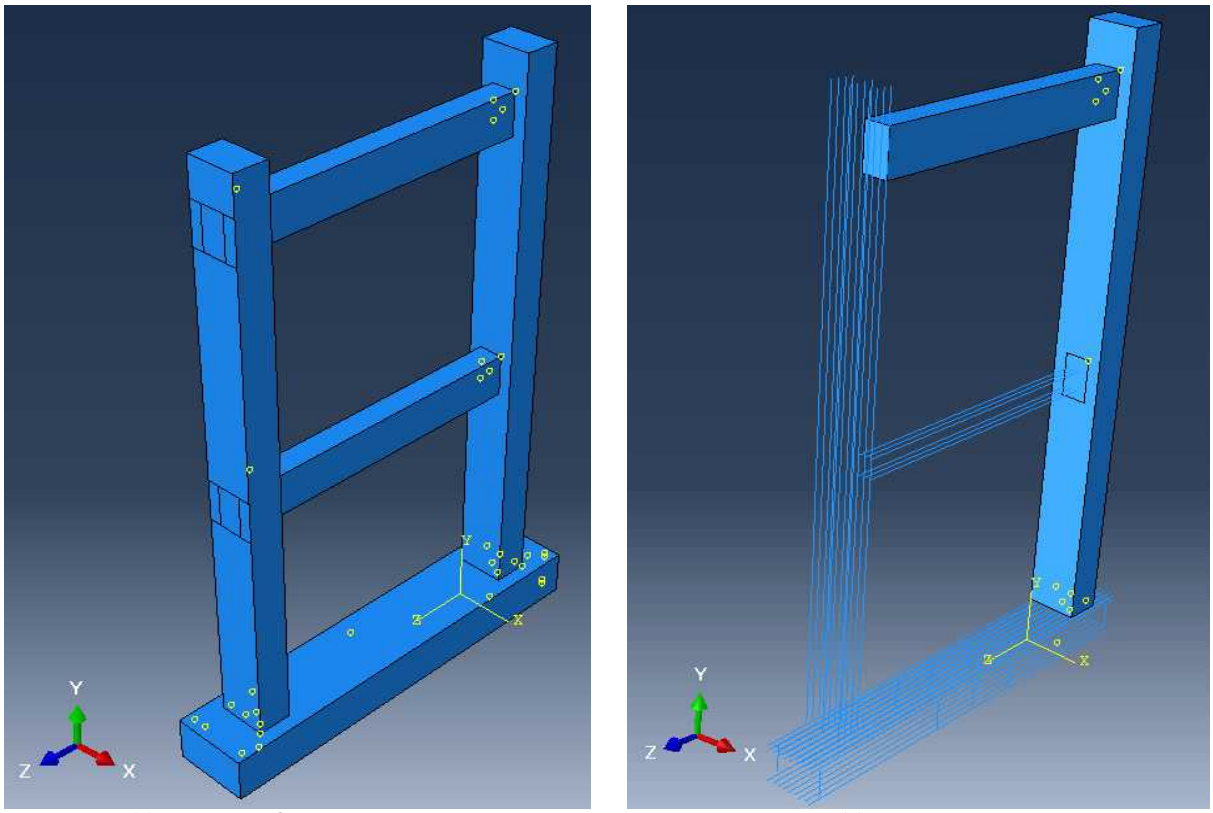
6. The investigation into the effects of the boundary conditions on the plate displacement which reported in the form time-history showed that the clamped plate significantly provided a better blast resistance than the simply supported plate.

Having looked at the results of this study, it is worth noting that a valuable point of the presented method is its ease of use, especially for engineers. Although the effect of the nonlinearity of the material was included in the method, the inclusion of the geometrical nonlinearities would help to improve the accuracy of the method. As a possible future study, it would be worthy to consider the geometrical nonlinearity to construct a simple method.

■ 모형실험결과와 해석결과 비교를 통한 해석모델 검증

1, 2차년도 해석결과와 실증실험 대상의 축소실험을 비교하여 3차년도 실증실험에 선행하는 문제들을 파악하고, 실증실험전 사전 준비완료.

This report is to present the evaluation of the validity of finite element method (FEM) model of a two-storey reinforced concrete frame with results obtained from the experiments. For this aim, the commercially available FEM package ABAQUS was employed. The illustration of the model created in ABAQUS is provided in 그림 2-60.



(a) Façade of the model **(b) Rebar**

그림 2-60 Illustration of the two-storey reinforced concrete frame modeled in ABAQUS

To validate the model, the load-displacement obtained from Experimental and numerical investigations were plotted in a comparative graph as shown in 그림 2-2.

As can be seen from the graph given in 그림 2-2, a good agreement was achieved between both experimental and FEM results. Despite having a good agreement, it can be seen that the numerical model is slightly conservative than the experimental. A reason for this can be referred to the discrepancy between details of models: the numerical model was simplified, especially, for the rebar net. The underestimation of the maximum load baring capacity might be due to the less contribution of steel rebar in numerical model.

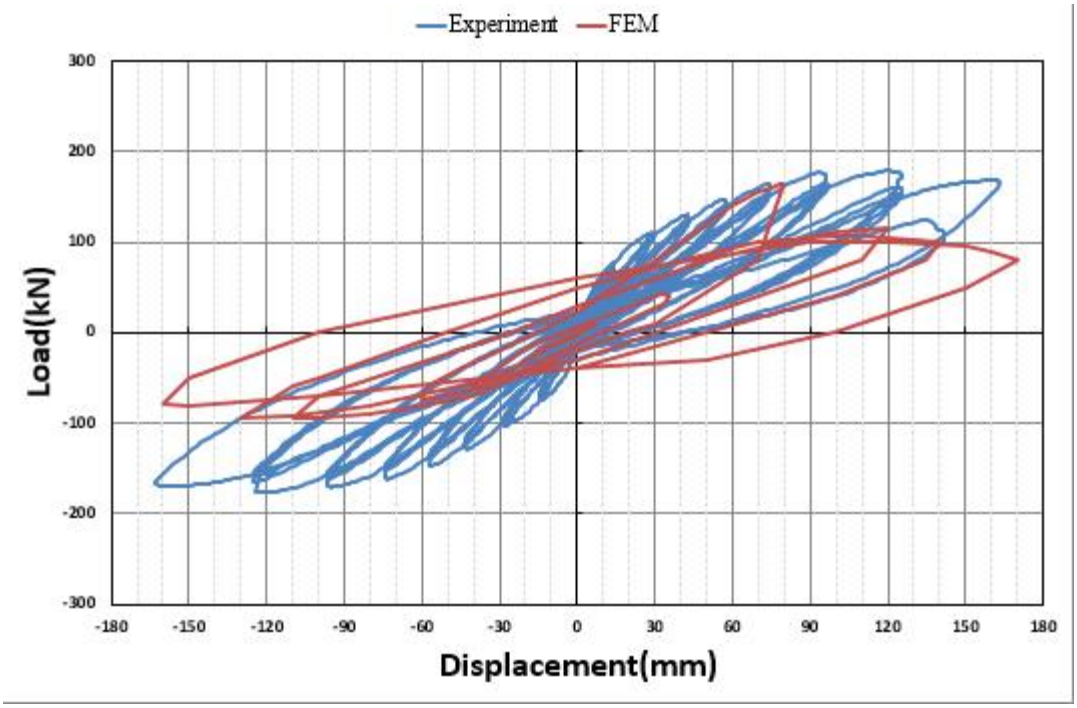
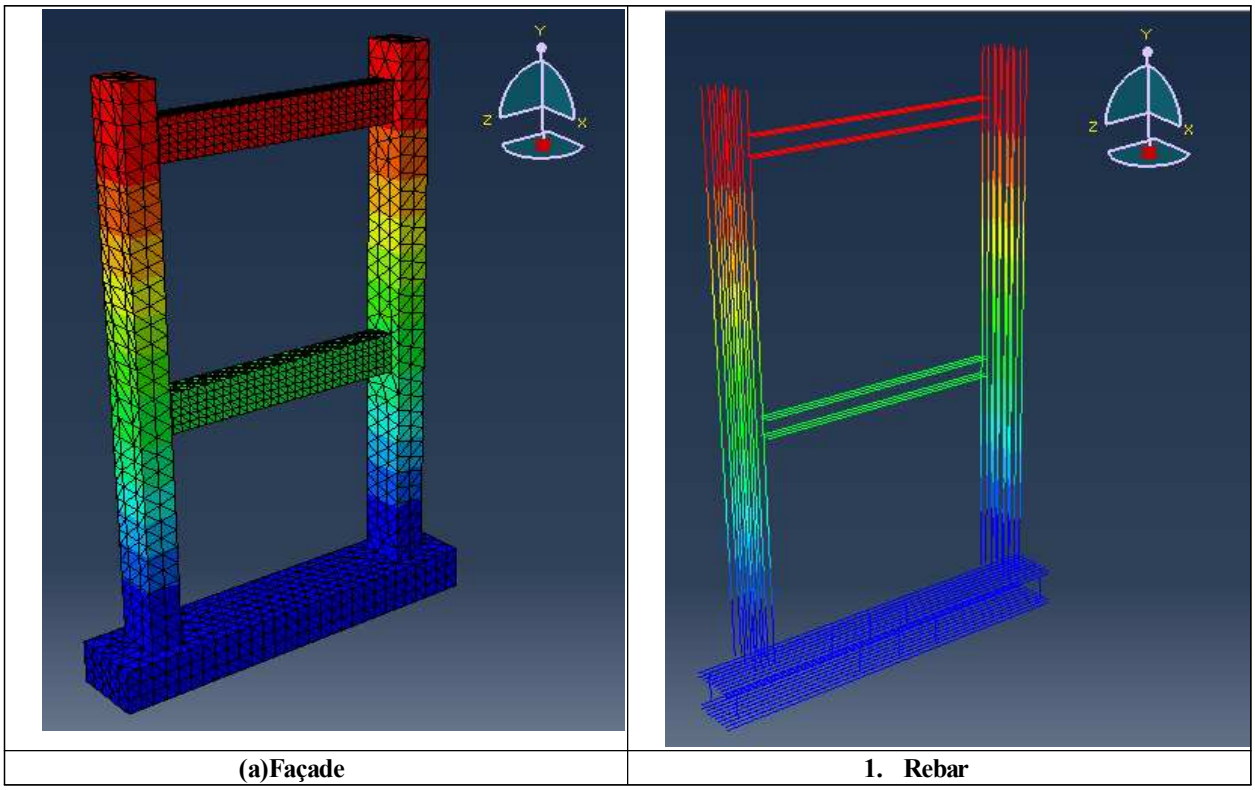


그림 2-61 Comparative graph presenting the load-displacement relation obtained from experimental work and FEM analysis

To visualize the variation of the displacement through the model, the spectrograms of deformed shape of the frame are provided in Fig .3: 그림 2-62(a) shows the displacement of the total model and 그림 2-62(b) shows the displacement variation of the steel rebar.



(a)Façade	1. Rebar

그림 2-62 Variation of displacement in the model

The spectrograms of the displacement of the model show that the maximum displacement occurs at the top on which the highest amount of the load was subjected. The lowest amount of displacement was observed on the foundation where the fixed boundary conditions were applied.

(나) 협동연구기관(Georgia Institute of Technology)

① 개발 목표 :

3D 모델 기반 구조체 변위 및 파손 정량화 기법

② 개발 내용 및 범위(그림을 이용하여 시스템 구성도, 구조 등을 구체적으로 표현)

①	재난 및 이벤트 전/후 3D 모델 매칭

- Vworld 3D Map 혹은 설계도면을 활용하여 국내 재난 이전 3D 기초 모델 확보
- 3D 기초 모델과 재난 후 변형 모델과의 공통된 특징점 추출
- Nearest-neighbor 매칭기법을 활용하여 기초 모델 및 변형 모델 매칭 기술 개발

②	구조체 변형 및 손상 정량화

- 빌딩의 높이 (H) 및 폭 (W), drift angle, 구조물의 회전, 구조물 상단의 전단변형 측정
- 붕괴된 구조체 검출 및 물성 확인

③	측정 데이터 연동

- 주관기관의 클라우드 기반 재난 데이터베이스와 연동
- 주관기관의 해석 결과와 상호 비교 및 검증

④	무인항공체 이미지 및 적외선 카메라 데이터 퓨전 방식 개발

- 무인항공체에 설치된 적외선 카메라와 디지털카메라 이미지 데이터 퓨전
- 3D 모델 기반 적외선 카메라 데이터 이미징



그림 2-63 2차년도 주요연구내용

③ 연구성과물

○ 재난 전/후 모델 매칭 기술

■ Open3D 라이브러리를 활용한 재난 전/후 모델 비교 알고리즘 개발

▪ Plane 혹은 Coner 포인트를 활용한 3차원 모델 매칭 기술 활용

- RANSAC 알고리즘을활용하여3차원 평면 추출
- 평면 법선벡터를 활용한 회전요소R 계산
- 모서리 값을 활용한 변환행렬 계산

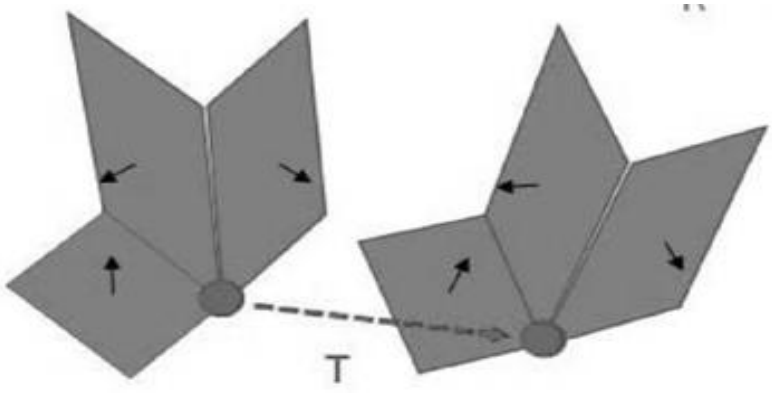


그림 2-64 법선벡터 및 edge 추출을 통한 모델 매칭 기술

▪ Python 기반 3D 모델 비교 및 변위 시각화 알고리즘 구현

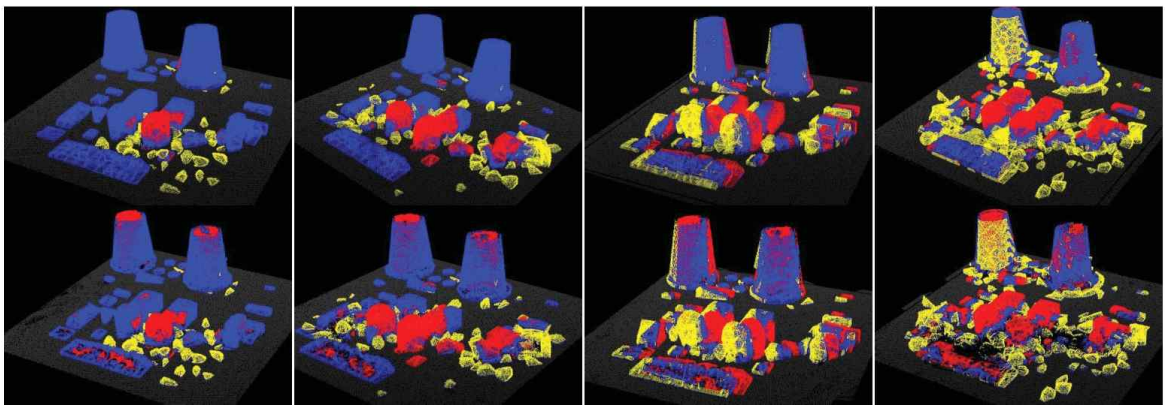
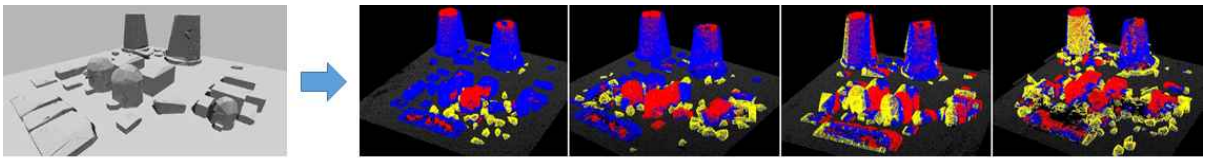


그림 2-65 3D 모델 매칭 및 변위 시각화 기술

○ 구조체 변형 및 손상 정량화 기술 개발

■ 재난 시뮬레이션을 통한 재난 전/후 모델 비교

▪ 핵발전소 3차원 모델을 활용하여 2가지 재난 (폭발/지진)과 2가지 강도 (중/강)에 대해서 시뮬레이션을 실시



재난 전 모델

재난 종류별/강도별 손상도 모델 (왼쪽부터 폭발(중)(강), 지진(중)(강)

그림 2-66 재난 강도별 모델 비교 시각화

▪ 손상도 검출 정확도 검증

표 2-25 손상도 검출 정확도 (Chen, J. and Cho, Y. (2019))

	배경 (Precision)	배경 (Recall)	잔해 (Precision)	잔해 (Recall)	손상부위 (Precision)	손상부위 (Recall)
Undamaged	1.00	0.57	-	-	-	-
폭발(중)	0.84	0.48	1.00	0.90	0.18	0.80
폭발(강)	0.76	0.44	1.00	0.81	0.46	0.99
지진(중)	0.62	0.36	1.00	0.65	0.48	0.74
지진(강)	0.61	0.32	1.00	0.63	0.61	0.75
평균	**0.71**	**0.40**	1.00	**0.75**	**0.43**	**0.82**

○ 무인 항공체 이미지 및 적외서 카메라 데이터 퓨전 방식 개발

■ 딥러닝 기술을 활용한 적외선 카메라 이미지에서 사람 검출 알고리즘 (Park et al., 2020)

▪ CNN 기반 사람검출 알고리즘 구현

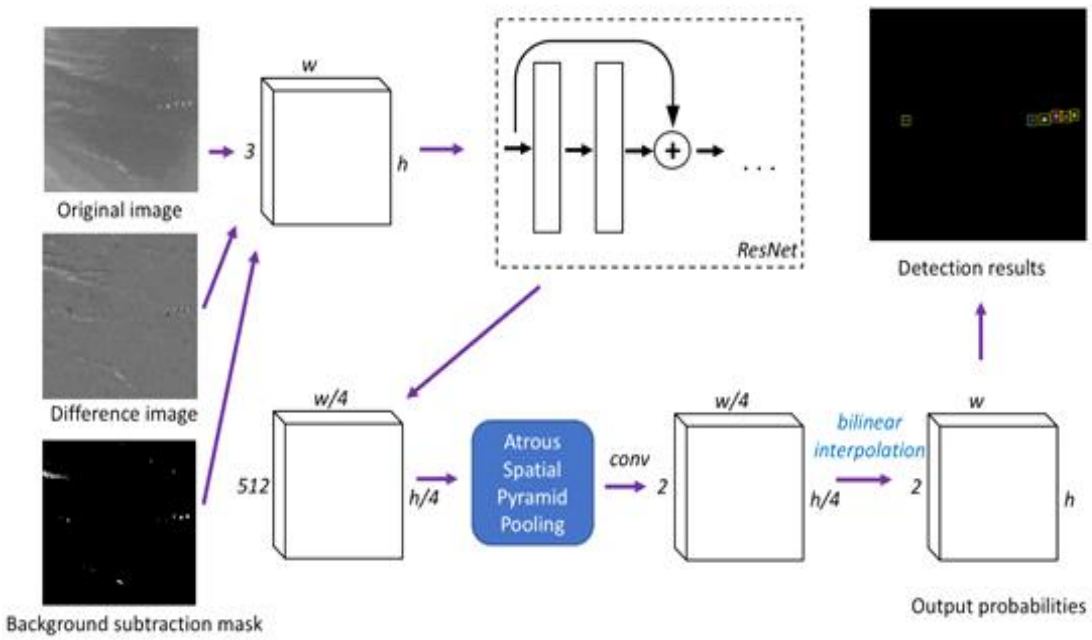


그림 2-67 적외선 이미지 내 사람 검출 딥러닝 아키텍쳐

▪ 알고리즘 정확도 검증

표 2-26 IR 이미지 내 사람검출 알고리즘 정확도

Method	Precision	Recall	F1-score
Simple thresholding	0.040	0.871	0.076
Adaptive thresholding	0.083	0.312	0.131
Background subtraction	0.534	0.951	0.684
K-means clustering	0.037	0.966	0.071
Our method	0.726	0.919	0.811
Our method*	0.759	0.948	0.843

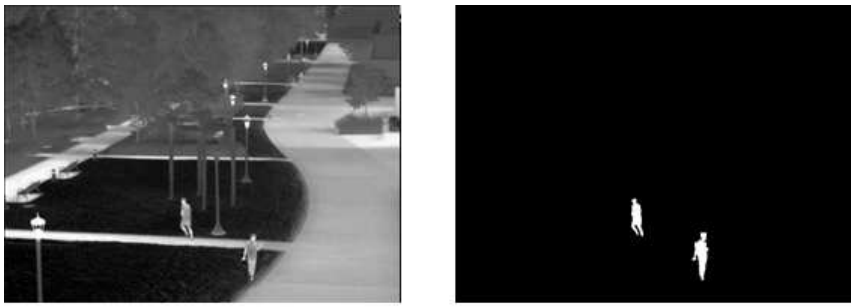


그림 2-68 사람검출 알고리즘 결과

■ 적외선 카메라 이미지 데이터 퓨전 기술

▪ 3D point cloud - 적외선 카메라 이미지 데이터 퓨전 및 시각화 구현

$$\begin{bmatrix} u \\ v \\ w \end{bmatrix} = K\,[R \mid t] \begin{bmatrix} x \\ y \\ z \\ 1 \end{bmatrix}$$

$$K = \begin{bmatrix} f_x & 0 & c_x \\ 0 & f_y & c_y \\ 0 & 0 & 1 \end{bmatrix}$$

적외선 카메라 캘리브레이션

$$x = \frac{1}{\Delta\theta}\tan^{-1}\frac{v}{w}$$

$$y = \frac{1}{\Delta\theta}\tan^{-1}\frac{w}{\sqrt{u^2+v^2}}$$

3차원 포인트 클라우드 - 적외선 카메라 이미지 매칭

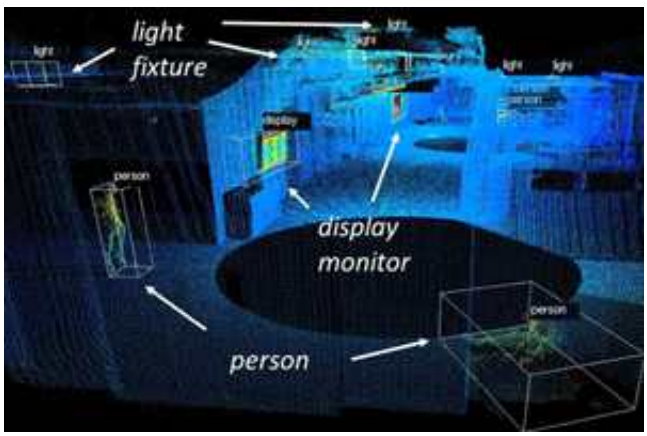


그림 2-69 적외선 이미지 3D 퓨전 기술

(3) 3차 연도

(가) 주관연구기관(서울대학교 산학협력단)

① 개발 목표

건물의 외관변형도를 고려한 구조물의 전체 및 주요부재에 대한 위험도를 나타내는 매핑시스템 개발

② 개발 내용 및 범위(그림을 이용하여 시스템 구성도, 구조 등을 구체적으로 표현)

①	구조물의 Full-scale 실증실험
	• 3가지의 데이터 측정방법 동시에 진행: 1) 지진하중에 의한 구조물의 변위 및 응력, 2) 지상 LiDAR를 이용한 외관변형도 측정, 3) 해외 공동연구기관 및 참여기업과 협력하여 드론을 이용한 구조물의 변형도 측정
②	3가지 실험결과(구조물 직접계측, LiDAR 계측, 드론계측)와 유한요소해석결과의 비교분석을 통한 개발된 모델검증
	• 유한요소해석결과에 의한 위험도와 3가지실험결과에 기반한 위험도의 비교를 통한 해석모델 검증 및 보완
③	실증실험 및 해석모델 수치해석결과를 활용한 건물변형도-내부손상도 매핑 모델 개발
	• 건물변형도를 구성하는 주요변수 (건물높이, 건물폭, 건물의 sidesway, drift angle, 건물회전 등)와 건물의 손상도와의 상관관계를 Contour 및 정량화된 수치로 보이는 매핑 모델 개발
	• 지반특성, 지진규모, 구조물의 재료적 특성, 건물변형도 수치를 알면 건물의 손상도를 파악할수 있는 Web기반의 매핑 모델 개발

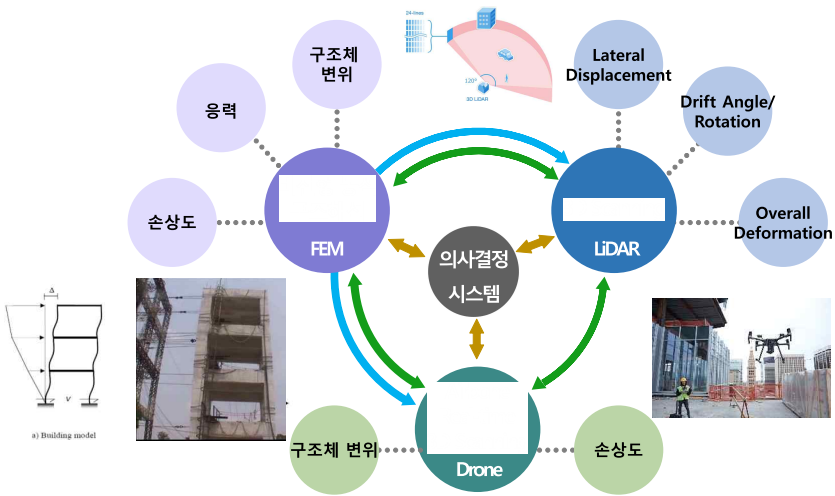


그림 2-70 3차년도 주요연구내용

■ 실험결과와 유한요소 해석결과의 비교검증

지진하중에 의한 구조물의 변위 및 응력, 지상 LiDAR를 이용한 외관변형도 측정, 드론을 이용한 구조물의 변형도 측정 결과와 유한요소 해석결과와의 비교 검증을 통하여 유한요소해석의 결과를 보완하고 정량화된 수치로서 제시하는 모델 개발.

1. 모형실험 및 해석 개요

In order to validate the numerical method of this study, a two-storey reinforced concrete frame was considered to be investigated by experimental works considering the cyclic loads. The load was applied to the upper parts of the frame such that two third of the load was applied to the column where the upper beam is installed while the remaing load applied to the column where the lower beam is installed. The load was applied using a hydraulic jack to the desired points. The illustration of the model constructed for experimental work is provided in 그림 2-71



그림 2-71 Photo of the frame constructed for the experimental work

Then, this frame was analyzed using ABAQUS, and the results were compared with those obtained form the experiment. The model created in ABAQUS is provided in 그림 2-72.

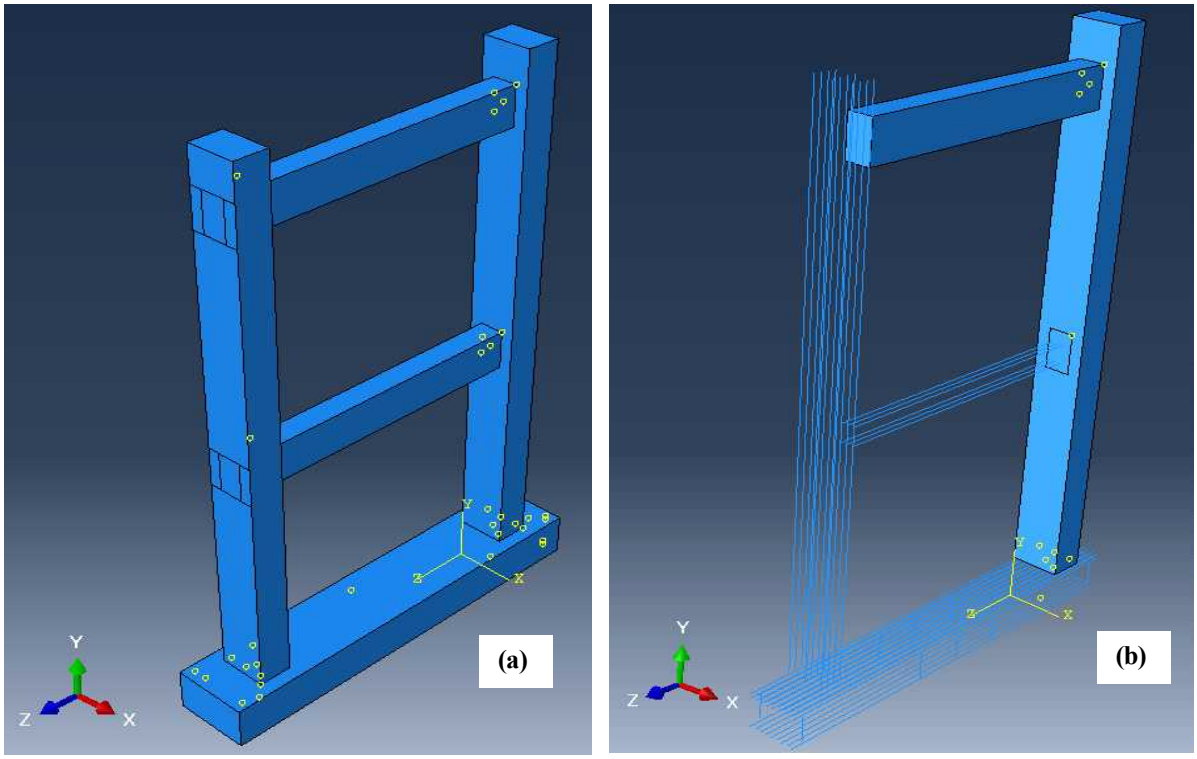


그림 2-72 Illustration of the two-storey reinforced concrete frame modeled in ABAQUS: (a) total view of the frame, and (b) rebar layout

(a) 하중-변위 그래프

The load-displacement obtained from the experimental and numerical investigations were plotted in a comparative graph as shown in 그림 2-73.

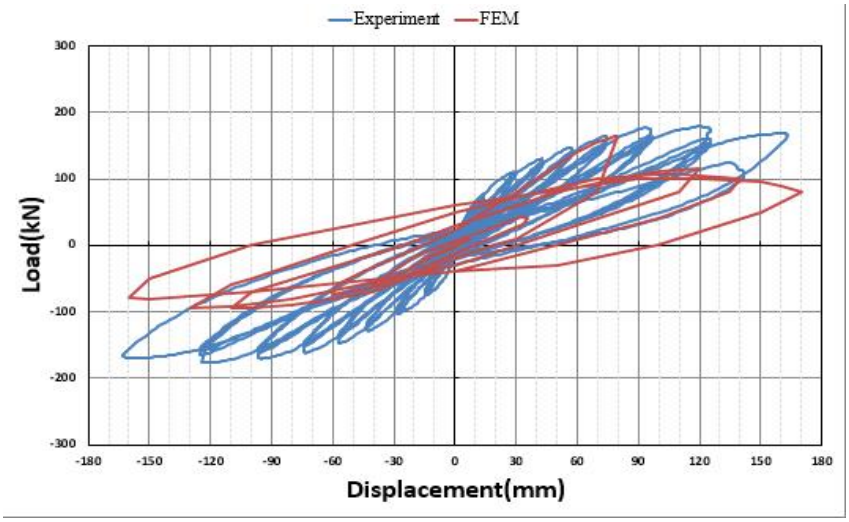


그림 2-73 Comparative graph presenting the load-displacement relation obtained from experimental work and FEM analysis

As can be seen from the graph given in 그림 2-73, a good agreement was achieved between the results of experiment and FEM analysis.

(b) 변위

In the first attempt, the frame which was investigated through experimental work was analyzed using the

To visualize the variation of the displacement through the model, the spectrograms of deformed shape of the frame are provided in 그림 2-74(a) showing the displacement of the total model and 그림 2-74(b) showing the displacement variation of the steel rebar, respectively.

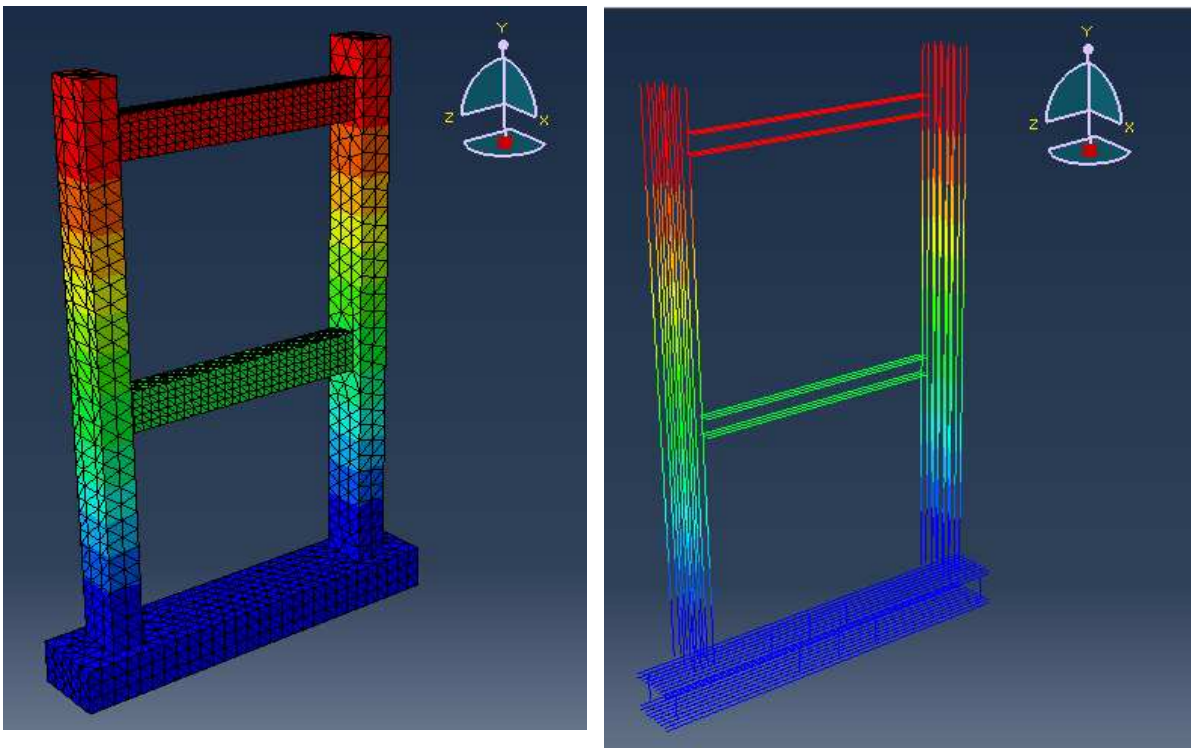


그림 2-74 Variation of displacement in the model: (a) concrete frame, (b) rebar

The spectrograms of the displacement of the model show that the maximum displacement occurs at the top on which the highest amount of the load was subjected. The lowest amount of displacement was observed on the foundation where the fixed boundary conditions were applied.

2. 모형실험결과와의 비교

The seismic-induced damages in frame buildings were evaluated considering the construction materials (concrete, and steel), number of stories, plan layout, and irregularities.

2.1 스틸 프레임

To model the steel frame, the structural steel of 400 MPa strength, elastic modulus of 200 GPa, and Poisson's ratio of 0.3 was used. The nonlinearity of the material was defined based on the stress-strain relation depicted in 그림 2-75.

For the beam of all stories IPE500 was considered and the box profile was adopted for the column with respect to the number of stories.

All of the cases of the buildings are subject to a loading pattern comprising the live and dead loads applied to the floors and interior and exterior walls as defined in 표 2-27. Furthermore, to account for a seismic load required for the seismic analysis a real recorded data was adopted as shown in 그림 2-76.

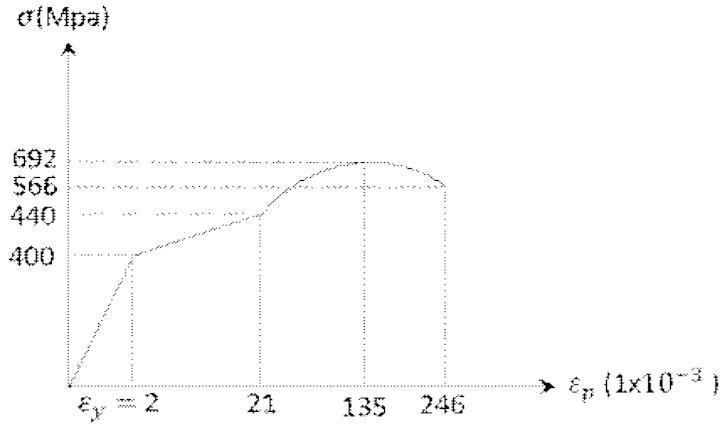


그림 2-75 Stress-strain relationship of the structural steel

표 2-27 Loading pattern

Loading position	Floor (kN/m^2)	Roof (kN/m^2)	Building exterior wall (kN/m)	Roof exterior wall (kN/m)
Dead load	11.38	9.26	7.68	1.99
Live load	3.14	2.35	-	0.98

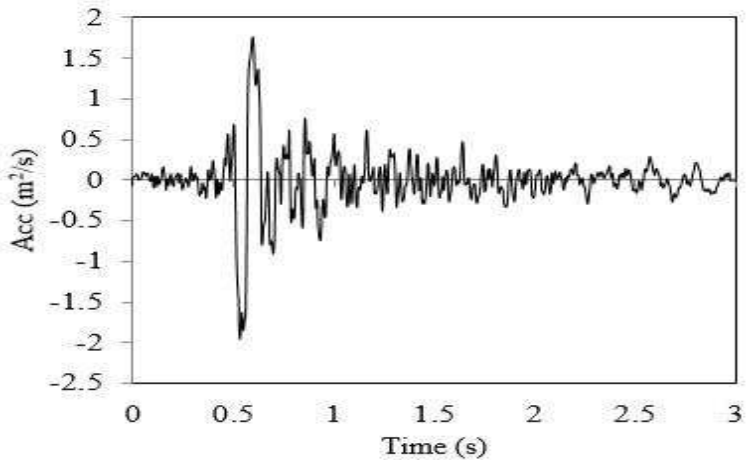


그림 2-76 Time-history of the applied seismic laod

2.1.1 층 수

To investigate the effect of the number of stories on the amount and pattern of the damages due to the applied seismic load, a series of frames with different number of stories were considered; 8, 10, 12, 15 and 20. The aim is to derive a criteria for predicting the internal displacement with respect to the external displacmenet and damage occurred in the high-rise buildings. For this type of analysis, a regular square-shaped plan of five spans of 3200 mm was considered. The illustration of the plan of the buildings is provided in 그림 2-77 while the 3D view of a typical frame is given in 그림 2-78.

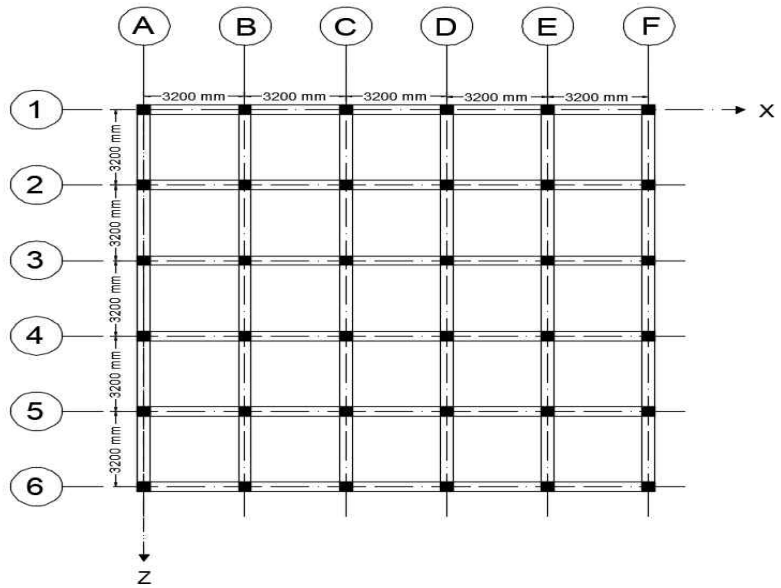


그림 2-77 Illustration of the regular plan

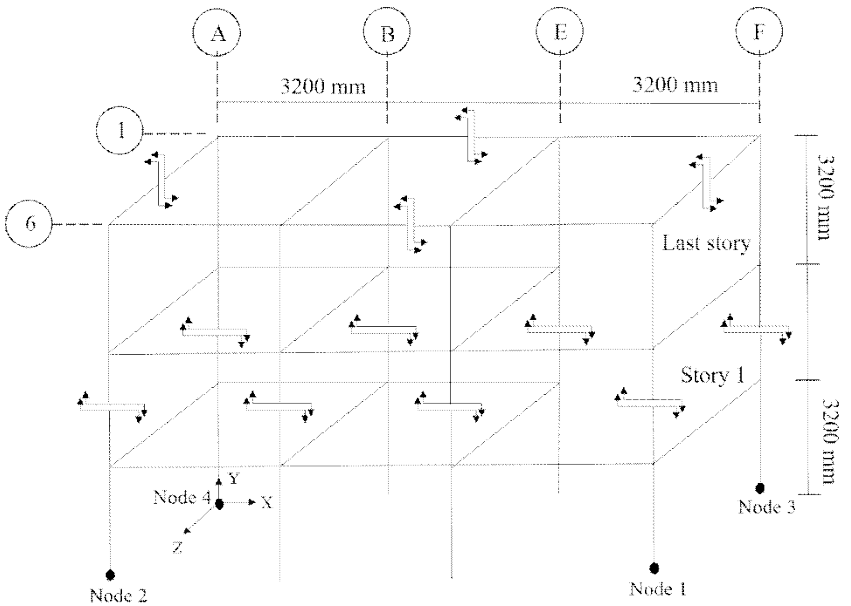
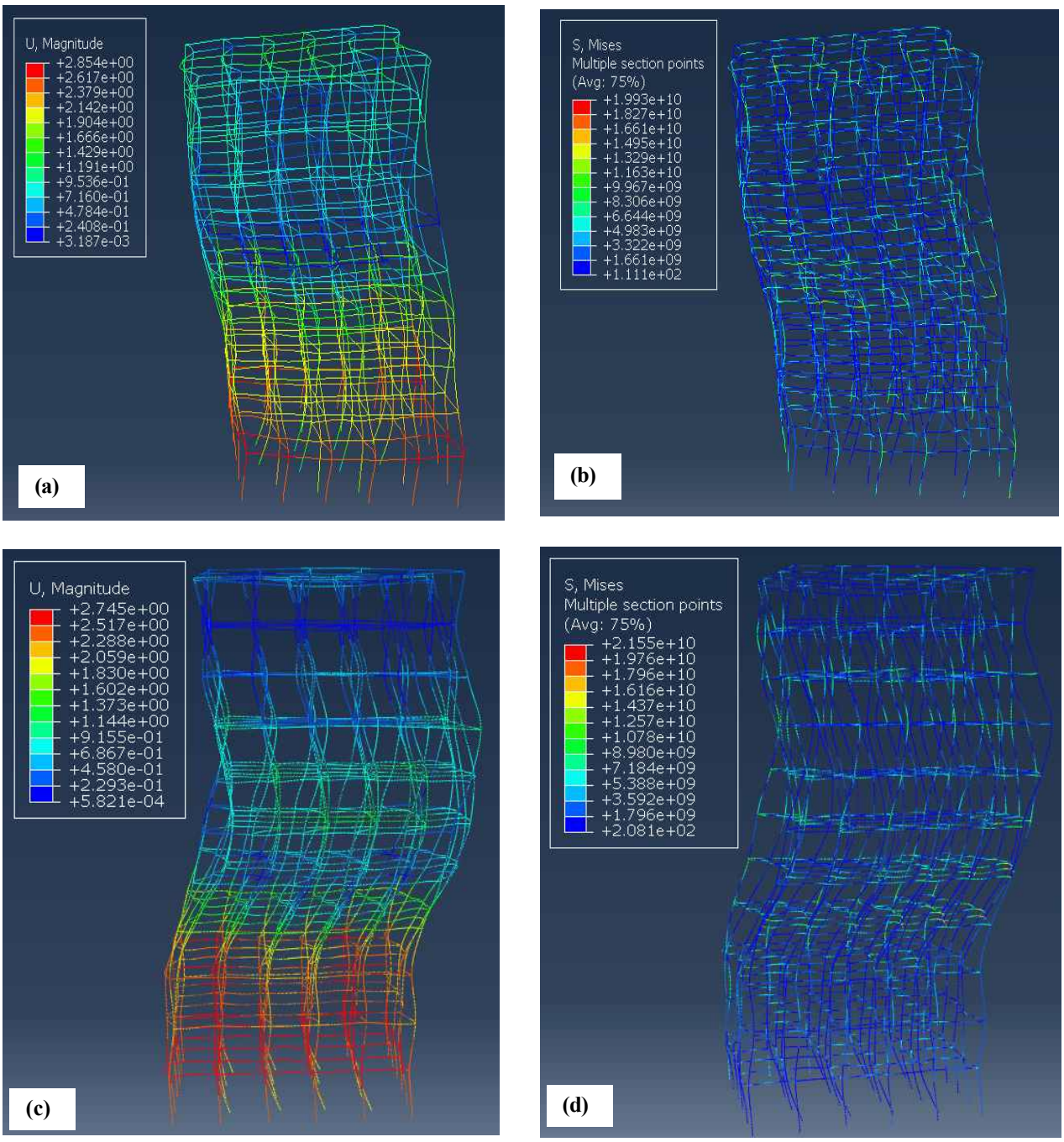
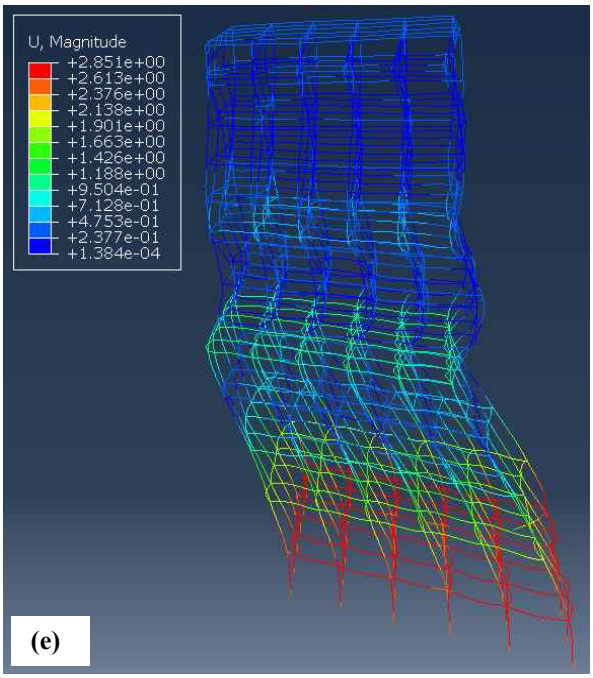


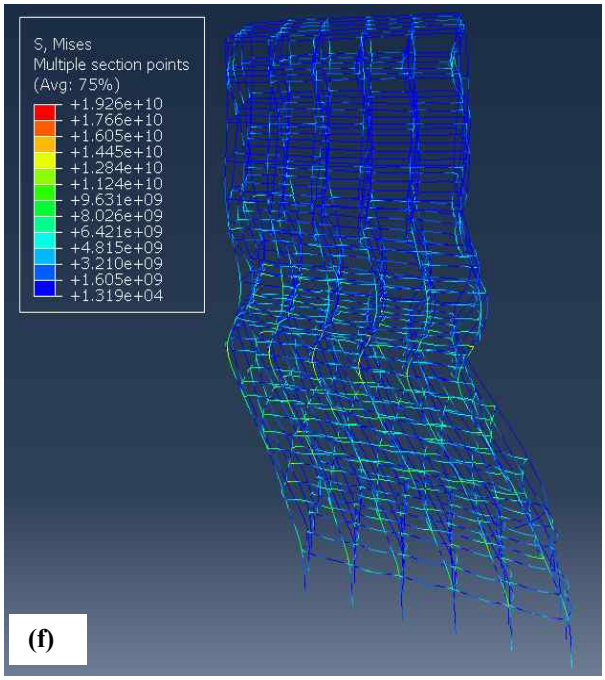
그림 2-78 Typical 3D view of the frame

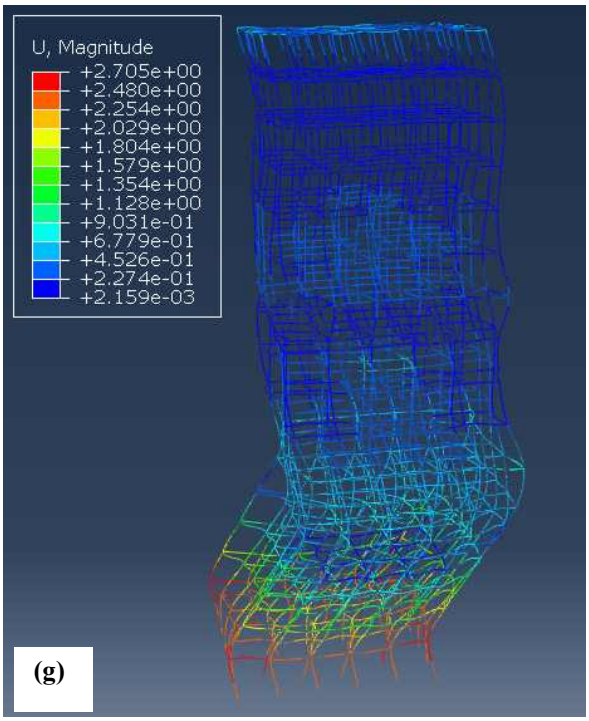
(a) 하중 및 변위

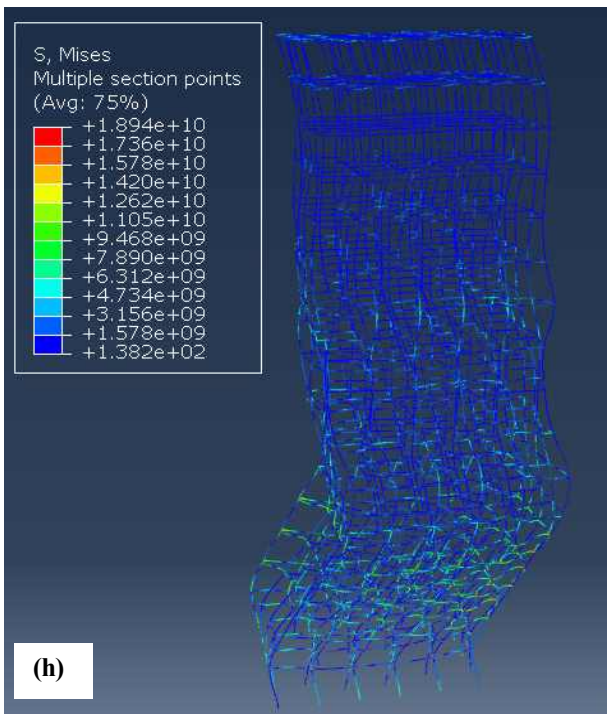
To derive a criteria for the seismic-induced damages of buildings, in the first step, the behavior of the frames in terms of displacement and stress were investigated. The spectrogram plotted on the deformed shapes of the frames of different stories after the first peak of applied seismic load are provided in 그림 2-79.




U, Magnitude
+2.851e+00
+2.613e+00
+2.376e+00
+2.138e+00
+1.901e+00
+1.663e+00
+1.426e+00
+1.188e+00
+9.504e-01
+7.128e-01
+4.753e-01
+2.377e-01
+1.384e-04
(e)


S, Mises
Multiple section points
(Avg: 75%)
+1.926e+10
+1.766e+10
+1.605e+10
+1.445e+10
+1.284e+10
+1.124e+10
+9.631e+09
+8.026e+09
+6.421e+09
+4.815e+09
+3.210e+09
+1.605e+09
+1.319e+04
(f)


U, Magnitude
+2.705e+00
+2.480e+00
+2.254e+00
+2.029e+00
+1.804e+00
+1.579e+00
+1.354e+00
+1.128e+00
+9.031e-01
+6.779e-01
+4.526e-01
+2.274e-01
+2.159e-03
(g)


S, Mises
Multiple section points
(Avg: 75%)
+1.894e+10
+1.736e+10
+1.578e+10
+1.420e+10
+1.262e+10
+1.105e+10
+9.468e+09
+7.890e+09
+6.312e+09
+4.734e+09
+3.156e+09
+1.578e+09
+1.382e+02
(h)

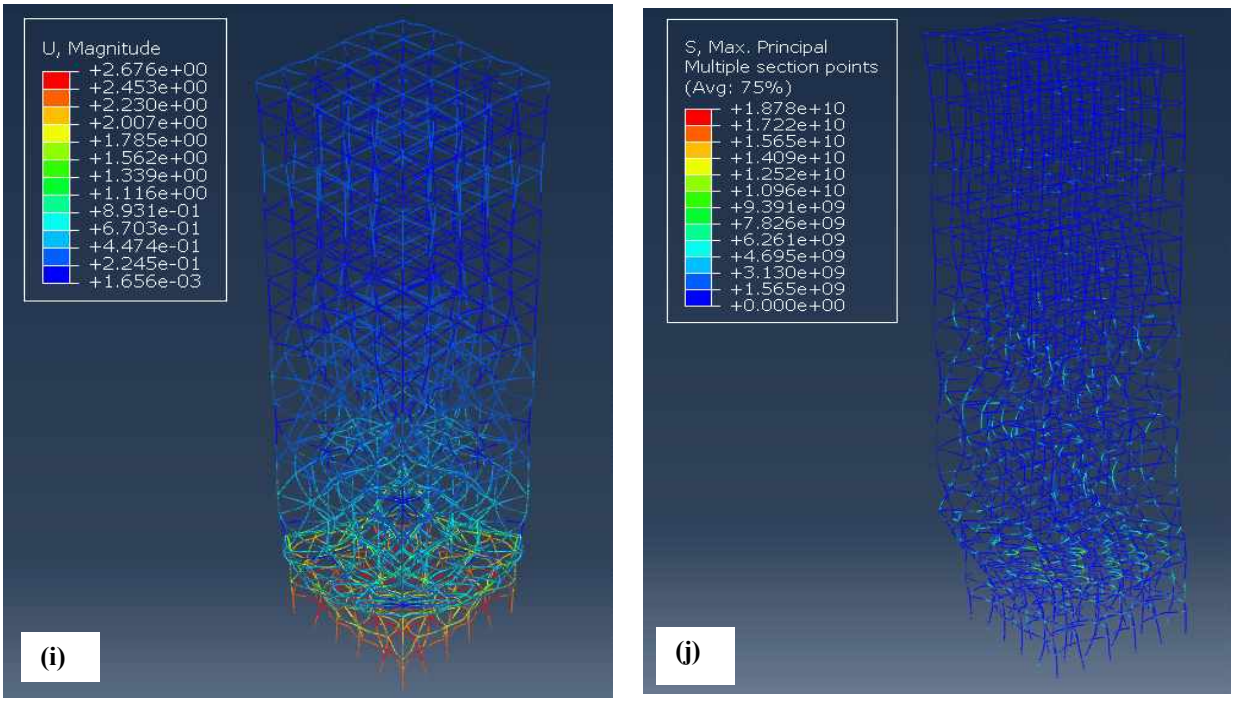


그림 2-79 Spectrograms of the displacement and stress of frames of different stories: (a) 8-story (displ.), (b) 8-story(stress), (c) 10-story(displ.), (d) 10-story(stress), (e) 12-story (displ.), (f) 12-story(stress), (g) 15-story(displ.), (h) 15-story(stress), (i) 20-story(displ.), (j) 20-story(stress)

(b) 층변위

In order to study the local displacement of the building in each story, the story drift is to be calculated by using the 식 (21)

$$d_i = \frac{U_i - U_{i-1}}{h_i} \tag{21}$$

where is story drift, is displacement of the ith story , is the displacement of the (i-1) story, and is the height of the story. The story drifts of the each building are plotted for each story such that the absica is specified to the drift (%), and the ordinate indicates the number of story. The graphs representing the variation of the story drift along the building height are presented in 그림 2-80.

In order to relate the deformation of the internal structural members to the structural behavior of the external members, a dimensionless ratio was defined as the ratio of the displacement of the internal members to the external members. The variation of the average amounts of displacement ratio with respect to number of story is illustrated in 그림 2-81.

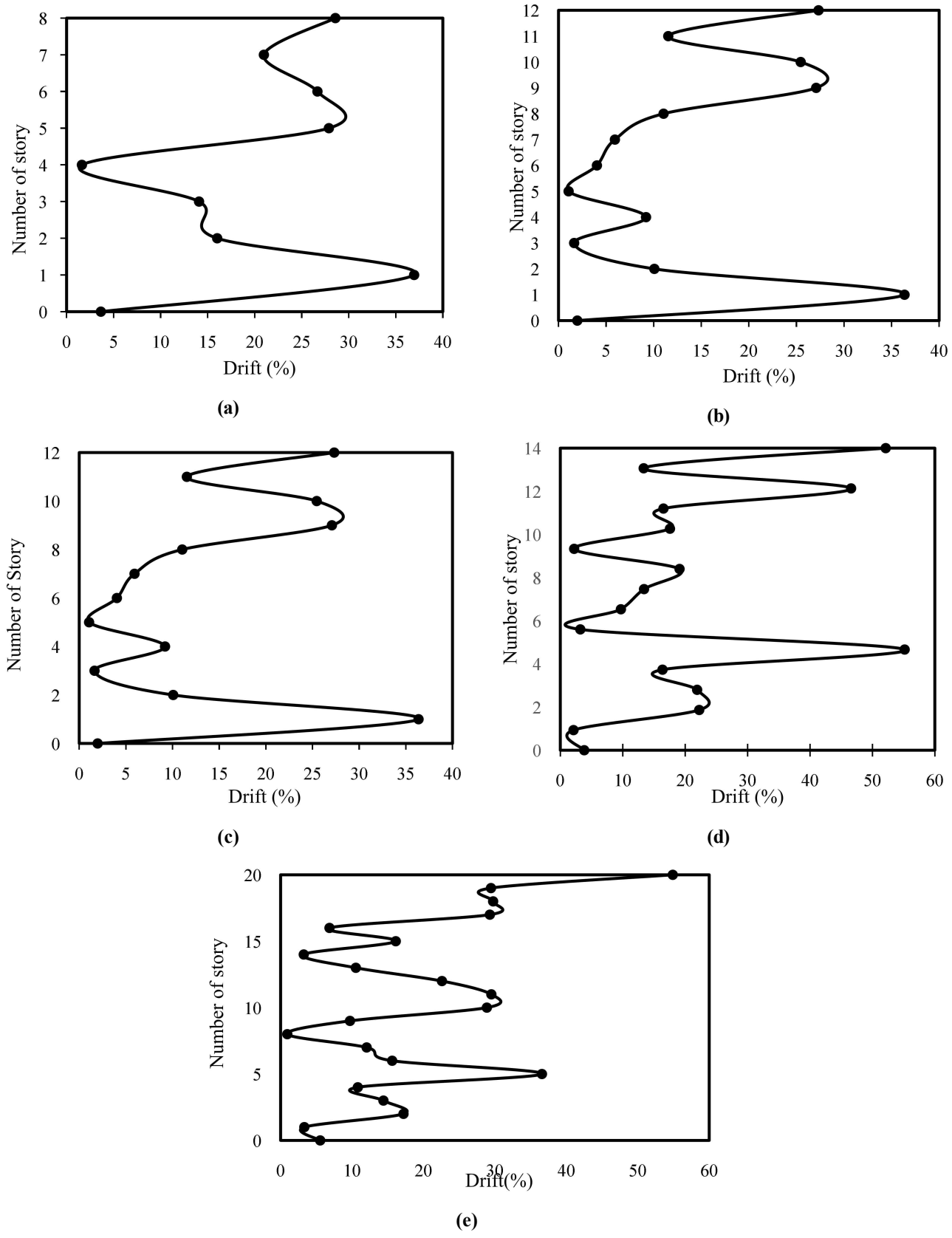


그림 2-80 Story drift due to the load combination of seismic load a building dead and live loads for a variety of buildings stories; (a) 8-story, (b) 10-story, (c) 12-story, (d) 15-story, and (e) 20-story

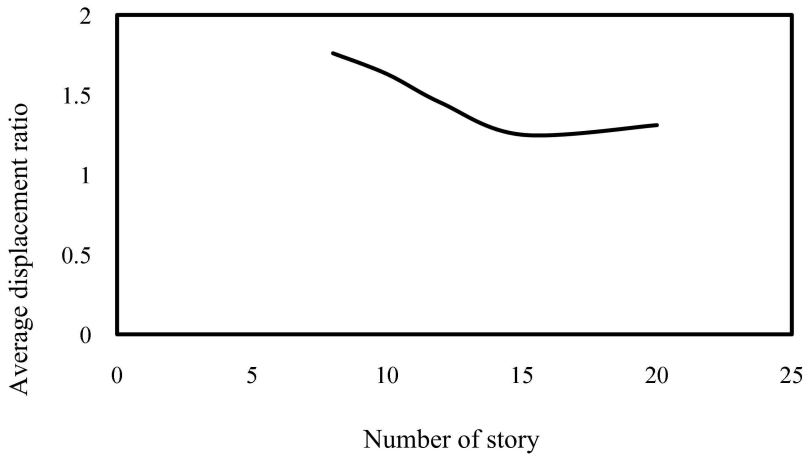


그림 2-81 Variation of average amount of displacement ratio

Based on this graph the following equation can be suggested for the prediction of the average displacement ratio of a building with a specific number of stories with the coefficient of determination of R2=0.9733.

$$U_r = 0.0042N^2 - 0.1403N + 2.2229 \quad (22)$$

where U_r is displacement ration and N is the number of stories.

(c) 제안된 식의 일반화

(c-1) 층 수

To evaluate the generalization of the 식 (22), it was considered to investigate the displacement of the seismic loaded of a 5-story building.

The displacement ratios are provided in 표 2-28, and the story drift is provided in 그림 2-82. Then, the average displacement ratios were calculated using presented formula and their variations with respect to the actual displacement obtained form FEM analysis using ABAQUS were determined as shown in 표 2-29.

표 2-28 Displacement ratio for a 5-story building obtained from FEM

Level(m)	19.8	16.5	13.2	9.9	6.6	3.3	0
Roof	6	5	4	3	2	1	Ground
Displ. ratio	1.84	1.51	1.47	1.64	1.75	1.91	3.6

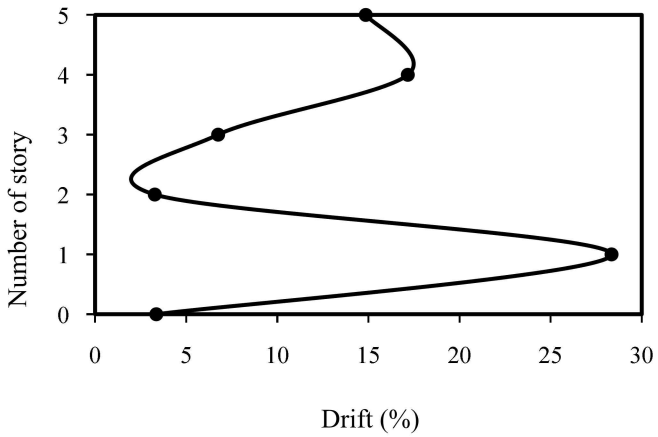


그림 2-82 Story drift of the 5-story building

표 2-29 Comparison between the displacement ratios obtained from FEM and suggested formula

Number of Story of buildings	Displ. ratio (FEM)	Displ. Ratio (Formula)	Variation (%)
5	1.96	2.14	8.41
8	1.76	1.79	1.68
10	1.63	1.59	2.52
12	1.45	1.43	1.40
15	1.25	1.29	3.1
20	1.31	1.30	0.77

(c-2) 하중

To evaluate the generalization of the formula, the building of 5-story was subjectetd to a seismic load of a lower magnitude of 0.1 of the real magnitude.

The seismic analysis of the 5-story building subject to a seismic load with magnitude of 0.1 of the real seismic load was performed and the story drift of the frame was achieved as illustrated in 그림 2-83.

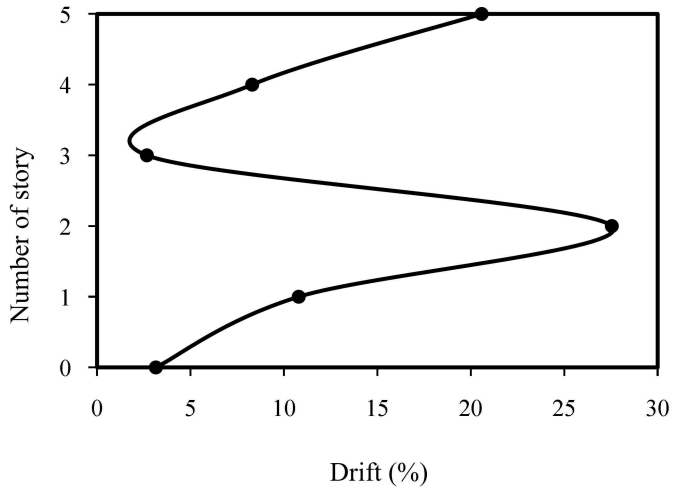


그림 2-83 Story drift of the 5-story building subject to a seismic load of a 0.1 magnitude of real load

The displacement ratios of the 5-story building are provided in 표 2-30. From 표 2-30 an average displacement ratio of 1.98 was achived. The variation of displacement ratio obtained from FEM with respect to the displacement ratio calculated from presented formula is 7.38%, so the generalization of the presented formula is validated for different load magnitudes too.

표 2-30 Dispalcement ratio of the 5-story building for a seismic load of one-tenth magnitude

	6(roof)	5	4	3	2	1	0
mid/corner	1.51	1.90	2.07	1.21	1.99	1.85	3.33

2.2 콘크리트 프레임

In this part it is tried to evaluate the seismic response of the concrete frames and obtain a criteria for the prediction of the displacement of interior structural elements with respect to the those of exterior elements. For this aim, five buildings of different stories were considered; 8-story, 10-story, 12-story, 15-story, and 20-story. The frame is fixed at the bottom and a uniform column size and reinforcement ratio along building height were considered.

For the analysis of this report, the concrete of compressive strength of 20.0 MPa, elastic modulus of 21.2 GPa, and Poisson's ratio of 0.20 was considered for the concrete. To model the plastic behavior of the concrete, the concrete damage plasticity was adopted as defined in 표 2-30. Furthermore, the compressive and tensile behaviors of the concrete are provided in the graphs given in 그림 2-83(a) and (b), respectively.

표 2-31 Concrete characteristics and damage plasticity model

Parameter	Density (kg/m3)	Elastic modulus (GPa)	Poisson's ratio	Dilation angle	Eccentricity	$\frac{f_{b0}}{f_{c0}}$	k	Viscosity parameter
value	2400	21.2	0.2	30.5	0.1	1.16	0.667	0

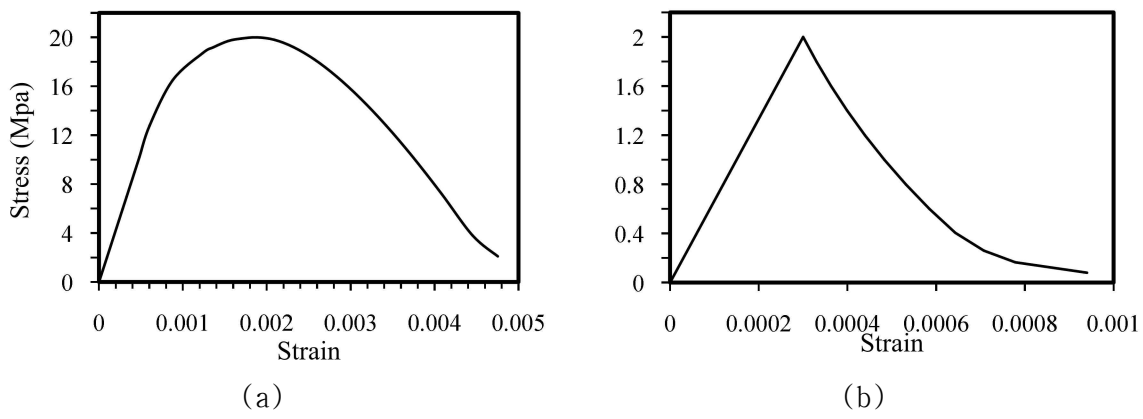
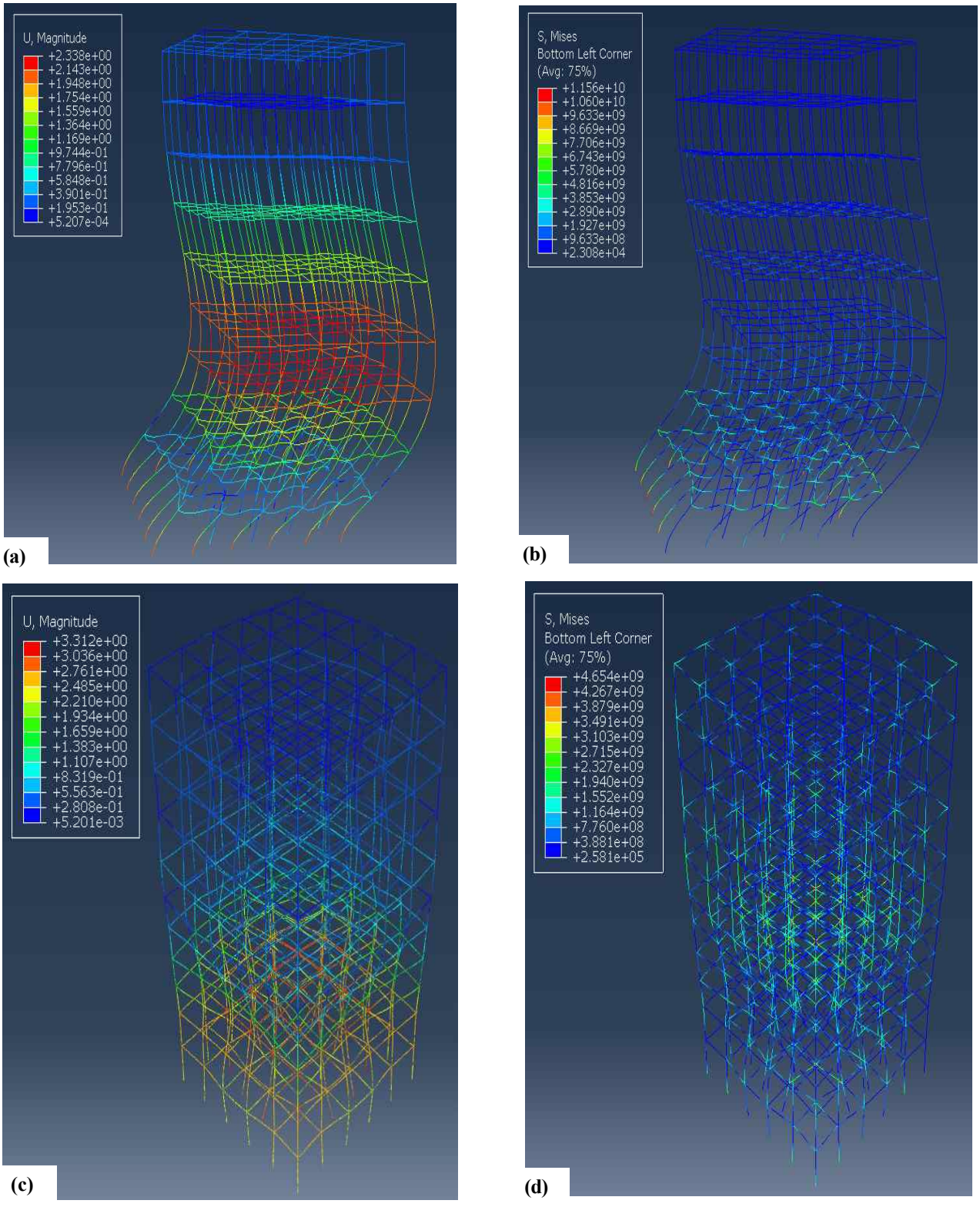
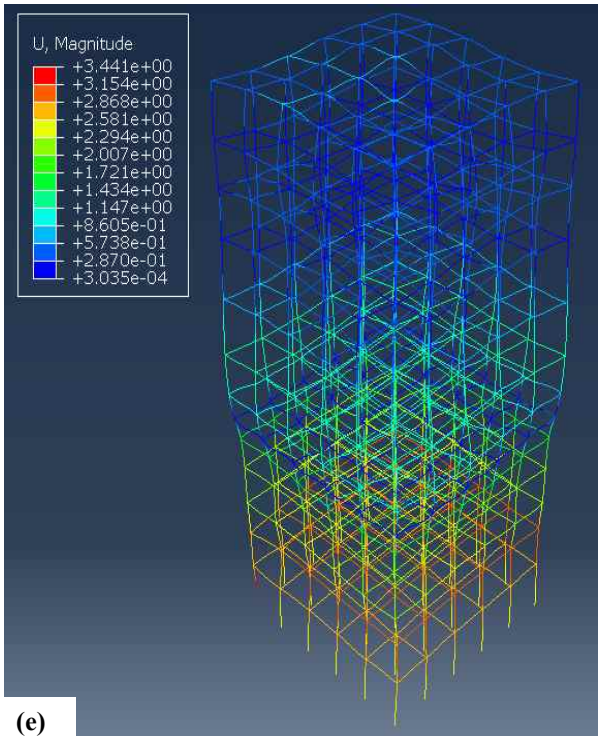


그림 2-84 Nonlinear properties of concrete; (a) compressice, (b) tensile

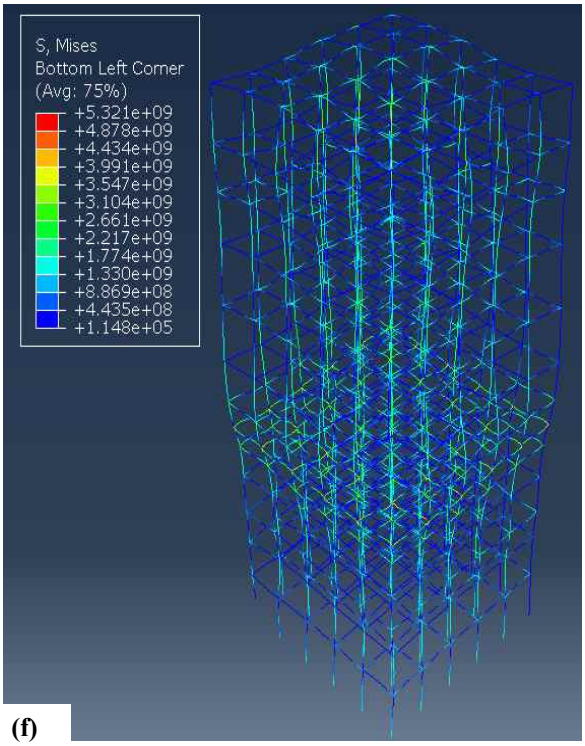
2.2.1 변위 및 응력

To derive a criteria for the seismic-induced damages of concrete buildings, the behavior of the frames in terms of displacement and stress were investigated. The variation of displacement and stress over the height of the concrete frames of different stories after the first peak of applied seismic load are provided in 그림 2-84.

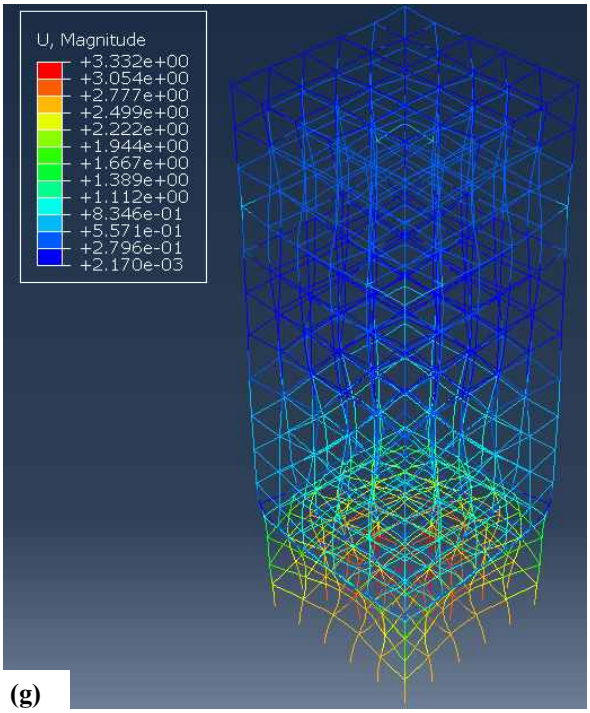



U, Magnitude
+3.441e+00
+3.154e+00
+2.868e+00
+2.581e+00
+2.294e+00
+2.007e+00
+1.721e+00
+1.434e+00
+1.147e+00
+8.605e-01
+5.738e-01
+2.870e-01
+3.035e-04

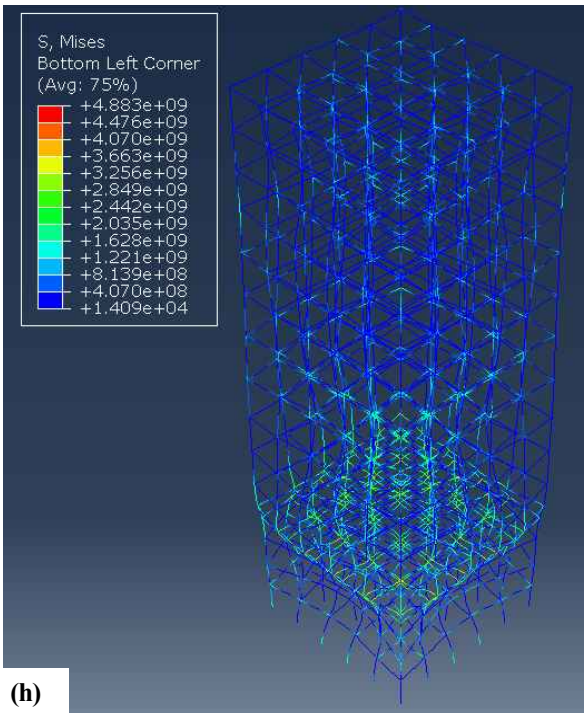
(e)


S, Mises
Bottom Left Corner
(Avg: 75%)
+5.321e+09
+4.878e+09
+4.434e+09
+3.991e+09
+3.547e+09
+3.104e+09
+2.661e+09
+2.217e+09
+1.774e+09
+1.330e+09
+8.869e+08
+4.435e+08
+1.148e+05

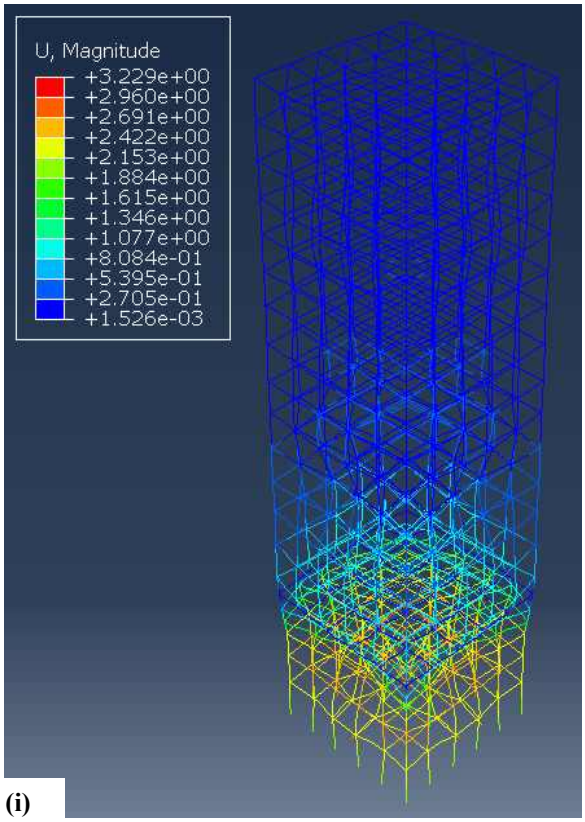
(f)


U, Magnitude
+3.332e+00
+3.054e+00
+2.777e+00
+2.499e+00
+2.222e+00
+1.944e+00
+1.667e+00
+1.389e+00
+1.112e+00
+8.346e-01
+5.571e-01
+2.796e-01
+2.170e-03

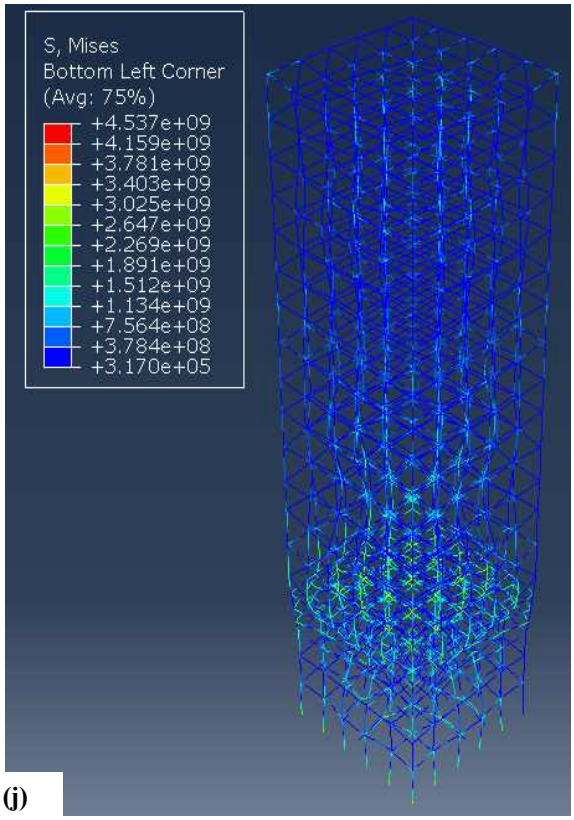
(g)


S, Mises
Bottom Left Corner
(Avg: 75%)
+4.883e+09
+4.476e+09
+4.070e+09
+3.663e+09
+3.256e+09
+2.849e+09
+2.442e+09
+2.035e+09
+1.628e+09
+1.221e+09
+8.139e+08
+4.070e+08
+1.409e+04

(h)



(i)



(j)

그림 2-85 Variation the displacement and stress of concrete frames of different stories: (a) 8-story (displ.), (b) 8-story(stress), (c) 10-story(displ.), (d) 10-story(stress), (e) 12-story (displ.), (f) 12-story(stress), (g) 15-story(displ.), (h) 15-story(stress), (i) 20-story(displ.), (j) 20-story(stress).

To find a criterion for prediction of the deformation of the internal structural members by having the displacement of the external members the displacement ratios were calculated as that of steel frames. The variation of the average amounts of displacement ratio concerning the number of story is depicted in 그림 2-87.

Based on this graph the following equation canbe suggested for the prediction of the average displacement ratio of a building with a specific number of stories with the coefficient of determination of R2=0.9557.

$$U_r = 0.0042N^2 - 0.1403N + 2.2229 \quad (23)$$

where Ur is displacement ration and N is the number of stories.

2.2.2 제안된 식의 일반화

(a) 층 수

To generalize the 식 (23), a concrete frame of 5 story was evaluated and the corresponding displacement due to seismic load and building live and dead loads were achieved. Accordingly, the displacement ratios are provided in 표 2-32, and the story drift is provided in 그림 2-88. Then, the average displacement ratios were calculated using presented formula and their variations with respect to the actual displacement obtained form FEM analysis using ABAQUS were determined as shown in 표 2-33.

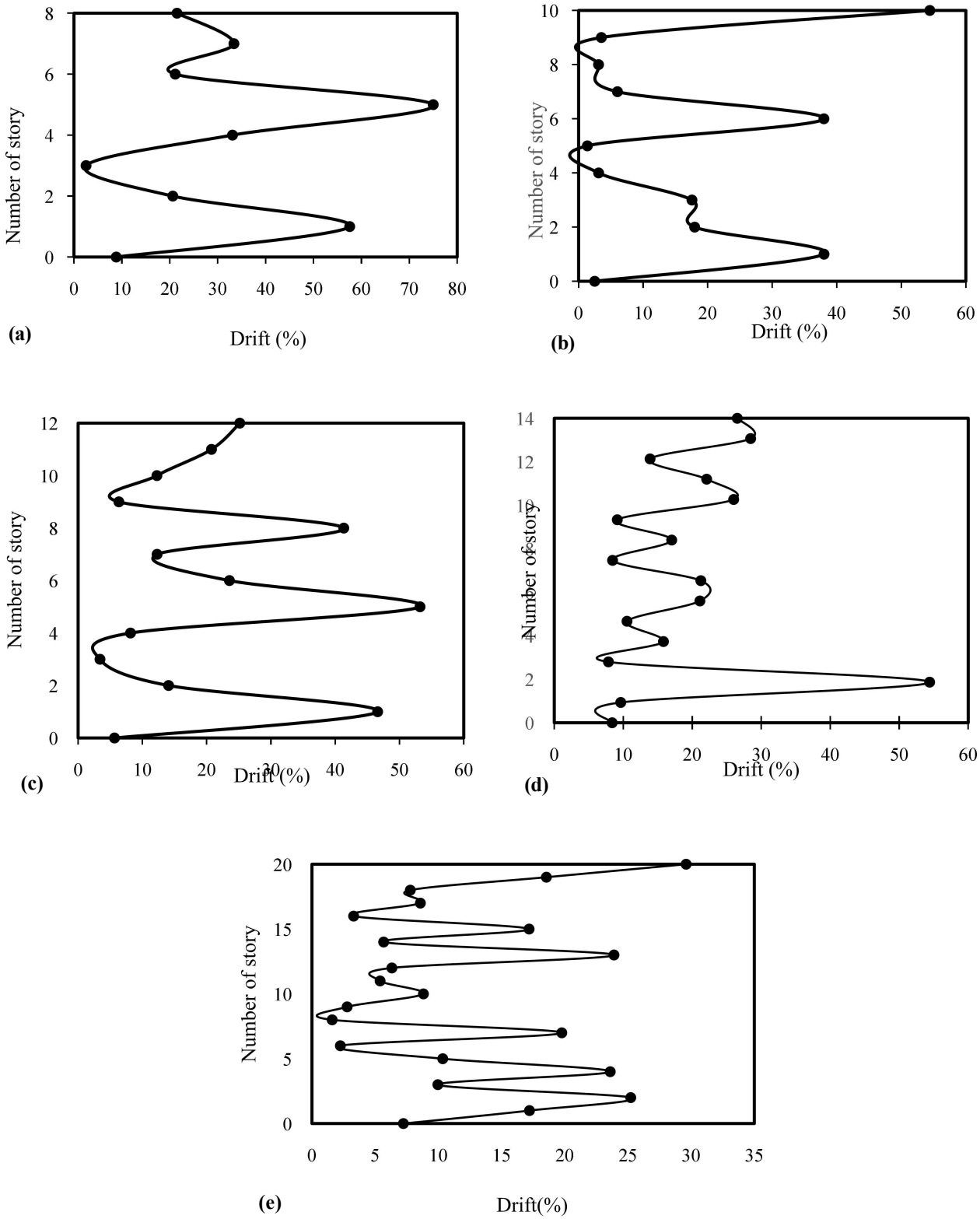


그림 2-86 Story drift due to the load combination of seismic load a building dead and live loads for a variety of buildings stories; (a) 8-story, (b) 10-story, (c) 12-story, (d) 15-story, and (e) 20-story

표 2-32 Displacement ratio for a 5-story concrete building obtained from FEM

Level(m)	19.8	16.5	13.2	9.9	6.6	3.3	0
Roof	6	5	4	3	2	1	Ground
Displ. ratio	1.44	1.31	1.27	1.4	1.74	1.91	3.6

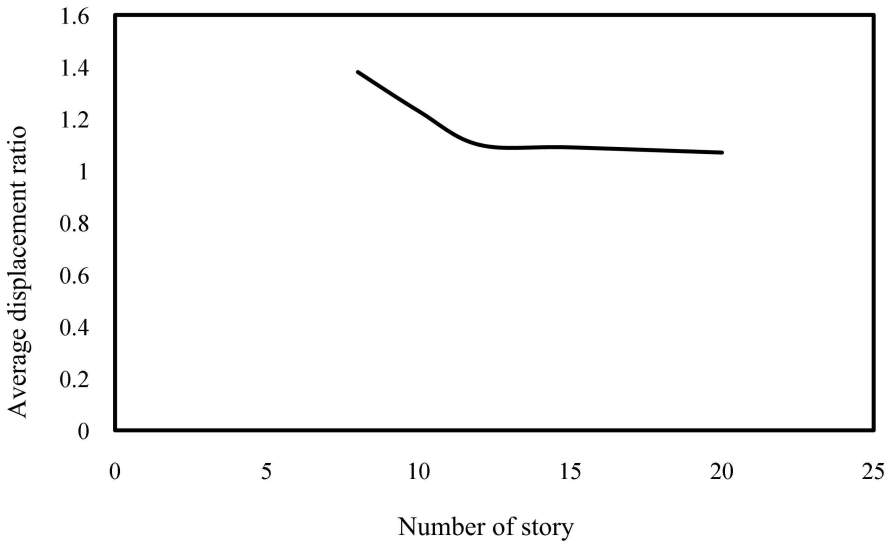


그림 2-87 Variation of average amount of displacement ratio

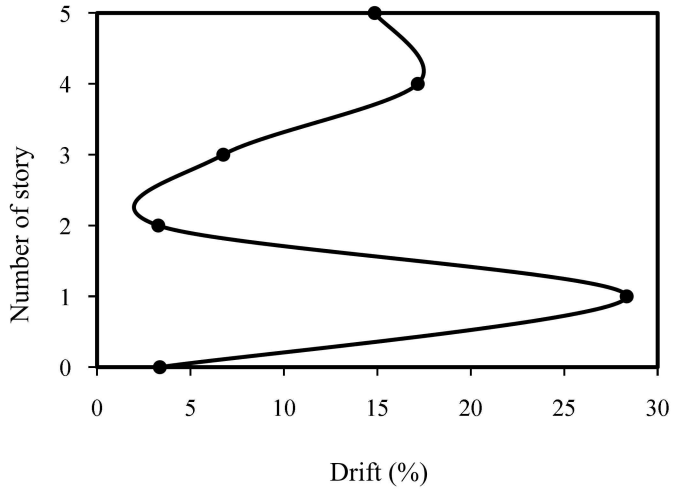


그림 2-88 Story drift of a 5-story concrete frame

표 2-33 Comparison between the displacement ratios obtained from FEM and suggested formula

Number of Story of buildings	Displ. ratio (FEM)	Displ. Ratio (Formula)	Variation (%)
5	1.53	1.63	5.93
8	1.38	1.37	0.78
10	1.23	1.24	0.80
12	1.1	1.14	3.85
15	1.09	1.06	2.50
20	1.07	1.10	2.45

(b) 하중

To evaluate the generalization of the formula, the building of 5-story was subjectetd to a seismic load of a lower magnitude of one-tenth of the real seismic load magnitude. The seismic analysis of the 5-story concrete building subject to a seismic load with magnitude of 0.1 of the real seismic load was performed and the story drift of the frame was achieved as illustrated in 그림 2-89.

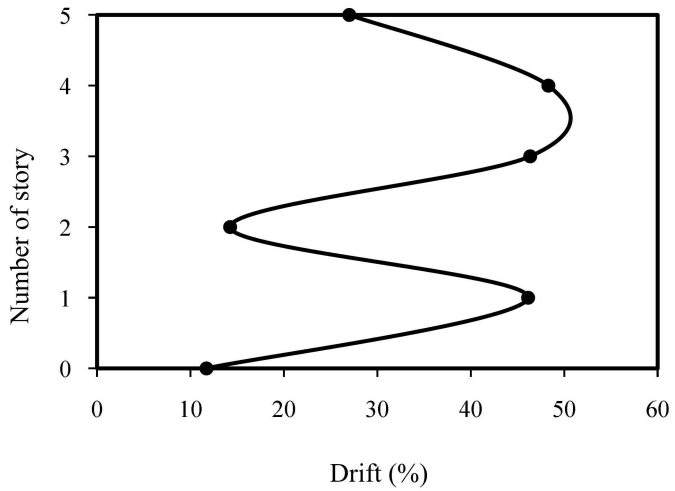


그림 2-89 Story drift of the 5-story concrete building subject to a seismic load of a 0.1 magnitude

The displacement ratios of the 5-story building are provided in 표 2-34. From 표 2-34 an average displacement ratio of 1.54 was achived. The variation of displacement ratio obtained from FEM with respect to the displacement ratio calculated from presented formula is 5.31%, so the generalization of the presented formula is validated for different load magnitudes too.

표 2-34 Dispalcement ratio of the 5-story building for a seismic load of one-tenth magnitude

roof	6	5	4	3	2	1	0
mid/corner	0.91	0.93	1.54	1.11	1.05	1.76	3.48

3. 드론계측 결과와의 비교

3.1 전체 거동과 파괴

A two-story reinforced concrete parking deck was tested to find the most vulnereable parts and behavior of the structure subject to the seismic loads. The illustration of the destructued structure at Guardian Center is provided in 그림 2-90.

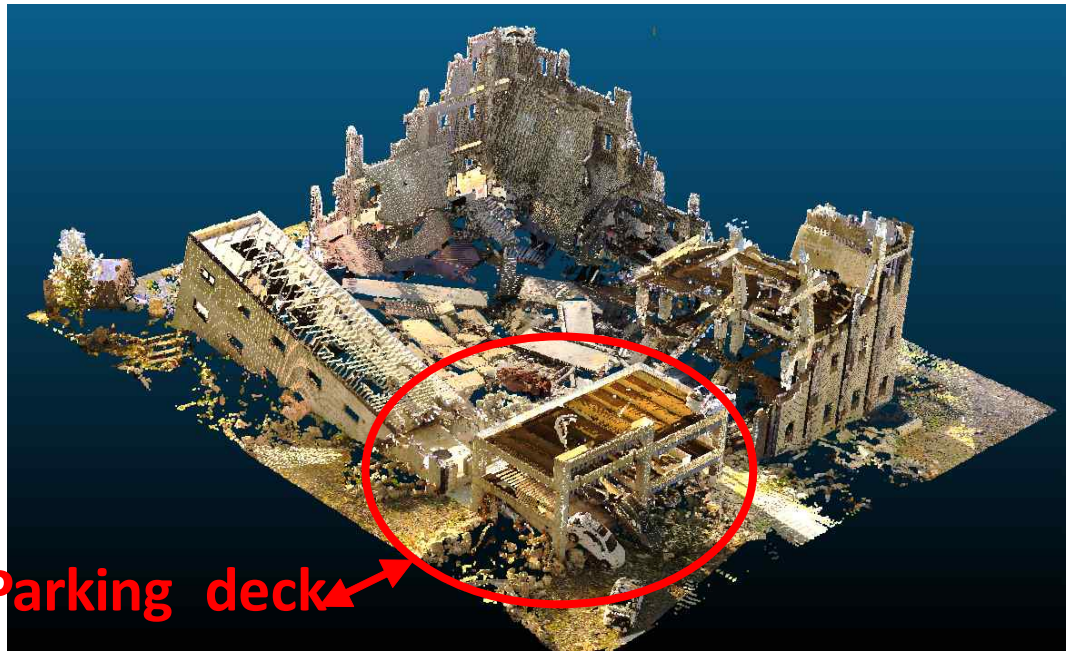


그림 2-90 Illustration of the destructed structure and the parking deck at Guardian Center

To have a better illustration of the parking deck, its focused front and back views are provided in 그림 2-91.

As can be seen form the 그림 2-91, the concrete part of the lower areas of the column are totally crushed and destructed and the only parts which still resist are the reinforcing rebar which they may soon collapse due to the further laoding. It show that the applied load affect the lower parts of the column mostly and they need very special considerations for both design and construction. Since the concrete is weak in the shear parts, it is highly suggested to reinforce this parts with steel or shape memory alloy (SMA) fibers, i.e. the fiber reinforced concrete can be used instead of plain concrete. The existence of fibers help to bridge the cracks in the shear parts and increase the shear capacity of the column along with the rebars. Furthermore, the ultra high-performance concrete can be used to enhance the seismic resitance of the parking deck.

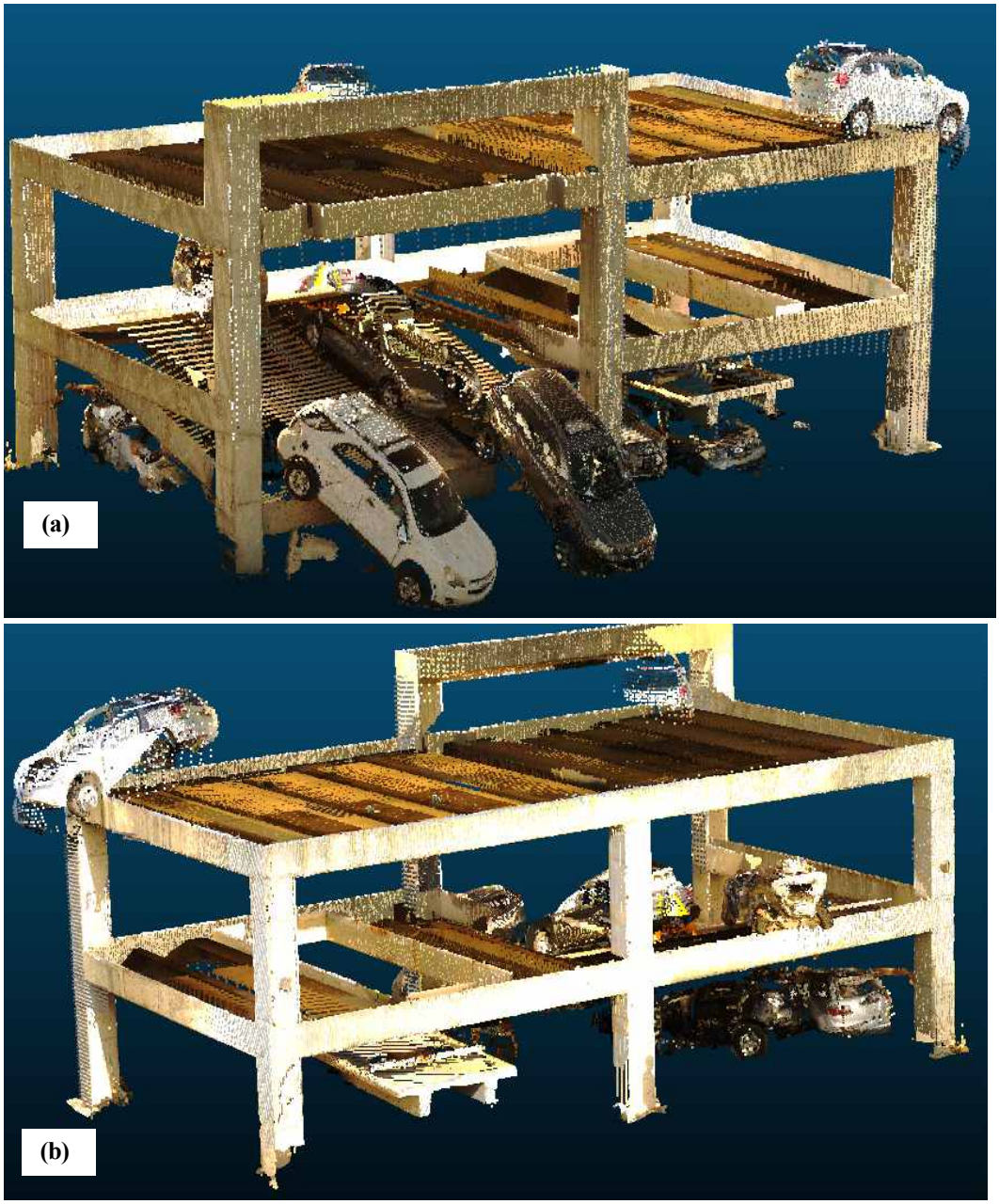


그림 2-91 Focused views of the damaged parking deck; (a) front view, (b), back view

3.2 구조 요소의 손상 평가

The post-evaluation of the parking deck dameged due to the applied seismic laod was carried out and the amounts of the damages of the structural elements were extracted. 표 2-35 shows the average damage and tilt of each structural element, namely, beam, column and slab. In this table 100% indicates no damage, and 0.0% shows completely damaged.

표 2-35 Damage portion of the structural elements

	Beam	Column	Slab
Damage	67.92	93.48	76.96
tilt	-	1.68	3.59

As can be seen from 표 2-35, the most resistant and stable structural element is column and the most vulnereable one is beam, thus, in the desing and construction of the parking deck,

beams should be paid special considerations to be more resistant against the applied seismic loads. Damege occurred to beam might be because of the tilt of column and slab which applied shear to the beam-to-column joints and twist it against its longitudinal central axis. Besides, the bending moments applied to the beam increased the stress in the beam, especially, in the sear part and result in crushing of the concrete.

4. 요약

This report dealt with investigation of the concrete frame high-rise buildings and steel-frame high-rise buildings subject to seismic load. For this aim the finite element (FE) analysis was carried out using ABAQUS. The FE method was validated using the experimental works done on a concrete frame. Then, the attempts have been made to derive the equations for predicting the internal displacement from external displacmenet. Thses equations can be used for post-investigation of the earthquakes to predict the internal damage of the destructued or damaged buildings. This may help the rescue team to distinguish between completely damaged parts and partial damaged regions in which there might be some people sucked and can be saved. In the final step, a parking deck of concrete was evaluated and its damaged parts were addressed and discussed.

5. 유효성 평가 결과 국문 요약

콘크리트 프레임 고층 구조물과 스틸 프레임 고층 구조물의 지진 하중에 의한 피해를 실제 콘크리트 프레임 결과와 비교하였다. 가디언 센터 내의 손상된 구조물에 대한 조지아텍의 스캔 결과와 본 연구에서 도출한 콘크리트 프레임 구조물의 외관변형도 및 내부손상도의 차이는 약 4.7% 로 신뢰할 수 있는 결과를 도출하였다고 볼 수 있다. (하중 및 변위 (P.113) 및 구조요소의 손상 평가 (P.115))

따라서 본 연구의 외관변형도-내부손상도 매핑시스템은 유효하다고 평가할 수 있으며, 그 결과는 지진 후의 파괴되거나 손상된 건축물의 내부적인 손상을 예측하는데 사용 가능하다고 평가할 수 있다.

(나) 협동연구기관(Georgia Institute of Technology)

① 개발 목표

한/미 공동 Test-Bed 구축 및 시스템 검증

② 개발 내용 및 범위(그림을 이용하여 시스템 구성도, 구조 등을 구체적으로 표현)

①	재난 현장 Test-Bed 구축

- 재난 시뮬레이션 현장 Test-Bed 확보 (Guardian Centers in GA, USA)
- 현장시험 기획 및 설계
- Test-Bed 기초 설계 자료 취득
- 한/미 공동 현장검증시험 실시

②	시스템 검증

- 설계 도면 활용 재난 이전 기초모델 작성
- 무인항공기 활용 포인트 클라우드 데이터 취득
- 1차년도 개발된 오브젝트 검출 알고리즘 정확도 검증
- 2차년도 개발된 구조체 변위 및 손상평가 시스템 검증

③	시스템 통합

- 개별 모듈 통합 시스템 구축
- 주관기관에서 개발될 위험도 분석 모델과 연동
- 통합 시스템 효율성 및 생산성 검증



그림 2-92 3차년도 주요연구내용

○ 재난 시뮬레이션 현장 Test-Bed 구축

■ 재난 시뮬레이션 현장 Test-Bed 확보

▪ Guardian Centers in GA, USA

- 대상 구조물: 콘크리트 구조, Steel 구조

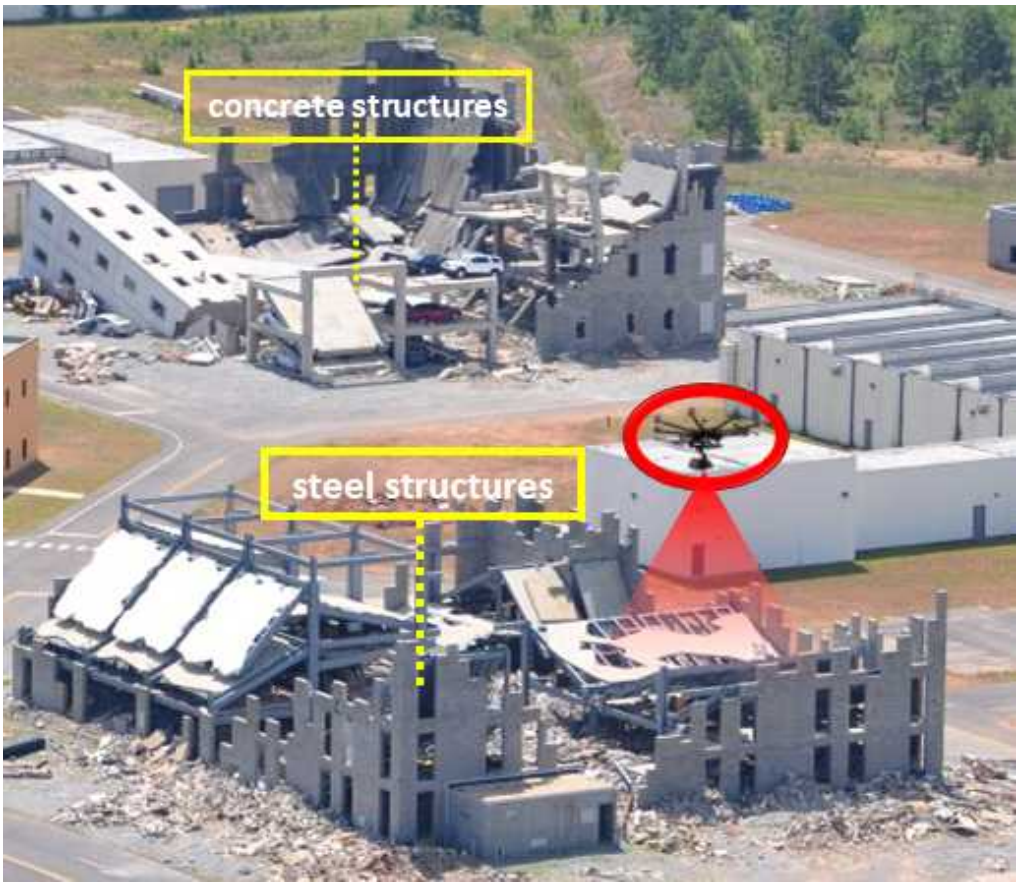


그림 2-93 Test-Bed 모의 재난 지역 무인 데이터 취득

- 데이터 취득: 무인시스템 (무인항공기, 레이져스캐닝 로봇)





그림 2-94 무인 시스템을 활용한 Test-Bed 지역 데이터 취득

■ 시스템 검증

▪ 무인항공기 기반 재난지역 3D 포인트 클라우드 데이터 취득 및 모델링

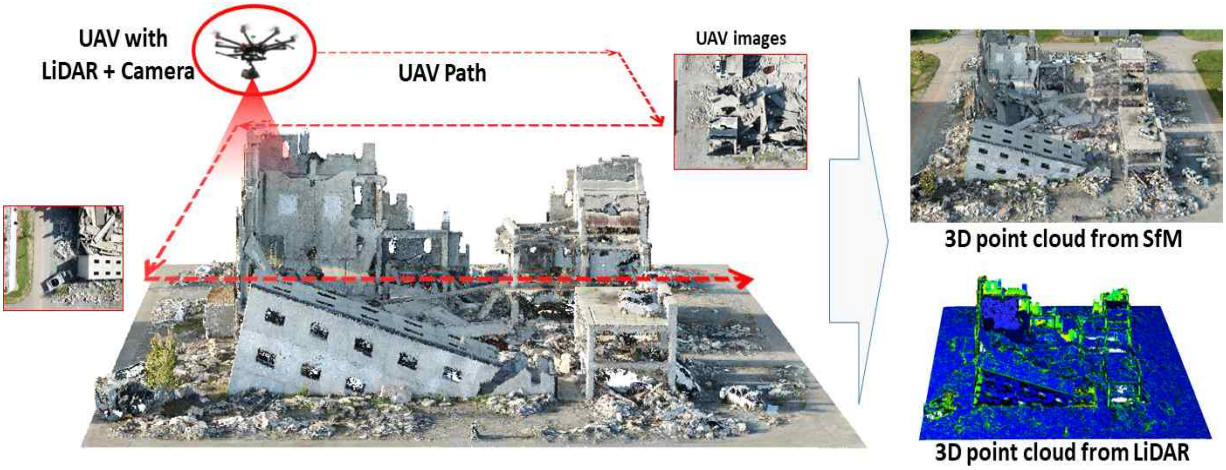


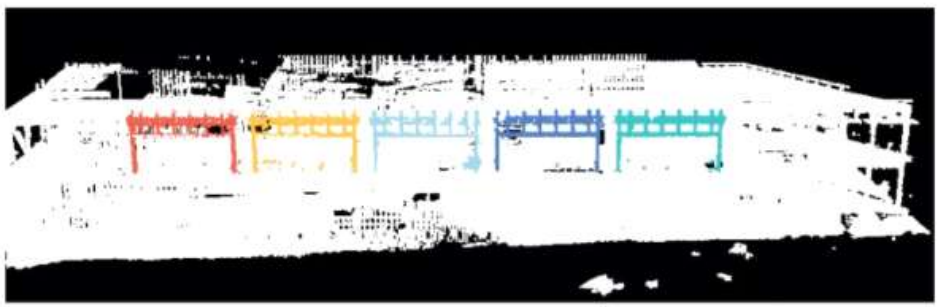
그림 2-95 이미지와 레이져를 활용한 재난지역 3D 모델링

▪ 오브젝트 검출 알고리즘 검증

- User Exemplar 기반 빌딩 요소 검출



(a) User selected exemplar (steel structure frame)



(b) Ground truth

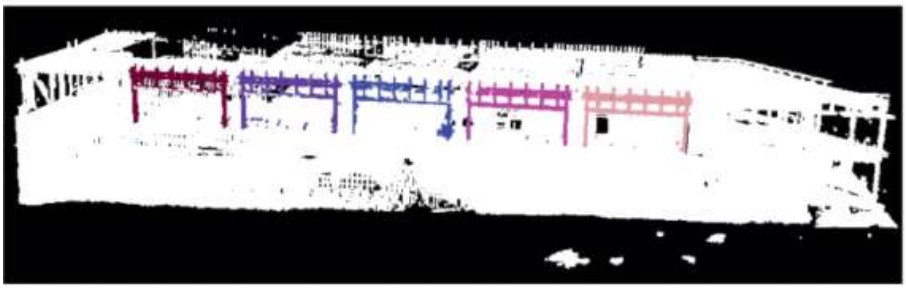


그림 2-96 User Exemplar 기반 스틸프레임 검출 결과

- User Exemplar 기반 빌딩 요소 검색 알고리즘 성능

Precision: 97%, Recall: 92%

▪ 손상평가 시스템 검증

- Unsupercised Learning 기반 크랙 분류 기술 (CrackEmbed)

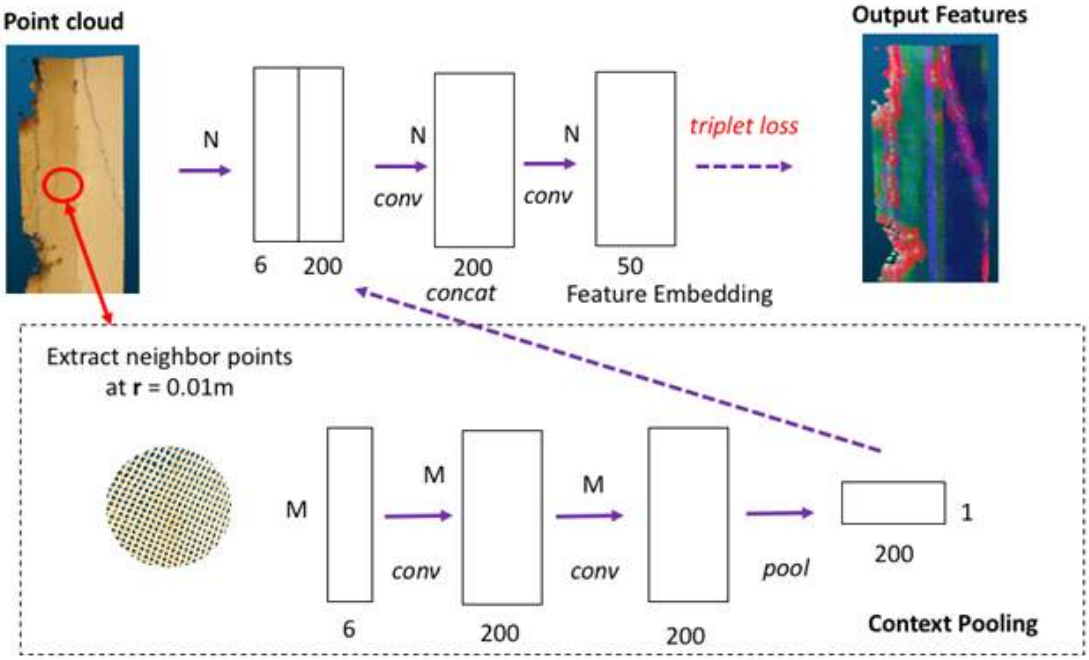


그림 2-97 CrackEmbed 네트워크 아키텍쳐

- 검증 대상 구조물: Guardian Center 콘크리트 빌딩 슬래브 구조

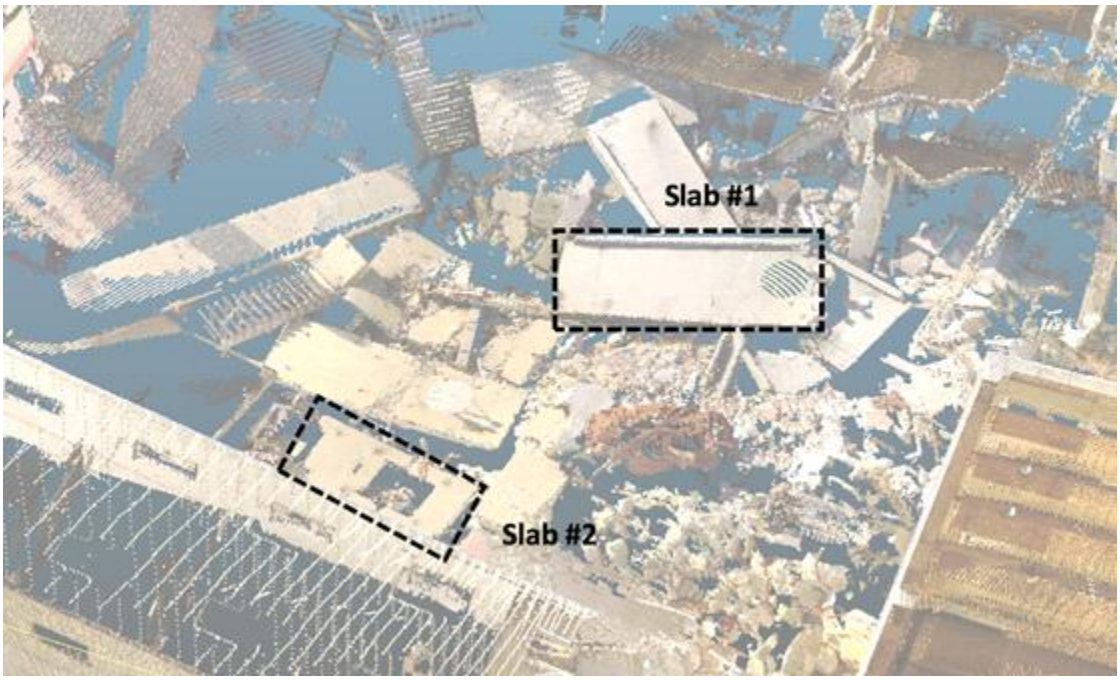


그림 2-98 검증 대상 슬래브 구조물

- 검증결과

표 2-36. 크랙 검출을 위한 특징점 서술자의 성능비교

Feature	Precision	Recall	F1-score	Length error (m)	Width error (m)
RGB color	**0.72**	0.57	0.63	0.027	0.021
Intensity	0.60	0.61	0.60	0.006	0.008
Normal	0.52	0.40	0.45	0.146	0.148
Curvature	0.47	0.44	0.44	0.049	0.040
FPFH	0.61	0.08	0.14	0.083	0.086
PointNet++	0.60	0.34	0.41	0.052	0.068
CrackEmbed	0.69	**0.75**	**0.71**	**0.004**	**0.004**

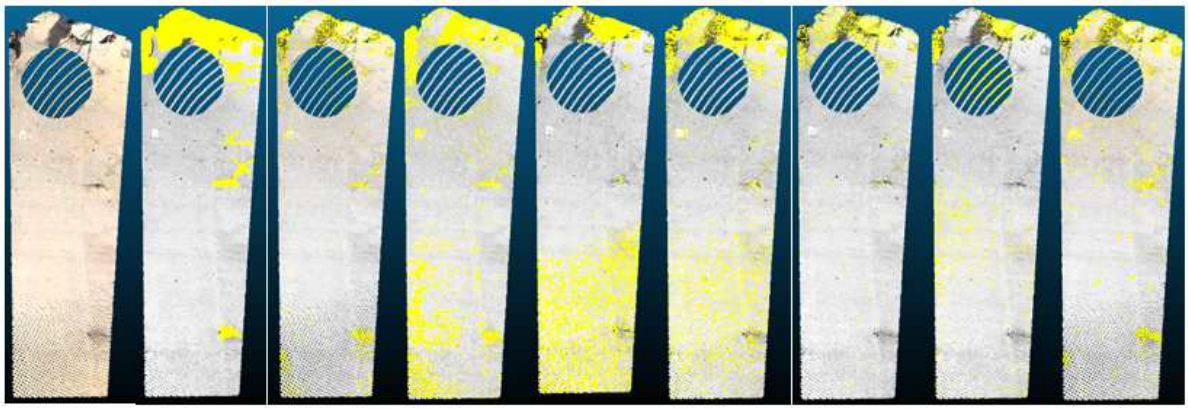


그림 2-98 왼쪽부터, (a) 원본데이터, (b) Ground Truth, (c) RGB color (d) intensity (e) normal (f) curvature (g) FPFH (h) PointNet++ (i) CrackEmbed

○ 시스템 통합 지원

■ 포인트 클라우드를 활용한 구조해석용 3D 모델링

▪ 오브젝트 검출 알고리즘을 통한 포인트 클라우드 새그멘테이션

- Guardian Center Parking Deck

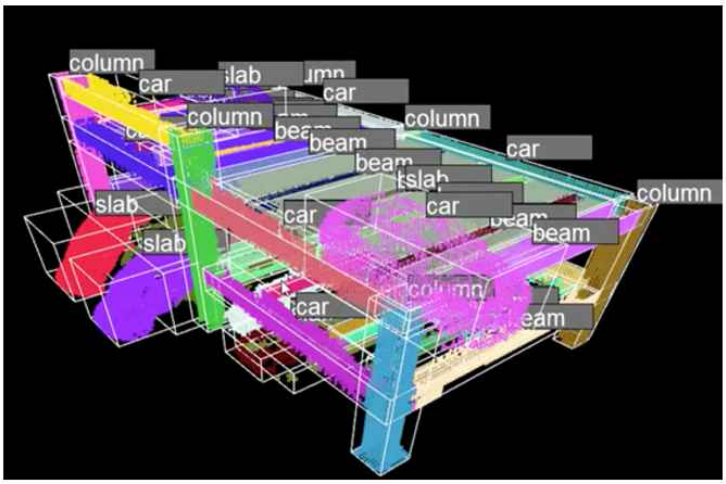


그림 2-99 Test-Bed 지역 포인트 클라우드 새그멘테이션

▪ 3D Cad 모델 변환

- Point to 3D 모델링 (ply -> obj)

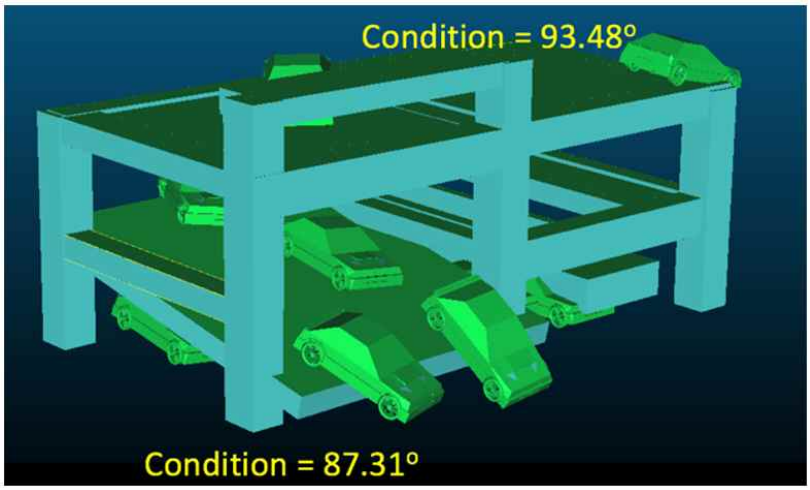


그림 2-100 구조해석을 위한 3D 캐드모델

○ 드론 기반 이미지 활용시, pointcloud와 이미지 정합 관련 발생 문제점 해결방안

- 본 연구는 레이저 스캔을 통해 생성되는 point cloud에 드론 이미지를 정합하는 방식이 아닌, Structure from Motion 방식을 활용하여 드론 이미지를 활용해 3차원 point cloud를 생성하였으며, 본 연구에서는 드론을 통해 제작된 point cloud와 LiDAR를 통해 생성되는 포인트 클라우드를 병합하는 기술을 제안함

○ LiDAR 데이터와 사진측량 데이터의 병합처리 방식

- 드론 이미지를 통해 생성되는 3D Point Cloud는 지상 레이저 스캔으로 생성되는 3D Point Cloud와 비교하여 정밀도/정확도가 떨어지며, 특히 수직 구조물에 대한 정밀도가 수평 구조물에 비해 현저히 낮음

- 이러한 이유로 본 연구에서는 지상 레이저 스캔으로 생성된 Point Cloud와 드론 이미지로 생성되는 Point Cloud를 정합하는 방법론을 제시함 (Park et al., 2019)

- 기존 3차원 모델을 자동으로 정합하는 방법들은 두 모델에서 동시에 존재하는 3차원 특징점을 활용하는 방식을 사용하였으나, 드론 이미지로 생성되는 point cloud와 지상 레이저 스캐너를 통해 생성되는 point cloud는 데이터를 취득하는 위치가 서로 달라 중첩되는 부분이 작고 모델의 형상이 다르기 때문에 3차원 특징점 추출이 어려움

- 따라서 본 연구에서는 각 포인트 클라우드 제작 시 수집되는 2D이미지에서 공통 특징점을 추출하고 그 특징점이 위치한 픽셀이 3차원 포인트 클라우드에 투영되는 좌표를 추적하여 추적된 공통 3차원 좌표점들을 기반으로 변환매트릭스를 생성하여 이를통해 3차원 포인트 클라우드를 정합하는 방식을 제안함 (그림 2-101)

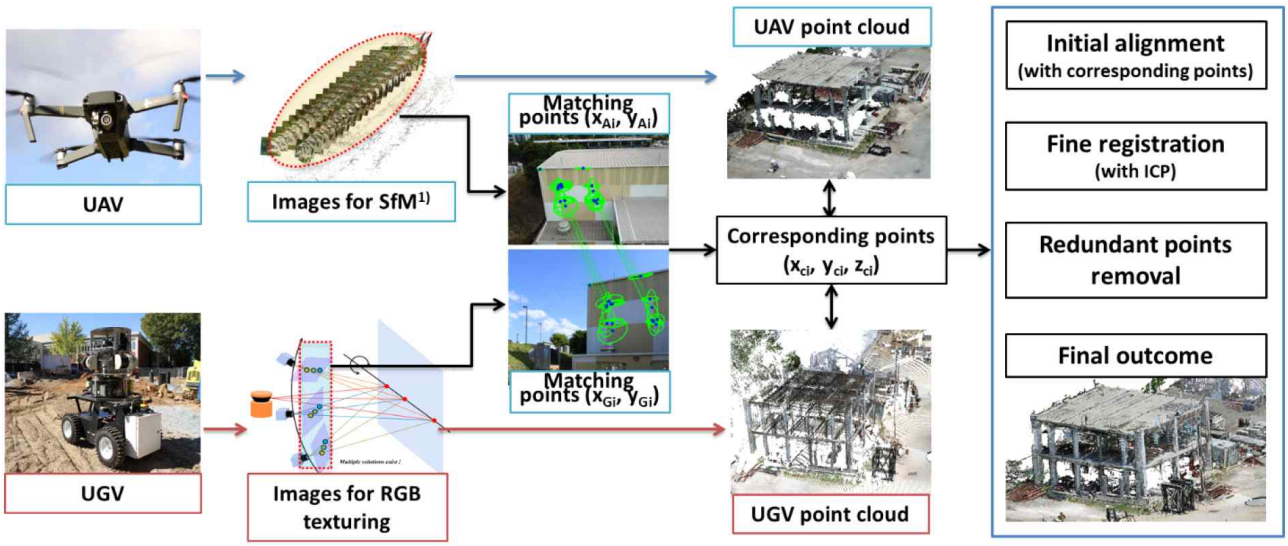


그림 2-101 3차원 포인트 클라우드 정합 순서

- 제안된 모델 정합 방식은 MODS 알고리즘을 사용하여 2D 이미지들 사이의 공통 특징점을 추출하였으며, 이는 기존 SIFT 혹은 SURF 알고리즘에 비해 FOV가 크게 차이나는 이미지들에서도 훨씬 더 많은 매칭포인트를 추출할 수 있음

3. 목표 달성도 및 관련 분야 기여도

가. 목표 달성도

(1) 연차별 목표 달성도

구분(연도)	세부 과제명	세부 연구 목표	연구개발 수행 내용	연구 결과
1차 연도 (2018)	재난 대응 및 복구 지원을 위한 급속 손상도평가 및 의사결정시스템 개발	지진에 의한 고층 아파트의 거동특성 파악 및 3차원 해석모델 개발	해석모델 개발을 위한 고층아파트 재원 및 지진하중에대한 주요변수 파악	• 20층 고층아파트에 대한 Modal Analysis를 통한 Critical areas 및 주요변수 파악
			Response-Spectrum Analysis를 통한 Peak Response 파악	• Response-Spectrum Analysis를 통한 변위 및 하중에대한 Critical Sections 파악
			비선형 동적해석(Nonlinear Dynamic Analysis)을 통해 구조물의 비선형 거동특성 파악 및 3차원 해석모델 개발	• 선형해석을 기반으로 비선형동적해석 3차원해석모델 개발 및 검증
			해석모델을 이용한 수치해석을 통해 매핑 모델에 사용될 주요변수 파악	• 비선행동적해석 모델을 이용한 수치해석으로 최종 매핑모델에 사용할 주요변수 파악
			소규모 모형실험을 위한 주요변수 파악 및 실험준비	• 모형실험 시편도면 제작 및 수정 • 시편제작 및 계측업체 선정 및 계측방법 수립
			소규모 모형실험 수행	• 시편제작 및 계측 업체와 계약체결 • 계측방법 및 장소선정완료 • 실험 및 계측 완료
	재난대응 및 복구를 위한 무인비행체 기반 재난지역 3차원 매핑 및 이미지 분석기법 개발	무인항공기 기반 재난지역 이미지 데이터 취득	모의 재난지역 선정 및 데이터 취득	• 모의 재난지역 데이터 취득: 2건
		무인항공기 이미지를 활용한 재난지역 3차원 모델링	모의 재난지역의 고밀도 3D-RGB 포인트 클라우드 모델 생성	• 3차원 포인트 클라우드 모델 제작: 2건 • 드론 및 지상레이져 스캔 데이터 융합 기술 개발
		머신러닝 기반 오브젝트 자동검출 및 분류기법 개발	머신러닝 기술을 활용한 오브젝트 검출 및 분류 알고리즘 개발	• 알고리즘 개발 및 검증 : 1건
2차 연도 (2019)	재난 대응 및 복구 지원을 위한 급속 손상도평가 및 의사결정시스템 개발	지진하중 및 내부폭파에 의한 고층 아파트의 파괴거동 해석모델 개발 및 모형실험	해석모델 검증 및 보완	• 2층 철골구조물 실물 모형실험과 해석결과 비교를 통해 모델 검증 및 보완
			지진하중에 이은 내부폭파에 종속된 고층 아파트의 유한요소해석	• 실제 지진하중 및 폭파, 지반강성등을 고려한 해석 모델개발

			모델개발	
			실증실험을 위한 대상 구조물 선정 및 구조물 변위 및 손상도 측정방법 연구	• 실증단지 구조물과 유사한 철근콘크리트 구조물에대한 손상도 데이터(Fragility Curves)도출
	재난대응 및 복구를 위한 무인비행체 기반 재난지역 3차원 매핑 및 이미지 분석기법 개발	3D 모델 기반 구조체 변위 및 파손 정량화 기법	재난 및 이벤트 전/후 3D 모델 매칭	• 모의재난 모델을 생성하여 재난 전/후 모델 정합
			구조체 변형 및 손상 정량화	• 재난 전/후 구조물 변위 측정 기술 구현
			적외선 카메라 데이터 퓨전 방식 개발	• 3차원 모델에 적외선 카메라 이미지 텍스쳐링 기법 개발
3차 연도 (2020)	재난 대응 및 복구 지원을 위한 급속 손상도평가 및 의사결정시스템 개발	건물의 외관변형도를 고려한 구조물의 전체 및 주요부재에 대한 위험도를 나타내는 매핑 시스템 개발	실증실험을 위한 대상 구조물 선정 및 구조물 변위 및 손상도 측정방법 연구	• 미국 조지아주 Guardian Center Test-Bed 내 현장 실증 구조물과 연계된 분석
			구조물의 Full-scale 실증실험	• 미국 조지아주 Guardian Center Test-Bed 내 현장 실증 구조물과 연계된 분석을 통한 해석결과 검증
			3가지 실험결과(구조물 직접계측, LiDAR 계측, 드론계측)와 유한요소 해석결과의 비교분석을 통한 개발된 모델검증	• 주관기관의 유한요소해석 모델과 Guardian Center 현장실험 데이터와의 비교를 통한 모델검증
			실증실험 및 해석모델 수치해석결과를 활용한 건물변형도-내부손상도 매핑 모델 개발	• 공동연구기관 데이터와 비교검증을 통한 매핑 시스템 개발
	재난대응 및 복구를 위한 무인비행체 기반 재난지역 3차원 매핑 및 이미지 분석기법 개발	한/미 공동 Test-Bed 구축 및 시스템 검증	재난 현장 Test-Bed 구축	• 미국 조지아주 Guardian Center Test-Bed 구축 및 현장 실험 실시
			시스템 검증	• 오브젝트 검출 알고리즘 정확도 검증
			시스템 통합	• 주관기관 위험도 분석 모델과 연동

구분	핵심 성과물(CTE)		단위 성과물		성과점검기준									양적성과 현황		
						질적 성과지표	목표치	달성치	측정방법	검증방법	가중치	해당기관	예산(백만원)	목표치	달성치	가중치
주관	A	재난대응 및 복구를 위한 무인비행체 기반 재난지역 3차원 매핑 및 이미지 분석기법	A-1	지진에 의한 고층 아파트의 거동특성 파악 및 3차원 해석모델 개발	①	해석모델 개발	1건	1건	전문가 자문을 통한 모델 유효성 증명	자문보고서	10%	서울대	60	논문 : 2 건	논문 : 3 건	10%
			A-2	지진하중 및 내부 폭파에 의한 고층아파트의 파괴거동 해석모델 개발 및 모형실험	①	해석모델 개발	1건	1건	전문가 자문을 통한 모델 유효성 증명	자문보고서	10%	서울대	80	논문 : 2 건	논문 : 1 건	10%
					②	모형제작 및 모형실험	1건	1건	실험분석	실험분석 보고서	10%	서울대	85			10%
			A-3	건물의 외관변형도를 고려한 구조물의 전체 및 주요 부재에 대한 위험도를 나타내는 매핑시스템 개발	①	매핑시스템 개발	1건	1건	전문가 자문을 통한 모델 유효성 증명	자문보고서	20%	서울대	70	논문 : 2 건 출원 : 1 건 S/W : 1 건	논문 : 3 건 출원 : 건 S/W : 건	20%
공동	B	재난대응 및 복구를 위한 무인비행체 기반 재난지역 3차원 매핑 및 이미지 분석기법	B-1	드론 및 무인로봇을 활용한 재난지역 3차원 모델링 및 오브젝트 검출기법 개발	①	모델링 및 검출기법 개발	1건	1건	전문가 자문을 통한 모델 유효성 증명	자문보고서	10%	Georgia Tech	98	논문 : 1 건	논문 : 1 건	10%
			B-2	3D 모델 기반 구조체 변위 및 파손 측정기법	②	측정기법 개발		1건	전문가 자문을 통한 모델 유효성 증명	자문보고서	20%	Georgia Tech	118	논문 : 1건	논문 : 3 건	20%
			B-3	한/미 공동 Test-Bed 구축 및 시스템 검증	③	시스템 개발		1건	전문가 자문을 통한 모델 유효성 증명	자문보고서	20%	Georgia Tech	123	논문 : 1 건 S/W : 1 건	논문 : 2건 S/W : 1건	20%
계											100%		634	특허출원 :1 건 등록 : 건 논문 : 9건 시제품 : 건 S/W : 2건	특허출원 : 1건 등록 : 건 논문 :13건 시제품 : 건 S/W : 1건	100 %

(2) 정량적 연구성과 목표 및 달성도

구분			목표	달성도(%)	비고
국외 논문 게재	SCI		9	144%	13 편
	비SCI				
	계		9	144%	13 편
국내 논문 게재	SCI				
	비SCI				
	계				
특허 출원	국내		1	100%	출원번호: 1020200171015
	국외				
	계		1	100%	
특허 등록	국내				
	국외				
	계				
인력 양성	석사				2 명 (석사학위 2명)
	박사				
	계				2 명 (석사학위 2명)
기술 이전	계약 건수				
	계약액				
	징수액				
국제 표준화	기고서 제출				
	기고서 채택				
	표준안 채택				
국내 표준화	기고서 제출				
	기고서 채택				
	표준안 채택				
등록·기탁 대상 성과물	보고서 원문				
	연구시설·장비				
	기술요약정보				
	생명자원	생명정보			
		생물자원			
		신품종			
	소프트웨어		2	50%	등록번호: C-2020-045819
	화학물				
기타	시제품				
	성과 홍보				
	일자리 창출				

(3) 성과 목표에 대한 평가

성과 목표	자체 평가
건물외관변형도와 건물내외부 손상도의 상관관계를 보이는 매핑시스템	• 건물변형도를 구성하는 주요변수 (건물높이, 건물폭, 건물의 sidesway, drift angle, 건물회전 등)와 건물의 손상도와의 상관관계를 Contour 및 정량화된 수치로 보이는 매핑 모델 개발 • 지반특성, 지진규모, 구조물의 재료적 특성, 건물변형도 수치를 알면 건물의 손상도를 파악할 수 있는 Web기반의 매핑 모델 개발 • 예방목적으로는 사전분석을 통해 보수/보강의 기준을 제시할 수 있음. • 실전 및 사후 대응목적으로는 지역의 건물정보가 사전에 확보될경우는 지진발생시 드론을 통한 빠른 계측 및 결과분석을 통해 재난구조의 우선순위에 가이드라인을 제공하며 보수/보강의 정도를 파악하게 함
재난대응 및 복구를 위한 무인비행체 기반 재난지역 3차원 매핑 및 이미지 분석기법	• (머신러닝 기반 오브젝트 자동검출 알고리즘) 머신러닝 기술을 활용하여 3차원 포인트 클라우드 모델에서 변형된 빌딩 요소(기둥, 벽, 바닥판 등)를 자동으로 검출하고 분류해 주는 기법
지진하중 및 내부 폭파에 의한 고층아파트의 파괴거동 해석모델 개발 및 모형실험	- 해석모델의 검증 및 보완을 위해 실물크기의 모형 철골구조물에대한 지진하중 제하 실험을 성공적으로 완료 (본문에 첨부된 실험보고서 참조) - 모형 실물 실험결과와 해석모델의 비교를 통해 해석모델의 검증 및 보완을 수행하여 3차년도에 있을 실증단지 실험을 위한 기반 구축 - 해석모델의 고도화를 위해 지진하중 및 내부폭파 하중을 고려하였고, 건물의 불규칙성 및 지반의 강성을 추가적으로 고려한 해석 모델을 개발하였고, 현재 연구결과를 정리한 논문 2편이 리뷰중
3D 모델 기반 구조체 변위 및 파손 정량화 기법	- 본 연구에서는 Rigid Body Physics를 사용하여 인공 재난 전/후 모델을 지진의 강도 및 폭발의 강도를 달리하여 생성하는 방식을 개발하였으며, 기존의 유한요소법 (1.07초/element) 및 iDEM 방식 (0.35초/element)에 비해 크게 향상된 시뮬레이션 성능을 보임 (0.008초/element) - 본 파손 정량화 방식의 총 소요 시간은 아래와 같음 ● 데이터 취득 (2500 평방미터 기준) - 무인기: 8분 - 지상로봇: 18분 ● 모델 매칭 시간: 1분 이하 ● 손상 검출 시간: 5분 이하 ● 본 정량화에 사용한 3D 시뮬레이션 모델 제원 - 크기: 45 x 43 x 12 (m) - 단위 Voxel 크기: 0.5 m - 파일포맷: .OBJ (3D mesh) - 하드웨어: Intel Xeon E3-1246 (35.GHz) CPU and an NVIDIA GTX 1080 GPU - 대상 기술은 3차원 voxel 그리드가 아닌 다운 샘플링한 포인트 클라우드를 사용하여 기계학습 및 추론을 실시함으로써 기존 3D 오브젝트 검출 방식에 비해 메모리 사용량과 추론시간을 1/10 수준으로 낮추는데 성공함 - 재난 발생 후 현장 데이터 수집을 위한 SLAM 기반 무인

	데이터 수집 장치의 최적경로 추정방식을 구현하였으며, 손상 및 잔해 검출율이 80% 이상으로 상당히 높게 측정됨 (손상 검출율: 82 %) - 본 연구에서는 Rigid transformation 방식을 통해 레이저 스캐닝 데이터와 적외선 카메라 데이터를 정합하고 시각화하였으며, 정합된 데이터로 실시한 사람검출 시험에서 92% 이상의 높은 검출율을 보임

나. 관련 분야 기여도

- 본 연구과제는 재난 이후 현장 대응 방안 수립을 지원할 수 있는 기초시스템을 개발하는 것으로 우리나라 재난 대응 역량의 향상에 기여함. 복합재난의 경우, 단순재난과 차별화된 대응전략을 제공하고, 재난 현장의 파악에 겪는 어려움을 경감하여, 재난 대응 및 그 복구에 필요한 시간과 노력을 줄여줌. 이를 통하여 재난에 의한 인적, 물적피해를 대폭 감소함.
- 무인기를 이용한 3차원 스캐닝 및 모델링 기술을 재난 현장에 적용하여 구조 및 복구 과정에서의 추가적인 인명피해를 최소화함. 재난 현장에서의 빠른 정보 취득 및 위험도 판단을 통하여 구조 작업의 효율을 높이고, 무인기를 활용한 위험지역 정찰을 통하여 구조대의 인명피해까지 경감함.
- 외부 변형도를 통하여 내부 손상도를 파악하여, 단순하게 재난 현장의 위험도를 파악하는 것에 그치지 않고, 노후 건축물 혹은 건설현장의 붕괴 위협을 실시간으로 파악하는 기술에 응용 가능함. 반복적인 하중이 가해지는 교량 및 기타 구조물의 모니터링 기술로 활용 가능함.

다. 목표 미달성 시 원인(사유) 및 차후대책(후속연구의 필요성 등)

4. 연구개발성과의 활용계획 등

가. 연구결과의 활용방안

(1) 최종목표의 국가적 활용방안

재난대응 및 복구 지원을 위한 급속 손상도 평가 및 의사결정시스템 개발	
재난/재해 대응 국가적 원천기술 확보	선진기술의 도입, 다재간의 협력을 통한 지진 대응에 대한 **국가적 원천기술의 확보 가능**
복합적 재난/재해 대응 및 관리 시나리오 구축	다양한 지진 발생과 피해 양상을 반영한 대응 시나리오 개발과 무인 기기를 활용한 시뮬레이션을 통하여 **효율적 대응 및 관리 가능**
현장 대응 중심의 의사결정 시스템 구축	지진 발생 현장 즉시 대응이 가능해지며, 대응 시나리오 기반의 **현장에서의 신속한 의사결정 가능**



그림 5-1 최종목표의 국가적 활용방안

(2) 연구결과의 구체적 활용방안

재난대응 및 복구 지원을 위한 급속 손상도 평가 및 의사결정시스템 개발	
기술적 활용방안	현장 대응 중심의 기술을 이용한 지진 발생 현장에서의 신속한 대처
	선진 기술의 공유와 이해를 통한 선진국의 기술이전 기피 현상 극복
	무인 원격화 기술을 사이버물리시스템으로 확장
사회적 활용방안	신속한 복구시스템을 통한 지진에 대한 전사회적 트라우마 예방 가능
	현장 대응 기술 도입으로 인한 안전사고 위험성 감소
	예상 불가능한 지진 발생 상황에서의 성공적 대처로 국가적 이미지 향상
경제적 활용방안	개발 기술을 바탕으로 후진국 시장 진출을 통한 Global Frontier 역할 수행
	인공지능형 현장 복구 기술로 피해규모 최소화 가능
	시나리오 기반의 신속한 현장 대응으로 최단시간 인명구조 및 추가피해 감소

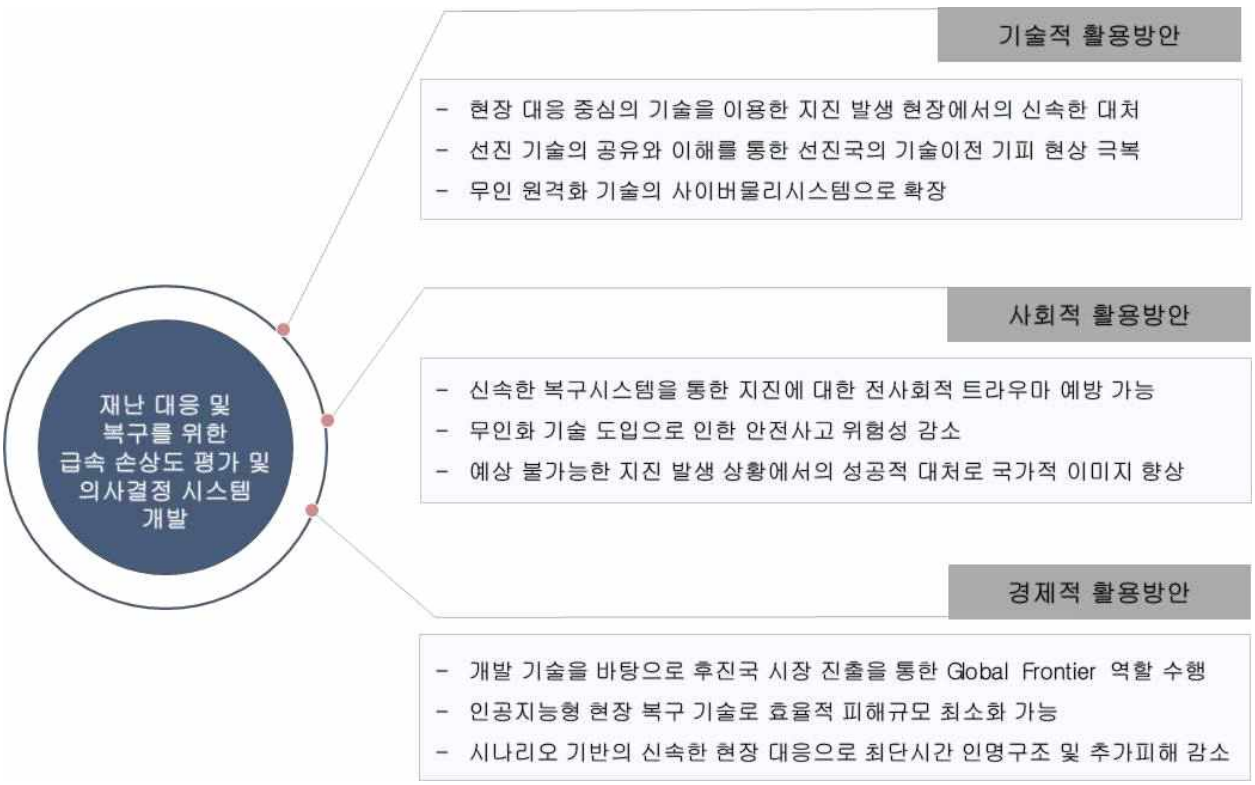


그림 5-2 연구결과의 구체적 활용방안

(3) 고층건출 해석용 DB 구축방안 및 기술활용전략

• 고층건물 해석용 DB구축방안

- 고층아파트의 다양한 제원(형상, 재질)을 고려한 재난시의 손상도 데이터를 웹기반으로 사전 구축하여, 재난시 무인항공체로부터의 데이터와 연동시키는 개념임.
- 재난의 위급성을 감안하여 클라우드기반의 DB구축으로 무인항공체 측정데이터가 실시간으로 사전구축 데이터와 매칭되며, 가장 근사한 경우의 상세손상도평가 데이터가 실시간으로 재난총지휘부에 전달된다.
- 데이터 전달시 의사결정에 도움을 줄 구조전략도 함께 전송됨.

• 기술활용전략

- 지방자치단체별로 BIM등을 활용하여 재난위험지역의 고층건물의 3D모델을 사전에 구축하고 각각의 건물에대한 사전구조해석을 수행하여 DB를 구축한후 클라우드 기반의 서버네트워크를 구축해둠.
- 무인항공체 대기위치를 동별로 마련하여 응급상황발생시 최근접거리의 무인항공체가 투입됨.
- 중앙정부에 총괄 클라우드기반의 서버네트워크와 연동하여 작동하는 개념.
- 재난안전처 '지진피해 대응시스템'에서 예측하는 피해를 기반으로 하여 무인항공체의 스캔 우선도를 선정함.

(4) 드론사용 불가능 할 경우 손상도 평가방안

기상이나 주변 환경으로 인해 드론 활용이 불가능한 상황을 대비하여, 사람이 직접 촬영하는 방식 혹은 지상용 모바일 로봇을 적용하여 재난지역에 대한 3차원 포인트 클라우드 데이터를 추출하는 방안을 준비할 예정임. 이를 위해 상대국 (조지아텍)에서 기보유중인 3차원 스캐닝 모바일 로봇을 사용할 예정임.

(5) 재난 대응 로봇과 연계

개발 중인 무인 구조로봇이나 기타 재난대응로봇 등과 연동하여 재난 현장에서 자율적으로 정보를 수집하고 판단하는 시스템 개발에 활용 가능함. 구조 로봇이 총지휘부에 현장 상황을 전달하여 실시간으로 구조 작업의 위험도 파악 및 진행상황을 점검함.

붙임. 참고 문헌

Ajamy, A., Asgarian, B., Ventura, C.E., Zolfaghari, M.R. (2018). “Seismic fragility analysis of jacket type offshore platforms considering soil-pile-structure interaction”, Engineering Structures, 174, 198-211.
https://doi.org/10.1016/j.engstruct.2018.07.066.

Al-Thairy, H. (2018). Behavior and failure of steel columns subjected to blast loads: Numerical study and analytical approach,” Advances in Materials Science and Engineering, 1-20. https://doi.org/10.1155/2018/1591384.

Altunışık, A.C., Kalkan, E. (2016). “Investigation of earthquake angle effect on the seismic performance of steel bridges”, Steel and Composite Structures, An Int'l Journal, 23(4). 855-874. https://doi.org/10.12989/scs.2016.22.4.855.

Amabili, M., Balasubramanian, P., Garziera, R., Royer-Carfagni, G. (2020). Blast loads and nonlinear vibrations of laminated glass plates in an enhanced shear deformation theory. Composite Structures, 252, 112720. https://doi.org/10.1016/j.compstruct.2020.112720.

Amini, M. R., Simon, J. and Nemat-Nasser, S. (2010). Numerical modeling of effect of polyurea on response of steel plates to impulsive loads in direct pressure-pulse experiments, Mechanics of Materials, 42, pp. 615 – 627. https://doi.org/10.1016/j.mechmat.2009.09.009.

Benavent-Climent, A., Morillas, L., Escolano-Margarit, D. (2014). “Inelastic torsional seismic response of nominally symmetric reinforced concrete frame structures: Shaking table tests”, Engineering Structures, 80, 109-117.
https://doi.org/10.1016/j.engstruct.2014.08.047.British Standards Institution. (2004). BS EN 1992-1-1: Eurocode 2: Design of concrete structures - Part 1- 1: General rules and rules for buildings. Brussels: BSI.

British Standards Institution. (2005). BS EN 1993-1-1: Eurocode 3: Design of steel structures - Part 1-1: General rules and rules for buildings. Brussels: BSI.

Brunesi, E., Nascimbene, R. & Casagrande, L. (2016). Seismic analysis of high-rise mega-braced frame-core buildings. ELSEVIER: Engineering Structures, Vol. 115, pp. 1-17.

Bojorquez, E., Iervolino, I. (2011). “Spectral shape proxies and nonlinear structural response”, Soil Dynamics and Earthquake Engineering, 31, 996-1008.
https://doi:10.1016/j.soildyn.2011.03.006.

Byfield MP. (2006). Behaviour and design of commercial multistorey buildings subjected to blast. Journal of Performance of Constructed Facilities, 20(4), 324 – 329. https://doi.org/10.1061/(ASCE)0887-3828(2006)20:4(324).

Cancellara, D., De Angelis, F. (2019). “Dynamic assessment of base isolation systems for irregular in plan structures: Response spectrum analysis vs nonlinear analysis”, Composite Structures, 215, 98-115.
https://doi.org/10.1016/j.compstruct.2019.02.013.

Chen, H., Liew, J.Y.R. (2005). Explosion and fire analysis of steel frames using mixed element approach. Journal of Engineering Mechanics, 131(6), 606-615. https://doi.org/10.1061/(ASCE)0733-9399(2005)131:6(606).

Chen, X., Shi, G. (2016). Finite element analysis and moment resistance of ultra-large capacity end-plate joints, Journal of Constructional Steel Research, 126, 153-162. https://doi.org/10.1016/j.jcsr.2016.07.013.

Choi, E., Mohammadzadeh, B., Kim, D., Jeon, J.S. (2018). “A new experimental investigation into the effects of reinforcing mortar beams with superelastic SMA fibers on controlling and closing cracks”, Composites Part B: Engineering, 137, 140-152.

https://doi.org/10.1016/j.compositesb.2017.11.017.

Choi, E., Mohammadzadeh, B., Hwang, J.H., Kim, W.J. (2018). “Pullout behavior of superelastic SMA fibers with various end-shapes embedded in cement mortar”, Construction and Building Materials, 167, 605-616.
https://doi.org/10.1016/j.conbuildmat.2018.02.070.

Choi, E., Mohammadzadeh, B., Hwang, J.H., Lee, J.H. (2019). “Displacement-recovery-capacity of superelastic SMA fibers reinforced cementitious materials”, Smart Structures and Systems, 24(2). 157-171.
https://doi.org/10.12989/sss.2019.24.2.157.

Choi, E., Chae, S.W., Park, H., Nam, T.H., Mohammadzadeh, B., Hwang, J.H. (2018). “Investigating self-centering capacity of superelastic shape memory alloy fibers with different anchorages through pullout tests”, Journal of Nanoscience and Nanotechnology, 18, 6228-6232.
https://doi:10.1166/jnn.2018.15635.

Choi, E., Mohammadzadeh, B., Kim, H.S. (2019). “SMA bending bars as self-centering and damping devices”, Smart Materials and Structures, 28, 025029.
https://doi.org/10.1088/1361-665X/aaf5e3.

Chopra, A. K. (2001) Dynamic of Structures: Theory and Application to Earthquake Engineering, Prentice Hall Inc., New Jersey, USA. http://dx.doi.org/10.12989/sem.2008.29.4.411.

Chung, K.F., Ko, C.H., Wang, A.J. (2005). “Design of steel and composite beams with web openings-Verification using finite element method”, Steel and Composite Structures, An Int'l Journal, 5(2). 203-233.
https://doi.org/10.12989/scs.2005.5.2_3.203.

Civalek, O., Ersoy, H. (2008). Frequency analysis of moderately thick uniform isotropic annular plates by discrete singular convolution method, Structural Engineering and Mechanics, An Int’l Journal, 29(4), 411-422.

Clubley, S.K. (2014) Long duration blast loading of cylindrical shell structures with variable fill level, Thin-Walled Structures, 85, 234-249. https://doi.org/10.1016/j.tws.2014.08.021.

D. Bonorchis, G.N. Nurick. (2007). The effect of welded boundaries on the response of rectangular hot-rolled mild steel plates subjected to localised blast loading, Int. J. Impact Eng. 34 (11) 1729–1738. https://doi.org/10.1016/j.ijimpeng.2006.11.002.

Dasgupta, B. (2017). “Evaluation of methods used to calculate seismic fragility curves”, U.S. Nuclear Regulatory Commission.
https://www.nrc.gov/docs/ML1712/ML17122A268.

Davani, M.R., Hatami, S., Zare, A. (2016). “Performance-based evaluation of strap-braced cold-formed steel frames using incremental dynamic analysis” Steel and Composite Structures, An Int'l Journal, 21(6). 1369-1388.
http://dx.doi.org/10.12989/scs.2016.21.6.1369.

Devi, U., Amanat, K.M. (2015). Non-linear finite element investigation on the behavior of CFRP strengthened steel square HSS columns under compression, International Journal of Steel Structures (2015), 15(3), 671-680. https://doi.org/10.1007/s13296-015-9013-7.

Dya, A.F.C., Oretaa, A.W.C. (2015). “Seismic vulnerability assessment of soft storey irregular buildings using pushover analysis”, Procedia Engineering, 125, 925–932.
https://doi.org/10.1016/j.proeng.2015.11.103

Eslami-Majd, A., Rahbar-Ranji, A. Deformation behaviour of corroded plates subjected to blast loading. Ships and Offshore Structures, 10(1), 79-93. https://doi.org/10.1080/17445302.2014.889371.

Fan, H., Li, Q.S., Tuan, A. Y., & Xu, L. (2009). Seismic analysis of the world’s tallest building. ELSEVIER: Journal of Constructional Steel Research, Vol. 65, pp. 1206-1215.

Farzin, M., Dibajian, S.H. (2012). An Introductory & Training Book for ABAQUS Software, Isfahan University of Technology publications, Iran.

Forni, D., Chiaia, B., Cadoni, E. (2017). Blast effects on steel columns under fire conditions, Journal of Constructional Steel Research, 136, 1-10. https://doi.org/10.1016/j.jcsr.2017.04.012.

Gharababaei, H., Darvizeh, A., Darvizeh, M. (2010). Analytical and experimental studies for deformation of circular plates subjected to blast loading, Journal of Mechanical Science and Technology, 24(9), 1855-1864. https://doi.org/10.1007/s12206-010-0602-2.

Georgoussis, G., Tsompanos, A., Makarios, T. (2015). "Approximate seismic analysis of multi-storey buildings with mass and stiffness irregularities", Procedia Engineering, 125, 959-966. https://doi.org/10.1016/j.proeng.2015.11.147.

Goel, M.D., Matsagar, V.A., Gupta, A.K. Marburg, S. (2012). An Abridged Review of Blast Wave Parameters, Defence Science Journal, 62(5), 300-306. https://doi.org/10.14429/dsj.62.1149.

Gulkhan, P., Korucu, H. (2011). High-velocity impact of large caliber tungsten projectiles on ordinary Portland and calcium aluminate cement based HPSFRC and SIFCON slabs. Part II: numerical simulation and validation, Structural Engineering and Mechanics, An International Journal, 40(5), 617-636. https://doi.org/10.12989/sem.2011.40.5.595.

HAZUS, (1999). "Earthquake loss estimation methodology-Technical manual", Federal Emergency Management Agency and National Institute of Building Science. http://www.fema.gov/plan/prevent/hazus.

Heidarpour, A., Bradford, M.A. (2011). Beam–column element for non-linear dynamic analysis of steel members subjected to blast loading. Engineering Structures, 33(4), 1259-1266. http://dx.doi.org/10.1016/j.engstruct.2011.01.003.

Hoffman, S.T., Fahnestock, L.A. (2011). "Behavior of multi-storey steel buildings under dynamic column loss scenarios", Steel and Composite Structures, An Int'l Journal, 11(2). 149-168. https://doi.org/10.12989/scs.2011.11.2.149.

Hou, W., Xu, S., Ji, D., Li, Q., Zhang, P. (2019). "Seismic performance of steel plate reinforced high toughness concrete coupling beams with different steel plate ratios", Composites Part B: Engineering, 159, 199-210. https://doi.org/10.1016/j.compositesb.2018.09.100.

Hosseini, M., Hashemi, B., & Safi, Z. (2017). Seismic design evaluation of reinforced concrete buildings for near-source earthquakes by using nonlinear time history analyses. ELSEVIER: Procedia Engineering, Vol. 199, pp. 176-181.Hsu, H.L., Juang, J.L., Chou, C.H. (2011). "Experimental evaluation on the seismic performance of steel knee braced frame structures with energy dissipation mechanism", Steel and Composite Structures, An Int'l Journal, 11(1). 77-91. http://dx.doi.org/10.12989/scs.2011.11.1.077.

Huang, Z., Richard Liew, J.Y. (2016). Steel-concrete-steel sandwich composite structures subjected to extreme loads, International Journal of Steel Structures, 16(4), 1009-1028. https://doi.org/10.1007/s13296-016-0026-7.

Imbalzano, G., Linforth, S., Ngo, T.D., Lee, P.V.S., Tran, P. (2018). Blast resistance of auxetic and honeycomb sandwich panels: Comparisons and parametric designs, Composite Structures, 183, 242-261. https://doi.org/10.1016/j.compstruct.2017.03.018.

Israel, J.J., Tovar, A. (2013). Investigation of Plate Structure Design under Stochastic Blast Loading," 10th World Congress on Structural and Multidisciplinary Optimization, May 19 – 24, Orlando, Florida, USA.

Jones, N. (2012). Damage of plates due to impact, dynamic pressure and explosive loads, Latin American Journal of Solids and Structures, 10, 767-780. https://doi.org/10.1590/S1679-78252013000400006.

Kang, J.S., Davidson, J.S. (2013). Structural effects of concrete lining for concrete-lined corrugated steel pipes. Structure and Infrastructure Engineering, 9(2), 130-140. https://doi.org/10.1080/15732479.2010.532809.

Khan, U., Al-Osta, M.A., Ibrahim, A. (2017). Modeling shear behavior of reinforced concrete beams strengthened with externally bonded CFRP sheets, Structural Engineering and Mechanics, An Int'l Journal, 61(1), 125-142. http://dx.doi.org/10.12989/sem.2017.61.1.125.

Kim, H.J., Yi, N.H., Kim, S.B., Nam, J.h., Ha, J.h., Kim, J.J. (2011). Debonding failure analysis of FRP-retrofitted concrete panel under blast loading, Structural Engineering and Mechanics, An Int'l Journal, 38(4), 479-501. https://doi.org/10.12989/sem.2011.38.4.479.

Kim, S., Lee, J. (2015). Blast resistant performance of bolt connections in the earth covered steel magazine, International Journal of Steel Structures, 15(2), 507-514. https://doi.org/10.1007/s13296-015-6019-0.

Kim, S., Lee, K. (2013). "Seismic performance of wind-designed diagrid tall steel buildings in regions of moderate seismicity and strong wind", Steel and Composite Structures, An Int'l Journal, 14(2). 155-171. http://dx.doi.org/10.12989/scs.2013.14.2.155.

Kircil, M.S., Polat, Z. (2006). "Fragility analysis of mid-rise R/C frame buildings", Engineering Structures, 28, 1335-1345. http://doi:10.1016/j.engstruct.2006.01.004.

Koneshwaran, S., Thambiratnam, D.P., Gallage, C. (2015). Blast Response of Segmented Bored Tunnel using Coupled SPH–FE Method, Structures, 2, 58-71. https://doi.org/10.1016/j.istruc.2015.02.001.

Larcher, M. (2007). Simulation of the effects of an air blast wave, Scientific and Technical Research series – ISSN 1018-5593, Luxembourg: Office for Official Publications of the European Communities.

Lee, A.D., Shepherd, P., Evernden, M.C. (2020). Large deflections in thin rectangular plates subjected to uniform load: Pitfalls in the application of analytical methods. Structures, 27, 1419-1432. https://doi.org/10.1016/j.istruc.2020.06.029.

Lee, D., Ha, T., Jung, M., Kim, J. (2014). "Evaluating high performance steel tube-framed diagrid for high-rise buildings", Steel and Composite Structures, An Int'l Journal, 16(3). 289-303. http://dx.doi.org/10.12989/scs.2014.16.3.289.

Lee, K., Kim, T., Kim, J. (2009). Local response of W-shaped steel columns under blast loading. Structural Engineering and Mechanics, 31(1), 25-38. https://doi.org/10.12989/sem.2009.31.1.025.

Lee, K., Shin, J. (2016). Equivalent single-degree-of-freedom analysis for blast-resistant design, International Journal of Steel Structures, 16(4), 1263-1071. https://doi.org/10.1007/s13296-016-0073-0.

Li, S., Li, X., Wang, Z., Wu, G., Lu, G., Zhao, L. (2017). Sandwich panels with layered graded aluminum honeycomb cores under blast loading, Composite Structures, 173, pp. 242-254. https://doi.org/10.1016/j.compstruct.2017.04.037.

Li, S., Zuo, Z., Zhai, C., Lili, X. (2017). "Comparison of static pushover and dynamic analyses using RC building shaking table experiment", Engineering Structures, 136, 430-440. https://doi.org/10.1016/j.engstruct.2017.01.033.

Li, X.D., Yin, J.P., Zhao, P.D., Zhang, L., Xu, Y.X., Wang, Q., Zhang, P. (2020). The effect of stand-off distance on damage to clamped square steel plates under enclosed explosion, Structures, 25, 965-978. https://doi.org/10.1016/j.istruc.2020.03.066.

Li, Y., Wu, W., Zhu, H., Wu, Z., Du, Z. (2017). The influence of different pre-formed holes on the dynamic response of square plates under air-blast loading. Engineering Failure Analysis, 78, 122-133. http://dx.doi.org/10.1016/j.engfailanal.2017.03.002.

Li, Z., Chen, W., Hao, H. (2019). Numerical study of blast mitigation performance of folded structure

with foam infill, Structures, 20, 581-593. https://doi.org/10.1016/j.istruc.2019.06.012.

Li, Z., Li, H., Liu, L., Zuo, H. (2020). Propagation of blasting seismic wave in viscoelastic full space and half space under infinitely long cylindrical charge. Journal of Applied Geophysics, 181, 104137. https://doi.org/10.1016/j.jappgeo.2020.104137.

Lian, M., Su, M., Guo, Y. (2015). "Seismic performance of eccentrically braced frames with high strength steel combination", Steel and Composite Structures, An Int'l Journal, 18(6). 1517-1539. http://dx.doi.org/10.12989/scs.2015.18.6.1517.

Liew, J.Y.R. (2008). Survivability of steel frame structures subject to blast and fire, Journal of Constructional Steel Research, 64(7-8), 854-866. https://doi.org/10.1016/j.jcsr.2007.12.013.

Linzell, D.G., Nadakuditi, V.P. (2011). "Parameters influencing seismic response of horizontally curved, steel, I-girder bridges", Steel and Composite Structures, An Int'l Journal, 11(1). 21-38. https://doi.org/10.12989/scs.2011.11.1.021.

Liu, S., Zhou, Y., Zheng, Q., Zhou, J., Jin, F., Fan, H. (2019). Blast responses of concrete beams reinforced with steel-GFRP composite bars, Structures, 22, 200-212. https://doi.org/10.1016/j.istruc.2019.08.010.

Liu, Y., Yan, J., Li, Z., Huang, F. (2019). Improved SDOF and numerical approach to study the dynamic response of reinforced concrete columns subjected to close-in blast loading, Structures, 22, 341-365. https://doi.org/10.1016/j.istruc.2019.08.014.

Lopez-Arancibia, A., Altuna-Zugasti, A.M., Aldasoro, H.A., Pradera-Mallabiabarrena, A. (2015). Bolted joints for single-layer structures: numerical analysis of the bending behavior, Structural Engineering and Mechanics, An International Journal, 56(3), 355-367. https://doi.org/10.12989/sem.2015.56.3.355.

Mario, D., Barbara, P. (2008). "A review of research on seismic behavior of irregular building structures since 2002", Bulletin Earthquake Engineering, 6, 285-308. https://doi.org/10.1007/s10518-007-9052-3

Markose, A., Rao, C.L. (2017). Mechanical response of V shaped plates under blast loading," Thin-Walled Structures, 115, 12-20. https://doi.org/10.1016/j.tws.2017.02.002.

Mijušković, O., Šćepanović, B., Žugić, L., Ćorić, B. (2020). Analytical approach to elastic stability problems of plates with different boundary conditions subjected to combined bending, shear and patch loading. Structures, 24, 335-350. https://doi.org/10.1016/j.istruc.2020.01.016.

Mirzababaie Mostofi, T., Babaei, H., Alitavoli, M. (2016). Theoretical analysis on the effect of uniform and localized impulsive loading on the dynamic plastic behavior of fully clamped thin quadrangular plates, Thin-Walled Structures, 109, 367-376. https://doi.org/10.1016/j.tws.2016.10.009.

Mitra, R. (2008). Seismic modeling and analysis of a four story steel moment frame building and comparison of methods of its simulation using SAP-2000. Master's Thesis, Department of Civil Engineering, University of Missouri, Kansas City, Missouri.

Moghimi, H., Driver, R.G. (2015). Performance assessment of steel plate shear walls under accidental blast loads, Journal of Constructional Steel Research, 106, 44-56. https://doi.org/10.1016/j.jcsr.2014.11.010.

Mohammadzadeh B. (2016). Investigation into dynamic responses of isotropic plates and sandwich plates subjected to blast loads, Doctoral dissertation, Seoul, Korea: Sejong University.

Mohammadzadeh, B., Bina, M., Hasounizadeh, H. (2012). "Application and comparison of mathematical and physical models on inspecting slab of stilling basin floor under static and dynamic forces", Applied Mechanics and Materials, 147, 283-287. https://doi.org/10.4028/www.scientific.net/AMM.147.283.

Mohammadzadeh, B., Noh, H.C. (2014). "Investigation into central-difference and Newmark's beta method in measuring dynamic responses", Advanced Materials Research, 831, 95-99. https://doi.org/10.4028/www.scientific.net/AMR.831.95.

Mohammadzadeh, B., Noh, H.C. (2017). “Analytical method to investigate nonlinear dynamic responses of sandwich plates with FGM faces resting on elastic foundation considering blast loads”, Composite Structures, 174, 142-157.
https://doi.org/10.1016/j.compstruct.2017.03.087.

Mohammadzadeh, B., Choi, E., Kim, W.J. (2018). Comprehensive investigation of buckling behavior of plates considering effects of holes, Structural Engineering and Mechanics, An International Journal, 68(2), 261-275. https://doi.org/10.12989/sem.2018.68.2.261.

Mohammadzadeh, B., Noh, H.C. (2019). “An analytical and numerical investigation on the dynamic responses of steel plates considering the blast loads”, International Journal of Steel Structures, 19(2). 603-617.
https://doi.org/10.1007/s13296-018-0150-7.

Mohammadzadeh, B., Noh, H.C. (2017). Analytical method to investigate nonlinear dynamic responses of sandwich plates with FGM faces resting on elastic foundation considering blast loads, Composite Structures, 174, 142-157. http://dx.doi.org/10.1016/j.compstruct.2017.03.087.

Mohammadzadeh, B., Noh, H.C. (2016). Investigation into buckling coefficients of plates with holes considering variation of hole size and plate thickness, MECHANIKA, 22(3), 167-175. http://dx.doi.org/10.5755/j01.mech.22.3.12767.

Mohammadzadeh, B., Noh, H.C. (2013). Investigation into Central-Difference and Newmark’s Beta Methods in Measuring Dynamic Responses,” Advanced Materials Research, 831, 95-99. https://doi.org/10.4028/www.scientific.net/AMR.831.95.

Mohammadzadeh, B., Noh, H.C. (2015). Numerical analysis of dynamic responses of the plate subjected to impulsive loads, International Journal of Civil, Environmental, Structural, Construction and Architectural Engineering, 9(9), 11194-1197.

Mohammadzadeh, B., Noh, H.C. (2014). Use of buckling coefficient in predicting buckling load of plates with and without holes, Journal of Korean Society of Advanced Composite Structures, 5(3), 1-7. http://dx.doi.org/10.11004/kosacs.2014.5.3.001.

Mohammadzadeh, B., Choi, E., Kim, W.J. “Comprehensive investigation of buckling behavior of plates considering effects of holes”, Structural Engineering and Mechanics, 68(2). 261-275.
https://doi.org/10.12989/sem.2018.68.2.261.

Mohammadzadeh, B., Choi, E., Kim, D. (2019). “Vibration of sandwich plates considering elastic foundation, temperature change and FGM faces”, Structural Engineering and Mechanics, 70(5). 601-621.
https://doi.org/10.12989/sem.2019.70.5.601.

Mohammadzadeh, B., Jung, S., Lee, T.H., Le, Q.V., Cha, J.H., Jang, H.W., Lee, S.H., Kang, J., Shokouhimehr, M. (2020). “Manufacturing ZrB2–SiC–TaC Composite: Potential Application for AircraftWing Assessed by Frequency Analysis through Finite Element Model”, Materials, 13, 2213.
https://doi:10.3390/ma13102213.

Momeni, M., Hadianfard, M.M., Bedon, C., Baghlani, A. (2019). Numerical damage evaluation assessment of blast loaded steel columns with similar section properties, Structures, 20, 189-203. https://doi.org/10.1016/j.istruc.2019.04.002.

Moriello, D.S., Bosi, F., Torii, R., Tan, P.J. (2020). Failure and detachment path of impulsively loaded plates. Thin-Walled Structures, 155, 106871. https://doi.org/10.1016/j.tws.2020.106871.

Naguib, M., Salem, F. A., & El-Bayoumi, K. (2015). Dynamic analysis of high-rise seismically isolated buildings. American Journal of Civil Engineering, Vol. 3(2). pp. 43-50.

Najam, F., & Warnitchai, P. (2017, January). A modified response spectrum analysis procedure to determine nonlinear seismic demands of high-rise buildings with shear walls. In Proceedings of the 16thWorldConferenceonEarthquakeEngineering. Santiago Chile: National Information Centre of

Earthquake Engineering.

Nam, J. W., Kim, J.H.J., Kim, S.B., Yi, N.H., Byun, K.J. (2008). A study on mesh size dependency of finite element blast structural analysis induced by non-uniform pressure distribution from high explosive blast wave, KSCE Journal of Civil Engineering, 12(8), 259-265. https://doi.org/10.1007/s12205-008-0259-x.

Ngo, T., Mendis, P., Gupta, A. & Ramsay, J. (2007). Blast Loading and Blast Effects on Structures – An Overview, Loading on Structures, EJSE Special Issue, 76-91. https://doi.org/10.1016/j.proeng.2017.09.388.

Nurick, G.N., Shave, G.C. (1996) The deformation and tearing of thin square plates subjected to impulsive loads - an experimental study. International Journal of Impact Engineering, 18(1), 99-116. https://doi.org/10.1016/0734-743X(95)00018-2.

Oikonomou, A., Bougiatioti, F. (2011). "Architectural structure and environmental performance of the traditional buildings in Florina, NW Greece", Building and Environment, 46(3). 669-689. https://doi.org/10.1016/j.buildenv.2010.09.012.

Ozakgul, K. (2015). Evaluation of energy response of space steel frames subjected to seismic loads, Structural Engineering and Mechanics, An Int'l Journal, 54(4), 809-827. https://doi.org/10.12989/sem.2015.54.4.809.

Ozmen, C., Unay, A.I. (2007). "Commonly encountered seismic design faults due to the architectural design of residential buildings in Turkey", Building and Environment, 42, 1406-1416. https://doi.org/10.1016/j.buildenv.2005.09.029.

Özuygur, A.R. (2016). "Performance-based seismic design of an irregular tall building-A case study", Structures, 5, 112-122. https://doi.org/10.1016/j.istruc.2015.10.001.

Parajuli, H.R., Shrestha, R.K. (2018). "Generation of Synthetic Ground Motion", Journal of Geological Resource and Engineering, 6, 105-111. https:// doi:10.17265/2328-2193/2018.03.002.

Pedro, N., Simoes da Silva, L., Bento, R., Simoes, R. (2009). "Calibration of model parameters for the cyclic response of end-plate beam-to-column steel-concrete composite joints", Steel and Composite Structures, An Int'l Journal, 9(1). 39-58. https://doi.org/10.12989/scs.2009.9.1.039

Peng, Y., Yang, P. (2008). Dynamic plastic response of clamped stiffened plates with large deflection. Journal of Marine Science and Application, 7, 82-90. https://doi.org/10.1007/s11804-008-7071-3.

Peng, Y., Yang, P., Hu, K. (2020). Nonlinear dynamic response of blast-loaded stiffened plates considering the strain rate sensitivity. Marin Structures, 70, 102699. https://doi.org/10.1016/j.marstruc.2019.102699.

Rajendran, R., Lee, J. M. (2009). Blast loaded plates, Marine Structures, 22, 99–127. https://doi.org/10.1016/j.marstruc.2008.04.001.

Rajendran, R., Narasimhan K. (2006). Deformation and Fracture Behavior of Plate Specimens Subjected to Underwater Explosion-A Review, International Journal of Impact Engineering, 32, 1945–1963. https://doi.org/10.1016/j.ijimpeng.2005.05.013.

Rashid, J.Y.R., James, R.J. (2009). Failure Analysis and Risk Evaluation of Lifeline Structures Subjected to Blast Loadings and Aircraft/Missile Impact, International Workshop on Structural Response to Impact and Blast, Haifa, Israel.

Reddy, J.N. (2006). Theory and analysis of elastic plates and shells, Second Edition, CRC Press, Taylor & Francis Group.

Reyes-Salazar, A., Cervantes-Lugo, J.A., Lopez-Barraza, A., Bojórquez, E., Bojorquez, J. (2016). "Seismic response of 3D steel buildings with hybrid connections: PRC and FRC", Steel and

Composite Structures, An Int'l Journal, 22(1). 113-139.
http://dx.doi.org/10.12989/scs.2016.22.1.113.
http://dx.doi.org/10.12989/scs.2014.17.4.471

Richard Liew, J.Y., Chen, H. (2004). Explosion and fire analysis of steel frames using fiber element approach. Journal of Structural Engineering, 130(7), 991-1000. https://doi.org/10.1061/(ASCE)0733-9445(2004)130:7(991).

Rolfe, E., Kelly, M., Arora, H., Hooper, P.A., Dear, J.P. (2017). Failure analysis using X-ray computed tomography of composite sandwich panels subjected to full-scale blast loading, Composites Part B: Engineering, 129, 26-40. https://doi.org/10.1016/j.compositesb.2017.07.022.

Sabuwala, T., Linzell, D., Krauthammer, T. (2005). Finite element analysis of steel beam to column connections subjected to blast loads. International Journal of Impact Engineering, 31(7), 861-876. https://doi.org/10.1016/j.ijimpeng.2004.04.013.

Schiffer, A., Tagarielli, V.L. (2015). The response of circular composite plates to underwater blast: Experiments and modelling. Journal of Fluids and Structures, 52, 130-144. https://doi.org/10.1016/j.jfluidstructs.2014.10.009.

Sheehan, T., Chan, T.M., Lam, D. (2015). "Mid-length lateral deflection of cyclically-loaded braces", Steel and Composite Structures, An Int'l Journal, 18(6). 1569-1582.
http://dx.doi.org/10.12989/scs.2015.18.6.1569

Shim, C.S., Yun, N.R., Shin, D.H., Yu, I.H. (2013). Design of protective structures with aluminum foam panels, International Journal of Steel Structures, 13(1), 1-10. https://doi.org/10.1007/s13296-013-1001-1.

Shooshtari, A., Khadem, S.E. (2018). A multiple scales method solution for the free and forced nonlinear transverse vibrations of rectangular plates, Structural Engineering and Mechanics, An Int'l Journal (2006), 24(5), 543-560. http://dx.doi.org/10.12989/sem.2006.24.5.543.

Syed, Z.I., Raman, S.N., Ngo, T., Mendis, P., Pham, T. (2018). The Failure Behaviour of Reinforced Concrete Panels Under Far-field and Near-field Blast Effects, Structures, 14, 220-229. https://doi.org/10.1016/j.istruc.2018.03.009.

Takahashi, K., Watanabe, K. (2010). Advanced Numerical Simulation of Gas Explosion for Assessing the Safety of Oil and Gas Plant, Numerical Simulations - Examples and Applications in Computational Fluid Dynamics, Prof. Lutz Angermann (Ed.), ISBN: 978-953-307-153-4, InTech, JGC Corporation , Japan (2010), 377-389.

Takin, K., Hashemi, B.H., Nekooei, M. (2016). "The relationship between time-varying eccentricity of load with the corner lateral displacement response of steel structure during an earthquake", Steel and Composite Structures, An Int'l Journal, 20(4). 801-812.
http://dx.doi.org/10.12989/scs.2016.20.4.801.

Tavakoli, H.R., Kiakojouri, F. (2014). Numerical Dynamic analysis of Stiffened Plates Under Blast Loading, Latin American Journal of Solids and Structures, 11, 185-199. https://doi.org/10.1590/S1679-78252014000200003.

Teeling-Smith, R.G., Nurick, G.N. (1991). The deformation and tearing of thin circular plates subjected to impulsive loads. International Journal of Impact Engineering, 11(1), 77-91. https://doi.org/10.1016/0734-743X(91)90032-B.

Urgessa, G.S., Arciszewski, T. (2011). Blast response comparison of multiple steel frame connections. Finite Elements in Analysis and Design, 47(7), 668-675. https://doi.org/10.1016/j.finel.2011.01.009.

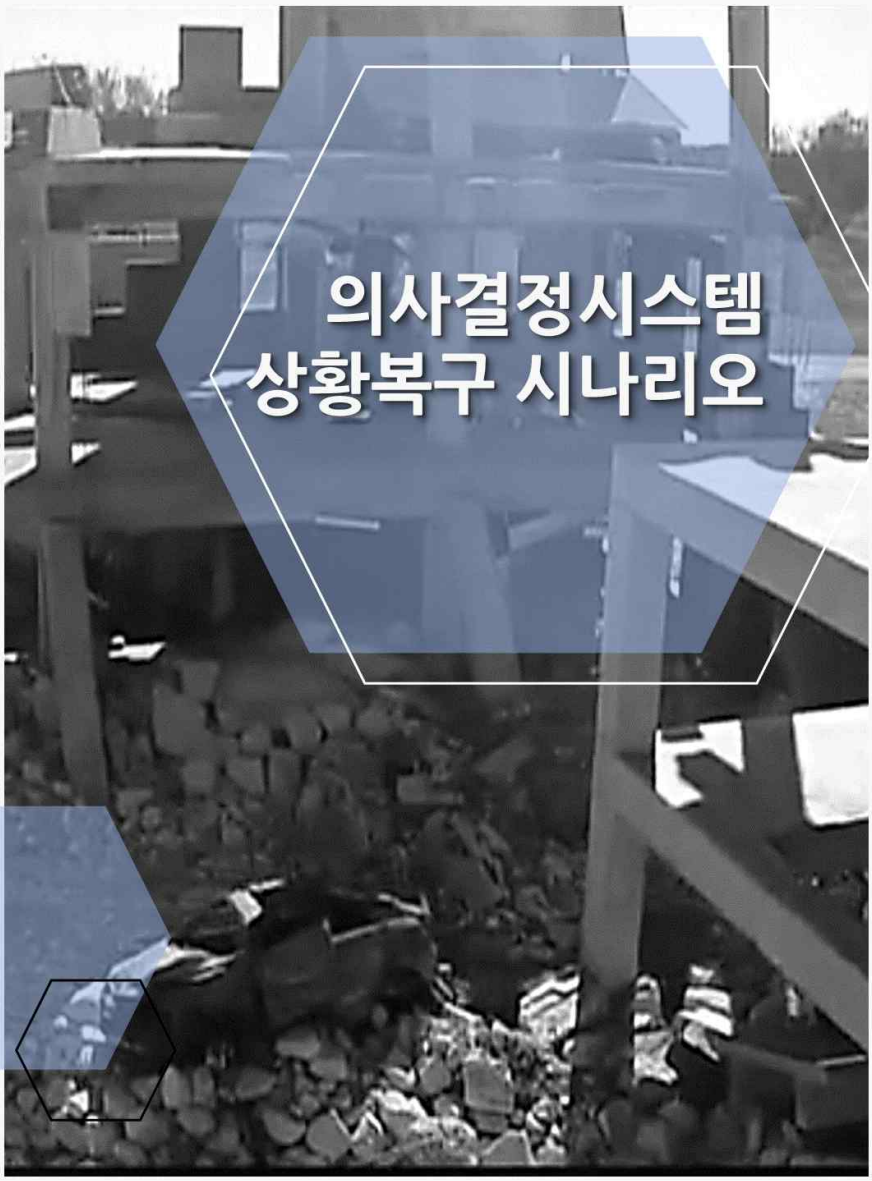
Vapper, M., Lasn, K. (2020). Blast protection of concrete columns with thin strips of GFRP overlay, Structures, 25, 491-499. https://doi.org/10.1016/j.istruc.2020.02.011.

Vasilopoulos, A.A., Bazeos, N., Beskos, D.E. (2008). "Seismic design of irregular space steel frames using advanced methods of analysis", Steel and Composite Structures, An Int'l Journal, 8(1). 53-83.

http://dx.doi.org/10.12989/scs.2008.8.1.053.
Virella, J.C., Godoy, L.A. (2009). “Dynamic response of empty steel tanks with dome roof under vertical base motion”, Steel and Composite Structures, An Int'l Journal, 9(2). 119-130. http://dx.doi.org/10.12989/scs.2009.9.2.119.
Ventsel, E., Krauthammer, T. (2001) Thin Plates and Shells- Theory, Analysis and Applications, The Pennsylvania State University, Pennsylvania, Marcel Dekker, Inc.
Wang, F.C., Zhao, H.Y. (2020) Experimental investigation on blast furnace slag aggregate concrete filled double skin tubular (CFDST) stub columns under sustained loading, Structures, 27, 352-360. https://doi.org/10.1016/j.istruc.2020.05.046.
Xu, Y., Bai, Y., Paik, J.K., Dai, W. (2020). An improved method for quantitative risk assessment of unconfined offshore installations subjected to gas explosions, Structures, 566-577. https://doi.org/10.1016/j.istruc.2020.03.019.
Yuan, Y., Tan, P.J. (2013) Deformation and Failure of Rectangular Plates Subjected to Impulsive Loadings, International Journal of Impact Engineering, 59, 46-59. https://doi.org/10.1016/j.ijimpeng.2013.03.009.
Zhang, J., Ye, Y., Qin, Q. (2019). On dynamic response of rectangular sandwich plates with fibre-metal laminate face-sheets under blast loading. Thin-Walled Structures, 144, 106288. https://doi.org/10.1016/j.tws.2019.106288.
Zhao, N., Yao, S., Zhang, D., Lu, F., Sun, C. (2020). Experimental and numerical studies on the dynamic response of stiffened plates under confined blast loads. Thin-Walled Structures, 154, 106839. https://doi.org/10.1016/j.tws.2020.106839.
국립재난안전연구원. (2013). 지진재해 피해 추정 기술 분석. 서울:국립재난안전연구원
한국과학기술평가원. (2019). 2018년 기술수준평가.
행정안전부. (2019). 2018 재해연보. 세종:행정안전부.

부 록

의사결정시스템 예시



재난 대응 및 복구 지원을 위한 급속 손상도 평가 및 의사결정시스템 개발

연구책임자	강 준 석
주관연구기관	서울대학교
공동연구기관	Georgia Institute of Technology
연구기간	2018.04.10. ~ 2020.12.31.
사업명	국토교통기술촉진연구사업

세부과제 #1

건물외관 변형도와 건물내외부 손상도의 상관관계를 보이는 매핑 시스템 개발

세부과제 #2

재난대응 및 복구를 위한 무인 비행체 기반 재난지역 3차원 매핑 및 이미지 분석기법 개발

● **개요**

최근 빈번히 발생하고 있는 동해안 지역의 지진. 임의의 아파트 혹은 건물에 지진이 발생할 경우, 의사결정자는 피해를 최소화하기 위해 어떤 선택을 해야 할까?

서울대학교에서는 지진이 발생하였을 때 건물 내외부에서 발생할 수 있는 손상 정도를 사전 해석하여 빅데이터를 구축하였다.

서울대학교의 구조 빅데이터 기술력이 Georgia Tech 공과대학 현장상황분석 능력과 통합되어 재해재난 구조에 최적화된 맵핑 시스템 개발했다.

본 기술은 구조물의 내/외부 상세 손상도를 빠르게 요약 제시하여 의사결정자에게 판단에 필요한 가이드라인 (손상범위 및 규모의 정량화, 구조상황에 대한 가이드라인 제공)을 제공한다. 의사결정자는 신속한 상황판단으로 인명피해 및 SOC 피해 최소화에 기여한다.

상황발생 조치 시나리오

시나리오 #1

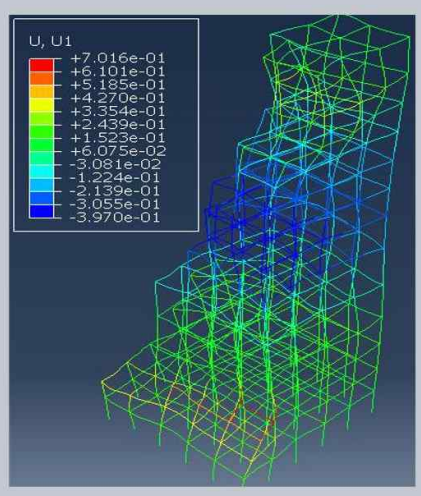
- 발생 위치 : 대한민국 OO시 OO동 OOO 아파트
- 재난 규모 : 지진강도 4.0
- 인명 규모 : 450명
- 골든 타임 : 상황조치까지 40분
- 컨트롤 타워 : OO시 OO구
- 조치 협력기관 : 소방청, 재난대응센터, 지역거점 병원

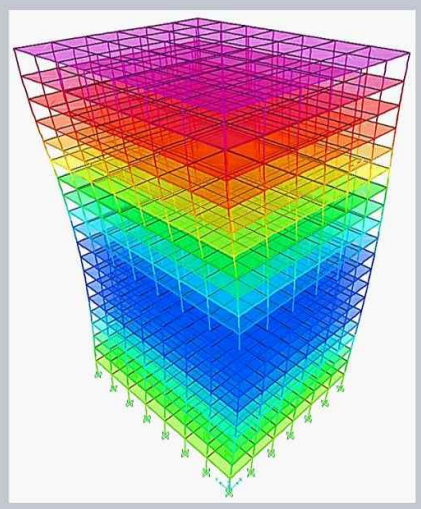


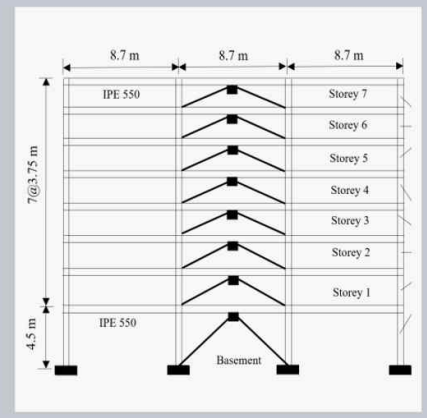
재난대응 컨트롤 타워

사전연구단계

세부과제 #1
건물외관 변형도와 건물내외부 손상도의 상관관계를 보이는 매핑 시스템 개발







1 단계. 건물 내/외부 손상도 Data-base 구축

세부과제 1을 통해 수행된 DB 구축은 최우선적으로 해석모델 개발을 위해 고층 아파트 재원 및 지진 하중에 대한 주요변수 파악한다. 판 지진대에 위치한 지역을 대상으로 아파트의 데이터를 수집하며, 20층 이상 40층 이하의 고층 아파트에 대한 형상 및 층수에 대한 Data-base를 구축한다.

지진 규모(MMI : modified Mercalli intensity)는 국내에서 발생가능한 4~8 사이로 설정하며, 구조물의 재료적 특성을 이용해 내진설계 유무를 고려한다. 아파트 높이, 폭, 각도, 구조물 상단의 변형 등과 내부 손상도의 상관관계를 파악하는 등 해석모델을 이용한 수치해석을 통해 매핑 모델에 사용될 주요 변수를 파악한다.

2 단계. 지진하중 및 내부 폭파에 의한 건물 손상 Data 수집

LiDAR를 이용해 건물을 계측하고, 이를 해석 결과와 상호 비교하여 상관관계를 분석한다. 단일 건물의 지진위험도를 전체 구조물 및 주요 부재에 대해 정량화 하며, 정량화된 손상도는 1단계부터 5단계까지 분류된다.

건물 내부에서 발생할 수 있는 화재, 폭파 등의 여러가지 재난 상황별로 유형을 정의하고, 각 케이스로 인해 주요 부재의 손상도 변화를 해석한다. 부재 손상도를 고려하기 위한 폭파 변수 (BF : Blast Factor)가 제안되며, 이는 지진 하중 하에서의 위험도와 곱해져 위험도를 보정하는 방법을 제시한다.

데이터를 축적하기 위한 실험은 유한요소 해석(FEM : Finite Element Method)이 사용되며, 이를 검증하기 위한 실증 실험을 실시한다. 현재 진행된 미국의 가디언 센터 이외에 국내에 마련된 시설을 이용하여, 예비 데이터를 구축과정을 검증한다.

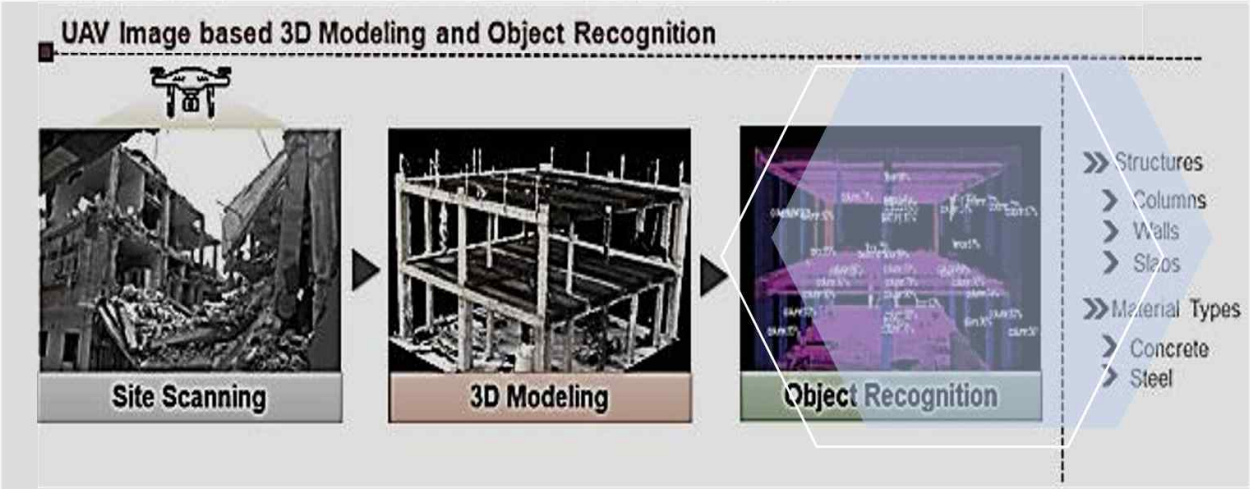


3 단계. 건물의 외관 변형도를 활용한 주요 위험도 유형 분류

건물의 외관 변형도를 활용하여 전체 주요 부재에 대한 위험도를 나타내는 매핑 시스템을 개발하고 이를 유형화하여, 재난 발생 시 신속 대응할 수 있는 정보제공 플랫폼을 구축한다. 본 유형 분류를 위해서 3가지의 데이터 측정 방법이 동시에 진행되며, 1) 지진 하중에 의한 구조물 변위 및 응력 파악 2) 지상 LiDAR를 이용한 외관변형도 측정 3) UAV를 활용한 구조물 변형도 측정 등이 수행된다.

세 가지의 실험 결과와 2단계에서 수행된 유한요소 결과 값을 비교 분석하여 보다 정확도 높은 위험도 해석모델을 개발하고 이를 검증 보완한다. 건물 변형도를 구성하는 주요변수와 건물 손상도의 상관관계를 Contour 및 정량화된 수치로 보이는 매핑을 개발하여 Data를 축적하며, 이는 의사결정자가 즉시 판단할 수 있도록 Web 기반으로 제공된다.





사전연구단계

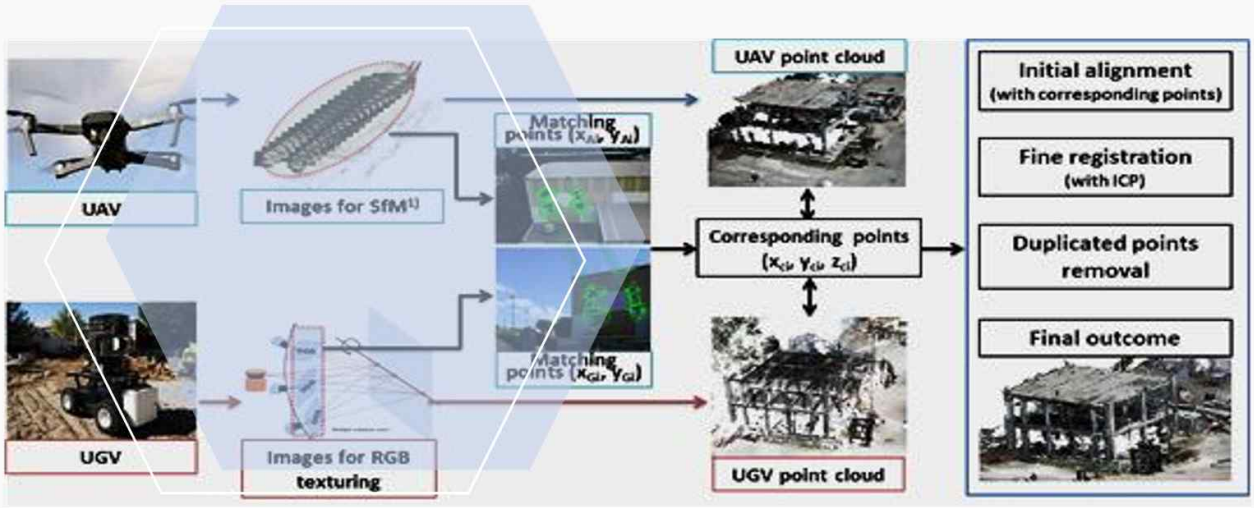
세부과제 #2
재난대응 및 복구를 위한 무인비행체 기반 재난지역 3차원 매핑 및 이미지 분석기법 개발

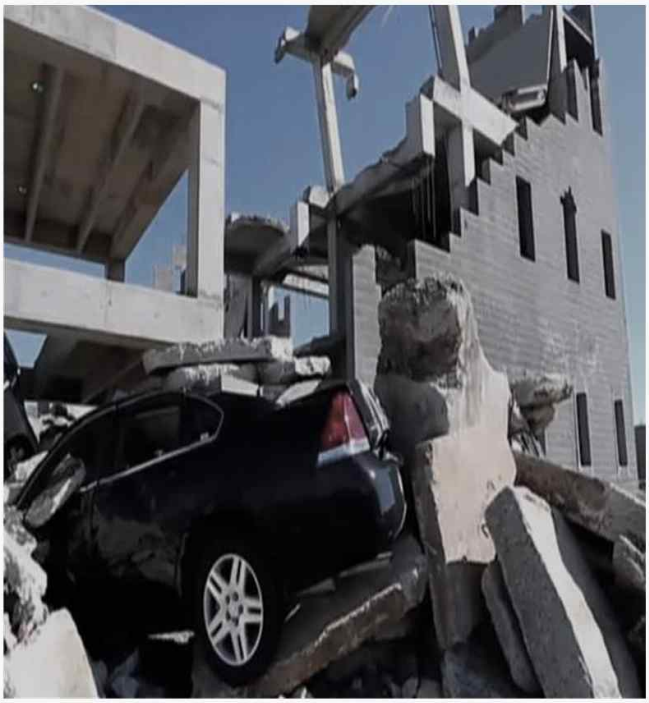
1 단계. 무인항공기를 활용한 재난지역 3차원 모델링 / 오브젝트 검출기법 개발

세부 과제 #2의 핵심 기술은 무인항공기 기반으로 재난지역의 이미지 데이터를 취득하는 것으로, 객체 단위 혹은 타운 단위의 스캐닝 데이터를 수집한다. SfM (Structure from Motion) 알고리즘 기반으로 이미지 분석을 실시하고, 고밀도의 RGB 클라우드 모델을 생성하는 기술을 개발한다.
본 단계에서는 머신러닝을 기반으로 오브젝트가 자동 검출되며 분류되는데, 이는 재난 시에 효율적으로 사용될 수 있도록 포인트 클라우드의 다운 샘플링 및 노이즈 제거 기법이 구현된다. 손상과 비 손상된 오브젝트 분류를 위해서 머신러닝을 통해 트레이닝 모델이 정형화 되며, 지명상태 뿐만 아니라 손상 시 잔해를 검출할 수 있는 기술까지 개발된다.

2 단계. 구조체 파손 정량화 기법을 통한 손상 모델 매칭

Vworld 3D Map과 구조체의 설계도면을 활용한 재난 이전의 3D 기초 모델 확보 및 빅데이터를 구축한다. Nearest-neighbor 매칭 기법을 활용하여 3D 기초모델과 재난 후 변형 모델과의 공통 특징을 추출한다. 이를 활용한 구조체 손상의 정량화를 이루며, 구조물의 전단변형 측정은 물론, 붕괴된 구조체 검출 및 물성치를 확인할 수 있다.
매칭된 모델은 측정 데이터로 연동되어, 클라우드 기반의 재난 데이터 베이스와 연동된다. 무인항공체에 설치된 적외선 카메라와 디지털 카메라 이미지 데이터를 퓨전하여, 의사결정자에 판단을 도울 수 있는 3D 모델 기반 적외선 카메라 데이터 이미징을 개발된다. 측정된 데이터는 세부과제 #1과 상호 비교 검증하여 최적의 복구 경로(ORP : Optimized Rescue & Restoration Pathways)를 제시한다.





지진발생 단계

1 단계. 지진 발생 및 진도 확인 단계

본 단계는 OO시 OO동 OOO 아파트에 진도 4.0 이상의 큰 규모의 지진이 발생을 가정한 상태입니다. 컨트롤 타워에서는 해당 요일, 시간대, 사건발생 시기 등을 고려하여 아파트 내부에 거주자 및 연령층 등을 신속히 유추합니다. 컨트롤 타워에서는 가장 먼저, 지진 발생시 시민들이 고려해야할 사항을 전파하고, 이후에는 복구 및 복원 / 지진 상황에 맞는 의사결정 단계로 즉시 도입하게 됩니다.

컨트롤 타워는 의사결정을 위하여, 지진 발생과 대규모 피해가 시작됨과 동시에 상시 대기중인 무인 항공체를 출동하여 건물 외부의 손상도를 스캐닝하고 각 부재별 손상도를 파악합니다. 모든 스캐닝은 30분 내에 시행되며, 실시간으로 데이터를 분석하여 의사결정자가 위치한 컨트롤 타워로 전송됩니다.

2 단계. 구조해석 사전 매칭 단계

무인 항공체가 30분 내에 실시간으로 부재의 손상도 파악 및 전송을 하는 동안, '컨트롤 타워 구조 안전성 Data Base 팀'의 Golden Time 도 동시에 시작합니다. 진도 규모와 피해 대상지, 건물의 형태 등을 통해서 사전에 구축된 Data Base를 선별하게 됩니다.

구조나 형태에 따라서 분류된 25,000개의 손상 데이터 중에서 약 30%의 유사 데이터가 우선 선정됩니다. 데이터 선정은 6,000개에서 7,500개 사이로 선정되며 현장 스캔 된 데이터의 정확도가 높을수록 우선 선정된 데이터의 수는 적어집니다. 구조해석 Data Base의 매칭은 20분 내로 실시되며, 매칭이 종료됨과 동시에 최적의 복구 시스템 분석이 시작됩니다.



상황조치 및 의사결정 단계

1 단계. 지진 발생 및 상황 확인 단계

상황조치는 무인항공체의 분석 데이터가 전송됨과 동시에 즉시 시작됩니다. 개발된 매칭 알고리즘을 이용하여 드론 스캐닝 자료와 가장 유사한 최적의 손상 케이스를 확정합니다. 본 작업은 5분 내에 모두 매칭되며, 의사결정자가 시민 및 지자체, 협력기관에게 조치 할 수 있는 사항 들을 안내합니다.

의사결정자에게는 신속한 결정을 내릴 수 있도록, 최소한의 정보를 가시적으로 표현하여 제공됩니다. 예를 들면, 하기와 같은 정보를 제공할 수 있습니다.

"OO 아파트의 12시 방향 외관과 내부의 손상도가 20% 이상입니다. 신속한 복구 지원체계를 도입해주시고, 지진의 규모가 0.3 이하일 때 102동 A라인에 위치한 주민분들을 빨리 대피해주시기 바랍니다."

대피 및 복구 단계

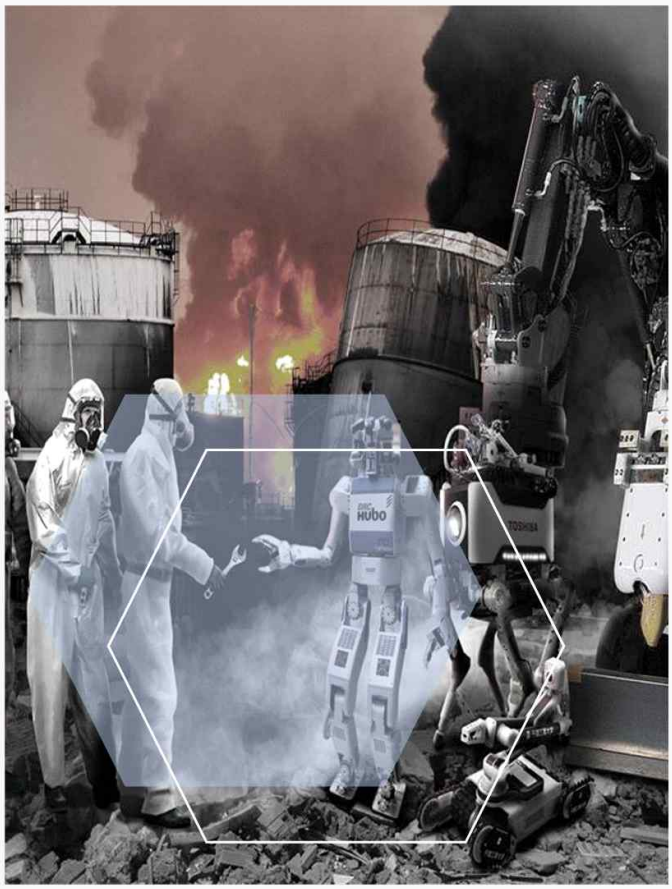
1 단계. 의사결정단계

데이터 제공이 끝난 후에는 컨트롤타워에 위치한 의사결정자의 상황조치 결정이 시작됩니다. 재해재난의 경우, 해당 지역의 컨트롤 타워에서 결정권을 가지고 선제적으로 행동하는 선조치 후보고 형식의 매뉴얼을 따릅니다.

크게 세 가지의 단계로 구분하여 의사결정이 시작됩니다. 첫 번째는 시민 안전조치 단계입니다. 본 단계는 시민들에게 가장 안전한 위치로 대피하기 위함으로, 인명피해를 최소화하는 것을 가장 큰 목표로 합니다. 구조체의 손상도 정도와 여진의 상태에 따라서 건물 외부의 대피시설(강당 등)로 이동 시킬 것인지, 내부의 안전한 공간으로 이동시킬 것인지가 결정됩니다.

이후에는 화재진압 및 복원/복구 단계가 이루어집니다. 지진으로 인해 발생한 화재는 사회 경제적으로 추가적인 피해를 일으킬 수 있기 때문에, 소방청 등의 기관과 긴밀한 협력을 시도하며 지역의 주요 병원과 구조시스템을 가동합니다. 무인 복구 드론 / 복구 로봇 등은 손상된 건물 부위를 복구하는 작업을 시행합니다.

이후에는 생필품 보급 및 시민 안정 단계로서, 시민들이 안정적으로 복구할 수 있는 체계를 지원합니다. 본 복구 의사결정 시스템은 여러 시설들에 대해 동시다발적으로 수행되며, 한 지역이 모두 복원될 때까지 반복됩니다.



사진출처 : 조선일보

의사결정시스템 기대효과

복합적 재난대응 시장 구축
- 무인구조 및 복구 시나리오 적용을 통한 원친기술 시장 창출

국제적 수준의 재난대응 선진국
- 지진 피해 상황에 대한 시나리오 예측함으로써, 국가적 이미지 제고

신뢰도 높은 재난대응
- 재난 발생 시 신속한 현장 대응 및 효율적 현장 복구로 국민들의 국가 재난대응 신뢰도 향상

경제적 가이드라인 제공
- 인공지능형 현장 대응 기술 개발로 기계와 인력을 효율적으로 분배, 경제적 시너지 기대

재난 대응 및 복구 지원을 위한 급속 손상도 평가 및 의사결정시스템 개발

의사결정시스템 상황복구 시나리오

주관 : 서울대학교

(우) 08826 서울시 관악구 관악로 1

공동 : Georgia Institute of Technology

North Ave NW, Atlanta, GA 30332 미국

주 의

1. 이 최종보고서는 국토교통부에서 시행한 국토교통기술촉진연구사업의 연구보고서입니다.

2. 이 최종보고서 내용을 발표하는 때에는 반드시 국토교통부에서 시행한 사업의 연구개발성과임을 밝혀야 합니다.

3. 국가과학기술 기밀 유지에 필요한 내용은 대외적으로 발표 또는 공개하여서는 안 됩니다.